LA--11933-PR

DE91 000513

The Manuel Lujan, Jr. Neutron Scattering Center LANSCE Experiment Reports 1989 Run Cycle

Compiled by
Dianne K. Hyer
Maria A. DiStravolo

Los Alamos
NATIONAL LABORATORY
Los Alamos, New Mexico 87545

Contents

High Density Powder Diffraction (HIPD) 1
Experiment reports 4

Neutron Powder Diffractometer (NPD) 65
Experiment reports 68

Single Crystal Diffractometer (SCD) 111
Experiment reports 114

Low-Q Diffractometer (LQD) 135
Experiment reports 138

Surface Profile Analysis Reflectometer (SPEAR) 201
Experiment reports 204

Filter Difference Spectrometer (FDS) 211
Experiment reports 214

Constant-Q Spectrometer (CQS) 235

New Instruments 239
PHAROS
meV Spectrometer

LANSCE User Group 245
Science Seminar
Abstracts
November 1989

Index 263

The Manuel Lujan, Jr. Neutron Scattering Center
LANSCE Experiment Reports
1989 Run Cycle

Compiled by
Dianne K. Hyer and Maria A. DiStravolo

ABSTRACT

This year was the second in which LANSCE ran a formal user program. A call for proposals was issued before the scheduled run cycles, and experiment proposals were submitted by scientists from universities, industry, and other research facilities around the world. An external program advisory committee, which LANSCE shares with the Intense Pulsed Neutron Source (IPNS), Argonne National Laboratory, examined the proposals and made recommendations.

At LANSCE, neutrons are produced by spallation when a pulsed, 800-MeV proton beam impinges on a tungsten target. The proton pulses are provided by the Los Alamos Meson Physics Facility (LAMPF) accelerator and an associated Proton Storage Ring (PSR), which can alter the intensity, time structure, and repetition rate of the pulses. The LAMPF protons of Line D are shared between the LANSCE target and the Weapons Neutron Research facility, which results in LANSCE spectrometers being available to external users for unclassified research about 60% of each six-month LAMPF run cycle. Measurements of interest to the Los Alamos National Laboratory may also be performed and may occupy up to an additional 20% of the available beam time. These experiments are reviewed by an internal program advisory committee. Ninety-five proposals were submitted for unclassified research and eight proposals for research of a programmatic nature to the Laboratory. Oversubscription for instrument beam time by a factor of two was evident with 439 total days requested and only 246 available for allocation.

Our definition of beam availability is when the proton current from the PSR exceeds 50% of the planned value. The PSR ran at 50 μA current (average) at 20 Hz for most of 1989. The overall beam availability averaged as follows:

- 80% during cycle 53 (May 15 to June 15)
- 71% during cycle 54 (June 28 to August 9)
- 74% during cycle 55 (August 18 to September 26)

All of the scheduled experiments were performed (excluding those few withdrawn because of problems with samples), and experiments in support of the LANSCE research program were accomplished during the discretionary periods.

High Density Powder Diffractometer (HIPD)

High Intensity Powder Diffractometer (HIPD)

The High Intensity Powder Diffractometer (HIPD) is designed to study the atomic structures of materials that are available only in polycrystalline or noncrystalline form. In the HIPD the pulsed neutron beam is directed through a collimator onto a cylindrical or flat plate sample supported in a vacuum chamber. Neutrons are detected by banks of detectors located at various angles to the incident beam. The data from each detector are collected as a function of time of flight (TOF) and stored in a FASTBUS memory module, which is controlled by a micro-VAX II computer. Because the neutron TOF is directly proportional to the neutron wavelength, the measured diffraction pattern yields exact information on the atomic arrangement in the sample. The HIPD offers exceptionally high data rates with nearly three decades of range in momentum transfer or d-spacing. An ambient-temperature, high-intensity water moderator provides a usable neutron flux at wavelengths out to 4 Å. Low backgrounds permit the routine use of wavelengths down to 0.1 Å. The HIPD is intended primarily for studies of liquids and amorphous solids, for magnetic diffraction studies, and for crystallographic studies of samples that are either very small or are in extreme environments of temperature, pressure, or magnetic fields. This instrument is also appropriate for experiments that require time-resolved diffraction measurements.

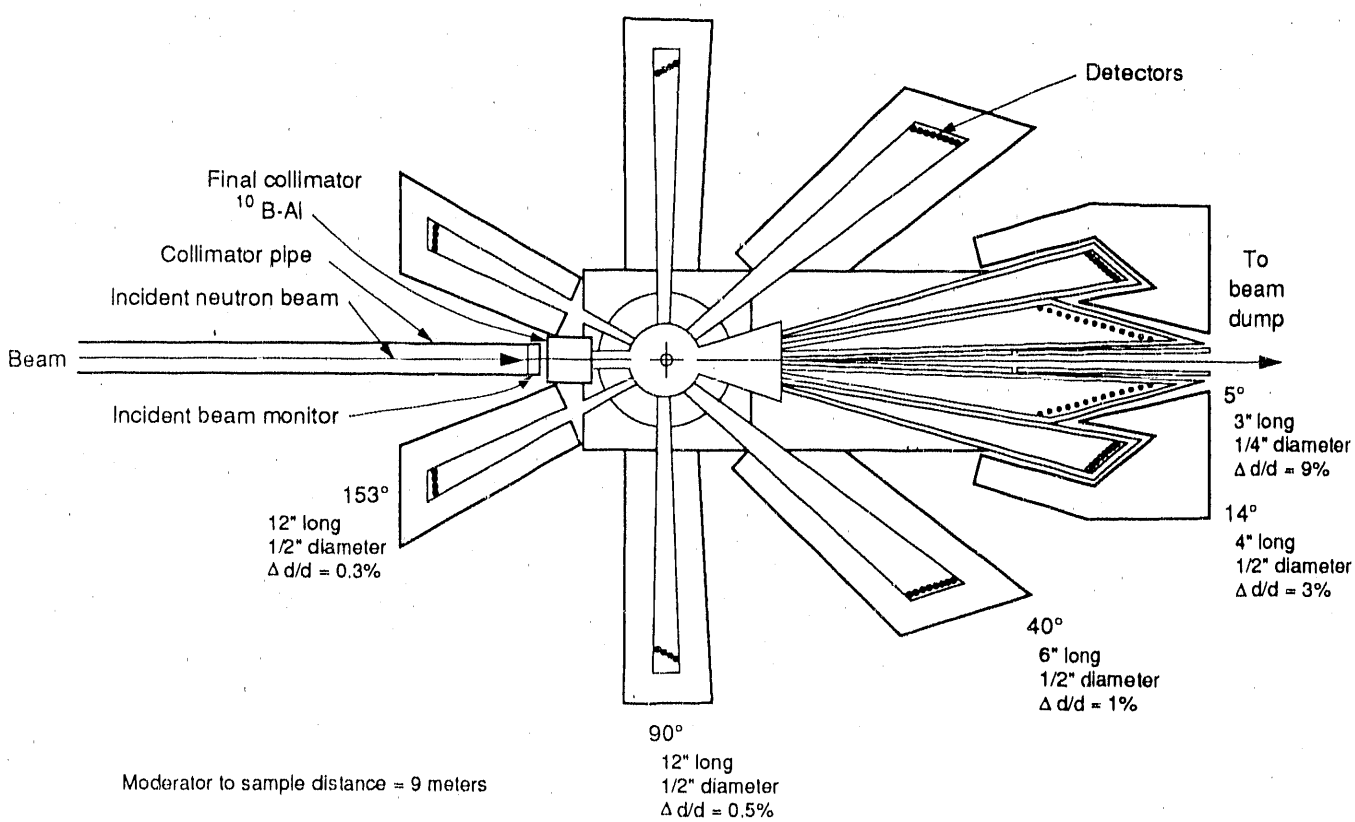

Instrument Details

Wavelength range, λ	0.05 - 4.0 Å
Beam width	1.23 cm
Beam height	2.54 - 5.08 cm, variable
Q range	0.1 - 200 $Å^{-1}$
Range of scattering angle	5° - 153°
Moderator	Chilled water at 10° C
Sample environment	13 - 300 K, closed cycle refrigerator; furnace is planned for 1500° C
Sample size	0.01 - 20 cm^3
Experiment duration	5 minutes - 1 day, depending on sample size

Robert Von Dreele, instrument scientist
John Thomas, instrument technician

Instrument used: *(please type)*	Local contact:	Proposal number: *(for LANSCE use only)*
HIPD	A. C. Lawson & R. B. Von Dreele	D-10.0

Title:

Magnetic Structure of UPdSn

Report received: *(for LANSCE use only)*

Authors and affiliations:

R. A. Robinson, LANSCE, LANL
A. C. Lawson, MST Division, LANL
K. H. J. Buschow, Philips Research Labs., Eindhoven

Experiment report:

A few years ago, a systematic study of the magnetic properties of a number of ternary uranium compounds was made by Palstra et al.[1]. Many of these compounds showed evidence of gaps in their band structures and a few were thought to be antiferromagnetic. One of us [2] had already studied UNiSn on a reactor powder diffractometer at NBS and this summer, we studied some of the other antiferromagnets on HIPD at LANSCE. The most dramatic results were on the hexagonal compound UPdSn, which has a Néel temperature of 29K. We took data both above and below T_N, at 45K and 10K. The high temperature data fit well to the $CaIn_2$ structure [1], with space group $P6_3/mmc$, except for three impurity lines which we have so far been unable to identify. The data from one of the two 40° banks are shown in the Figure. In the low temperature pattern, there are clearly 7 extra peaks, which are indexed in the lower figure. We interpret these as being magnetic, with cell doubling in the hexagonal plane. These are some of the best magnetic neutron diffraction data taken on an accelerator-based neutron source [3-6], with observable reflections out to a d-spacing of 8Å. The analysis of these data is incomplete, but we have established that our data are inconsistent with all of the collinear structures catalogued for this space group by Prandl[7]. We have found a simple non-collinear structure that appears to fit our data, but have not completed the analysis yet. However, we have every confidence that these data are good enough to determine the magnetic structure and the uranium moment.

Experiment report *(continued)*:

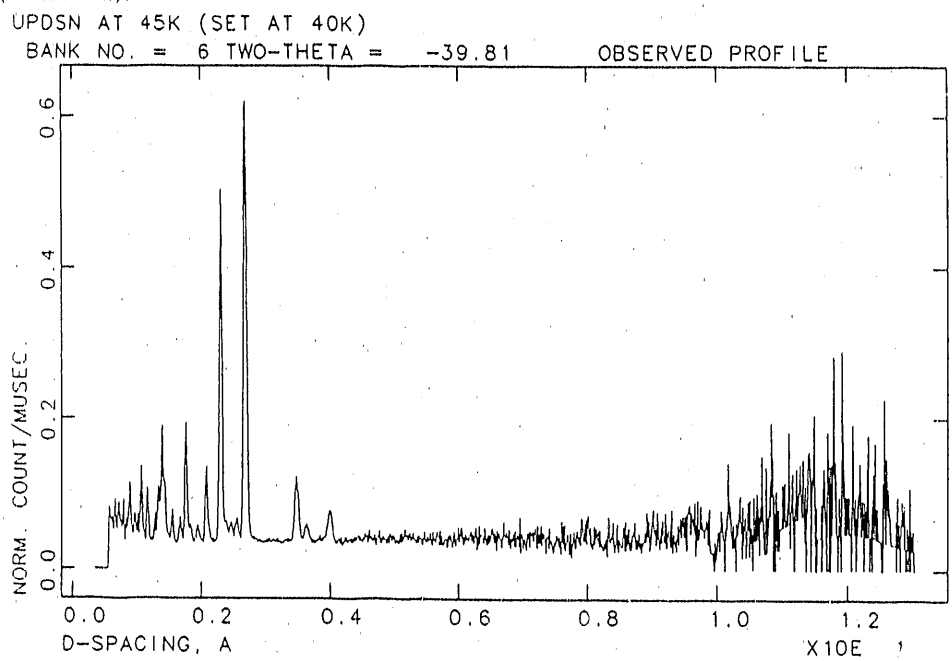

(a) Portion of the 45K diffraction pattern in one of the 40° banks on HIPD, on UPdSn.

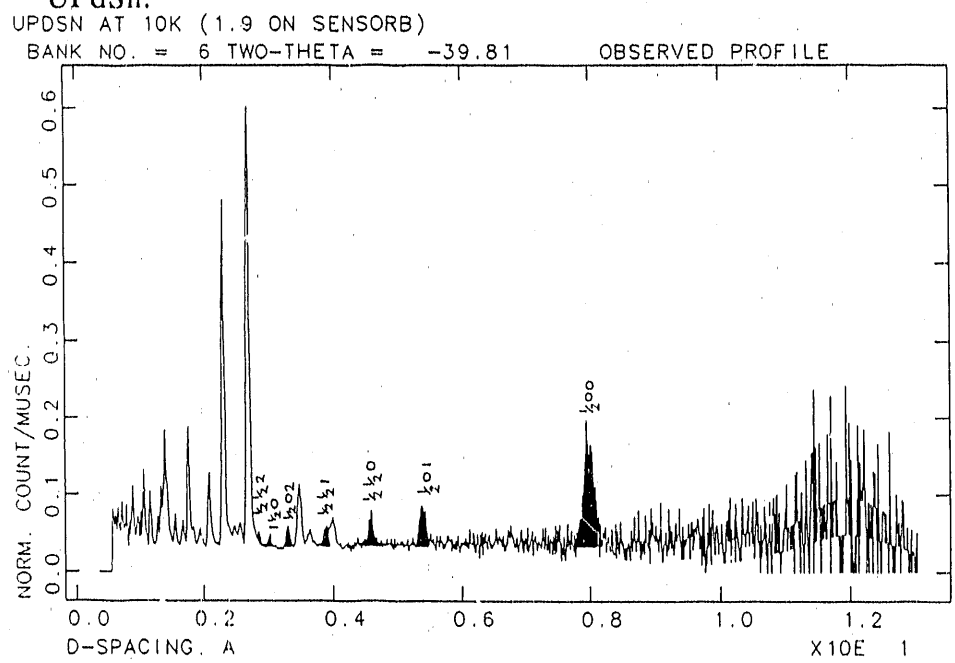

(b) Portion of the 10K diffraction pattern in one of the 40° banks on HIPD, on UPdSn. The extra peaks are shaded in black and indexed in the hexagonal cell.

References:

[1] T. T. M. Palstra, G. J. Niewenhuys, R. F. M. Vlastuin, J. van den Berg, J. A. Mydosh and K. H. J. Buschow, J. Magn. Magn. Mater. 67, 331 (1987).

[2] M. Yethiraj, R. A. Robinson, J. J. Rhyne, J. A. Gotaas and K. H. J. Buschow, J. Magn. Magn. Mater. 79, 355 (1989).

[3] G. P. Felcher, J. D. Jorgensen and R. P. Wäppling, J. Phys. C: Solid State Phys. 16, 6281 (1983).

[4] A. C. Lawson, A. Williams, J. L. Smith, P. A. Seeger, J. A. Goldstone, J. A. O'Rourke and Z. Fisk, J. Magn. Magn. Mater. 50, 83 (1985).

[5] A. C. Lawson, A. Williams, J. G. Huber and R. B. Roof, J. Less-Common Metals 120,113 (1986).

[6] A. L. Giorgi, A. C. Lawson, J. A. Goldstone, K. J. Violin and J. D. Jorgensen, J. Appl. Phys. 63, 3604 (1988).

[7] W. Prandl, in "Neutron Diffraction", ed. H. Dachs, Springer-Verlag, Berlin 1978, p.113.

Instrument used: *(please type)*	Local contact:	Proposal number: *(for LANSCE use only)*
HIPD	Robert Von Dreele	D-31.0

Title:	Report received: *(for LANSCE use only)*
Neutron Powder Diffraction Study of $[Na(ND_3)_4]^{+I-}$	2/7/90

Authors and affiliations:

Dr. Victor G. Young, Jr.	Department of Chemistry Arizona State University
Dr. William S. Glaunsinger	Department of Chemistry Arizona State University
Mr. Gary L. Burr	Department of Chemistry Arizona State University
Dr. Robert B. Von Dreele	P-LANSCE Los Alamos National Laboratory

Experiment report:

It is known that alkali metal halides form stable complexes with water and alcohols. However, little is known concerning similar complexes containing ammonia or simple amines, even though there are several literature reports on their physical properties. One reason for this is that all of these complexes have a high partial pressure of ammonia (or amine) at room temperature which makes handling difficult and hazardous. Some properties of these complexes which make them attractive for study at present are those of fast ionic conductors and thermal storage systems. The first member of this class to be studied by neutron powder diffraction is $[Na(ND_3)_4]^{+I-}$. Data sets were collected at 28, 100 and 200 K on HIPD. All data revealed a sample that had a high degree of preferred orientation and neither NaI or solid ND_3 was present as a minor phase. Visual examination of the sample after data collection suggested that the sample may have been one large single crystal. The data is currently being indexed with the cell fitting programs VISSER and TREOR. It is likely that this data lacks the quality needed for a structural solution, but it should provide cell constants and possibly a spacegroup which could be used after a method is devised to powder and transfer this complex without ammonia loss. Diffraction profiles of two individual tubes of the +153 detector are provided below to demonstrate the severity of the preferred orientation.

Experiment report *(continued)*:

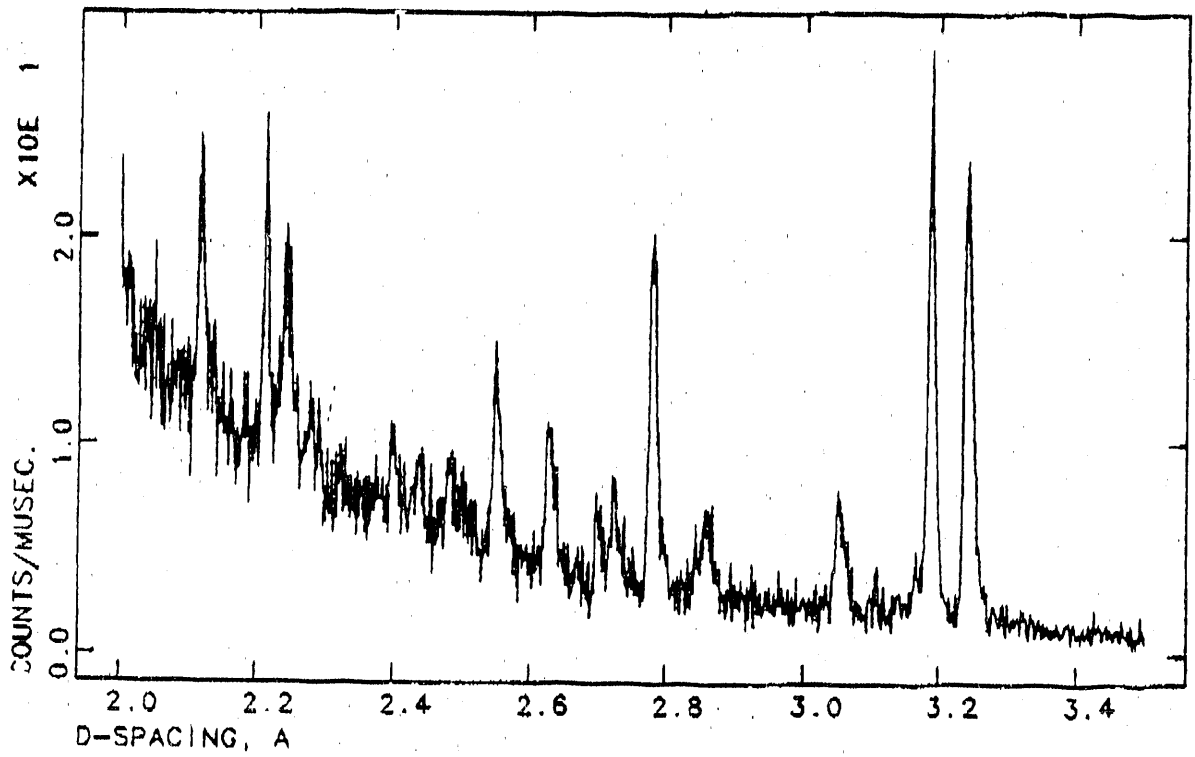

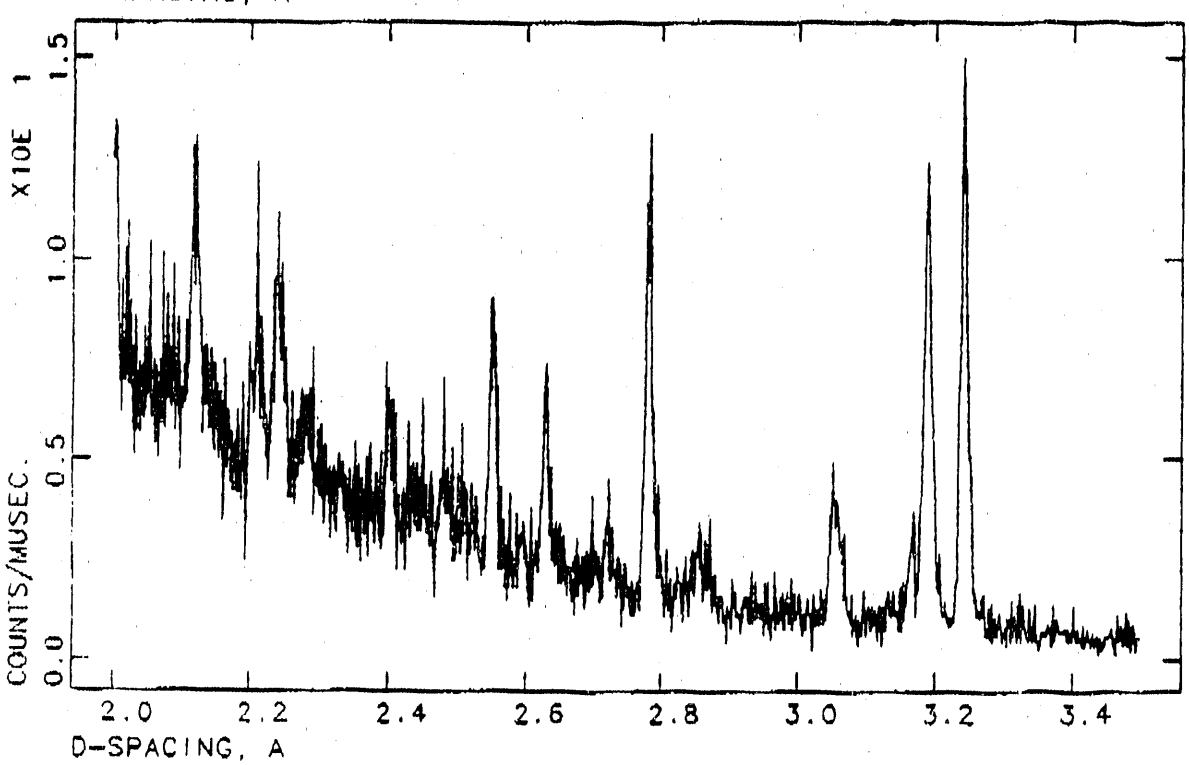

Instrument used: (please type)	Local contact:	Experiment no:
HIPD	R. B. Von Dreele	D-32.1

Title:
"Neutron Powder Diffraction Study of $Ag_{0.25}TiS_2$"

Authors and affiliations:

G.L. Burr, V.G. Young, Jr., and W.S. Glaunsinger,
Department of Chemistry, Arizona State University
M.J. McKelvy, Center for Solid State Science, Arizona State University
R.B. Von Dreele, LANSCE, Los Alamos National Laboratory

Report received:
(to be filled in by LANSCE)

Dates of experiment: July 27, 1989

- ☐ Approved by external program committee
- ☐ Approved by internal program committee
- ☐ Part of LANSCE discretionary time

Experiment report:

$Ag_{0.25}TiS_2$ has been studied by neutron powder diffraction at 300 K. The diffraction pattern is consistant with a mixed phase material. The phases are stage-I($p\bar{3}m1$ where a-3.416A and c-6.1A) and stage-II($p\bar{3}m1$ where a-3.416A and c-6.1A) $Ag_{0.25}TiS_2$. We are presently working toward the solutions of these structures using Rietveld refinements. The data set from the 153 degree detector bank is shown below.

Experiment report (continued):

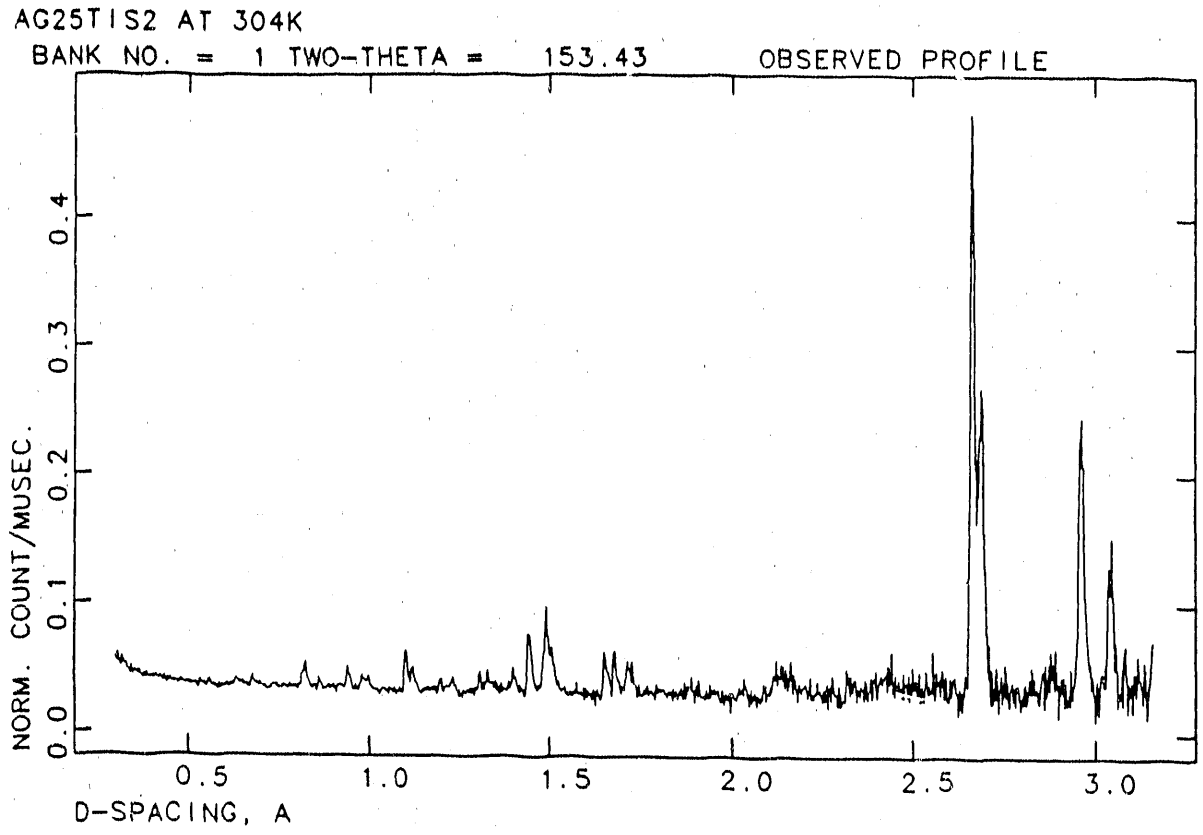

Los Alamos
Los Alamos National Laboratory
Los Alamos, New Mexico 87545

Form number 1195 (12/87)

Instrument used: (please type)	Local contact:	Experiment no:
HIPD	R.B. Von Dreele	D-32.2

Title:

"Neutron Powder Diffraction Study of $(Ag^{+})_{0.25}(ND_3)_{0.75}TiS_2^{0.25-}$"

Authors and affiliations:

Report received:
(to be filled in by LANSCE)

G.L. Burr, V.G. Young, Jr., and W.S. Glaunsinger, Dept. of Chemistry, ASU
M.J. McKelvy, Center for Solid State Science, ASU
R.B. Von Dreele, LANSCE, Los Alamos National Laboratory

Dates of experiment: August 23, 1989

- ☐ Approved by external program committee
- ☐ Approved by internal program committee
- ☐ Part of LANSCE discretionary time

Experiment report:

$Ag^{+}_{0.25}(ND_3)_{0.75}TiS_2^{0.25-}$ has been studied by neutron powder diffraction at 300 K. Due to the large contribution to the background from the quartz sample container required to maintain a ND_3 pressure above the sample, the data refinement was not sucessful. The locations of deuterium positions were not resolvable. The data set from the 153 degree detector bank is shown below. Furthur work using a newly fabricated vanadium sample container, which is capable of maintaining the required ammonia pressure above the sample without the need for a quartz container, is anticipated.

periment report (continued):

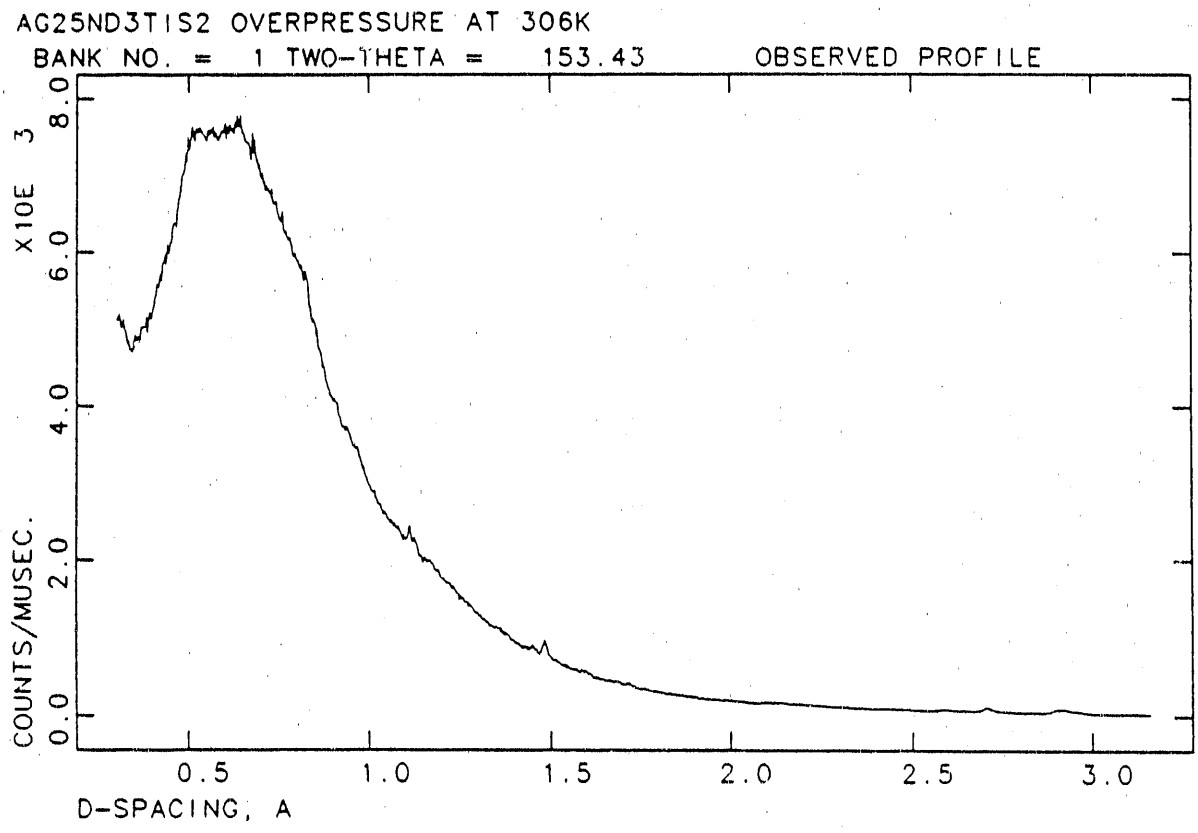

Instrument used: *(please type)*	Local contact:	Proposal number: *(for LANSCE use only)*
HIPD	R. B. VonDreele	D-13.0
Title: The structure of Magnesium Deuteroxide		**Report received:** *(for LANSCE use only)*

Authors and affiliations:

Daniel Partin and Michael O'Keeffe.
Arizona State University

Experiment report:

Brucite is a layered structure consisting of octahedra of oxygen around magnesium, with deuterium bonded to the oxygen and directed into the area between the layers (see figure).

Magnesium deuteroxide has a hexagonal unit cell with a 3.1444(2) A, c 4.7645(4) A, volume of 40.793(6) A^3, and spacegroup P-3m1. X^2 5.918.

Atom		X	Y	Z	u11	u33	u12
Mg	1(a)	0	0	0	0.006(4)		
O	2(d)	1/3	2/3	0.2220(3)	0.0250(8)	0.0052(9)	0.0125(4)
D	2(d)	1/3	2/3	0.4168(2)	0.0265(6)	0.016(1)	0.0132(3)

There was very little difference between the low temperature (10k) and the room temperature runs.

There were difficulties in the refinement, for example, being unable to adequately model the Lorentzian broadening in the diffracted peaks (see figure).

Experiment report *(continued)*:

Results to date are:
unit cell is cubic with a 18.3030(1) A, volume of 6161.5 A^3 and spacegroup Im3m.

Atom		X	Y	Z
Ba	48(j)	0.15077(9)	0	0.31021(9)
Ba	24(h)	0	0.36350(8)	0.36350(8)
Ba	16(f)	0.17666(7)	0.17666(7)	0.17666(7)
Cu	48(i)	0.25	0.14970(4)	0.35030(4)
Cu	24(h)	0	0.12600(6)	0.12600(6)
Cu	12(e)	0	0.2032(1)	0
Cu	12(e)	0	0.4322(2)	0
O	48(k)	0.07418(4)	0.14454(5)	0.34571(7)
O	48(k)	0.26746(5)	0.26746(5)	0.08488(7)
O	12(d)	0.25	0	0.5
O	12(e)	0	0.3343(2)	0
O	48(j)	0.1011(3)	0	0.4469(2)

References:

Instrument used: *(please type)*	Local contact:	Proposal number: *(for LANSCE use only)*
HIPD	R. B. Von Dreele	D-14,1

Title:	Report received: *(for LANSCE use only)*
Neutron Powder Diffraction Study of Ba3N2	

Authors and affiliations:

Nathaniel E. Brese and Michael O'Keeffe
Department of Chemistry
Arizona State University
Tempe, AZ 85287 USA

Experiment report:

Ba_3N_2 is formed by reaction of the elements at between 600 and 800°C. Both its X-ray and neutron powder diffraction patterns are plagued by extremely broad peaks (see Fig. 1). Since broad peaks greatly increase the difficulty in indexing the pattern, we could not discern a reliable unit cell. Programs such as TREOR and VISSER did yield several small monoclinic cells, but all the cells required indexing of strong peaks with unlikely indices.

We are currently trying to develop flux growth methods, so that crystals can be produced without the inordinate strain evident in the powder samples.

Experiment report *(continued)*:

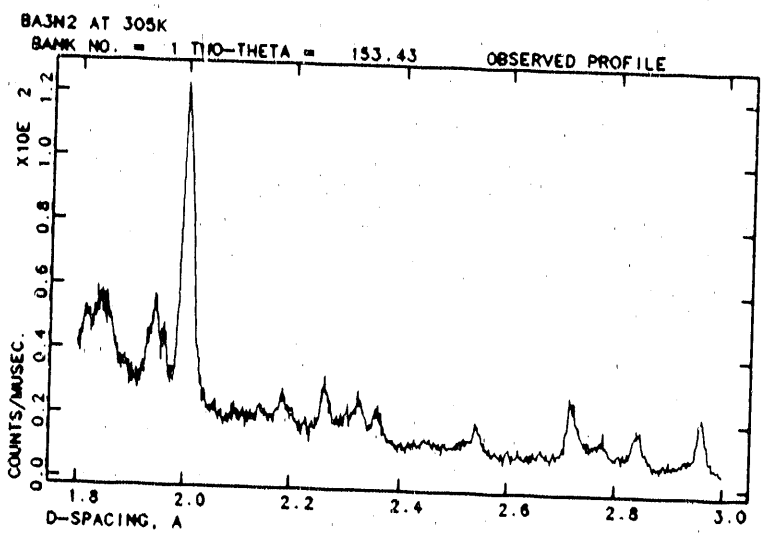

References:

Instrument used: *(please type)*	Local contact:	Proposal number: *(for LANSCE use only)*
HIPD	R. B. Von Dreele	D-14.2

Title:

Neutron Powder Diffraction Study of SrD2 and SrND

Report received: *(for LANSCE use only)*

Authors and affiliations:

Nathaniel E. Brese, Michael O'Keeffe

Department of Chemistry
Arizona State University
Tempe, AZ 85287 USA

R. B. Von Dreele

Manuel Lujan, Jr. Neutron Scattering Center
Los Alamos, NM 87545 USA

Experiment report:

It has been suggested that Sr2N is actually Sr2NHx (1,2). Further, we showed that Sr2N can be made without any hydrogen contamination (3). In order to explore the susceptibility of Sr2N to intercalation by hydrogen, we reacted our Sr2N neutron sample with D2 and obtained amixture of Srd2 and SrND. Their structures were refined using time-of-flight neutron diffraction data.

SrD2 and SrND crystallize with the PbCl2 and rocksalt structures, respectively. Crystal data for SrD2: Pnma, a 6.3707(4), b 3.8714(3), c 7.3021(5), V 180.09(2), Z 4, Dx 3.38. Sr atoms center irregular tricapped trigonal prisms with 2 of the D atoms being significantly farther away from the Sr atom. The Sr-D distances are 2.811(4) (2x), 2.703(4) (2x), 2.577(4), 2.491(5), 2.444(3) (2x), and 2.415(5). Crystal data for SrND: Fm3m, a 5.4472(2), V 161.6?(1), Z 4, Dx 4.26. The center of mass of the rotationally-disordered ND dipole was fixed at the center of the unit cell; the dipole was directed at the 48 vertices of a truncated cuboctahedron. The N-D distance was fied at 1.01; Sr has N neighbors between 2.615 and 2.833A and D neighbors between 2.008 and 3.1898. The data collected at 300K were refined to a final Rwp of 0.042 and Rp of 0.031. The reduced Chi-squared was 4.055 for 7572 profile points and 55 variables.

Experiment report *(continued)*:

Submitted to the Journal of Solid-State Chemistry.

References:

1. J. -F. Brice, J. -P. Motte and J. Aubry, Rev. Chim. Miner. 12, 105 (1975).
2. F. Hulliger and F. Levy (Eds.), "Structural Chemistry of Layer-type Phases", D. Reidel, Dordrecht, Holland (1976).
3. Ne. E. Brese and M. O'Keeffe, J. Solid-State Chem., submitted for review

Instrument used: *(please type)*	Local contact:	Proposal number: *(for LANSCE use only)*
HIPD	Robert B. Von Dreele	D-16.1

Title:
STUDIES OF LONG-RANGE ANTIFERROMAGNETIC ORDERING IN Bi_2CuO_4

Report received: *(for LANSCE use only)*

Authors and affiliations:

Eddie W. Ong, Los Alamos National Laboratory and Department of Chemistry, Arizona State University.

George H. Kwei, Robert A. Robinson and Robert B. Von Dreele, Los Alamos National Laboratory

B.L. Ramakrishna, Department of Chemistry, Arizona State University.

Experiment report:

The discovery of the high transition temperature superconductors [1] has led to a great deal of work on the structure and magnetic properties of the oxocuprates [2,3]. A number of the early studies used neutron diffraction to study antiferromagnetic ordering in La_2CuO_4 and oxygen-deficient nonsuperconducting $YBa_2Cu_3O_{6+\delta}$ [4]. More recently, magnetic susceptibility, electron paramagnetic resonance and neutron diffraction studies of related oxocuprates have been reported. Evidence for antiferromagnetic ordering has been seen in neutron powder diffraction studies of Y_2BaCuO_5 and $Y_2Cu_2O_5$ [5-7]. Currently, the class of oxocuprates with the formula A_2CuO_4 is being studied intensively. It was found that the structures adopted by these compounds depended strongly on the size of the trivalent cation (A = rare earth), as demonstrated by the so-called T, T' and T* phases [8,10]. One of the more interesting oxocuprates that has been studied is Bi_2CuO_4.

The replacement of bismuth for the rare earths resulted in a radically different structure. Unlike many of the the oxocuprates which have bridging units such as Cu-O-Cu or Cu-O-O-Cu in planar arrays, the copper ions in Bi_2CuO_4 are coordinated by square planes of oxygen ions, which in turn are stacked above each other in a staggered fashion, forming one-dimensional copper ion chains. The copper atoms are not bridged by any intervening oxygen ions and the Cu-Cu distance is only 2.9 Å, only slightly larger than that in metallic copper. This situation allows several possibilities for the exchange interactions between the copper ions. These may include exchange through orbital overlap as well as the superexchange through the oxygen and/or bismuth ions. The dependence of the magnetic susceptibility on temperature shows a broad maximum, typical of low dimensional antiferromagnets, near 50 K [3]. However, the origin of its magnetic behavior is clouded somewhat by the differences in the proposed structures for Bi_2CuO_4 [11,12]. The structural uncertainties and the possibility of antiferromagnetic ordering led us to undertake a joint x-ray/neutron powder diffraction study of Bi_2CuO_4 to determine its structure, at both ambient and low temperatures. DC magnetometry was used to track its magnetic response as a function of field and temperature. ESR was used to probe the local electronic environments of the copper ions. This combination of techniques provides both long-range and short-range descriptions of the magnetic structure of Bi_2CuO_4.

Experiment report *(continued)*:

Simultaneous refinement of the room temperature x-ray and neutron data was used to obtain accurate cell parameters and atomic positions. Neutron diffraction data at 13 K and 300 K show that the appropriate space group is P4/ncc at both temperatures and reveal the appearance of a two magnetic peaks at the lower temperature which can be indexed as 1 0 0 and 2 1 0 reflections.

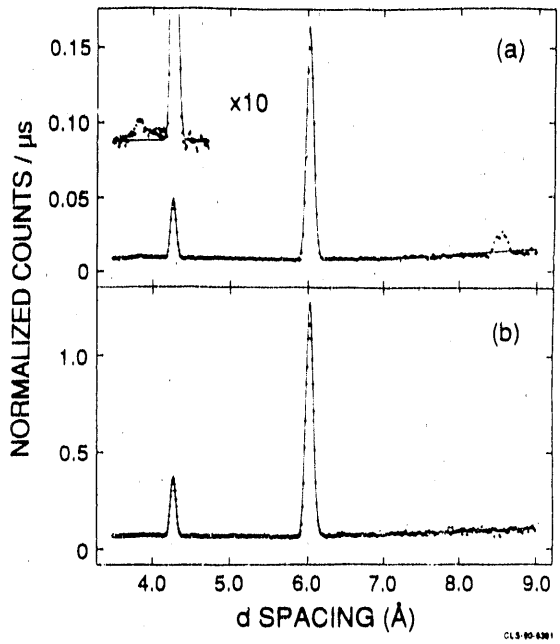

The figure at left shows a comparison of portions of the neutron powder diffraction patterns measured on the -40° detector bank for Bi_2CuO_4 at 13 K and 304 K. Panel (a) shows the normalized data in the d spacing range 3.5-9.0 Å taken at 304 K, while panel (b) shows the data taken at 13 K and the magnetic peaks at d spacings of 3.8 and 8.5 Å. While these reflections are clearly indicative of long-range antiferromagnetic order, on the basis of these powder data alone, one cannot determine the moment direction. But, on the assumption that the moments lie along the c-axis, the copper magnetic moment is $0.56\pm0.04\mu_B$. dc magnetometry was performed at temperatures from 1.66 to 400 K and fields ranging from 0.5 to 50 kOe. The magnetization showed no field saturation even at 1.66 K and 45 kOe. The susceptibility showed a maximum near 50.4 K with a Curie tail observed at low temperatures. Antiferromagnetic interactions dominated at all temperatures. The magnetic behavior is like that of a three-dimensional antiferromagnetic system. ESR experiments were done over the temperature range 4.3 to 300 K. For temperatures above 50 K, one broad line with g = 2.09 was observed. The resonance field shifted to higher values for T < 37 K, with an eventual splitting of the line below 15 K. These can be associated with antiferromagnetic resonant modes, consistent with an ordered antiferromagnetic phase.

[1] J. G. Bednorz and K. A. Müller, Z. Phys. B **64**, 189 (1986).
[2] B.L. Ramakrishna and E.W. Ong, J. Appl. Phys. **64**, 5953 (1988).
[3] K. Sreedhar and P. Ganguly, Inorg. Chem. **27**, 2261 (1988).
[4] See S. K. Sinha, D. Vaknin, M. S. Alvarez, A. J. Jacobson, J. Newsam, J. T. Lewandowski, D. C. Johnston, C. Stassis, J. M. Tranquada, T. Freltoft, H. Moudden, A. I Goldman, P. Zolliker, D. E. Cox and G. Shirane, Physica B**156** &**157**, 854 (1989) and references therein.
[5] E. W. Ong, B. L. Ramakrishna and Z. Iqbal, Sol. State. Commun. **66**, 171 (1988).
[6] T. Chattopadhyay, P. J. Brown, U. Köbler and M. Wilhelm, Europhys. Lett. **8**, 685 (1989).
[7] J. Aride, S. Flandrois, M. Taibi, A. Boukhari, M. Drillan and J.L. Soubeyroux, Solid State Commun. **72**, 459 (1989).
[8] S-W. Cheong, Z. Fisk, J.D. Thompson, and R.B. Schwartz, Physica C**159**, 407 (1989).
[9] J. Akimitsu, S. Suzuki, M. Watanabe and H. Sawa, Jap. J. Appl. Phys. **27**, L1859 (1989).
[10] Y. Tokura, H. Takagi and S. Ushida, Nature **337**, 345 (1989).
[11] J.-C. Boivin, D. Thomas and G. Tridot, Compt. Rend. Acad. Sc. Paris **276**, 1105 (1973).
[12] R. Arpe and Hk. Müller-Buschbaum, Z. Anorg. Chem. **426**, 1 (1976).

Instrument used: *(please type)*	Local contact:	Proposal number: *(for LANSCE use only)*
HIPD	Robert B. Von Dreele	D-16.2

Title:

STUDIES OF LONG-RANGE ANTIFERROMAGNETIC ORDERING IN Bi_2CuO_4

Report received: *(for LANSCE use only)*

Authors and affiliations:

Eddie W. Ong, Los Alamos National Laboratory and Department of Chemistry, Arizona State University.

George H. Kwei, Robert A. Robinson and Robert B. Von Dreele, Los Alamos National Laboratory

B.L. Ramakrishna, Department of Chemistry, Arizona State University.

Experiment report:

The results of an investigation of Bi_2CuO_4 using: (1) x-ray and neutron powder diffraction, (2) dc magnetometry, and (3) electron spin resonance, is presented. Simultaneous refinement of the room temperature x-ray and neutron data was utilized to obtain accurate cell parameters and atomic positions. Neutron diffraction data at 13 K and 300 K show that the appropriate space group is P4/ncc at both temperatures and reveal the appearance of a two magnetic peaks at the lower temperature which can be indexed as 1 0 0 and 2 1 0 reflections. While they are clearly indicative of long-range antiferromagnetic order, on the basis of these powder data alone, one cannot determine the moment direction. But, on the assumption that the moments lie along the c-axis, the copper magnetic moment is $0.51\pm0.01\mu_B$. dc magnetometry was performed at temperatures from 1.66 to 400 K and fields ranging from 0.5 to 50 KOe. The magnetization showed no field saturation even at 1.66 K and 45 KOe. The susceptibility showed a maximum near 50.4 K with a Curie tail observed at low temperatures. Antiferromagnetic interactions dominated at all temperatures. The magnetic behavior is like that of 3-D antiferromagnetic system. ESR experiments were done over the temperature range 4.3 to 300 K. For temperatures above 50 K, one broad line with g = 2.09 was observed. The resonance field shifted to higher values for $T < 37$ K, with an eventual splitting of the line below 15 K. These can be associated with antiferromagnetic resonant modes, consistent with an ordered antiferromagnetic phase.

Instrument used: *(please type)*	Local contact:	Proposal number: *(for LANSCE use only)*
NPD HIPD	Joyce A. Goldstone Robert B. Von Dreele	D-8.0

Title:

$TlBa_{1.2}La_{0.8}CuO_5$: A SUPERCONDUCTOR PRODUCED BY REDUCTION, RATHER THAN OXIDATION, OF THE CuO_2 PLANES

Report received: *(for LANSCE use only)*

Authors and affiliations:

M.A. Subramanian, E.I. Du Pont de Nemours.

George H. Kwei, Joyce A. Goldstone and Robert B. Von Dreele, Los Alamos National Laboratory.

John B. Parise, Department of Earth and Space Sciences, SUNY at Stony Brook.

Experiment report:

Doping of La^{3+} for Ba^{2+} in $TlBa_2CuO_5$, to introduce holes into the CuO_2 planes, leads to superconductivity in the material $TlBa_{1.2}La_{0.8}CuO_5$ (with $T_c \approx 52$ K). The structure (P4/mmm) has been refined using neutron powder diffraction data co'lected at 305 K [a = 3.8479(3) and c = 9.0909(6) Å] and 15 K [a = 3.8444(1) and c = 9.0744(3) Å]. An increase in the Cu-O in-plane bond distance from that in $TlBa_2CuO_5$ is consistent with a lowering of the formal oxidation state of copper from its value of 3+. Substantial static site disorder is observed in the Tl-O(3) planes, presumably to allow for better Tl^{3+}-O coordination. Examination of the thermal parameters for the CuO_6 octahedra shows that this disorder in turn produces a local tilting of the octahedra and a resultant puckering of the CuO_2 planes.

To be published in Physica C (1 February 1990).

Instrument used: *(please type)*	Local contact:	Proposal number: *(for LANSCE use only)*
HIPD	A. C. Lawson	D-21.0

Title:

TEXTURE OF COLD-ROLLED ALUMINUM
BY PULSED NEUTRON DIFFRACTION

Report received: *(for LANSCE use only)*

Authors and affiliations:

D. Sivia, M. Yethiraj, P-LANSCE
A. C. Lawson, J. Vaninetti, MST-5
D. Viskoe and T. Claytor, WX-3
Los Alamos National Laboratory
Los Alamos NM 87545

Experiment report:

Metallurgical "texture" is the distribution of orientation of the grains comprising a polycrystalline specimen. In certain applications, it is important to know the texture so that mechanical properties of a component can be predicted. Texture can be determined by diffraction techniques; neutron diffraction is particularly advantageous when it is desired to sample the entire volume of a large specimen.

Our sample was a laminated aluminum sphere of 2" diameter using 1/16" circular cold-rolled plates. This configuration, known as "the Armadillo," was chosen to avoid awkward shape corrections in our initial experiments. The Armadillo was mounted on a two-circle goniometer with the normals of the laminates in the diffraction plane of the High Intensity Powder Diffractometer (HIPD) at the zero-settings of the goniometer angles. 36 data sets were obtained at different settings of the goniometer so that 144 distinct orientations were realized in the ±153° and ±90° detector banks. Data collection times were approximately 20 minutes for each orientation with LANSCE running at 30 μA. Two typical diffraction patterns are shown in Fig. 1, and it is evident that much shorter collection times would be sufficient for such a large sample.

Integrated intensities were obtained for the first 10 reflections of each pattern, and a procedure based on the "maximum entropy" principle was used to infer the Orientation Distribution Function (ODF) from the data. Pole figures were obtained directly from the data and by derivation from the ODF are in good agreement. Some of the derived pole figures are shown in Fig. 2. (As an example of the utility of the ODF, we were able to estimate the 511 pole figure from the ODF, even though no data were obtained directly for this reflection.)

Experiment report *(continued)*:

We consider that our initial experiments have been quite successful. In 1989 we checked the texture of a single laminate of the Armadillo and extended our measurements to 123-superconductors, but these data have not been analyzed yet. An important intermediate goal is the systemization of the data analysis, and our future plans include the study of anisotropic actinide materials. As compared to textures determined on the Single Crystal Diffractometer (SCD), our method suffers from relatively poor real-space resolution but has better q-space resolution

Fig. 1 Diffraction Patterns (Aluminum)

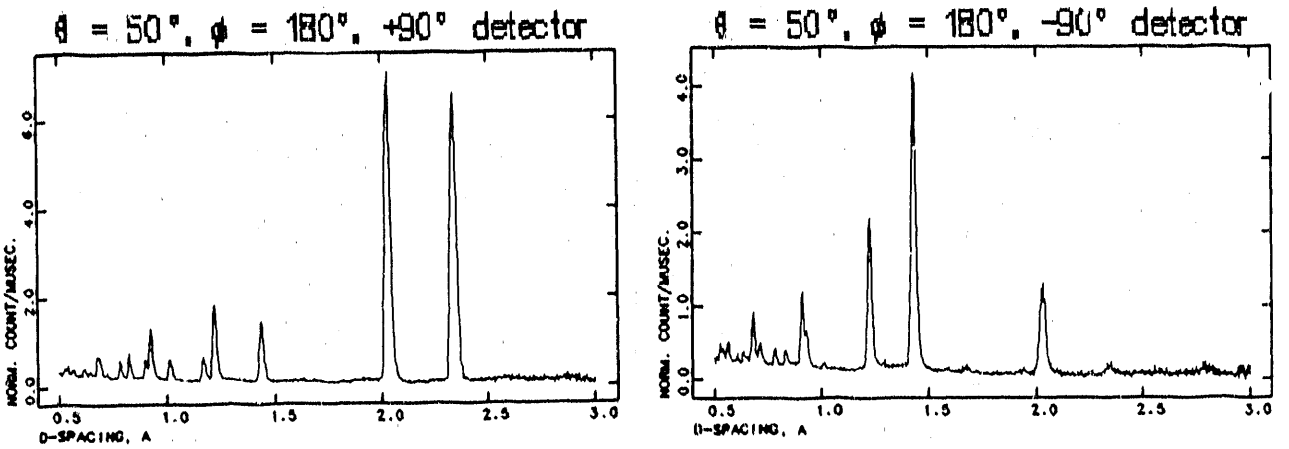

Fig. 2 Derived Pole Figures

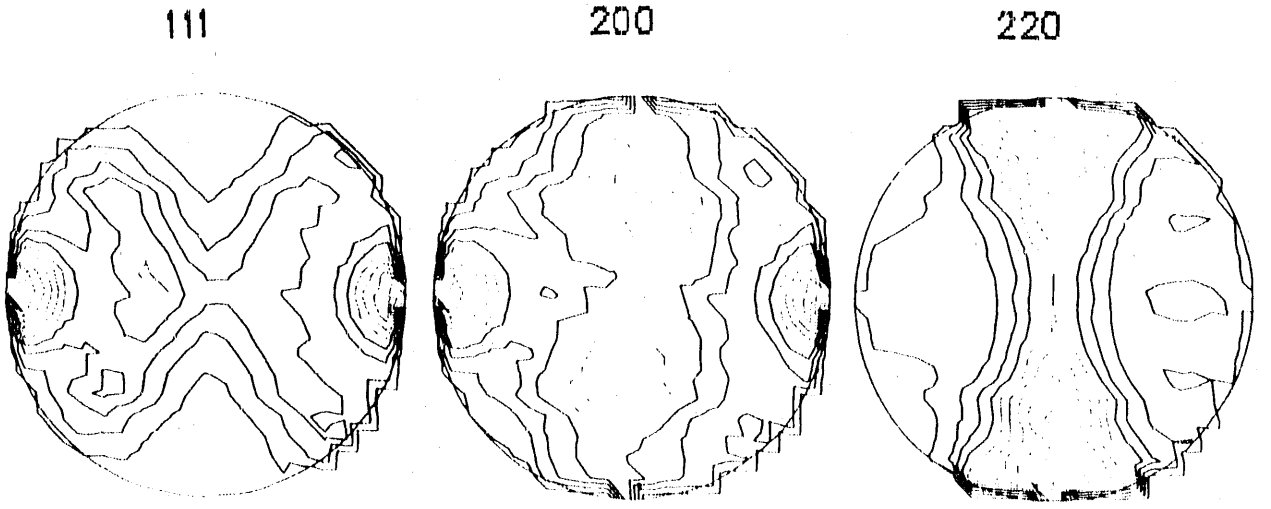

Instrument used: *(please type)*	Local contact:	Proposal number: *(for LANSCE use only)*
HIPD	R. B. Von Dreele	D-33.0

Title:

Structural and Magnetic Studies of some Uranium Ternaries

Report received: *(for LANSCE use only)*

Authors and affiliations:

R. A. Robinson, LANSCE, LANL
G. H. Kwei, CLS Division, LANL
A. C. Lawson, MST Division, LANL
R. B. Von Dreele, LANSCE, LANL
K. H. J. Buschow, Philips Research Labs., Eindhoven

Experiment report:

A few years ago, a systematic study of the magnetic properties of a number of ternary uranium compounds was made by Palstra et al.[1]. Many of these compounds showed evidence of gaps in their band structures and a few were thought to antiferromagnetic. One of us [2] had already studied UNiSn on a reactor powder diffractometer at NBS and this summer, we studied some of the other antiferromagnets on HIPD at LANSCE. The most dramatic results, which are described in a separate report, were on the hexagonal compound UPdSn.

In addition, we studied the two compounds UNiAl and UNiGa, which were reported to form in the Fe_2P structure, and appeared to be antiferromagnetic below 21K and 38K respectively, on the basis of susceptibility measurements[1]. We made measurements at 10K and above the Néel temperature in each case. While the high temperature data fit well to the Fe_2P structure, we observed no extra intensity at low temperature and conclude that any ordered moment is below the sensitivity of our measurement.

Furthermore, we studied a sample with the stoichiometry UAgSb, which was thought to crystallise in the conventional $C1_b$ or MgAgAs structure, with a lattice parameter of 6.196Å and an antiferromagnetic ordering temperature of about 210K [3]. This is the same structure as many Mn-based Heusler alloys as well as UNiSn [2] and lattice parameters of just over 6Å are typical for this structure. We made measurements at 10K and 250K and portions of the pattern taken in one of the 40° banks are shown in the Figure. A number of extra lines are seen in the low-temperature data. These reflections are indicative of Type I antiferromagnetic order[4] on the FCC sublattice (occupied by Uranium atoms). The absence of a 100 reflection at ~6.2Å indicates that the moment is parallel to the [100] axis, just as in UNiSn [2]. However, there are a number of impurity lines in the pattern, which can be idexed to a simple FCC structure, with a lattice parameter of 4.082Å. These are presumably due to the element silver. Furthermore, the intensities of the other phase could not be made to agree with any ordering or occupation scheme in the MgAgAs structure. However, they did

Experiment report *(continued)*:

agree with USb, which has the rock-salt structure (and is FCC, just like the MgAgAs structure) with a lattice parameter of 6.2Å. Finally, the magnetic structure of USb was determined many years ago[5,6,7]. It is indeed Type I antiferromagnetic, with a moment of between 2.16μ_B and 2.78μ_B along the [100] direction and an ordering temperature of around 215K. Our data are in complete agreement with these results. We therefore conclude that our sample was a two-phase mixture of USb and Ag.

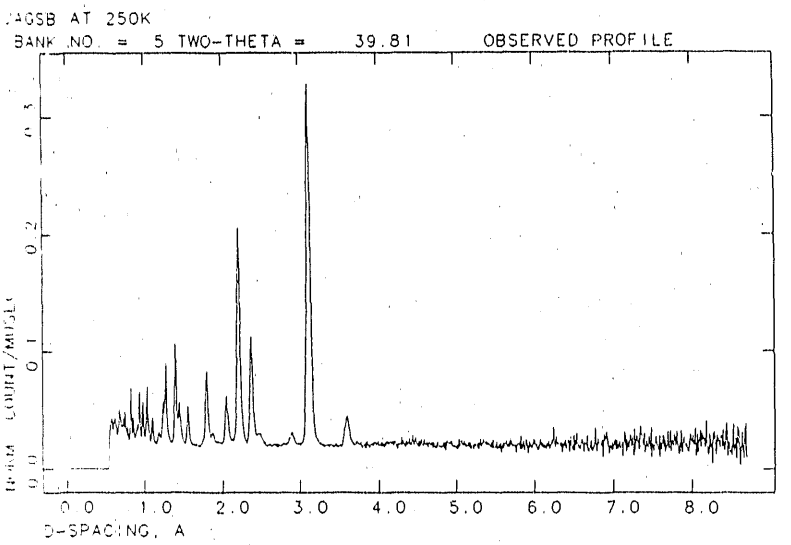

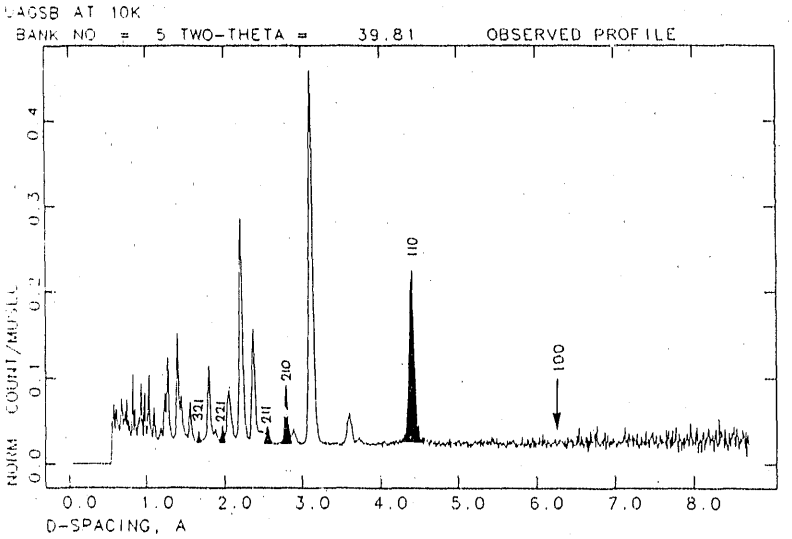

References:

[1] T. T. M. Palstra, G. J. Niewenhuys, R. F. M. Vlastuin, J. van den Berg, J. A. Mydosh and K. H. J. Buschow, J. Magn. Magn. Mater. 67, 331 (1987).

[2] M. Yethiraj, R. A. Robinson, J. J. Rhyne, J. A. Gotaas and K. H. J. Buschow, J. Magn. Magn. Mater. 79, 355 (1989).

[3] K. H. J. Buschow, unpublished data

[4] J. S. Smart, "Effective Field Theories of Magnetism", Saunders, Philadelphia, 1966, p.76.

[5] J. Leciejewicz, A. Murasik and R. Troć, Phys. Stat. Solidi 30, 157 (1968).

[6] M. Kuznietz, G. H. Lander and F. P. Campos, J. Phys. Chem. Solids 30, 1642 (1968).

[7] C. E. Olsen and W. C. Koehler, J. Appl. Phys. 40, 1135 (1969).

Instrument used: *(please type)*	Local contact:	Proposal number: *(for LANSCE use only)*
High Intensity Powder Diffractometer	Angus Lawson	205.0

Title:	Report received: *(for LANSCE use only)*
Neutron Diffraction of $LaNi_{4.7}Al_{0.3}$ Containing Helium-3	

Authors and affiliations:

W. C. Mosley and R. T. Walters
Westinghouse Savannah River Company
Post Office Box 616
Aiken, SC 29802

Experiment report:

Neutron diffraction experiments on three samples of $LaNi_{4.7}Al_{0.3}$, one containing helium-3 from exposure to tritium for twenty one months, were recently performed on the High Intensity Powder Diffractometer (HIPD) at the Los Alamos Neutron Scattering Center (LANSCE). The purpose of this work was to determine how the helium-3 atoms are present in the $LaNi_{4.7}Al_{0.3}$ structure by comparing neutron diffraction data for the tritium-exposed sample with those for unexposed samples. This information will assist in understanding how the ingrowth of helium-3 from tritium decay influences the behavior of lanthanum-nickel-aluminum intermetallic alloys that will be used for tritium processing in the Replacement Tritium Facility presently being constructed at the Savannah River Site.

Although the quality of the HIPD data for the tritium-exposed sample was greatly decreased by the vanadium secondary containment required because of an unacceptably high level of contamination detected on the aluminum sample holder, evaluation revealed that the relative intensities of the neutron diffraction peaks for the primary phase were like those for the unexposed samples. This observation indicates that the helium-3 atoms are not incorporated into the crystal structure of the primary phase. This interpretation is consistent with earlier results of x-ray diffractometry and desorption plateau pressure measurements that showed the sample of $LaNi_{4.7}Al_{0.3}$ exposed to tritium for twenty one months to be in the "recovered" state rather than the "expanded" state. Helium-3 produced by radioactive decay of tritium is believed to occupy sites at or near the triton sites in the crystalline lattice of the primary phase causing lattice expansion and decreases in the desorption plateau pressure. (Increased aluminum in $LaNi_{5-x}Al_x$ causes similar effects.) However, the sample exposed to tritium for twenty one months had been cycled many times and heated to high temperatures to remove the tritium. These treatments caused the crystalline lattice to recover to its original size and the desorption plateau pressures to recover to near their original values.

Experiment report: *(continued)*

The recent experiments at LANSCE showed that neutron diffractometry of lanthanum-nickel-aluminum intermetallic alloys containing helium-3 is feasible. Similar experiments should be performed on tritium-exposed alloys in the "expanded" state. Samples of alloys in the "expanded" state will be available within a few months from a tritium exposure program being conducted at the Savannah River Site. For future experiments, use of a thermal expansion seal on the aluminum sample holder may allow better decontamination and eliminate the need for secondary containment in vanadium.

References:

Instrument used: *(please type)*	Local contact:	Proposal number: *(for LANSCE use only)*
HIPD	R. von Dreele	212.0

Title:

Structures of the Three Phases of PaD_x

Report received: *(for LANSCE use only)*

Authors and affiliations:

J. W. Ward, B. Cort, A. C. Lawson, R. B. von Dreele, Los Alamos National Laboratory

J. C. Spirlet, European Institute for Transuranium Elements

Experiment report:

Protactinium forms three distinct hydride phases. Two of these are isomorphous to structures also found in the uranium hydride system; these are the α-UH_3 structure in which the uranium atoms occupy a bcc lattice and the β-UH_3 structure in which the uranium atoms occupy an A15 lattice. The third allotrope of PaH_x forms as a C15 cubic Laves phase, a unique structure in binary hydrides. The location of the hydrogen atoms is not known with certainty for any of the protactinium hydrides but are assumed by analogy to the better-known UH_3 system.

Both the A15 and C15 structures are characteristic of transition metal intermetallic compounds. Their appearance in the actinide hydrides is most surprising, as a metal playing a dual role without an apparent valence difference is unknown elsewhere. The effect is clearly due to the appearance of broadband, bonding 5f electrons. It is therefore of great interest to know the structures of these compounds.

Due to delays involved with shipping the protactinium sample from England, we were able to utilize only two of our allotted six days of neutron beam time and to therefore perform only a preliminary investigation of C15 PaD_x. The small protactinium sample did not deuteride completely, and the resulting phase composition indicated by the neutron diffraction data is 83% deuteride and 17% metal. The data refine reasonably well using the C15 crystal structure, but the crystal structure and composition are not consistent with the phase diagram. Because of the small sample size and the sample composition, the data are not of high enough quality to determine either the composition of the deuteride or the positions of the deuterium atoms with any degree of confidence.

We conclude that the vanadium sample holder for this small sample must be redesigned to reduce the background contribution to the diffraction data. We must also repeat the deuteriding cycle multiple times in order to produce a 100% deuteride sample for future experiments.

Experiment report: *(continued)*

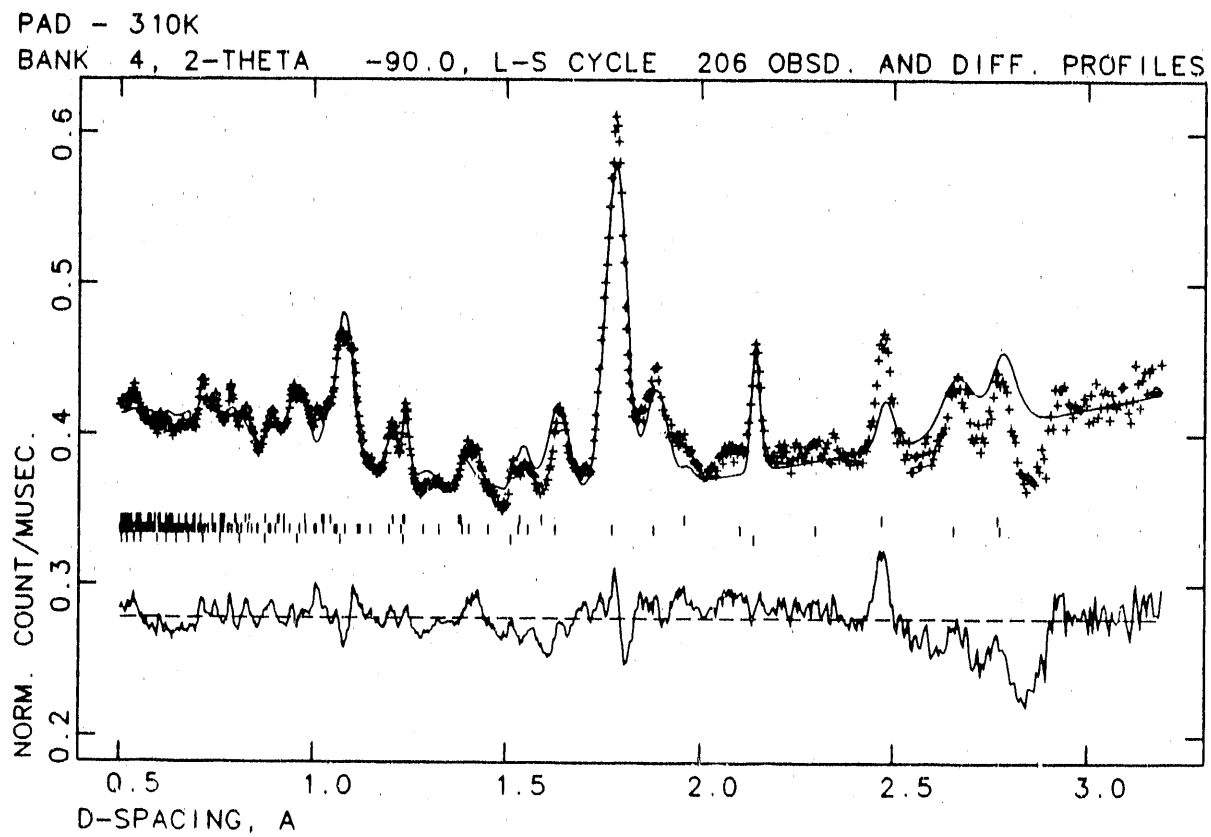

Figure 1. Neutron diffraction pattern for the C15 phase of PaD_x. The reflection markers for the three phases present are identified as follows: top - Pa metal, middle - C15 PaD_x, and bottom - vanadium from the encapsualtion. The negative peak near 2.8 Å is due to aluminum from a window in the beam that is not accounted for by the analysis code.

References:

Instrument used: *(please type)*	Local contact:	Proposal number: *(for LANSCE use only)*
HIPD	Dr R.B. Von Dreele	237.0

Title:

Particle size determination from extinction measurements in neutron diffraction patterns of α–alumina.

Report received: *(for LANSCE use only)* 2/23/90

Authors and affiliations:

W.Kalceff, T.M. Sabine
Department of Physics, University of Technology, Sydney,
P.O. Box 123, Broadway, N.S.W. 2007, Australia.

R.B. Von Dreele
LANSCE.

Experiment report:

A total of nine experimental runs were carried out at 305K on eight samples of α–alumina (kindly provided by J. Cline of NIST), with particle sizes of 2.59μm, 10.10μm, 14.55μm, 23.23μm, 38.04μm, 47.62μm, 61.18μm and 167μm. All the experiments were conducted in the final week of the run cycle, at a time when production problems were causing considerably reduced and fluctuating neutron beam intensities. The mean number of T_0s per run was $\simeq$ 109,000, a somewhat low (but adequate) value for the determination of statistically significant integrated intensities in the weaker reflections.

The integrated intensities for the strongest high–d lines were determined and the degree of extinction for each (hkl) was calculated by "normalizing" each data set to allow for differing sample sizes and irradiation times.

The observed extinction sizes were much smaller than predicted on the basis of the stated particle sizes (Kalceff et al 1989, 1990), suggesting that the mosaic block sizes are significantly smaller than the grains of the samples. Moreover, the apparent anisotropy in the extinction effects may imply the presence of screw dislocations directed along the hexagonal c–axis, as the strongest extinction effects were in the (00l) reflections and almost negligible in the (hk0) planes, even for the largest grain samples. When a full analysis of the data has been completed (including the x–ray results and high resolution transmission electron microscopy observations of the defect structure of the samples awaited from NIST), the extinction model may have to be modified to include anisotropy.

The results of the analysis will be presented at IUCr XV at Bordeaux in July; it is expected that a publication in Acta Cryst will ensue.

Experiment report *(continued)*:

A further experiment has been proposed by Von Dreele, Kalceff and Sabine (for the 1990 run cycle) to study the extinction effect in CaF_2 (fluorite), a material free of core defects and easily produced in a wide range of particle sizes.

Sabine (1990) has developed a theory for the simultaneous correction of diffraction data for the effects of extinction and absorption. It is believed that the present treatment of these effects, particularly as applied to x–ray data (where it is more evident by virtue of the scattering process), needs to be modified. This is particularly important in cases, as with GSAS, where simultaneous refinements of neutron and x–ray data are undertaken. The present neutron TOF alumina data, together with the expected x–ray data from NIST, will provide an ideal test case for the applicability of the new theory.

References:

1. Kalceff, W., Sabine, T.M. and Von Dreele, R.B., LANSCE User Group Science Seminar, Nov. 16–17, 1989, Los Alamos National Laboratory, ***Extinction in Alumina Powders.***
2. Kalceff, W., Sabine, T.M. and Von Dreele, R.B., Aust. Institute of Physics Condensed Matter Physics Meeting, Feb. 7–9, 1990, ***Extinction in α–alumina neutron TOF diffraction.***
3. Sabine, T.M. (1990) ***The flow of radiation in a real crystal,*** to appear in Vol. C, International Tables for Crystallography.

Instrument used: *(please type)*	Local contact:	Proposal number: *(for LANSCE use only)*
HIPD and NPD	Dr R.B. Von Dreele Dr J.A. Goldstone	238.0

Title:	Report received: *(for LANSCE use only)*
Neutron diffraction studies of SYNROC at temperatures ranging from 300K to 1500K.	2/23/90

Authors and affiliations:

W.Kalceff, T.M. Sabine
Department of Physics, University of Technology, Sydney,
P.O. Box 123, Broadway, N.S.W. 2007, Australia.

L. Vance
Australian Nuclear Science and Technology Organisation,
Private Mail Bag 1, Menai, N.S.W. 2234, Australia.

Experiment report:

Ten SYNROC samples were fabricated using the alkoxide route and Purex waste (simulating US commercial reactor waste) in preparation for these measurements. Waste loadings ranged from 0% (SYNROC–B) to 30% (SYNROC–C), at increments of 5%; three samples with loadings of 20%, 25% and 30% were also made using a neutralised precursor–waste mixture.

The research proposal submitted for the LANSCE work envisaged a set of runs at different temperatures to determine the stability of the major phases with temperature. Unfortunately there was insufficient time available on the instruments to complete the full set of measurements, and the HIPD furnace was not functioning. All samples were run on HIPD at 305K, and the 0% one was also done using NPD at 10K; the total beam time used was $\simeq$ 7 days, excluding time lost with aborted runs due to intermittent problems with the detector electronics.

Analysis of the data is at a stage where the lattice parameter variation of two of the major phases (hollandite and perovskite) has been determined, showing a Vegard's law–type increase in cell volume with waste loading, but the third major phase, zirconolite, is proving much more difficult to interpret. Recent work at ANSTO has shown that at a temperature below 1200° C zirconolite forms with a monoclinic variant of the fluorite structure; above this temperature, a zirkelite modification forms, with a pseudo–trigonal symmetry. We are seeking the mechanism active in the two cases; it is hoped that this will allow the form stabilized in SYNROC to be deduced.

Electron microscopy work is also in train at ANSTO to identify the remaining impurity phase(s) present in the SYNROC samples.

Experiment report *(continued)*:

Once the above questions have been resolved, it should be possible to refine the diffraction data to identify the sites into which the various waste atoms are deposited. It is planned to confirm these results by deliberately doping a new set of samples with varying compositions of waste atoms and performing neutron diffraction studies similar to the present ones on them.

The determination of temperature factors for the constituent phases in the samples cannot be done until all gross features of the diffraction data have been explained. The 10K and 305K data from NPD will be used to attempt a temperature parameter refinement on all phases present; high resolution x–ray diffraction data already collected at UTS and ANSTO will be used in a joint GSAS refinement with the neutron data.

Whether the data collected at LANSCE and ANSTO/UTS is adequately statistically significant to support the above analyses remains to be seen.

References:

1. Kalceff, W., October 1989, LANSCE Physics Colloquium, *SYNROC studies at LANSCE.*

2. Kalceff, W., Argyriou, J., Sabine, T.M., Aust. Institute of Physics Condensed Matter Physics Meeting, Feb. 7–9, 1990, *Crystalline distortions of SYNROC due to simulated–waste loading.*

Instrument used: *(please type)*	Local contact:	Proposal number: *(for LANSCE use only)*
HIPD	A.C. Lawson, MST-5	243.0

Title:	Report received: *(for LANSCE use only)*
OMEGA PHASE FORMATION IN SHOCK-LOADED TITANIUM ALLOYS	

Authors and affiliations:

G.T. Gray III Los Alamos National Laboratory, MST-5

A.C. Lawson Los Alamos National Laboratory, MST-5

Experiment report:

Although the response of titanium alloys to dynamic loading is beginning to be understood, little experimental data exists concerning the structure/property relationships of titanium alloys subjected to shock loading. These studies are complicated by the fact that pure α titanium undergoes a polymorphic phase transition from hexagonal to a more open hexagonal omega (ω) phase at high pressure. The ω-phase transformation in α-Ti under shock or hydrostatic soaking conditions exhibits a large hysteresis that is responsible for retention of the high-pressure ω phase to atmospheric pressure[1,2]. The ω-phase induced in pure Ti is observed to be morphologically similar to ω phase formed in as-quenched β-phase alloys based on Zr, Ti, and Hf [3]. Crystallographically the phase transformation is believed to be a diffusionless displacive transition[2,3]. The influence of alloying α titanium on the details of the substructure evolution and occurrence of the ω-phase transition has not defined a consistent pattern.

To investigate the influence of alloy chemistry, in particular interstitial oxygen content, on ω-phase formation, neutron diffraction experiments were conducted on 99.99 wt.% titanium shock-loaded at 11 and 23 GPa and A-70 Ti (3600 ppm oxygen wt.%) shocked at 11 GPa and "soft" recovered. The neutron experiments were conducted with the beam axis parallel to the prior shock direction of the samples, i.e. through-thickness; one sample was additionally studied with the neutron beam in the sample plane to investigate the effect of texture on the lattice parameter data. Neutron diffraction data were obtained at HIPD at LANSCE and the data refined using GSAS.

Metastable ω-phase titanium was found to be retained in the high-purity titanium following both shock pressures [11 GPa - RUN # 734 & 738(in-plane)] and [23 GPa - RUN # 737] but not in the high-oxygen-content A-70 alloy-RUN # 735. Diffraction data for the 11 GPa high-purity Ti showing ω-phase (Figure 1) and the absence of ω-phase in the shock-loaded A-70 Ti (Figure 2) are shown. The lattice constants for the α and ω-phases measured are listed in Table I. We attempted to determine whether our ω-phase is "rumpled" (i.e., whether the true space group is P(-3)m1 instead of P6/mm), but the refinements were inconclusive, probably because of preferred orientation effects in our highly textured samples. The refined preferred orientation parameters are not considered significant in view of the simplicity of the texture model currently in GSAS. We unsuccessfully attempted to determine the particle size for the ω-phase; either the particle size is too large (> ~ 1000 angstroms) or there is too much broadening from the large strains in both phases. These strains are caused by the epitaxial mismatch between the α and ω-phases; the "a" of the α-phase tries to match "c" of the ω-phase, and visa versa. The measured lattice constants and strains shown in Table I illustrate how the strain results

Experiment report: *(continued)*

from the slight mismatch of the lattice constants. While the exact mechanism by which interstitial oxygen suppresses ω-phase formation in Ti is still under study, tthe current lattice parameter data supports the idea that any alloying addition which increases the lattice mismatch such as oxygen, given the fixed "a" / "c" orientation relationship between the two phases, will probably reduce the tendency for phase formation or significantly increase the phase treansformation start pressure.

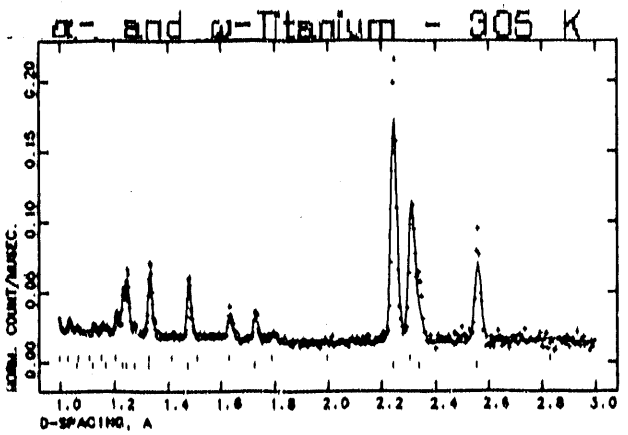

Figure 1: Shock-loaded High-Purity Ti

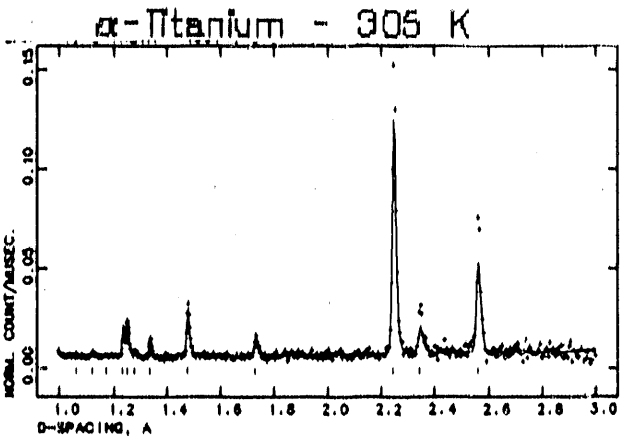

Figure 2: Shock-loaded A-70 Ti

Table 1. Strains and Lattice Constants for α- and ω-Titanium

Run #	734	735	737	738
volume fraction ω (%)	28	0	18	29
lattice constants (Å):				
a(α)	2.9506(2)	2.9520(1)	2.9516(2)	2.9493(2)
c(α)	4.6795(4)	4.6884(4)	4.679 (1)	4.6712(5)
a(ω)	4.614(1)	-	4.614(1)	4.611(1)
c(ω)	2.832(1)	-	2.831(1)	2.826(1)
strain from σ_1^2 (%):				
strain(α)	0.68	0.52	0.79	0.74
strain(ω)	0.74	-	0.91	0.93
strain from lattice constants (%):				
$(a(\alpha)-a_0)/a(\alpha)$	0.05	-	0.01	0.09
$(c(\alpha)-c_0)/c(\alpha)$	0.19	-	0.20	0.37
$(a(\alpha)-c(\omega))/a(\alpha)$	-4.02	-	-4.04	-4.18
$(c(\alpha)-a(\omega))/c(\alpha)$	-1.40	-	-1.39	-1.29

References:

1. Sikka, S.K., Vohra, Y.K. and Chidambaram, R., Progress Matls. Sci. 27 (1982) 245.
2. Kutsar, A.R. and German, V.N., in Titanium and Titanium Alloys, eds. J.C. Williams and A.F. Belov (New York, Plenum Press) (1982) 1633.
3. Rabinkin, A., Taliankar, M., and Botstein, O., Acta Metall. 29 (1981) 691.

Instrument used: *(please type)*	**Local contact:**	**Proposal number:** *(for LANSCE use only)*
HIPD	Robert Von Dreele	D-17.0
Title: Structure of the Solid Phases of Chloro-Iodomethane, $CD_2C\ell I$		**Report received:** *(for LANSCE use only)*

Authors and affiliations:

Bruce Torrie, Department of Physics, University of Waterloo, Waterloo, Ontario, Canada N2L 3G1

Robert Von Dreele and Allen C. Larson, LANSCE, Los Alamos National Laboratory

Experiment report:

This structure determination is a continuation of studies of the halogen derivatives of methane. Previous efforts were described in a review article [1] and in a series of articles of which the most recent deals with methylene bromide and methylene iodide [2]. Raman and infrared spectra of a variety of samples have been obtained and the structures of a subgroup of these have been determined using neutron powder profile techniques.

Spectroscopic results indicate that $CD_2C\ell I$ freezes at 245 K into a plastic phase and at 195 K a transformation to other phases takes place. Two ordered phases and a disordered phase have been produced by varying the cooling rate.

In the current experiment two phases were observed at 13 K. One of these is an ordered phase which can be indexed to give the selection rules for the space group Pnma. The other phase produced only a small number of Bragg peaks and is clearly disordered.

Experiment report: *(continued)*

References:

1. A. Anderson, B. Andrews and B.H. Torrie, J. de Chim. Phys. 82, 99 (1985).
2. D.A. Prystupa, B.H. Torrie, B.M. Powell and P.N. Gerlach, Molec. Phys. (to be published).

Instrument used: *(please type)*	Local contact:	Proposal number: *(for LANSCE use only)*
H I P D	Robert B. VonDreele	253.0

Title:

Structure and Dynamics of Related Silica Compounds

Report received: *(for LANSCE use only)* 2/2/90

Authors and affiliations:

B. J. Olivier and D. W. Schaefer
Department 1810
Sandia National Laboratories
P. O. Box 5800
Albuquerque, NM 87185

D. Richter, B. Farago and B. Frick
Institut Laue-Langevin
38042 Grenoble, France

Experiment report: Vitreous silica compounds are attractive since they can be prepared in different structural forms. Those of current interest include ; 1) *Fused quartz* , a simple glass. 2) Cab-*O-Sils* , low density colloidal aggregates created during flame hydrolysis. 3) *Aerogels* , extremely low density porous glasses commonly produced upon the hypercritical drying of silica gels.

Vibrational excitations in glasses have been extensively studied over the past few decades yet , the origin of the low energy vibrational spectra inherent in the tenuous solids mentioned above remains a central unsolved problem in solid state physics [1]. For example , it is well known that for vibrational frequencies below ~ 3 THz that the experimentally observed density of states in fused quartz is significantly greater then when calculated using Debye's theory.Buchenau et. al. [2] attribute the enhancement to the relative rotations of SiO_4 tetrahedra in conjunction with sound waves below 1 THz. The applicability of this model to the low energy modes of the less dense Cab-O-Sil and aerogel phases of silica is currently unknown . By studying the elastic and inelastic scattering spectra from silica related compounds we hope to understand the static and dynamic patterns in aerogels.

We have used the HIPD to obtain the integrated neutron scattered flux spetra from quartz and sundry aerogels as a function of the momentum transfer , $Q=4\pi\sin(\theta/2)/\lambda$. Figure 1 illustrates preliminary results showing the quartz static structure factor , S(Q) , as a function of Q .This , although a well known elastic scattering spectrum , is unique in its expansive range of Q . The importance of large Q will be discussed below.

Experiment report *(continued)*:

Figure 1. S(Q) vs. Q for Quartz

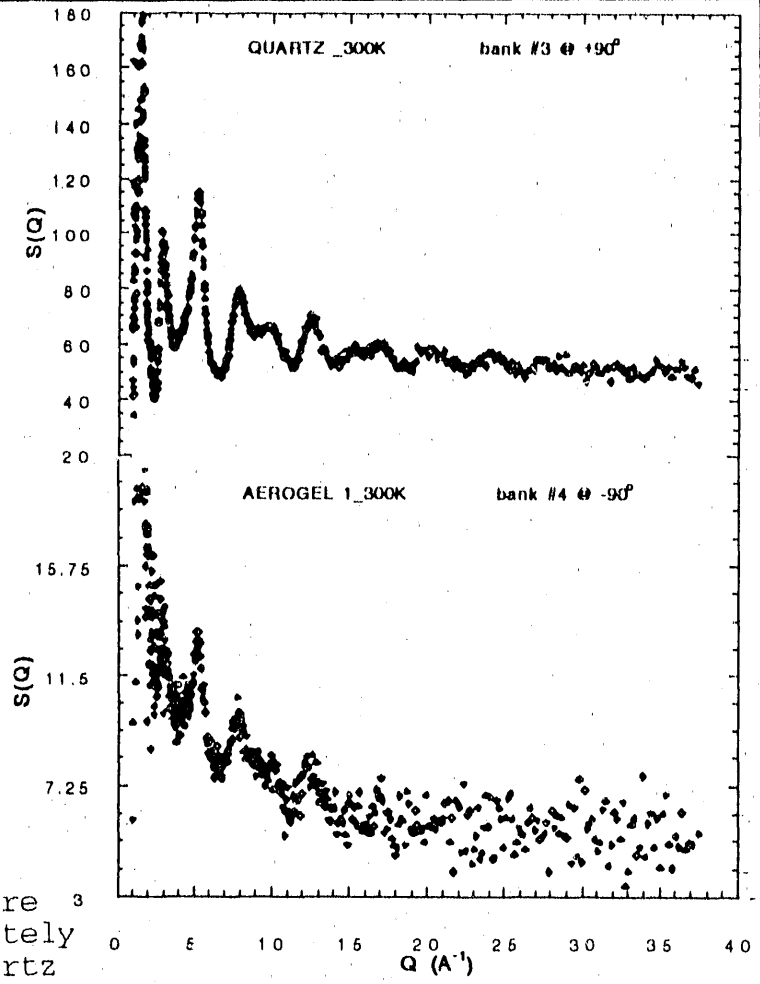

Figure 2. S(q) vs. Q for Polymeric Aerogel

Figure 2 is the intensity spectrum from a polymeric aerogel obtained at 300°K. The positions of the structure peaks of aerogel_1 approximately correspond to those from quartz although the strength hence resolution of the aerogel peaks are significantly diminished. This is not surprising since the number of scatterers present in the quartz far exceeds those in the aerogel sample. We acknowledge the decreasing trend in S(Q) in Fig. 2 and attribute this to extraneous counts at short time of flights.

In order for us to make any quantitative comparisons between these and other aerogel spectra taken at other neutron facilities [3] the intensities must be normalized. A proper normalization is with respect to the number of atoms , N present in the neutron beam. Since $S(Q\to\infty) \propto N$, the extensive Q range of our data should allow for normalization and quantification of our amorphous silica spectra.

References:

1. Amorphous Solids-Low Temperature Properties, ed. by W. A. Phillips (Springer-Verlag, Berlin, 1981).

2. U. Buchenau, M. Prager, N. Nucker, A. J. Dianoux, N. Ahmad and W. A. Phillips, Phys. Rev. B, **34**, 5665 (1986).

3. D. W. Schaefer, C. J. Brinker, D. Richter, B. Farago and B. Frick, Phys. Rev. Lett. ,submitted.P

Instrument used: *(please type)*	**Local contact:**	**Proposal number:** *(for LANSCE use only)*
HIPD	Robert Von Dreele	267.0
Title: Structure of Cyanamide, D_2NCN		**Report received:** *(for LANSCE use only)*

Authors and affiliations:

Bruce Torrie, Department of Physics, University of Waterloo
Waterloo, Ontario, Canada N2L 3G1

Robert Von Dreele and Allen C. Larson, LANSCE,
Los Alamos National Laboratory

Experiment report:

This structure determination is part of a continuing program at the University of Waterloo to study the structures and vibrations of molecular crystals by neutron powder profile techniques, X-ray diffraction and Raman and infrared spectroscopy. Calculations have been undertaken to match the experimental results to quantites derived using atom-atom potentials.

The purpose of the experiment was to determine the structure and to see how this evolves with temperature. Powder profiles were recorded at 13, 90, 210 and 305 K. (The melting point is 317 K.) Our recent Raman and infrared work indicated that there is only one phase between room temperature and 20 K and this was confirmed by the neutron results. The lattice parameters and space group, P_{bca}, were known from an X-ray study at room temperature [1] and these were used as a starting point for our structure determination.

Analysis of the data was performed using GSAS [2]. The dimensions of the molecule were known for the gas phase [3] and these were used in the rigid body routine of GSAS. An attempt was made to employ Patterson functions to find the orientations of the molecules but, in the end, approximate orientations were found using geometrical arguments and these orientations were refined by the least-squares routine. Finally the rigid body constraint was dropped and a full analysis of the 13 and 305 K data was carried out using atomic coordinates and isotropic temperature factors.

Experiment report: *(continued)*

References:

1. C.L. Christ, Acta Crystallogr. 4, 77 (1951).
2. A.C. Larson and R.B. Von Dreele, LAUR 86-748.
3. A. Attanasio, A. Bauder and Hs. H. Gunthard, Chem. Phys. 6, 373 (1974).

Instrument used: *(please type)*	**Local contact:**	**Proposal number:** *(for LANSCE use only)*
HIPD	Dr. Robert Von Dreele	272.0

Title:
Cation Distributions and Anharmonicity in High Temperature Cu_2S-Ag_2S Solid Solutions

Report received: *(for LANSCE use only)*
5-5-90

Authors and affiliations:
Bernhardt J. Wuensch and Catherine M. Heremans
Department of Materials Science and Engineering
Massachusetts Institute of Technology
Cambridge, Massachusetts 02139

Experiment report:

INTRODUCTION AND PREVIOUS WORK

The halides and chalcogenides of silver and copper represent the prototype cation-disordered fast-ion conductors--phases in which the cations are delocalized and extraordinarily mobile. The ionic electrical conductivity of such materials is some six to eight orders of magnitude larger than normal ionic solids, approaching values as large as 6 to 8 reciprocal ohm-cm for β-Ag_2S. Such conductivities are comparable to those of strong liquid electrolytes. The materials thus find application in electrochemically-based devices such as batteries, fuel cells and sensors. The phases in the Cu_2S-Ag_2S system are of basic interest as model materials toward understanding of the transport mechanism and diffusion path responsible for this behavior as the mobile cations constitute the dominant fraction of the scattering density. Calculated structure factors are thus extremely sensitive to the model constructed for the distribution and thermal vibration of the cations. Moreover, the present system is of great interest in ore mineralogy and geochemistry as many ore deposits descended from these high-temperature solid solutions.

The Ag and Cu halides and chalcogenides are based upon very simple anion packings. In previous work we have used single-crystal neutron techniques to establish the cation distribution and anharmonicity in bcc anion arrays [α-AgI (1), β-Ag_2S (2), β-Ag_2Se (3) and α- and β-Ag_3SI (4)], hcp arrays [β-Cu_2S (5)] and fcc arrays [α-Cu_2S (3) and α-Cu_2Se (3)]. These studies have been highly successful in providing insight into the origin of the cation mobility as a result of several factors: (a) use of neutron scattering provides a direct measure of the probability density function (pdf) of the cation nucleus, free of charge deformation effects, rather than a convolution of the pdf with the distribution of electrons on the atom as with x-rays; this has permitted distinction of anharmonicity from disorder over closely-spaced sites; (b) use of neutrons increases the number and accuracy of the recorded intensities (no decrease of scattering power with $\sin\theta/\lambda$, negligible absorption); (c) use of a recently-developed formalism which describes scattering from anharmonically-vibrating atoms; and (d) analysis of all structures as a function of temperature to distinguish position-averaged static disorder ("split atoms") from dynamic, time-averaged vibrational disorder

(anharmonicity).

The present study is an extension of such analyses to additional phases with fcc anion arrays. The objective is to analyze, as a function of temperature and composition, the structures of the solid solutions which extend across the Cu_2S-Ag_2S system at elevated temperatures ($T > 420°C$ for Cu_2S, 120°C for CuAgS, and 593°C for Ag_2S). The series is of especial interest as it constitutes the only system of which we are aware in which two cation species, with different bonding characteristics and site preferences (as reflected in their respective low-temperature structures), are simultaneously mobile. We examine only intermediate solid solutions. The structure of $Cu_{2-x}S$, for which nonstoichiometry greatly reduces the transition temperature, has been successfully studied with single-crystal methods (3). The high transition temperature of 593°C for Ag_2S approaches the limit of most of the heating devices which are available for diffraction measurements. Moreover, the higher temperatures of the stability range of this compound will greatly increase thermal vibration amplitudes. It is unlikely, therefore, that a number of detectable intensities sufficient to complete an analysis would be available. Indeed, the principal experimental challenge in the present work with any of these phases is the detection of a significant number of diffraction peaks, the intensity of which--even in neutron scattering--is greatly diminished by cation delocalization and unusually large thermal vibration amplitudes. Such is the inherent nature of these materials and the reason that their structures remain undetermined. The High Intensity Powder Diffractometer available at LANSCE thus constituted the most promising instrument available for conducting the present measurements.

EXPERIMENTAL REPORT

The fcc phases in the Cu_2S-Ag_2S cannot be quenched. Neither can single crystals be produced upon heating the low temperature phases (hcp anion packing for Cu_2S and bcc for Ag_2S) because of sluggish anion rearrangement and the disruptive nature of the phase transformation. Attempts to grow single crystals directly within the stability range of the fcc phases were unsuccessful due to immediate oxidation upon exposure to the atmosphere during attempts to transfer them to a diffractometer without cooling.

Rietveld analysis of powder diffraction profiles has accordingly been undertaken in the present work. It was desirable to synthesize the phases in situ in the temperature range of their stability in order to avoid possible degradation of the quality of the crystallites as a result of cycling through phase transformations. Fine powders of the elements in appropriate proportions were thus encapsulated in evacuated silica tubes and placed directly in the vacuum chamber of a furnace which had been newly-constructed for use on the HIPD. (The present experiments represented the initial trial of the furnace and it performed superbly!) The silica tubes served the dual purpose of maintaining the stoichiometry of the specimens which tend to lose sulfur at elevated temperature, as well as protecting the vacuum chamber and vanadium windows from possible attack by sulfur vapor. As elemental sulfur produces a very high vapor pressure at elevated temperature, the temperature of the capsules was slowly increased at first to initiate the reaction (which proceeds rapidly at all temperatures due to the mobility of the cations) and then increased to a temperature just above the phase transformation to complete formation of the fcc phase.

Table I. Compositions and Temperatures for HIPD Data Sets Successfully Recorded for Cu_2S-Ag_2S Solid Solutions

Composition		
$(Cu_{0.7}Ag_{0.3})_2S$	$(Cu_{0.5}Ag_{0.5})_2S$	$(Cu_{0.25}Ag_{0.75})_2S$
330°C	337°C	336°C
408°	430°	405°
492°	530°	500°
568°	630°	600°

The progress of the reaction was monitored by recording powder patterns during heating. when the diffraction pattern indicated the presence of no phase other than the desired fcc structure, the temperature was increased to the highest of the four at which data were to be recorded to insure complete reaction and homogeneity. Subsequent data sets were collected at lower temperatures at intervals uniformly spaced between limits imposed by the transformation temperature and an upper temperature dictated by prudent operation of the furnace. The compositions and temperatures at which powder profiles were successfully recorded are summarized in Table I. The temperatures cited are precise to ±2°C and represent averages of readings provided by two thermocouples attached to the top and bottom of the specimen, respectively, and which were connected to the temperature regulator of the furnace.

The experiments were highly successful in that the silica capsules remained intact, and in that the desired fcc phases were successfully synthesized in situ. The supposed fcc nature of the structures has been conclusively established and, at very least, lattice parameters and thermal expansion coefficients will be established as a function of composition and temperature with more precision and over a wider range of temperature. The LANSCE program system for structure analysis, GSAS, has been installed in our computation system and Rietveld analysis of the profiles is in progress. A complete and unambiguous determination of the cation distribution is proving to be a difficult exercise. The diffracted intensities are extremely weak, as anticipated, and only on the order of five to seven significant intensities will be available. (The exact number will not emerge until a final fit to the background intensity has been established for each pattern.) This is due to the difficulty of distinguishing very weak intensities from a high and unudulating background introduced by the silica capsule whose presence, unfortunately, was necessary for satisfactory execution of the experiments. Previous work at LANSCE has achieved successful modeling of this diffuse modulation, but these studies were larger than those of the present work by more than an order of magnitude. The feeble nature of the diffraction effects produced by our samples may be appreciated by noting that the largest intensity maximum provided by a specimen with a volume on the order of 10 cm^3 was exceeded by a diffraction peak arising from the fine-gauge thermocouple which had been attached to the specimen. This inherent problem is not a measure of the success of the experiments, however, as previous x-ray powder diffraction studies had provided no more than three, and often only one single, diffuse maximum barely distinguishable above background.

Rietveld analysis of an initial pattern has not yet enabled us to establish a unique distribution of cations among the octahedral and tetrahedral interstices which are available in an fcc array. Similar residuals were obtained for several likely models in view of the small number of significant intensities. As we have data for three different compositions, we are presently attempting to obtain a fit to the high background which is sufficiently accurate to permit extraction of structure factors. Difference maps between compositions will then be prepared in an attempt to reveal the sites which are preferentially occupied by Ag rather than Cu.

Experiment report: *(continued)*

References:

(1) R. J. Cava, F. Reidinger and B. J. Wuensch, Solid State Comm. 24, 411-416 (1977).

(2) R. J. Cava, F. Reidinger and B. J. Wuensch, J. Solid State Chem. 31, 69-80 (1980).

(3) M. Oliveria, R. K. McMullan and B. J. Wuensch, Solid State Ionics 28-30, 1332-1337 (1988).

(4) J.-J. Didisheim, R. K. McMullan and B. J. Wuensch, Solid State Ionics 18-19, 1150-1162 (1986).

(5) R. J. Cava, F. Reidinger and B. J. Wuensch, Solid State Ionics 5, 501-504 (1981).

Instrument used: *(please type)*	Local contact:	Proposal number: *(for LANSCE use only)*
HIPD	Greg Smith	#276.0

Title:

The molecular orientation of bilayer phospholipids.

Report received: *(for LANSCE use only)*

Authors and affiliations:

Gregory S. Smith, LANSCE
William Hamilton, LANSCE
Robert Von Dreele,LANSCE

Experiment report:

We have made a preliminary study of the relationship of the glycerol backbone to the position of the tails in the hexagonal in-plane lattice of the LßF phase of a phospholipid-water system. 1.5 grams of dimyristoyl phosphotidyl choline (DMPC) were obtained from Avanti Polar Lipids in which the fatty acid chain in the second position had been fully deuterated. If there is a structure associated with the backbone orientation, there is a deviation from the scattering one would expect for an in-plane hexagonal lattice.

The samples were prepared by mixing D2O with the DMPC to obtain 12% D2O by weight mixture. This put the sample in the LßF phase. Our initial estimate of 0.5 grams of DMPC per run was low. We saw no peaks in the scattering at all using 0.5 grams of DMPC. We then increased the amount of sample to 1.5 grams (our entire supply) mixed with D2O to get a 12% mixture. The plots of intensity versus d-spacing are shown in figures 1 and 2. The uncertainty in the peak positions due to weak scattering make an absolute determination of the structure difficult. However, there are several indications present in the data to support the hypothesis of backbone ordering. First, it is clear that the first two order lamellar peaks are present in the data at 55 and 27.5Å which is consistent with the lamellar plane spacing for the LßF phase. Also, there are weak peaks at 8.77 and 6.31Å. This is a strong indication of a larger unit cell

Experiment report *(continued)*:

than the usual 4.94Å which one measures for this phase. This supports the idea of backbone orientation. We are presently applying maximum entropy techniques to the problem to give us more certainty in the peak positions along with trying to index the peaks. We intend to make further measurements with more sample as well as with a sample for which both fatty acid chains are deuterated.

Figure 1

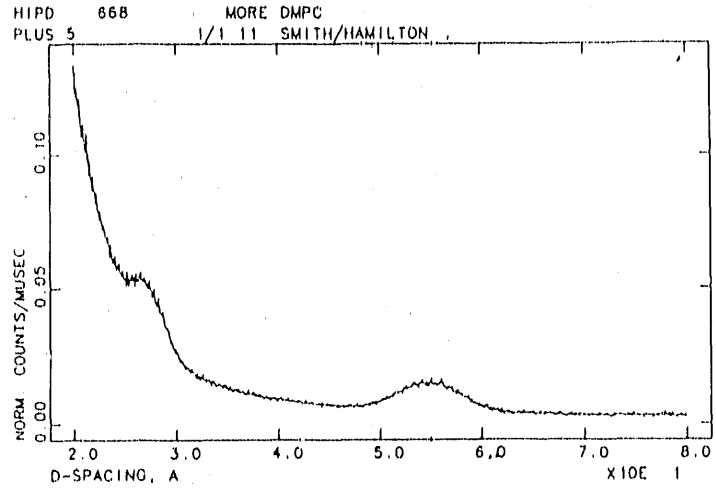

Figure 2

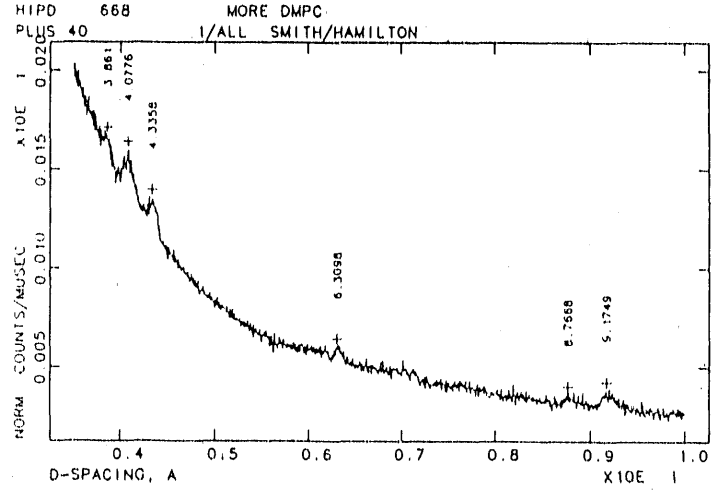

References:

(1) G. S. Smith, C. R. Safinya, D. Roux, and N. A. Clark, Mol. Cryst. Liq. Cryst.,**144**, 235(1987).

(2) G. S. Smith, E. B. Sirota, C. R. Safinya, and N. A. Clark, Phys. Rev. Lett., **60**, 813(1988).

(3) I. Hatta, S. Kato, K. Ohki, and K. Tsuchida, Mol. Cryst. Liq. Cryst., **139**, (1986).

Instrument used: *(please type)*	Local contact:	Proposal number: *(for LANSCE use only)*
HIPD	George H. Kwei	279.0

Title:	Report received: *(for LANSCE use only)*
STRUCTURE AND BULK SUPERCONDUCTIVITY FOR $BaPb_{.5}Bi_{.25}Tl_{.25}O_{3-\delta}$	

Authors and affiliations:

Zafar Iqbal, Allied Signal Inc.

George H. Kwei, Los Alamos National Laboratory

Eddie W. Ong and B.L. Ramakrishna, Department of Chemistry, Arizona State Univ.

Experiment report:

The layered hole-doped copper oxide based perovskite superconductors of compositions La-Ba(Sr,Ca)-Cu-O [1], Y-Ba-Cu-O [2], Bi-Sr-Ca-Cu-O [3], Tl-Ba-Ca-Cu-O [4] and Tl-Pb-Sr-Ca-Cu-O [5] and the electron doped Nd-Ce-Cu-O [6] and Nd-Cu-O-F [7] compositions, have been the center of intense interest in the field of oxide superconductivity. However, increasing interest is being focussed on the related (but non-magnetic) non-copper oxide materials with cubic or near-cubic perovskite structures such as $BaPb_{0.75}Bi_{0.25}O_3$, T_c = 13 K [8] - the first oxide high temperature superconductor, and its subsequently discovered analogs $BaPb_{0.75}Sb_{0.25}O_3$, T_c = 3.5 K [9] and $Ba_{0.6}K_{0.4}BiO_3$ with T_c = 30 K [10]. We report here on a reproducible synthesis route, structure and superconducting properties of the first thallium based analog in this series, of ideal composition $BaPb_{0.5}Bi_{0.25}Tl_{0.25}O_{3-\delta}$ (abbreviated as Ba-Pb-Bi-Tl-O), which was described recently by Sutto *et al* [11]. The compound $BaPb_{0.75}Tl_{0.25}O_3$ has also been synthesized in nearly single phase form but has to date not been found to be superconducting under the present synthesis conditions [12].

The most reproducible synthesis conditions involved the use of a welded gold tube with one opening that was only crimped so as to allow for interaction with the atmosphere of the reaction chamber. The reaction was carried out in a tube furnace in which the gold tube was place inside a quartz tube through which high purity gases were passed. Stoichiometric amounts of high purity BaO_2, PbO, Bi_2O_3 and Tl_2O_3 were ground together and reacted in three steps. In the first step, the oxides were fired at 775°C under flowing Ar for 1 to 1.5 hrs followed by rapid cooling in the same atmosphere. The product was then ground and fired again at 475°C under flowing O_2 for 1 hr followed by furnace cooling. In the final step, the product was annealed in a reduced oxygen atmosphere (5% O_2 and 95% Ar) for 3 hrs followed by rapid cooling in the same atmosphere.

The structures for three samples produced by annealing in different atmospheres were refined. ORTEP plot of the neutron structure of one unit cell of BPTBO, a superconducting sample produced by annealing in 5% O_2 and 95% Ar, at a sample temperature of 305 K. Each unit cell contains four formula units. For the sake of clarity, only bonds between Pb/Tl/Bi and the oxygens are shown. The Ba ions are located on the cell faces between the displaced O1; these displacements probably take place in order to provide the more favorable Ba-O distance of 2.75 Å given by the sum of the ionic radii. The thermal ellipsoids.are drawn as 95% probability surfaces.

Experiment report *(continued)*:

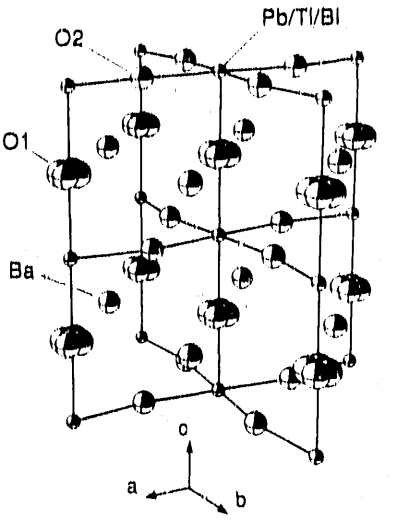

One of the objectives of this structural study was to determine the oxygen stoichiometry that distiguishes the superconducting sample annealed in 5% O_2 and 95% Ar from the nonsuperconducting sample annealed in Ar. Surprisingly, we find that the oxygen stoichiometry differs only by a little: 2.93 for the superconducting sample versus 2.87 for the nonsuperconducting sample.

An account of this work has been submitted to Physica C.

[1] J.G. Bednorz and K.A. Müller, Z. Phys. B**64**, 189 (1986).
[2] M.K. Wu *et al.*, Phys. Rev. Lett. **58**, 908 (1987).
[3] H. Maeda, Y. Tanaka, M. Fukutomi and T. Asano, Japan J. Appl. Phys. **27**, L209 (1988).
[4] Z.Z. Sheng and A.M. Herman, Nature **332**, 55 (1988).
[5] M.A. Subramanian *et al.*, Science **242**, 249 (1988); J.C. Barry, Z. Iqbal, B.L. Ramakrishnan, R. Sharma, H. Eckardt and F. Reidinger, J. Appl. Phys. **65**, 5207 (1989).
[6] Y. Tokura, H. Takagi and S. Uchida, Nature **337**, 345 (1989).
[7] A.C.W.P. James, S.M. Zahurak and D.W. Murphy, Nature **338**, 240 (1989).
[8] A.W. Sleight, J.L. Gillson and P.E. Bierstedt, Solid State Commun. **17**, 27 (1975).
[9] R.J. Cava *et al.*, Nature **339**, 291 (1989).
[10] L.F. Mattheis, E.M. Gyorgy and D.W. Johnson, Jr., Phys. Rev. B**37**, 3747 (1988); R.J. Cava *et al.*, Nature **332**, 814 (1988).
[11] T.E. Sutto, B.A. Averill and J. Ruvalds, University of Virginia, preprint (1989).
[12] Z. Iqbal *et al.*, in preparation.

Instrument used: *(please type)*	**Local contact:**	**Proposal number:** *(for LANSCE use only)*
HIPD	George H. Kwei	280.1

Title:

STRUCTURE AND VIBRATIONAL PROPERTIES OF La_2CuO_4 AND $YBa_2Cu_3O_7$

Report received: *(for LANSCE use only)*

Authors and affiliations:

George H. Kwei and Andrew C. Lawson, Los Alamos National Laboratory

Experiment report:

Ikeda *et al.* [1] recently reported surprisingly large atomic Debye temperatures for the constituent Cu and O atoms in La_2CuO_4 and $YBa_2Cu_3O_7$. These were determined from the recoil spectra of neutrons in the eV energy range. It was suggested that these large values arise from high-frequency modes which may in turn play a role in the mechanism for the high transition temperatures observed for the oxocuprate superconductors. Recent EXAFS experiments by Los Alamos scientists [2] have suggested other interesting temperature dependent structural features for $YBa_2Cu_3O_7$ near the superconducting transition: i.e. the Cu2-O4 bond becomes shorter or more harmonic, or both. Since this result is predicted in an excitonic model for superconductivity [3], there is a need to verify the predictions from EXAFS experiments.

We have been using pulsed-neutron powder diffraction data to provide estimates of the anisotropic thermal parameters of atoms in crystals and, therefore, information about the vibrational structure. Of special interest has been both the static and dynamical displacements of the in the high T_c oxide superconductors and the possible relationship between these and their superconducting behavior [4-6]. Recently, we also have been studying the vibrational properties of much simpler compounds and have been successful in determining atomic Debye temperatures from the thermal parameters obtained from Rietveld refinements of structural models using neutron powder diffraction data taken over a range of sample temperatures [7].

We have also been active using neutron diffraction to study the structures of a large number of superconducting materials.

Thus, the work by Ikeda *et al.* provides us with an opportunity to extend our determinations of vibrational properties to more complex systems and to assess the validity of the values obtained by eV neutron recoil spectroscopy. Furthermore, a study of the temperature dependence of the structure and thermal parameters for $YBa_2Cu_3O_7$ should provide a test of the results derived from EXAFS experiments.

Samples of the Debye temperatures obtained for the cations in $YBa_2Cu_3O_7$ are shown in the figure and do not support the unusually high values of the high Debye temperatures for the Cu ions obtained from neutron recoil spectroscopy. Similarly,and in contrast to the EXAFS results, the bond distances and thermal parameters for $YBa_2Cu_3O_7$ show no unusual temperature dependence near the superconducting transition temperature.

Experiment report *(continued)*:

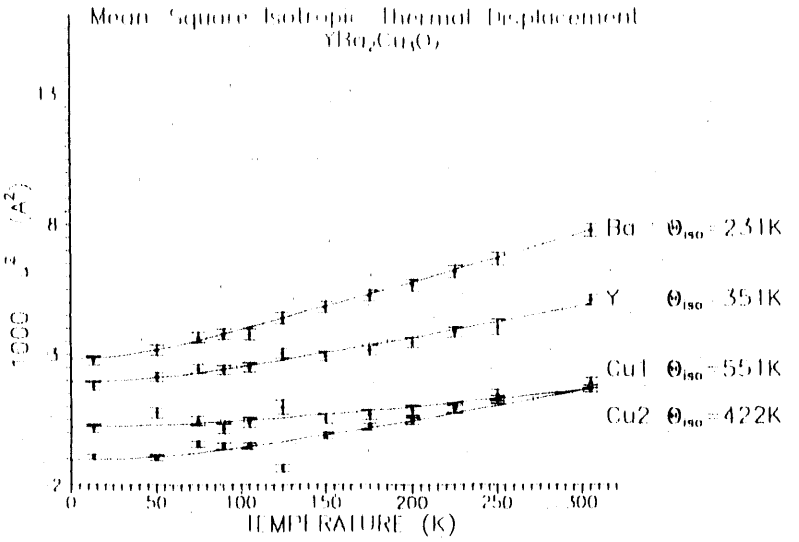

Recently, neutron recoil studies of $YBa_2Cu_3O_7$ have confirmed our Debye temperature determinations [8].

[1] S. Ikeda, M. Misawa, S. Tomiyoshi, M. Omori and T. Suzuki, Physics Lett. **A134**, 191 (1989).
[2] S.D. Conradson and I.D. Raistrick, Science **243**, 1340 (1989).
[3] Z. Tesanovic, A.R. Bishop and R.L. Martin, Solid State Commun. **68**, 337 (1988).
[4] A. Williams, G.H. Kwei, R.B. Von Dreele, A.C. Larson, I.D. Raistrick and D.L. Bish, Phys. Rev. B**37**, 7960 (1988).
[5] G.H. Kwei, J.A. Goldstone, J.D. Thompson, A. Williams and R.B. Von Dreele, Phys. Rev. B**39**, 7378 (1989).
[6] M.A. Subramanian, G.H. Kwei, J.B. Parise, J.A. Goldstone and R.B. Von Dreele, Physica C**160** (to be published).
[7] A.C. Lawson, A. Severing, J.M. Ward, C.E. Olsen, J.A. Goldstone and A. Williams, J. Less Common Metals (to be published).
[8] C. Bowman, private communication.

Instrument used: *(please type)*	Local contact:	Proposal number: *(for LANSCE use only)*
HIPD	George H. Kwei	280.2

Title: SUPERCONDUCTING-SUPEROXYGENATED CUPRATES: A JOINT X-RAY/ NEUTRON POWDER DIFFRACTION STUDY OF OXYGEN STOICHIOMETRY AND CATION ORDERING IN THE T* PHASE $La_{0.9}Sm_{0.9}Sr_{0.2}CuO_{4+\delta}$

Report received: *(for LANSCE use only)*

Authors and affiliations:

G.H. Kwei, S-W. Cheong, Z. Fisk, J.D. Thompson and R,B, Von Dreele, Los Alamos National Laboratory, and

J.E. Schirber, Sandia National Laboratory.

Experiment report:

The lanthanide cuprates R_2CuO_4 form the tetragonal T* phase structure when R is a mixture of early and later rare earths [1]. The structure of these materials resemble La_2CuO_4 (T-phase) in half of the unit cell and Nd_2CuO_4 (T'-phase) in the other half, and belong to the tetragonal space group P4/nmm. There are two lanthanide sites, one similar to that in the T phase (M-site) which is coordinated by nine oxygens and one similar to that in the T' phase (M'-site) coordinated by eight oxygens. Initially it appeared to be difficult to prepare single phase material with the T* structure, but it was soon discovered that addition of a small amount of Sr greatly enhances the range of phase stability [2]. Thus T* phase compounds of the type $La_{1.8-x}R_xSr_{0.2}CuO_4$, with R ranging from Pr to Ho, have been successfully prepared. Three of these Sr-doped compounds are superconducting when annealed in O_2: with x =0.9 and R=Sm, Eu and Gd, annealing at 150 K O_2 gives T_c's circa 20 K, while annealing at 3 Kbar O_2 gives T_c's of 37, 34 and 33 K. At present, it is not understood why the range of later lanthanides that produces superconducting materials is narrower than the range required to produce the T* phase or why the superconducting behavior changes so drastically with O_2 annealing for those that do superconduct. This remarkable behavior raises the very interesting questions of the effect of oxygen stoichiometry and cation ordering on superconductivity. In order to clarify this situation, we undertook a joint neutron/x-ray powder diffraction study of the low absorbing T* phase $La_{0.9}Sm_{0.9}{}^{152}Sr_{0.2}CuO_{4+\delta}$ annealed at both atmospheric pressures and 3 Kbar of O_2 to study these questions.

We find that the large cations again prefer the M site and that the smaller cations the M' site; however, we find that the ordering is not as complete as found by us previously for $La_{0.9}Gd_{0.9}Sr_{0.2}CuO_4$ using anomalous x-ray powder diffraction [3]. This result is reasonable in view of the smaller differences in ionic radii between La^{+3} and Sm^{+3}. We have not yet had a chance to refine structures that include defect oxygen sites for the extra oxygen, but fully expect that this should be possible (especially after our experience with the much more difficult problem of locating the extra oxygen in the phase separated $La_2CuO_{4+\delta}$). When this work is completed, we hope to have a much better understanding of the relationshiop between oxygen stoichiometry and cation ordering and superconductivity in the T* phase materials.

Experiment report *(continued)*:

References:

[1] J. Akimitsu, S. Suzuki, M. Watanabe and H. Sawa, Jap. J. Appl. Phys. **27**, L1859 (1988).
[2] S-W. Cheong, Z. Fisk, J.D. Thompson and R.B. Schwartz, Physica **C159**, 407 (1989).
[3] G.H. Kwei, R.B. Von Dreele, S-W. Cheong, Z. Fisk and J.D. Thompson, Phys. Rev. B (to be published 1 February 1990).

Instrument used: *(please type)*	Local contact:	Proposal number: *(for LANSCE use only)*
HIPD	George H. Kwei	281.1

Title:
DOPANT SITE-SELECTIVITY IN $YBa_2(Cu_{1-x}Fe_x)_3O_7$ ANNEALED IN REDUCING AND OXIDIZING ATMOSPHERES

Report received: *(for LANSCE use only)*

Authors and affiliations:

George H. Kwei, W. Larry Hults and James L. Smith, Los Alamos National Laboratory.

Experiment report:

Soon after the high T_c superconductor was first discovered, researchers in the field began transition metal doping studies of the Cu sites in order to gain a better understanding of the mechanisms responsible for superconductivity. Initial studies involved primarily resistance and magnetization studies [1], but more recently include x-ray and neutron diffraction studies and Mössbauer studies [2]. Although the site preference of many of the dopants for the chain Cu(1) sites and the plane Cu(2) sites have been reasonably well resolved, a few notable exceptions remain. One of these is the site preference of Fe dopants. There has been considerable controversy and neither x-ray, neutron or Mössbauer studies seem to agree.

Some time ago, Maeno and Fujita [3] suggested that, in keeping with the assumed site preference of chains for Fe^{+3} and planes Fe^{+2} [2], Fe dopes into chains when annealed at high temperatures in oxidizing environments and into planes when annealed in reducing environments. They also presented some data suggesting that this was indeed the case.

In order to test this interesting hypothesis, we have measured neutron powder diffraction patterns for two samples (with x = 0.06 and 0.12) each annealed using the same conditions used by Maeno and Fujita, e.g. at high temperatures in either oxygen or nitrogen, with a subsequent low temperature anneal in oxygen. We have completed refinement the structures for all data sets and find that for all samples Fe strongly prefers the chain Cu(1) sites, invalidating what would otherwise be an interesting hypothesis.

This work is now being written up for publication.

Experiment report *(continued)*:

References:

[1] G. Xiao, F.H. Streitz, A. Gavrin, Y.W. Du and C.L. Chien, Phys. Rev. B**35**, 8782 (1987).
[2] T.J. Kistemacher, Phys. Rev. B**38**, 8862 (1988) provides a review.
[3] Y. Maeno and H. Fujita, Physica **C153-155**, 1105 (1988).

Instrument used: *(please type)*	Local contact:	Proposal number: *(for LANSCE use only)*
HIPD	A. C. Lawson	100008.0

Title:

NEUTRON POWDER DIFFRACTION STUDY OF α- and β-UD_3

Report received: *(for LANSCE use only)*

Authors and affiliations:

A. C. Lawson (MST-5), J. Conant (WX-5), and G. Burr (P-LANSCE)
Los Alamos National Laboratory
Los Alamos NM 87545
W. Tadloch and D. Kirk
EG&G-Mound Laboratories
Miamisburg OH 45343

Experiment report:

UD_3 is known in two forms, α and β. Both forms have the same space group (Pm3n), and both are related to the Cr_3Si structure, which is normally found for transition metal compounds, rather than actinides. β-UD_3 has two crystallographically distinct uranium sites, and may be regarded as an intermetallic compound of uranium with uranium that is stabilized by hydrogen. (Such "self intermetallic" behavior is typical of the light actinide elements.) β-UD_3 becomes ferromagnetic below 160K, and the magnetic moment on the two uranium sites is identical within experimental error, as has been determined with three separate neutron diffraction experiments, including some earlier work at LANSCE [1]. α-UD_3 is also said to be ferromagnetic [2], but this claim is suspect, because the reported Curie temperature is the same as for β-UD_3, and because α-UD_3 is metastable and cannot be prepared without a considerable mixture of the β-form in the final product.

We have obtained neutron powder diffraction data on a sample of UD_3 containing nearly 50% of the metastable α-phase. Data were obtained at 15 different temperatures between 15K and room temperature on the High Intensity Powder Diffractometer (HIPD). Because of the ability of the Rietveld analysis method to deal with multiphase mixtures, the results of our investigation are phase specific.

Mulford, Ellinger and Zachariasen [3] solved the structure of α-UD_3 from powder x-ray data which permitted the location only of uranium atoms with certainty. Our neutron data allow the location of the deuterium atom. As predicted by Mulford et al., the structure of α-UD_3 is isomorphous with Cr_3Si (the famous β-W structure.)

Experiment report *(continued)*:

Our data show that α-UD_3 is non-magnetic. This is demonstrated by a comparison of diffraction patterns at different temperatures. Since no magnetic superlattice peaks associated with α-UD_3 were observed in our experiment, the β-form must be a simple ferromagnet if it is magnetic at all. The peak at 2.1 Å (the extreme left of the figures) comprises the 310-reflection of β-UD_3 and the 200-reflection of α-UD_3. Our data show that there is no magnetic intensity in this reflection, as the peak is fit perfectly with the nuclear structures alone. It follows that the α-form is non-magnetic. (It is known from the magnetic structure of β-UD_3 [1] that there is no magnetic intensity in the (310) reflection.)

The principal results of our study are:

- The x-ray crystal structure of Zachariasen and Mulford for α-UD_3 is confirmed.
- α-UD_3 is not magnetic above 15K.
- The striking minimum in lattice constant previously observed at the Curie temperature of β-UD_3 is confirmed, and a similar lattice constant minimum is observed for α-UD_3 despite its non-magnetic behavior.
- The Debye temperatures for the two phases, as determined from the Debye-Waller factors are nearly the same.

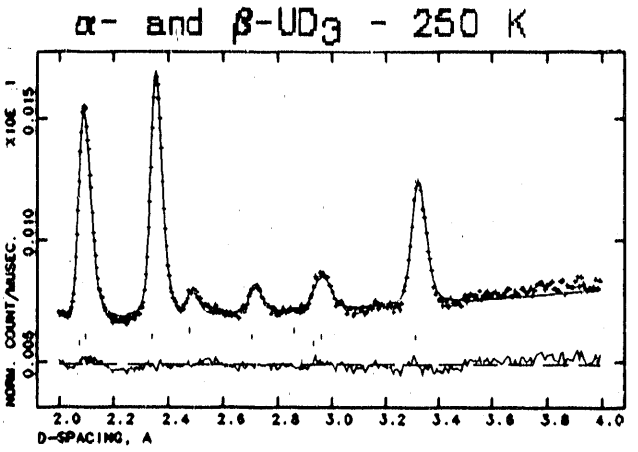

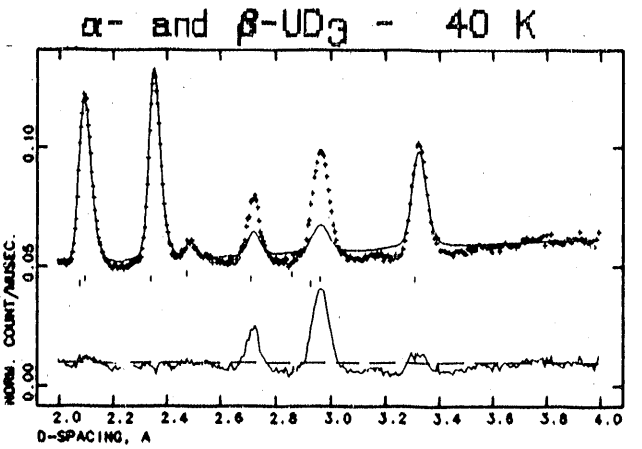

References:

1 A. C. Lawson, A. Severing, J. W. Ward, C. E. Olsen, J. A. Goldstone and A. Williams, J. Less-Common Metals, to be published (1990).

2 A. Silwa and W. Trzebiatowski, Bull Acad. Pol. Sci. Ser. Sci. Chem. 10 217 (1962).

3 R. N. R. Mulford, F. H. Ellinger and W. H. Zachariasen, J. Am. Chem. Soc. 76 297 (1954).

Instrument used: *(please type)*	Local contact:	Proposal number: *(for LANSCE use only)*
HIPD	A. C. Lawson	100009.0

Title:
STRAIN AND PARTICLE SIZE IN PALLADIUM POWDER -
A TEST OF THE IKEDA-CARPENTER-DAVID PROFILE FUNCTION

Report received: *(for LANSCE use only)*

Authors and affiliations:

A. C. Lawson, MST-5
J. W. Conant, WX-5
G. Burr and R. B. Von Dreele, P-LANSCE
Los Alamos National Laboratory
Los Alamos NM 87545

Experiment report:

We have been using time-of-flight neutron diffraction to study strain and particle size effects in materials. Neutron diffraction is useful when a bulk probe is required, and the time-of-flight method practiced at pulsed sources offers high resolution. The use of the Rietveld refinement technique to extract strain and particle size information from the diffraction data has the advantage of using many hkl-reflections simultaneously for the analysis.

The Rietveld method depends on the use of a peak-shape function that gives a realistic fit to the diffraction peaks over a wide range of d-spacing. There is always room for improvement. In this experiment we used some previously characterized palladium samples [1] to test a newly devised profile function based on the Ikeda-Carpenter peak shapes [2]. We used three palladium samples. The "alloy" was a $Pd_{0.9}Rh_{0.1}$ solid solution with about 0.2% strain and negligible particle size broadening (P > 1000 Å). The "Magic Barrel" palladium had 0.5% strain and P = 700 Å. The "palladium black" had the most severe line broadening, with 1.2% strain and P = 120 Å.

The figures show the fits obtained with the usual peak shape (Profile Function 1) [3] and with the new one (Profile Function 2) [4]. The fit is considerably better with the new profile function, and the refined profile coefficients are listed in the table. 1 (The units have been suppressed; they are the usual ones with μs and Å.) The derived values of strain and particle size did not change as a result of the better fit, but it seems certain that lower levels of detectable strain and particle size broadening can now be achieved. It should be noted that Profile Function 2 has shown some numerical instability when used on high resolution data from NPD. Further improvements in the profile functions can be anticipated.

Experiment report *(continued)*:

Alloy - Run HIPD 641

Profile Function 1

[Difc ≡ 5035, $\alpha_0 \equiv 0$, $\alpha_1 \equiv 1.02$, $\beta_0 \equiv 0.031$, $\beta_1 \equiv 0.0016$, $\sigma_0 \equiv 0$, per HIPD calibration ($\sigma_{1\,1} \equiv 35.0$)]

$\sigma_1 = 83(1)$

$\sigma_2 \equiv 0$

Profile Function 2

$\alpha_0 = 2.1(1)$

$\alpha_1 \equiv 0$

$\beta = 27.1(1)$

switch = 350(10)

$\sigma_1 = 33(2)$

$\gamma_1 = 2.4(2)$

all other σ's and γ's $\equiv 0$

Palladium Black - Run HIPD 642

Profile Function 1

$\sigma_1 = 1010(30)$

$\sigma_2 = 180(3)$

Profile Function 2

$\gamma_1 = 23(1)$

$\gamma_2 = 26(1)$

Magic Barrel - Run HIPD 643

Profile Function 1

$\sigma_1 = 230(4)$

$\sigma_2 \equiv 0$

Profile Function 2

$\gamma_1 = 10.9(4)$

$\gamma_2 = 1.0(3)$

α's, β, switch and other σ's and γ's fixed at values from alloy data.

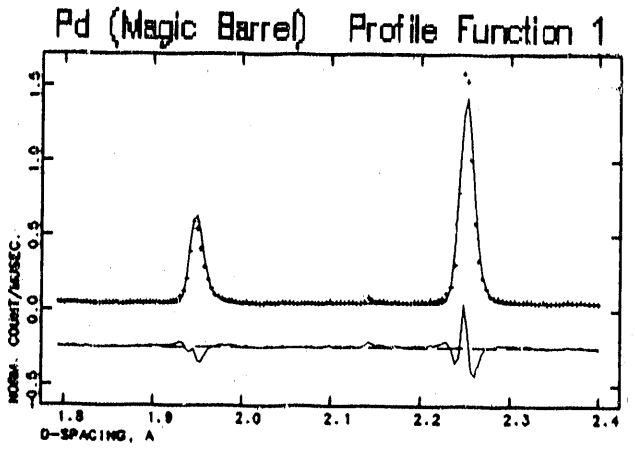

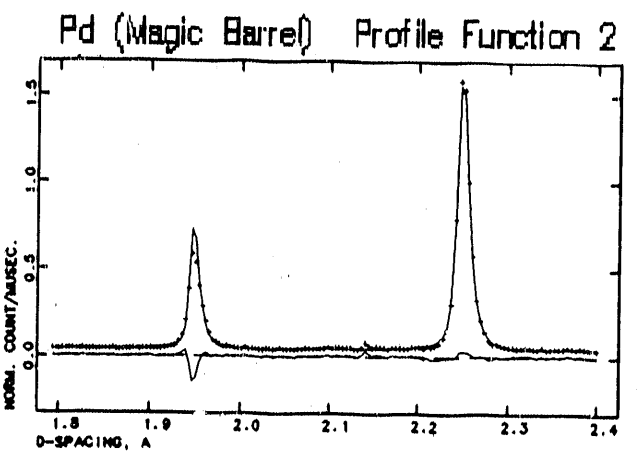

References:

1 A. C. Lawson et al., Advances in X-Ray Analysis (1989), to be published.

2 S. Ikeda and J. M. Carpenter, J. Nuc. Inst. Meth. A239 536 (1985).

3 R. B. Von Dreele, J. D. Jorgensen and C. Windsor, J. Appl. Cryst. 15 581 (1982) and R. B. Von Dreele, unpublished (1982).

4 W. I. F. David, J. Appl. Cryst. 19 63 (1986) and W. I. F. David, unpublished (1986)..

Instrument used: *(please type)*	Local contact:	Proposal number: *(for LANSCE use only)*
NPD / HIPD	Joyce Goldstone / Robert Von Dreele	278.0

Title:

Neutron Powder Diffraction from a Thermotropic Liquid Crystal

Report received: *(for LANSCE use only)*

Authors and affiliations:

Thomas P. Ricker, Joyce Goldstone and Robert VonDreele

Manuel J. Lujan Jr. Neutron Scattering Center (LANSCE)
Los Alamos National Lab.
Los Alamos, NM 87545

Experiment report:

INTRODUCTION: Thermotropic Liquid Crystals are organic molecules which self-organize into various ordered phases as the temperature is altered. Each of these phases is characterized by a distinct combination of partial orientational and translational order. Rod shaped thermotropic molecules are in general composed of a central rigid core with flexible aliphatic chains attached at each end. This class of molecule often exhibits smectic (layered) phases in which the molecules align end-to-end with a typical interlayer spacing of 30 Angstroms and an in-plane spacing of 5 Angstroms. Small angle neutron scattering (SANS) and powder diffraction experiments were undertaken to investigate the evolution of these parameters and to ultimately determine the molecular conformations and packing geometries present in the various phases.

EXPERIMENTAL RESULTS: High resolution neutron powder diffraction data was obtained on a three gram sample of the thermotropic liquid crystal: $D_{21}C_{10}O(C_6H_4)COO(C_6H_4)OC_6D_{13}$ encased in a standard vanadium sample holder using the Neutron Powder Diffractometer (NPD) and the High Intensity Neutron Powder Diffractometer (HIPD). This material exhibits the nematic, and several smectic liquid crystal phases. It is crystalline at room temperature.

Experiments on the NPD showed several well defined diffraction peaks in the 1 to 4 Angstrom regime for the crystalline phase, see Fig. 1. These peaks shift position in Q as the sample temperature was varied. As the sample is heated into the liquid crystalline phases only a few strong peaks remain, see Fig. 2. Data collection times were on the order of 24 hours per sample temperature.

Experiment report *(continued)*:

Experiments were performed on the HIPD to take advantage of this instrument's extended Q-range and its' shorter data collection times. Strong scattering was observed for the crystalline phase. Typical data is shown in figures 3a and 3b using the 40^{o} and 5^{o} detector banks respectively. The strong scattering peaks observed for the crystalline phase disappeared in the data for the smectic phases. Data collection times were are approximately 12 hrs.

CONCLUSIONS: We were successful in collecting scattering data from the crystalline phase of a thermotropic liquid crystal. The crystal structure of this material has yet to be determined pending the results of planned X-ray crystallography experiments. Scattering data from the smectic phases of our sample contain very few peaks. Information on molecular interactions in the smectic phases can be gained through a comparison of the liquid structure factors for like molecules with variously deuterated sites.

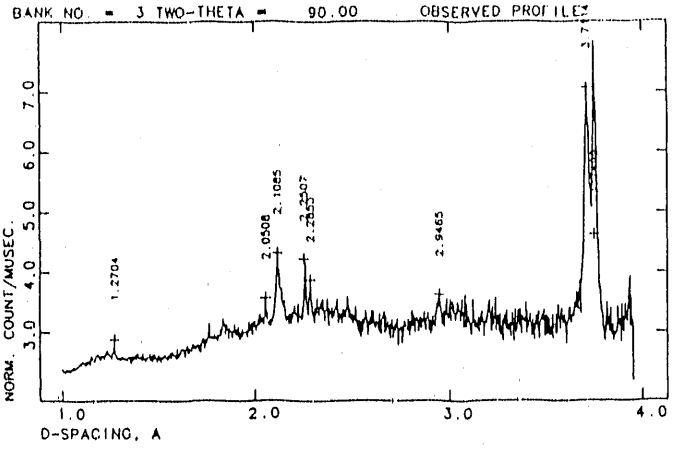

Figure 1: Neutron powder diffraction data for the crystal phase of $D_{21}C_{10}O(C_6H_4)COO(C_6H_4)OC_6D_{13}$, collected at room temperature on the Neutron Powder Diffractometer (NPD).

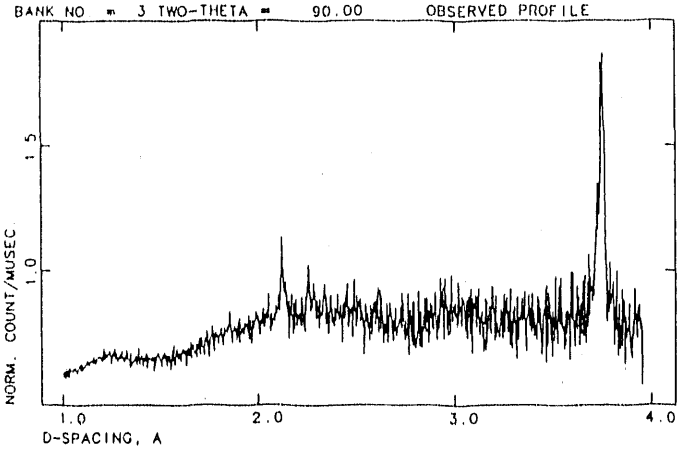

Figure 2: Powder diffraction data taken on NPD for the smectic C phase - sample temperature, 72^{o} C.

Experiment report *(continued)*:

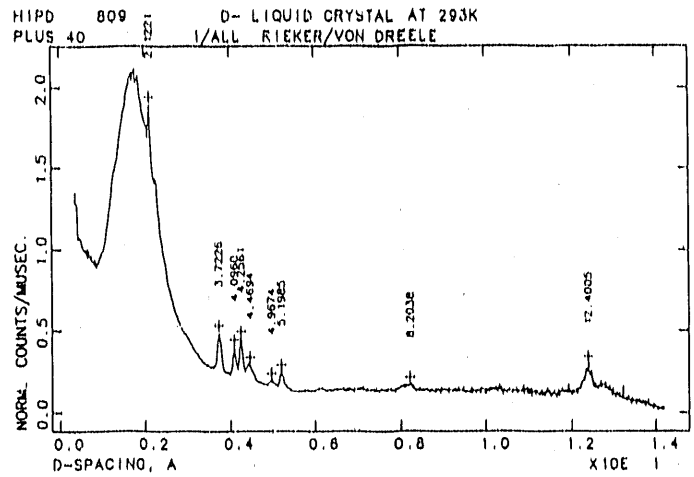

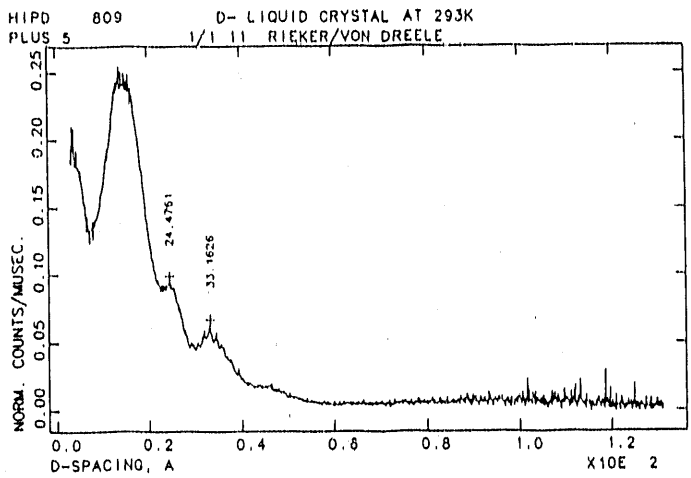

Figure 3: (a) Scattering data collected on the 40^{o} detector banks of the HIPD for the crystal phase of $D_{21}C_{10}O(C_6H_4)COO(C_6H_4)OC_6D_{13}$ taken at room temperature. (b) Data from the 5^{o} banks.

References:

Neutron Powder Diffractometer (NPD)

Neutron Powder Diffractometer (NPD)

The Neutron Powder Diffractometer (NPD) sample position is 32 m from the source. Standard collimation in the beam line produces a 5.0 x 1.0 cm beam at the sample position. Placed at five points along the beam, variable apertures permit adjustment of both the beam size on the sample and the viewed region of the moderator. The large evacuated sample can (74 cm inside diameter) has sufficient clearance to handle any special environment device necessary. Detectors are placed symmetrically at several angles to cover short d-spacings (0.25 to 3.9 Å) at a resolution ($\Delta d/d$=0.17%) to much longer d-spacings (~34 Å) at lower resolution ($\Delta d/d$=0.5-1.5%). Both sides of the instrument have identical resolution because the incident beam is normal to the moderator. The resolution of the instrument can be adjusted by changing the collimation and the detector-position resolution.

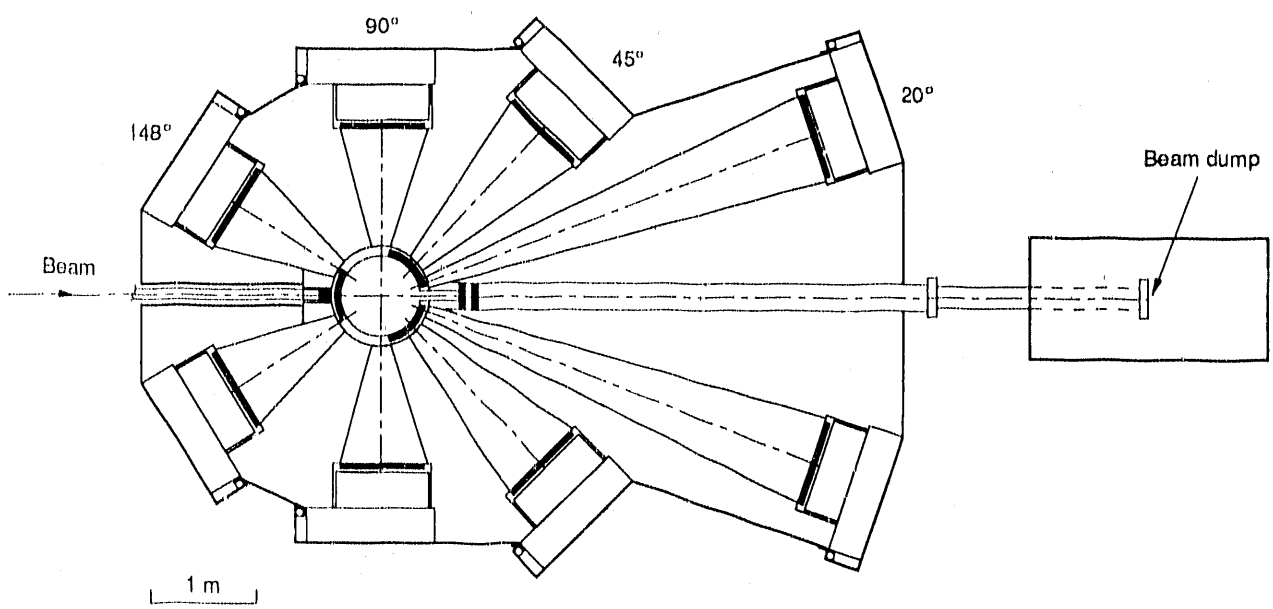

Instrument Details

Detector banks:	± 20° (1990)
	± 45° (1st in '89, 2nd in '90)
	± 90°
	± 148°
d-spacing range for 12- Hz operation (approximate):	
	± 20° 1.2 - 33.6 Å
	± 45° 0.65 - 12.7 Å
	± 90° 0.35 - 7.8 Å
	± 148° 0.25 - 5.2 Å
Resolution (determined by collimation):	
	± 20° 0.91 - 1.5%
	± 45° 0.37 - 0.62%
	± 90° 0.25%
	± 148° 0.15%
Moderator	Chilled water at 10° C
Sample environment	10 - 300 K, closed cycle refrigerator;
	room-temperature-access liquid-He dewar, 1.2 - 300 K;
	vacuum furnace, limit 700° C
Maximum beam size at sample:	
	5 cm (height) x 1 cm diameter
Experiment duration	8 - 48 hours

Joyce Goldstone, Instrument scientist
John Thomas, Instrument technician

Instrument used: *(please type)*	Local contact:	Proposal number: *(for LANSCE use only)*
NPD	Joyce A. Goldstone	D-4.0

Title:
SUPERCONDUCTING-SUPEROXYGENATED CUPRATES: STRUCTURE OF THE INTERSTITIAL OXYGEN DEFECT IN La_2CuO_{4+}

Report received: *(for LANSCE use only)*

Authors and affiliations:

George H. Kwei and Joyce A. Goldstone, Los Alamos National Laboratory

Bruno Morosin, James E. Schirber, Eugene L. Venturini and David S. Ginley, Sandia National Laboratory.

Experiment report:

Materials closely related to La_2CuO_4 continue to intrigue investigators. The first of the high T_c oxide superconductors were made by introducing holes into the CuO_2 planes by partially doping divalent Ba^{2+} for the trivalent La^{3+} [1]. Subsequently, the undoped parent compound, La_2CuO_4, was also found to become a superconductor, with a T_c near 30 K, when treated with excess oxygen [2-4]. Initially, there was some question as to whether cation deficiency or oxygen excess provided the hole doping necessary for superconducting behavior, but it soon became evident that it was the latter when careful studies of the La to Cu ratio in these materials showed them to be stoichiometric to within 1% [5]. As a consequence, there has been a great deal of interest in the role of the excess oxygen and its location in the parent crystal. However, in contrast to the cation doped La_2CuO_4 where Ba^{2+} substitutes for La^{3+} and the quantity and location of the dopants is not an issue, the parent La_2CuO_4 is essentially stoichiometric, and both the quantity and location of the excess oxygen in superoxygenated $La_2CuO_{4+\delta}$ remain important unresolved questions.

Magnetization data taken with the earlier samples implied low superconducting fractions (0.2 to 30%, depending on the pressure of O_2 used in the annealing procedure), and suggested that detailed diffraction studies of the intrinsic superconducting phase might be difficult. Nevertheless, the structure of the excess oxygen defect has been the subject of a number of studies. Neutron powder diffraction showed such samples to be single phase with the space group Bmab circa 320 K but to separate into two nearly identical orthorhombic phases with $a \approx 5.33$, $b \approx 5.40$ and $c \approx 13.1$ Å and probable space groups Bmab and Fmmm at lower temperatures [6]. The data suggested that a phase separation occurred upon cooling into a nonsuperconducting Bmab phase and a superconducting, probably oxygen-rich, Fmmm phase. Because of the limited material subjected to the higher 3 kbar oxygen annealing pressure, the diffraction analysis was carried out employing a larger quantity of 0.1 kbar O_2 treated sample which had an exclusion fraction of only 0.2-0.5% [6]. This low exclusion fraction was attributed to the crystallite grain size of the ceramic material; however, the diffraction determined fraction of Fmmm phase was ~30% compared to ~60% for the 3 kbar O_2 treated material. Because of the nearly identical structural arrangements in these phases, least-squares determined positional and thermal variables were highly correlated, and because of the low concentration of the excess oxygen, no detailed positional data on its location was obtainable.

Experiment report *(continued)*:

The location of the excess oxygen in the closely analogous $La_2NiO_{4+\delta}$ system was more easily elucidated because the Fmmm phase exists as a single phase above the miscibility gap (for $\delta > 0.13$) and samples with large values of the excess oxygen ($\delta \approx 0.18$) can be prepared by annealing at atmospheric pressures of O_2 [7]. The excess oxygen was found to occupy the (1/4,1/4,0.23) position; shifts in the positions of four of the nearest-neighbor oxygens were found to be necessary in order to make room for this occupancy. In that study, it was inferred from the remarkable similarity of the structures that the excess oxygen position might be the same in the two materials. However, it is well known that copper environments are usually more tetragonally distorted than those found in nickel compounds and such an analogy may not be valid. For example, significant differences in the lattice parameters for the two compounds (Cu as given above; for Ni, $a \approx 5.46$, $b \approx 5.53$ and $c \approx 12.55$ Å) exist because of these distortions.

Single crystal neutron diffraction data were employed to determine the crystal structure of superconducting $La_2CuO_{4+\delta}$ at room temperature and at 13 K by Chaillout *et al.* [8,9]. Data were taken on a twinned crystal and short neutron wavelengths were used so that the pairs of reflections from the twins were as close as possible. The diffraction pattern was indexed to a Bmab space group; within the standard deviations, the lattice parameters could not be considered significantly different from those previously determined and the peak widths appeared to preclude two phases undergoing a separation. By analogy to the structure of $La_2NiO_{4+\delta}$, they refined the low temperature structure for excess oxygen in a (1/4,1/4,z) site and found that it occupied a (1/4,1/4,0.24) site of the single Bmab phase (these authors actually used the equivalent setting of Cmca) with an occupancy of 0.032. The excess oxygen was found to displace three of the nearest neighbor apical oxygens, which left one short O-O bond (1.64 Å) between the excess oxygen and one of the displaced nearest neighbors. The close agreement between this bond length and that of the peroxide ion, O_2^{2-}, then suggested that the excess oxygen defect is inserted as a peroxide ion. However, since no tests for occupancy of the more favorable (3/4,3/4,z) site were made and since the symmetry of the displaced sites may artificially produce both shortened and lengthened O-O bonds, conclusions on the excess oxygen occupancy and the bond lengths between excess oxygen and displaced oxygen may just be an artifact of the model used. Recently, these authors have reported a large splitting of the 0 5 14 peak (in the Bmab setting) at 120 K and have ascribed this to phase separation. Curiously, and in apparent contradiciton to their earlier work, they then refer to the Bmab phase as the nonsuperconducting phase and state that the second phase, which is then presumably superconducting and contains the excess oxygen, must be monoclinic [10].

In order to clarify this situation, we have determined the structures of a high-pressure annealed sample of $La_2CuO_{4+\delta}$ with optimized superconducting properties (Tc = 40 K) using high resolution neutron powder diffraction data. We find that at room temperature, $La_2CuO_{4+\delta}$ is single phase belonging to the space group Bmab. At lower temperatures, the material separates into two similar orthorhombic phases. Rietveld refinement provides fits to the data that are consistent with an approximately stoichiometric nonsuperconducting Bmab phase and a superconducting, oxygen-rich, Fmmm phase. Structure and occupancy for the defect oxygen site in both the room temperature Bmab and low temperature Fmmm phases have been determined. Both the location of the excess oxygen in the two phases and the distortion of the neighboring lattice induced by the insertion of the defect oxygen are slightly different; these features therefore suggest that the nature of the defect is different in the two phases. These results show that the excess oxygen inserted by high pressure annealing is responsible for the miscibility gap at lower temperatures and that its presence in the Fmmm phase leads to bulk superconductivity in $La_2CuO_{4+\delta}$.

Experiment report *(continued)*:

[1] J. G. Bednorz and K. A. Müller, Z. Phys. B **64**, 189 (1986).
[2] P.M. Grant, S.S.P. Parkin, V.Y. Lee, E.M. Engler, M.L. Ramirez, G. Lim and R.D. Jacowitz, Phys. Rev. Lett. **58**, 2482 (1987).
[3] J. Beille, R. Cabanel, C. Chaillout, B. Chevalier, G. Demazeau, F. Deslandes, J. Etourneau, P. Lejay, C. Michel, J. Provost, B. Raveau, A. Sulpice, J.-L. Tholence and R. Tournier, C.R. Acad. Sci. Ser. 2 **304**, 1097 (1987).
[4] K. Sekizawa, Y. Takano, H. Yakigami, S. Tasaki and T. Inaba, Jap. J. Appl. Phys. **26**, L840 (1987).
[5] J.E. Schirber, B. Morosin, R.P. Merrill, P.F. Hlava, E.L. Venturini, J.F. Kwak, P.J. Nigrey, R.J. Baughman and D.S. Ginley, Physica **C152**, 121 (1988).
[6] J.D. Jorgensen, B. Dabrowski, S. Pei, D.G. Hinks, L. Soderholm, B. Morosin, J.E. Schirber, E.L. Venturini and D.S. Ginley, Phys. Rev. B**38** (1988) 11337; references therein contain a detailed background review.
[7] J.D. Jorgensen, B. Dabrowski, S. Pei, D.R. Richards and D.G. Hinks, Phys. Rev. B**40**, 2197 (1988).
[8] C. Chaillout, S-W. Cheong, Z. Fisk, M.S. Lehman, M. Marezio, B. Morosin and J.E. Schirber, Physica **C158** (1989) 183.
[9] C. Chaillout, S-W. Cheong, Z. Fisk, M.S. Lehman, M. Marezio, B. Morosin and J.E. Schirber, Physica Scripta **T29**, 97 (1989).
[10] C. Chaillout, J. Chenavas, S-W. Cheong, Z. Fisk, M.S. Lehman M. Marezio, B. Morosin, and J.E. Schirber, MM-HTSC Proceedings, July 1989 (to be published).

Instrument used: *(please type)*	Local contact:	Proposal number: *(for LANSCE use only)*
NPD	Joyce A. Goldstone	281.2

Title:
STRUCTURE AND OXYGEN STOICHIOMETRY FOR THE ELECTRON-DOPED CUPRATE SUPERCONDUCTOR $Nd_{1.85}Ce_{0.15}CuO_{4-d}$

Report received: *(for LANSCE use only)*

Authors and affiliations:

G.H. Kwei, S-W. Cheong, Z. Fisk, F.H. Garzon, J.A. Golstone and J.D. Thompson, Los Alamos National Laboratory.

Experiment report:

We have determined the structure of the newly discovered electron doped superconductor $Nd_{1.85}Ce_{0.15}CuO_{4-\delta}$ at 11 K and 300 K using high resolution neutron powder diffraction techniques. Both nonsuperconducting oxygenated and superconducting Zr-gettered (T_c = 24 K with shielding and Meissner fractions of 30 and 16% at 5 K, respectively) samples were investigated to study the effect of Zr gettering on the crystal structure and oxygen stoichiometry. Unlike $La_2CuO_{4+\delta}$, where a bulk superconducting oxygen-rich phase separates from La_2CuO_4, we find that the structure remains tetragonal (I4/mmm) for both samples at both temperatures. Structure and oxygen stoichiometry of the oxygenated and Zr-gettered samples remain remarkably similar at both temperatures, the only difference being a slight decrease (within three standard deviations) in the thermal parameters of the rare earth ions along the c-axis for the superconducting sample. Thermogravimetric analyses confirm the oxygen stoichiometry determined from neutron data by refinement of the oxygen occupancies.

This appeared as Physical Review B40, 9370 (1989).

Instrument used: *(please type)*	Local contact:	Proposal number: *(for LANSCE use only)*
NPD	Robert Von Dreele	B 251

Title:

ON THE STRUCTURE OF THE β–FORM OF MoO_3

Report received: *(for LANSCE use only)*

Authors and affiliations:

John B. Parise, Mineral Physics Institute *and* Department of Earth and Space Sciences, State University of New York, StonyBrook, NY11794-2100 and Eugene M. McCarron III, E.I. DuPont de Nemours, Experimental Station, PO Box 80356, Wilmington, DE19880-0356, Robert B.Von Dreele,and Joyce Goldstone, LANSCE, Los Alamos National Laboratory, Los Alamos, NM 87545.

Experiment report:

Recently the results of a structural study (1) using neutron powder diffraction, were reported for a new form of molybdenum trioxide, β'-MoO_3. This material was derived from the removal of hydrogen from the intercalated $HMoO_3$. The metastable form of MoO_3, from which these materials are derived, can be prepared in bulk from at least two novel low temperature routes (2,3). This precursor form has been designated β-MoO_3. No report of structural refinement based on diffraction data have been published. However, strong circumstantial evidence (2) based on a variety of comparisons with WO_3, which crystallizes with the distorted ReO_3-type structure, suggested that β-MoO_3 also possesses this type of structure. We have carried out structural studies which confirm this suggestion.

β-MoO_3 was obtained from the heat treatment of freeze dried powder (3); this was derived from liquid obtained from passing a solution of $Na_2MoO_4.2H_2O$ through a cation exchange column loaded with Rexyn 101(H).

Both high resolution neutron and x-ray diffraction data were collected on the NPD instrument at LANSCE and the x-7a beamline at the National Synchrotron Light Source, Brookhaven. Both powder diffractograms could be indexed on the basis of a mixture of two phases - the thermodynamically stable α-MoO_3 and β-MoO_3 (Table I). Preliminary analysis of data from the 148° neutron data bank (Fig 1) confirms the structure to be of the ReO_3-type with atomic parameters reported in Table I. The structures of β– and β'-MoO_3 are related, that of β– being a disordered variant of β' ; both consist of corner shared arrays of MoO_6- octahedra and are related to the polymorphs of WO_3.

Experiment report *(continued)*:

Table I. Atomic parameters for β-MoO_3 ($P2_1/c$, a=7.122,b=5.374, c=5.565, β=91.88).

NAME	x	y	z	FRAC	$U_{ISO} \times 10^2$
O(1)	0.25890	0.07960	-0.00508	1.0	2.9(2)
Mo(1)	0.00000	0.00000	0.00000	1.0	3.2(3)
Mo(2)	0.50347	-0.02227	0.12281	0.5	1.0(2)
O(2)	-0.04191	0.28354	0.20849	1.0	0.4(2)
O(3)	0.56314	0.31810	0.79685	1.0	6.0(4)

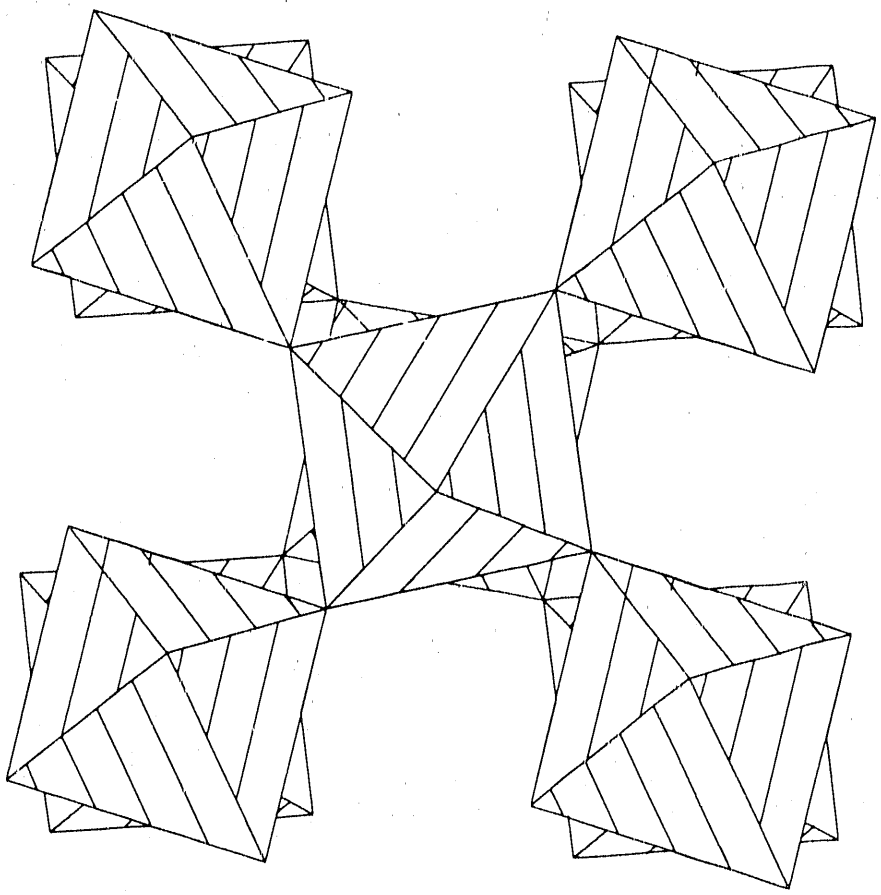

References:

References
1. Parise, J.B. et al Materials Res. Bull.,22, 803 (1987)
2. McCarron, E. M. III, J. Chem. Soc Chem. Comm., 336 (1986)
3. McCarron, E. M. III et al. Patent Pending (1990),

Instrument used: (please type)	Local contact:	Experiment no:
NPD	R. B. Von Dreele J. A. Goldstone	D-19.1

Title:

Neutron Powder Diffraction Study of Calcium-Ammonia Solvation Complexes in TiS_2

Authors and affiliations:

Report received:
(to be filled in by LANSCE)
2/2/90

E.W. Ong, V.G. Young Jr., G.L. Burr and W.S. Glaunsinger, Dept. of Chemistry, ASU;

R.B. Von Dreele and J.A. Goldstone, LANSCE, Los Alamos National Laboratory

Dates of experiment:

- ☒ Approved by external program committee
- ☐ Approved by internal program committee
- ☐ Part of LANSCE discretionary time

Experiment report:

$Ca_{0.132}(ND_3)_yTiS_2$ has been studied by neutron powder diffraction at both 20 and 300K. Due to the large contribution to the backgrounds from the quartz sample container, the data collections were not successful. The deuterium positions desperately needed were not resolvable for either sets of data. The 20K data set from the 148 detector bank is shown below. More work using the standard NPD vanadium containers with indium seal, without the quartz containment, is being requested.

Experiment report (continued):

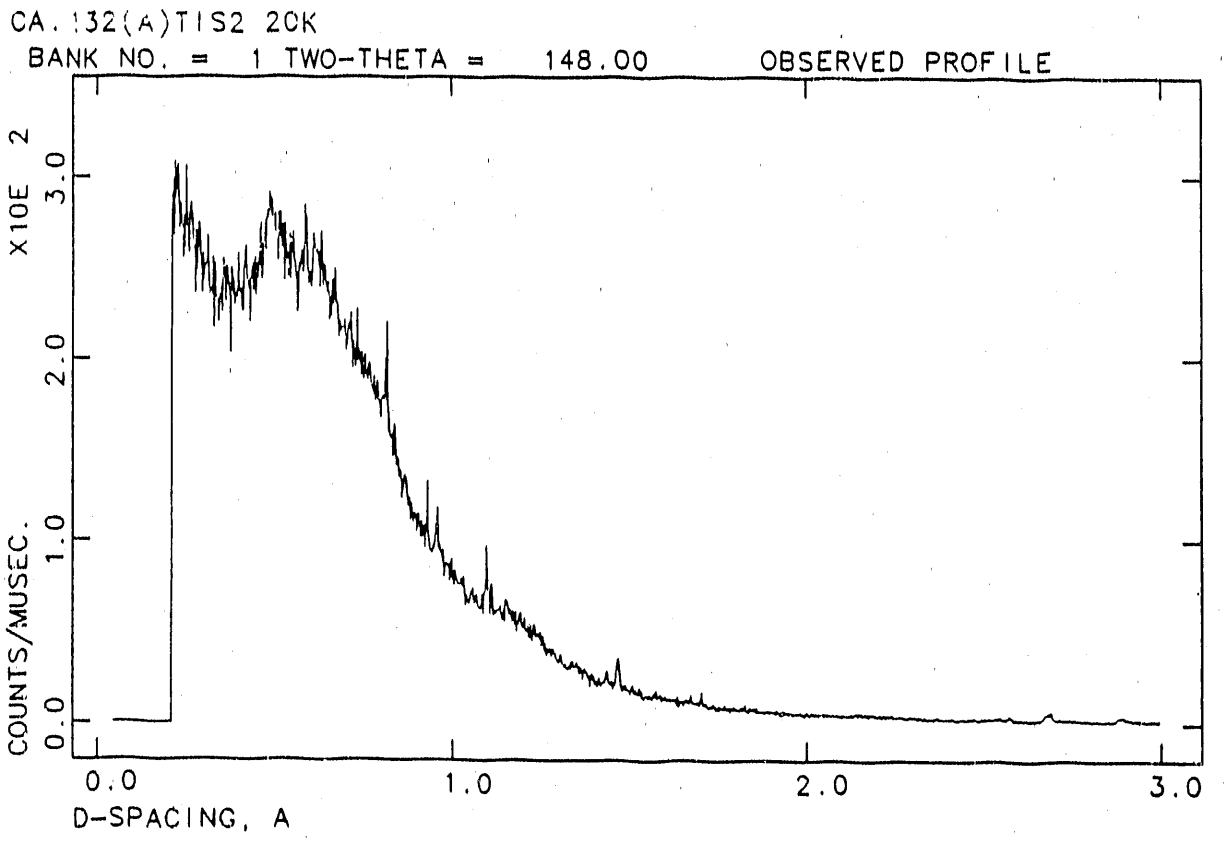

Los Alamos
Los Alamos National Laboratory
Los Alamos, New Mexico 87545

Form number 1195 (12/87)

Instrument used: (please type)	Local contact:	Experiment no:
NPD	R. B. Von Dreele J. A. Goldstone	D-19.2

Title:

Neutron Powder Diffraction Study of Calcium-Ammonia Solvation Complexes in TiS_2

Authors and affiliations:

Report received:
(to be filled in by LANSCE)
2/2/90

E.W. Ong, V.G. Young Jr., G.L. Burr and W.S. Glaunsinger, Dept. of Chemistry, ASU;

R.B. Von Dreele and J.A. Goldstone, LANSCE, Los Alamos National Laboratory

Dates of experiment:

- ☒ Approved by external program committee
- ☐ Approved by internal program committee
- ☐ Part of LANSCE discretionary time

Experiment report:

$Ca_{0.102}(ND_3)_y(ND_4^+)_{y'}TiS_2$ has been studied by neutron powder diffraction at both 20 and 300K. Due to the large contribution to the backgrounds from the quartz sample container, the data collections were not successful. The deuterium positions desperately needed were not resolvable for either sets of data. The 20K data set from the 148 detector bank is shown below.

Experiment report (continued):

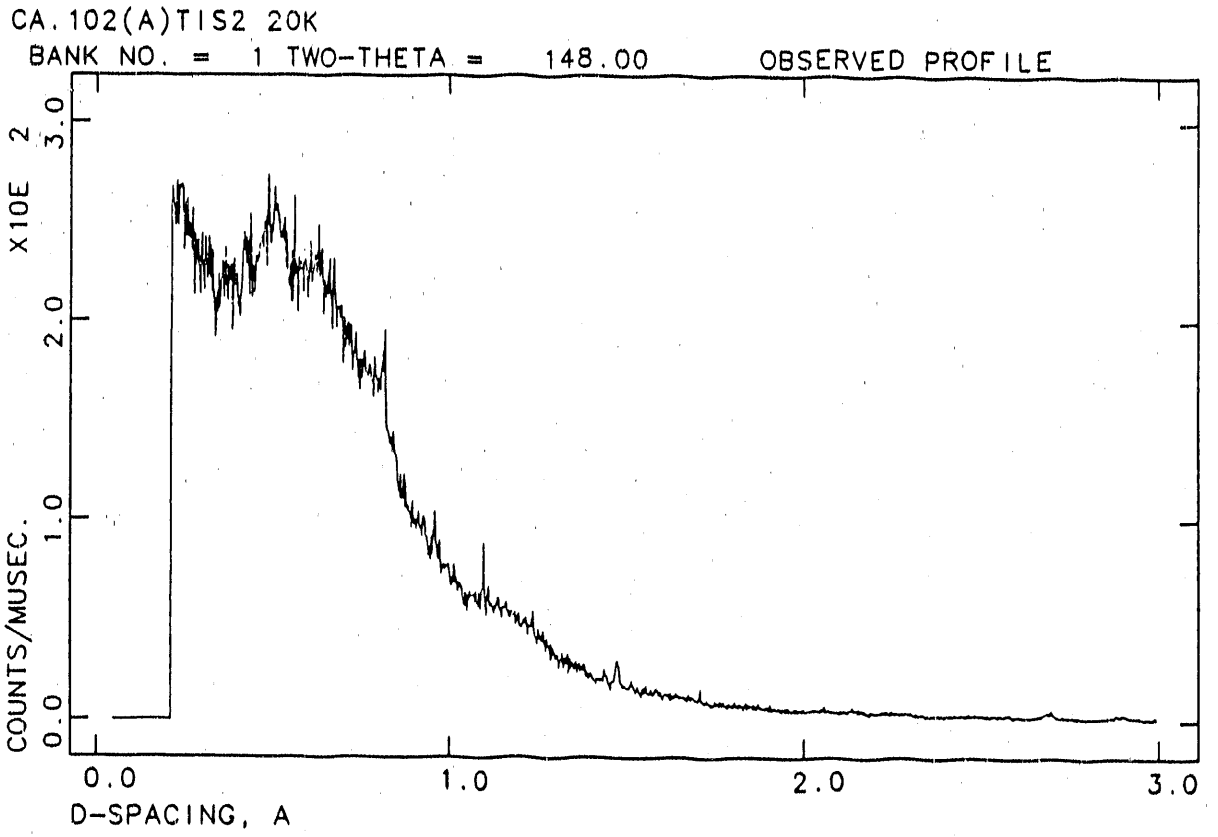

Instrument used: (please type)	Local contact:	Experiment no:
NPD	R.B. Von Dreele	203.1

Title: "Neutron Powder Diffraction Study of $(ND_4^+)_{0.25}(ND_3)_{0.62}TiS_2^{0.25-}$"

Authors and affiliations:

V.G. Young Jr. and W.S.Glaunsinger, Dept. of Chemistry, ASU;
M.J. McKelvy, Center for Solid State Science, ASU;
R.B. Von Dreele, LANSCE, Los Alamos National Laboratory

Report received:
(to be filled in by LANSCE)

Dates of experiment: July 20, 1989

- ☒ Approved by external program committee
- ☐ Approved by internal program committee
- ☐ Part of LANSCE discretionary time

Experiment report: $(ND_4^+)_{0.25}(ND_3)_{0.62}TiS_2^{0.25-}$ has been studied by neutron powder diffraction at both 300 and 20K. Due to the large contribution to the backgrounds from the quartz sample container, which was required to maintain the requisite ND_3 pressure over the sample, the data collections were not successful. In particular, the all important D positions were not resolvable for either data set. The 300K data set from the 148° detector bank is shown below. Further work using a newly fabricated vanadium sample container, which is capable of maintaining the required one atmosphere pressure of ND_3 over the above sample without the need for a quartz container, is anticipated.

Experiment report (continued):

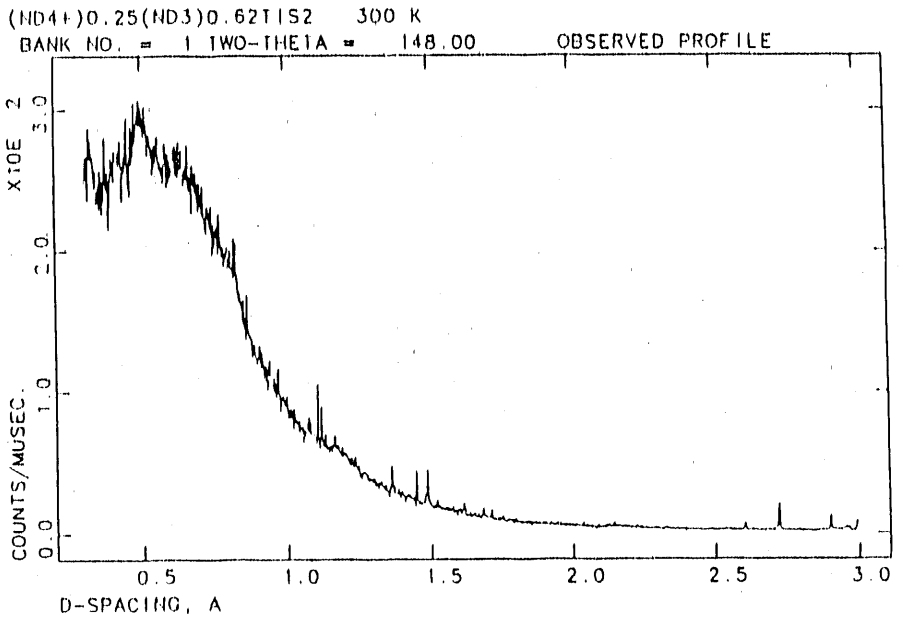

Los Alamos
Los Alamos National Laboratory
Los Alamos, New Mexico 87545

Form number 1195 (12/87)

Instrument used: (please type)	Local contact:	Experiment no:
NPD	R.B. Von Dreele	203.2

Title: " Neutron Powder Diffraction Study of $(ND_4^+)_{0.21}TiS_2^{0.21-}$

Authors and affiliations:

V.G. Young Jr. & W.S. Glaunsinger, Dept. Chemistry, ASU
M.J. McKelvy, Center for Solid State Science, ASU
R.B. Von Dreele, LANSCE, Los Alamos National Laboratory

Report received:
(to be filled in by LANSCE)

Dates of experiment:

July 21, 1989

- ☒ Approved by external program committee
- ☐ Approved by internal program committee
- ☐ Part of LANSCE discretionary time

Experiment report:

$(ND_4^+)_{0.21}TiS_2^{0.21-}$ has been studied by neutron powder diffraction at both 300 and 20K. The diffraction patterns are generally consistent with a six-layer trigonal unit cell with approximate cell parameters of a=3.41Å and c=41.8Å. The broad intensity band from 2.5 to 2.7Å, where the (107) and (108) reflections should reside, indicates significant local layer disorder for this intercalate [1]. We are presently working toward the solutions of these structures using Rietveld refinement. The 148° data taken at 20K is presented below.

[1] M.J. McKelvy, G.A. Wiegers, J.M. Dunn, V.G. Young Jr. and W.S. Glaunsinger, Solid State Ionics (submitted).

Experiment report (continued):

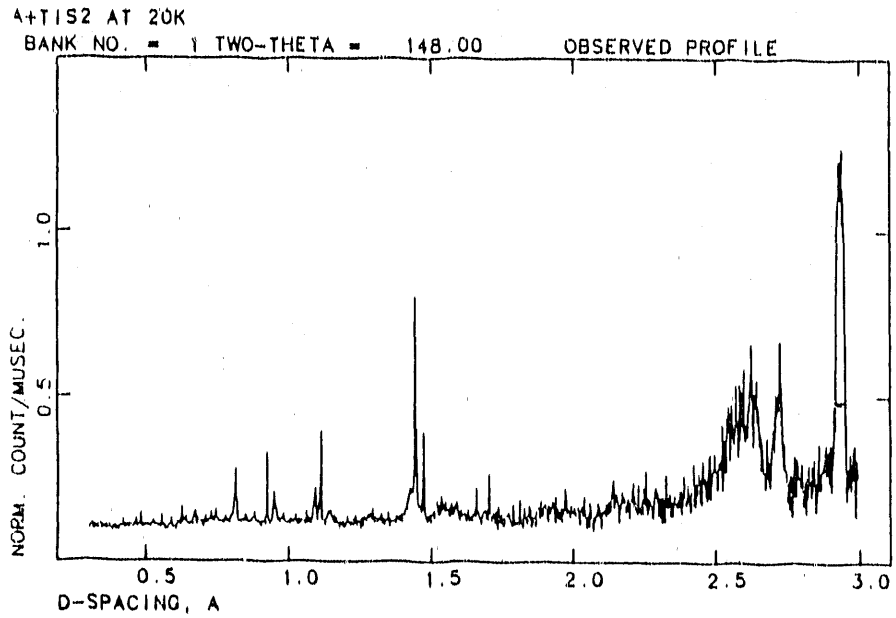

Los Alamos

Los Alamos National Laboratory
Los Alamos, New Mexico 87545

Form number 1195 (12/87)

Instrument used: (please type)	Local contact:	Experiment no:
HIPD	R.B. Von Dreele	203.3

Title: "Neutron Powder Diffraction Study of $(Na^{+})_{0.25}(ND_3)_{0.11}TiS_2^{0.25-}$"

Authors and affiliations:

G.L. Burr, V.G. Young, Jr., and W.S. Glaunsinger, Dept. of Chemistry, ASU
M.J. McKelvy, Center for Solid State Science, ASU
R.B. Von Dreele, LANSCE, Los Alamos National Laboratory

Report received: (to be filled in by LANSCE)

Dates of experiment: May 27, 1989

- ☐ Approved by external program committee
- ☐ Approved by internal program committee
- ☐ Part of LANSCE discretionary time

Experiment report:

$Na^{+}_{0.25}(ND_3)_{0.11}TiS_2^{0.25-}$ has been studied by neutron powder diffraction at 300 K. Due to the large contribution to the background from the quartz sample container used for this study, the data refinement was not sucessful. The locations of deuterium positions were not resolvable. The data set from the 153 degree detector bank is shown below. Furthur work using a vanadium sample container is anticipated.

Experiment report (continued):

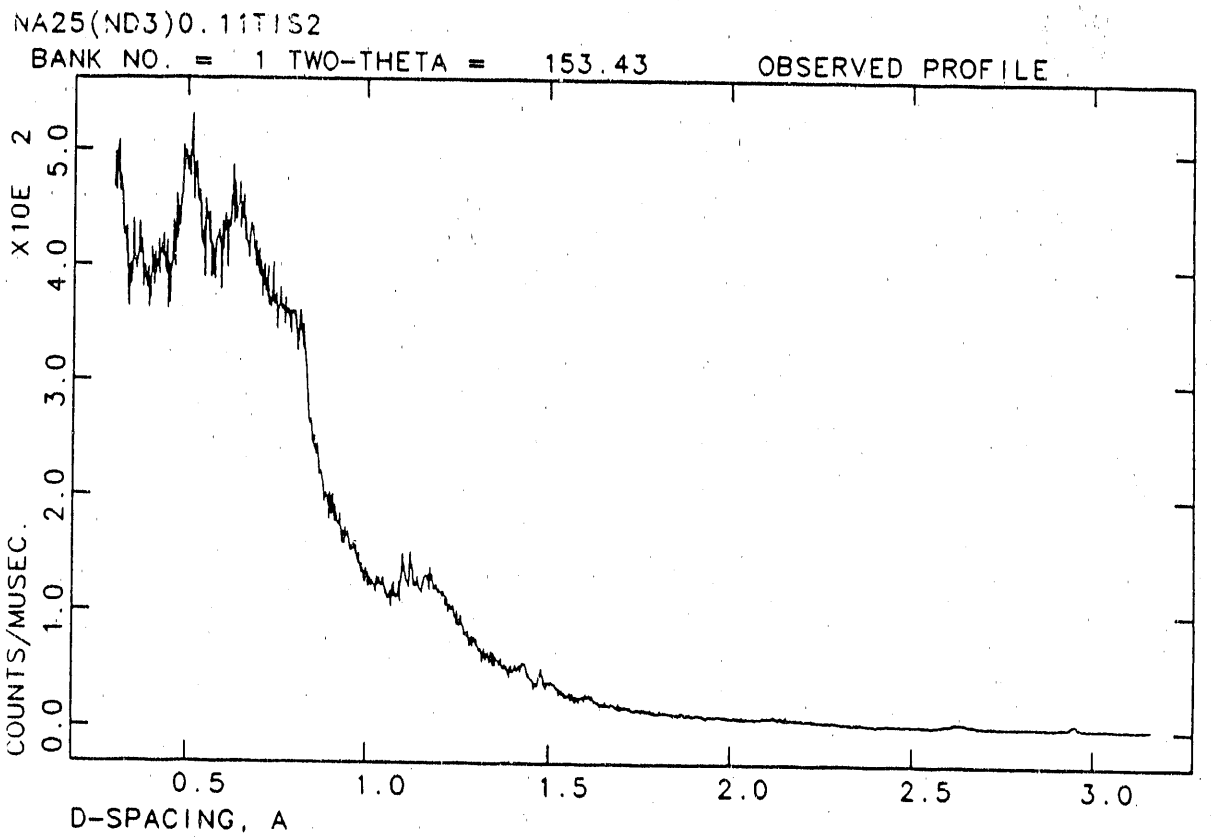

Los Alamos
Los Alamos National Laboratory
Los Alamos, New Mexico 87545

trument used: (please type)	Local contact:	Experiment no:
HIPD	R.B. Von Dreele	203.4

Title:
"Neutron Powder Diffraction Study of $(Na^+)_{0.25}(ND_3)_{0.75}TiS_2^{0.25-}$"

Authors and affiliations:

G.L. Burr, V.G. Young, Jr., and W.S. Glaunsinger, Department of Chemistry, ASU
M.J. McKelvy, Center for Solid State Science, ASU
R.B. Von Dreele, LANSCE, Los Alamos National Laboratory

Report received:
(to be filled in by LANSCE)

Dates of experiment: May 27, 1989

- ☐ Approved by external program committee
- ☐ Approved by internal program committee
- ☐ Part of LANSCE discretionary time

Experiment report:

$Na^+_{0.25}(ND_3)_{0.75}TiS_2^{0.25-}$ has been studied by neutron powder diffraction at 300 K. Due to the large contribution to the background from the quartz sample container required to maintain a ND_3 pressure above the sample, the data refinement was not sucessful. The locations of deuterium positions were not resolvable. The data set from the 153 degree detector bank is shown below. Furthur work using a newly fabricated vanadium sample container, which is capable of maintaining the required ammonia pressure above the sample without the need for a quartz container, is anticipated.

Experiment report (continued):

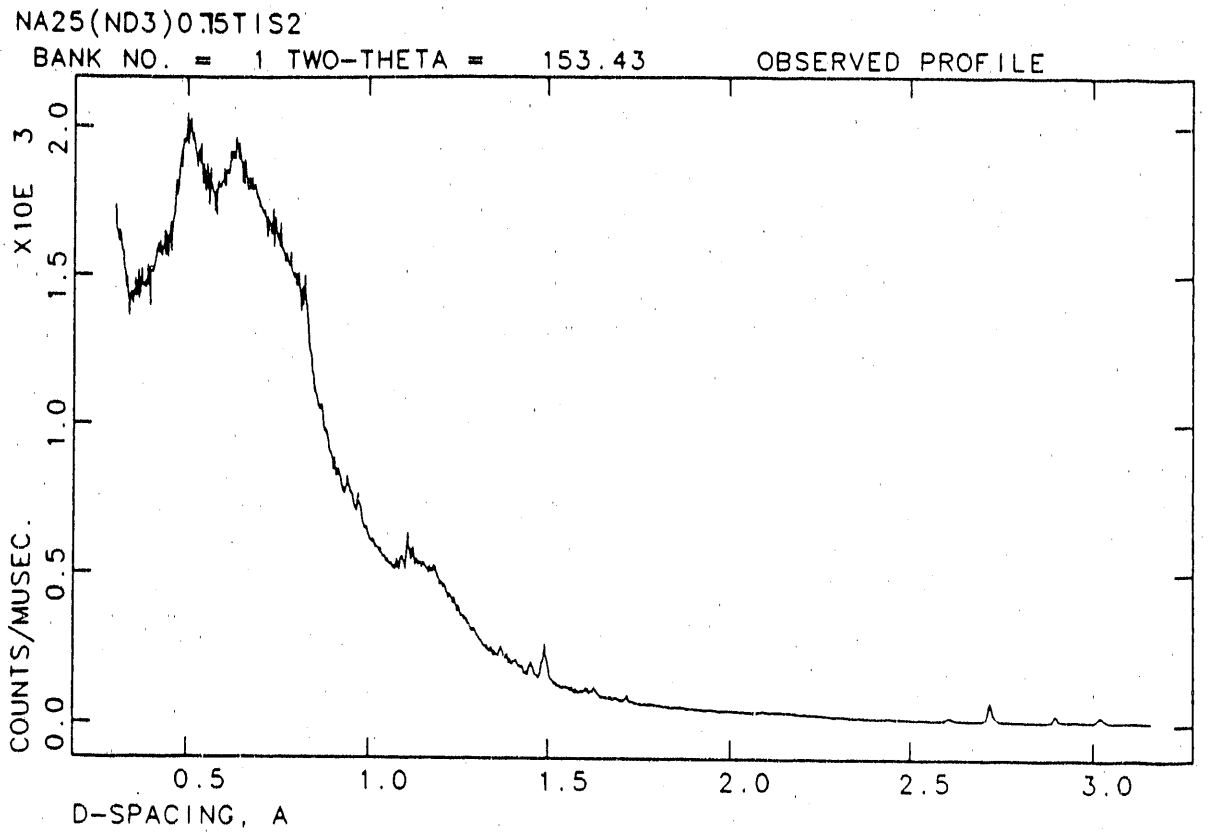

Los Alamos
Los Alamos National Laboratory
Los Alamos, New Mexico 87545

Form number 1195 (12/87)

Instrument used: *(please type)*	**Local contact:**	**Proposal number:** *(for LANSCE use only)*
NPD	Joyce A. Goldstone	218.0
Title: Neutron Diffraction Study of Neptunium Dideuteride		**Report received:** *(for LANSCE use only)*

Authors and affiliations:

J. A. Goldstone, Los Alamos National Laboratory, LANSCE MS H805, Los Alamos, NM 87545
A. C. Lawson, Los Alamos National Laboratory, MST-5 MS G730, Los Alamos, NM 87545
B. Cort , Los Alamos National Laboratory, NMT-5 MS E506, Los Alamos, NM 87545
E. Foltyn, Los Alamos National Laboratory, NMT-9, MS E502, Los Alamos, NM 87545

Experiment report:

This experiment started as a study of the phases of elemental neptunium. To avoid preferred orientation, we attempted to prepare a finely divided powder of Np metal through deuterating and dedeuterating bulk metal. Unfortunately, the dedeuterating process did not remove all the deuterium and the sample as prepared was essentially neptunium dideuteride. Data were collected on the sample over the temperature range of 15 to 620 K. This sample was an excellent deuteride, with little strain owing to the deuterating process in comparison to previous deuteride samples of Np. This sample was single phase and remained cubic over the entire temperature range investigated.

The structure is the classic CaF_2 ($Fm\bar{3}m$) in which there are two tetrahedral sites and one octahedral site per metal atom available for deuterium occupancy. Neutron diffraction data were fit using the Rietveld refinement code GSAS.[1] All diffraction data were successfully fit with using the space group $Fm\bar{3}m$ with neptunium occupying the (0,0,0) position and the deuterium in the (1/4,1/4,1/4) and (1/2,1/2,1/2) positions. No evidence of a phase transition to the tetrahedral structure observed in the higher deuterides of neptunium was observed.[2] Figure 1 shows a partial neutron diffraction pattern of NpD_2 at 15 K; the +'s are the observed data, the line through the data is the Rietveld fit, the lower curve is the difference between the observed data and the fit, and the vertical ticks mark the positions of allowed reflections for the space group. Figure 2 shows the lattice parameter versus temperature for all the runs; the fit through the data points is a parabola and the data seem to indicate a minimum in the lattice parameter around 240K. In addition to the lattice parameter data, the temperature dependence of the thermal displacement can be extracted from the fits. Figure 3 shows the thermal displacement versus temperature for both the neptunium and the tetrahedral site deuterium. The line drawn through each of the data sets is a Debye model fit to the thermal displacement with the extracted slopes, equal to Debye temperatures, given on the figure for each atom. The ratio of the Debye temperatures should be equal to the square root of the masses of the atoms; the mass ratio is 11 while the Debye temperature ratio is 7.

Experiment report *(continued)*:

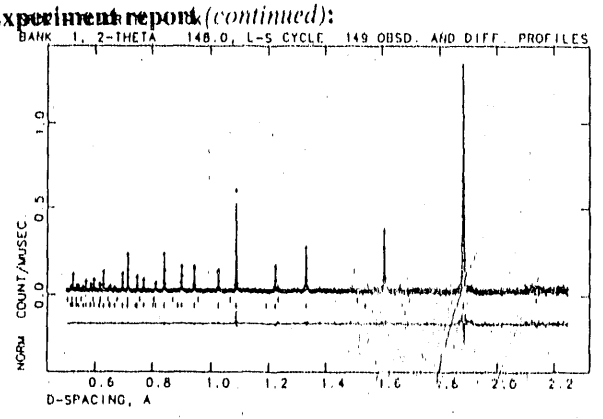

Figure 1: A partial neutron diffraction pattern of NpD_2 at 10 K; the +'s are the observed data, the line through the data is the Rietveld fit, the lower curve is the difference between the observed data and the fit, and the vertical ticks mark the positions of allowed reflections for the space group.

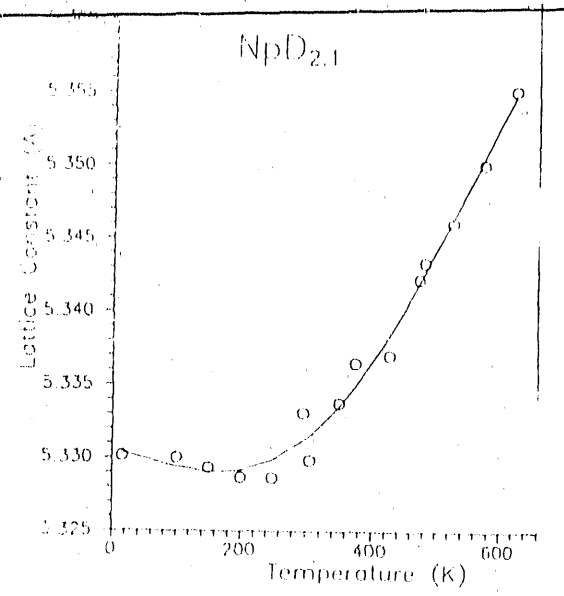

Figure 2: Lattice parameter versus temperature.

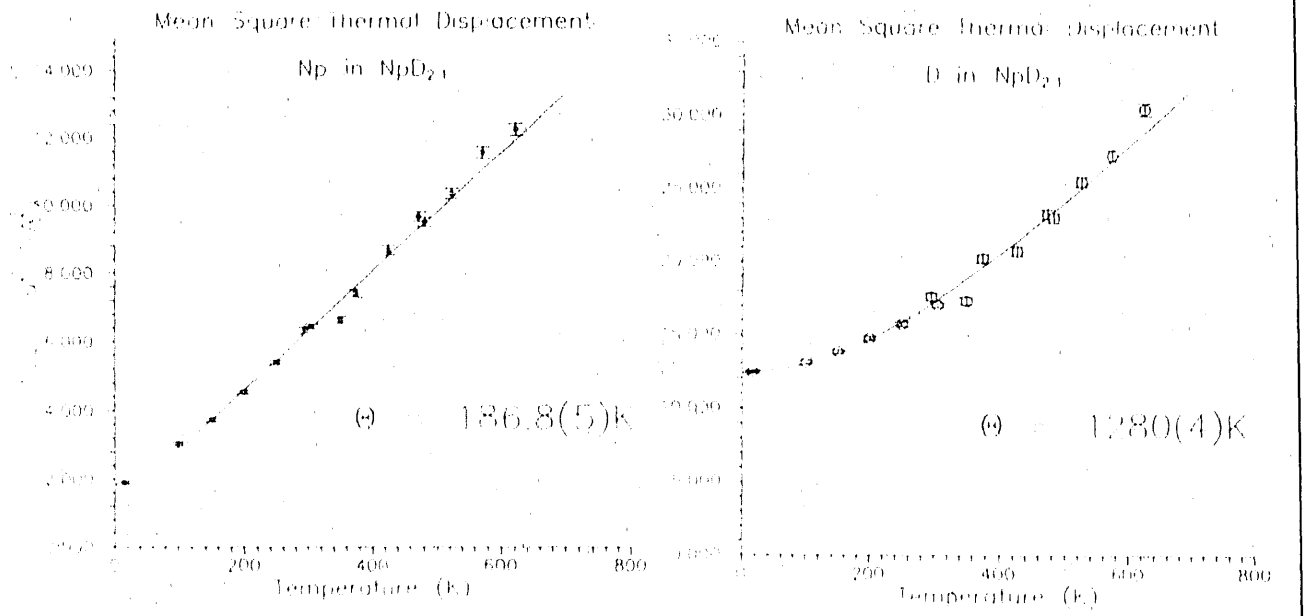

Figure 3: Thermal parameters for Np(left) and D(right) versus temperature with fitted Debye model and resultant Debye temperature.

References:

[1] A. C. Larson and R. B. Von Dreele, "Generalized Structure Analysis System", Internal Los Alamos Report, LA-UR 86-748

[2] J. A. Goldstone, Peter Vorderwisch, B. Cort, John W. Ward, and A. C. Lawson, "Optical Vibrational Frequency Distributions in Neptunium Hydride and Deuteride", Zeit. Phys. Chem. Neue Folge, **164** (1989) 1107.

Instrument used: *(please type)*	**Local contact:**	**Proposal number:** *(for LANSCE use only)*
NPD	Joyce A. Goldstone	226.0

Title:

Neutron Diffraction Study of Scandium Deuteride at Low Temperatures

Report received: *(for LANSCE use only)*

Authors and affiliations:

J. A. Goldstone, Los Alamos National Laboratory, LANSCE MS H805, Los Alamos, NM 87545
A. C. Lawson, Los Alamos National Laboratory, MST-5 MS G730, Los Alamos, NM 87545

Experiment report:

Scandium hydride behaves in a similar manner as the rare-earth dihydrides. The structure is the classic CaF_2 ($Fm\bar{3}m$) except that loading up to and beyond the dihydride composition under normal pressure conditions is not possible. In the $Fm\bar{3}m$ structure, there are two tetrahedral sites and one octahedral site per metal atom available for hydrogen occupancy. Only the tetrahedral site is observed to be occupied in scandium hydrides. Anomalous behavior has been reported in acoustic velocity measurements suggesting a phase transition around 240 K in $ScH_{1.99}$ [1]. ESR and x-ray data on $Sc_{0.995}Gd_{0.005}H_{1.98}$ indicate a possible phase transition below 140 K [2]. Since x-ray diffraction studies show no change in the scandium position nor the crystal structure, a neutron diffraction investigation was undertaken to examine possible changes in the position of the deuterium and/or ordering of the deuterium on the tetrahedral site.

Neutron diffraction patterns were collected for a sample of $ScD_{1.98}$ over the temperature range of 15 to 305 K. Data were fit using the Rietveld refinement code GSAS.[3] All diffraction data were successfully fit with using the space group $Fm\bar{3}m$ with scandium occupying the (0,0,0) position and the deuterium in the (1/4,1/4,1/4) position. No evidence of superlattice peaks arising from an ordering of the deuterium atoms was found. In addition, displacement of the deuterium off the high symmetry site to a more general (x,x,x) position did not improve the fit to the data. Figure 1 shows a partial neutron diffraction pattern of $ScD_{1.98}$ at 15 K. Figure 2 shows the lattice parameter versus temperature for all the runs; no indication of an anomalous change is observed over this temperature range. In addition to the lattice parameter data, the temperature dependence of the thermal displacement can be extracted from the fits. Figure 3 shows the thermal displacement versus temperature for both the scandium and the deuterium. The line drawn through each of the data sets is a Debye model fit to the thermal displacement with the extracted slopes, equal to Debye temperatures, given on the figure for each atom. The ratio of the Debye temperatures should be equal to the square root of the masses of the atoms; the mass ratio is 4.7 while the Debye temperature ratio is 3.7, so reasonable agreement exists.

The absence of a contraction of the lattice parameter at low temperatures in this $ScD_{1.98}$ sample does not rule out the possibly of a contraction of the lattice parameter in the scandium hydrides; this effect may be

Experiment report *(continued)*:
strongly isotope dependent. It may be worthwhile to investigate scandium hydride using neutron diffraction, a considerably more tedious task.

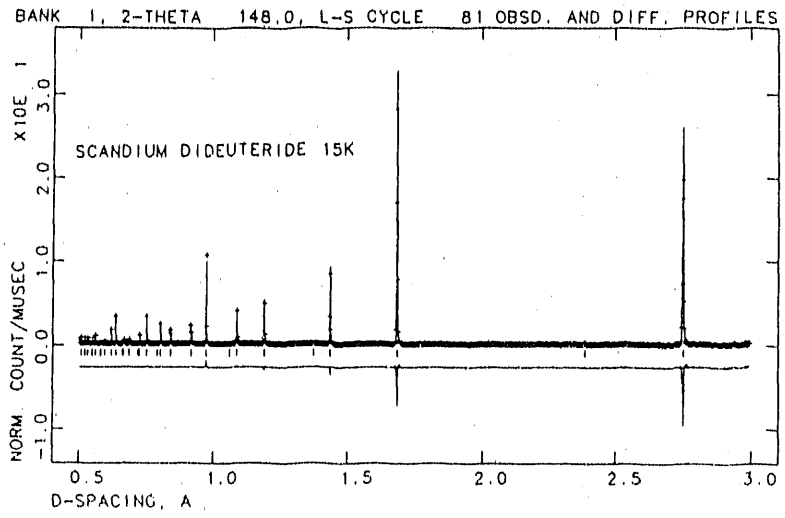

This figure shows a partial neutron diffraction pattern of ScD_2 at 15K; the +'s are the observed data, the line through the data is the Rietveld fit, the lower curve is the difference between the observed data and the fit, and the vertical ticks mark the positions of allowed reflections for the space group.

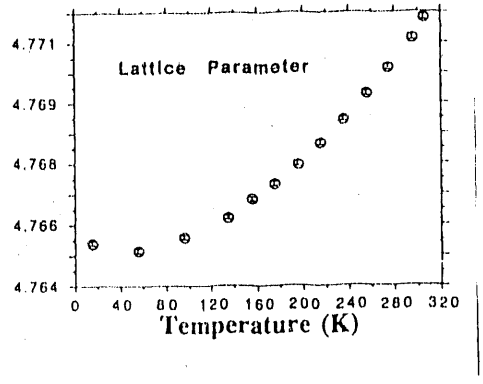

Figure 2: Lattice parameter versus temperature

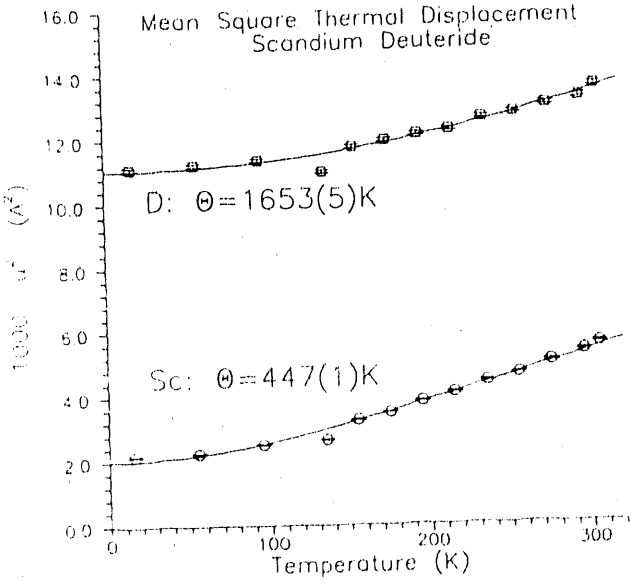

Figure 3: Thermal paramters versus temeprature with fitted Debye model (solid line) and resultant Debye temperature θ_D.

References:

[1] A. G. Beattie, J. Appl. Phys. 43 (1972) 3219.
[2] E. L. Venturini and B. Morosin, Physics Letters 61A (1977) 326.
[3] A. C. Larson and R. B. Von Dreele, "Generalized Structure Analysis System", Internal Los Alamos Report, LA-UR 86-748

Instrument used: *(please type)*	Local contact:	Proposal number: *(for LANSCE use only)*
NPD	Joyce A. Goldstone	2270

Title:

Investigation of Vacancies in High-Purity α-Plutonium

Report received: *(for LANSCE use only)*

Authors and affiliations:

J. A. Goldstone, Los Alamos National Laboratory, LANSCE MS H805, Los Alamos, NM 87545
A. C. Lawson, Los Alamos National Laboratory, MST-5 MS G730, Los Alamos, NM 87545
B. Cort , Los Alamos National Laboratory, NMT-5 MS E506, Los Alamos, NM 87545

Experiment report:

The existence of vacant sites in the α-phase of pure plutonium (monoclinic cell) has been inferred from neutron diffraction studies on GPPD at IPNS of pure plutonium. The reduced chi-squared value of the fit decreased by approximately a factor of two when vacancies were included. The objective of this investigation was to determine the location of the vacancies in the monoclinic lattice of a high purity, single phase α-plutonium sample. Neutron diffraction data (see figure) were collected on this sample at 305 and 15 K. Data were fit using the Rietveld refinement code GSAS [1] and the space group $P2_1/m$. All the eight types of Pu atoms in this cell occupy (x,1/4,z) type positions.

The diffraction patterns were fit under the following conditions: (1) site occupancies were varied independently and the thermal parameters of all Pu atoms were varied independently, but isotropic values were used; (2) site occupancies were fixed at 1 (full) and the thermal parameters of all Pu atoms were varied independently, but isotropic values were used; (3) site occupancies were independently varied and the thermal parameters of all Pu atoms were set equal and isotropic and varied; and (4) site occupancies were independently varied and anisotropic thermal parameters of all Pu atoms and varied independently. Tables 1 and 2 show the results of these fits for the 305 K data.

Table 1: Fraction and Isotropic Thermal parameters for Pu at ambient

			Uiso and fraction varied independently		Uiso constrained		Fraction constrained	
Atom #	x	z	Uiso	Frac	Uiso	Frac	Uiso	Frac
1	0.3381(2)	0.1585(1)	0.0102(3)	1.000	0.00775(9)	1.000	0.0084(2)	1.000
2	0.7730(2)	0.1717(1)	0.0112(4)	0.997(8)	"	0.986(5)	0.0093(3)	"
3	0.1336(2)	0.3399(1)	0.0044(3)	0.950(7)	"	1.013(5)	0.0053(2)	"
4	0.6573(2)	0.4544(1)	0.0053(3)	0.946(7)	"	0.998(5)	0.0068(2)	"
5	0.0293(1)	0.6202(1)	0.0078(4)	0.972(7)	"	0.998(5)	0.0075(3)	"
6	0.4688(2)	0.6511(1)	0.0084(4)	0.960(8)	"	0.974(5)	0.0091(3)	"
7	0.3289(2)	0.9265(1)	0.0083(4)	0.994(8)	"	1.017(5)	0.0068(2)	"
8	0.8715(2)	0.8955(1)	0.0070(4)	0.926(7)	"	0.958(5)	0.0094(2)	"
χ_r^2 / R_{wp}			1.264 / 3.02%		1.276 / 3.02%		1.273 / 3.04%	

Experiment report *(continued)*:

Table 2: Fraction and Anisotropic Thermal parameters for Pu at ambient

Atom #	x	z	U11	U22	U33	U13	Frac
1	0.3379(1)	0.1590(1)	0.0079(6)	0.0125(7)	0.0094(6)	0.014(5)	1.000
2	0.7726(2)	0.1716(1)	0.0103(7)	0.0120(8)	0.0086(8)	-0.0018(5)	0.995(8)
3	0.1340(2)	0.3403(1)	0.0065(6)	0.0027(60	0.0040(6)	0.0009(5)	0.948(7)
4	0.6574(2)	0.4544(1)	0.0067(6)	0.0080(6)	0.0056(6)	0.0027(4)	0.961(8)
5	0.0287(2)	0.6198(1)	0.0064(6)	0.0067(7)	0.0078(7)	0.0008(5)	0.967(7)
6	0.4687(2)	0.6514(1)	0.0130(7)	0.0126(9)	0.0052(7)	0.0035(5)	0.976(9)
7	0.3290(2)	0.9266(1)	0.0084(6)	0.0068(6)	0.0058(6)	0.0011(5)	0.980(8)
8	0.8717(2)	0.8954(1)	0.0063(7)	0.0108(7)	0.0074(7)	-0.0041(5)	0.931(7)
χ_r^2 / R_{wp}			1.241 / 2.99%				

The changes in χ_r^2 and R_{wp} are insignificant among these various fits. From these data, no conclusive evidence for the existence of vacant sites in α-plutoniun has emerged. Comparison of these results to the results obtained from the IPNS data on a different pure Pu sample show no systematic agreement on the location of vacancies in Pu It is concluded that it is best to set the vacancy concentration to zero.

In addition, the extra low temperature peak, observed in a different sample on HIPD [2], was not observed in this sample and addition experiments on NPD on the other sample did not show this extra peak.

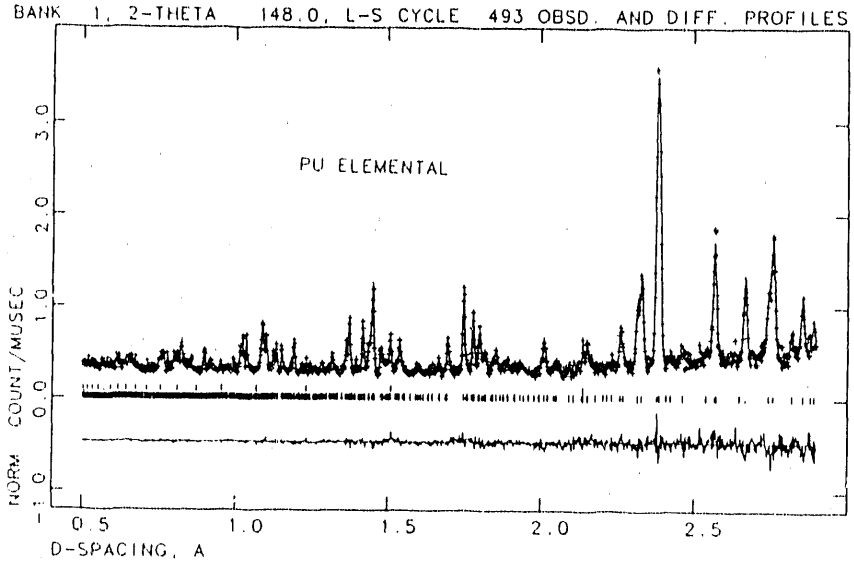

This figure shows a partial neutron diffraction pattern of α-Pu at 15 K; the +'s are the observed data, the line through the data is the Rietveld fit, the lower curve is the difference between the observed data and the fit, and the vertical ticks mark the positions of allowed reflections for the space group . The upper set of vertical ticks refers to the second phase evident in the diffraction pattern which arises from the double-walled vanadium encapsulation.

References:

[1] A. C. Larson and R. B. Von Dreele, "Generalized Structure Analysis System", Internal Los Alamos Report, LA-UR 86-748

[2] A. C. Lawson, A. Williams, B. Cort, LANSCE Experiment Reports LA-111638-PR (1988) 8.

Instrument used: *(please type)*	Local contact:	Proposal number: *(for LANSCE use only)*
NPD	Joyce Goldstone Robert Von Dreele	235.0

Title:	Report received: *(for LANSCE use only)*
Crystal Structures of CF_4	

Authors and affiliations:

Bruce Torrie, Department of Physics, University of Waterloo, Waterloo, Ontario, Canada N2L 3G1

Joyce Goldstone, Robert Von Dreele and Allen C. Larson, LANSCE, Los Alamos National Laboratory

Experiment report:

The crystal has a plastic phase and a fully ordered phase with a transition temperature of 76.2 K and a melting point of 89.5 K. X-ray studies [1] have been performed on both phases but grain growth occurs rapidly in the upper phase so only six reflections were measured and the intensities of these were not reliable. The structure of the upper phase, based on these results, is likely monoclinic, which is unusual for a plastic phase, but the pattern could not be indexed. For the low temperature structure, the space group $P2_1/C$ was originally chosen but the X-ray diffraction data was later reinterpreted in terms of a unit cell with space group C2/C [2].

CF_4 gas was transformed to a solid in a copper coil surrounded by liquid nitrogen. On melting the CF_4 was transferred to a vandium can immersed in liquid nitrogen where it rapidly refroze. The sample was then inserted in a top loaded cryostat and cooled to 4.2 K. After the first profile was recorded, the sample was warmed to 82 K and a series of profiles were recorded while the temperature remained constant. Total recording time for this phase was thirty hours and the ratio of peak intensity to background intensity decreased continuously.

The ordered low temperature phase was analyzed using GSAS [3] and the results confirm the X-ray results, as reinterpreted, but the accuracy of the present work is much greater and anisotropic thermal parameters were refined (not thermal parameters are given in reference [1]). Only seventeen peaks were clearly observed for the plastic phase and these are consistent with the six peaks seen previously with X-rays. Attempts have been made to index these peaks but none of the indexing schemes tried to date seem reasonable.

Experiment report: *(continued)*

References:

1. D.N. Bol'shutkin, V.M. Gasan, A.I. Prokhvatilov and A.I. Erenburg, Acta Crystallogr. B28, 3542 (1972).
2. Y.A. Sataty, A. Ron and F.H. Herbstein, J. Chem. Phys. 62, 1094 (1975).
3. A.C. Larson and R.B. Von Dreele, LAUR 86-748.

Instrument used: *(please type)*	Local contact:	Proposal number: *(for LANSCE use only)*
NPD	Robert Von Dreele	236.1

Title:

Structure Refinement of the Complex Rare Earth Oxides - Pr_9O_{16}

Report received: *(for LANSCE use only)* 1/31/90

Authors and affiliations:

Robert B. Von Dreele — LANSCE, MS H805, Los Alamos National Laboratory, Los Alamos, NM 87545

Leroy Eyring — Department of Chemistry, Arizona State University, Tempe, AZ 85287

Experiment report:

Two forms of the oxygen deficient rare earth oxide Pr_9O_{16} ("zeta" phase) were examined at room temperature on NPD. The "high temperature" form (annealed at 400°C) (Figure 1) was subsequently found to contain a considerable amount of $Pr_{10}O_{18}$ ("epsilon" phase). Because of the complexity of these two phases and their very great similarity no further analysis of the neutron diffraction data has been attempted. The "low temperature" form (Figure 2) is probably similarly contaminated but it is evident from a comparison ot the two patterns that it has a different structure than the high temperature form. Electron microscopy work currently in progress at Arizona State University suggest that the high temperature form slowly converts over many days to the low temperature form. A reexamination of "well aged" low temperature zeta phase material is warranted as this data shows the broadening effects of a high defect density.

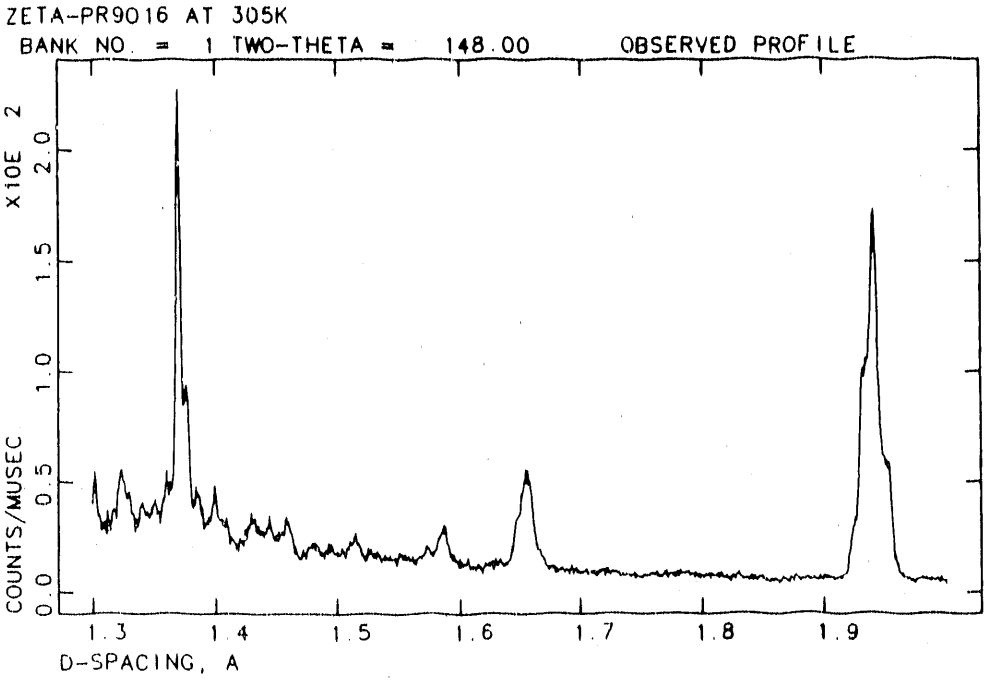

Experiment report *(continued)*:

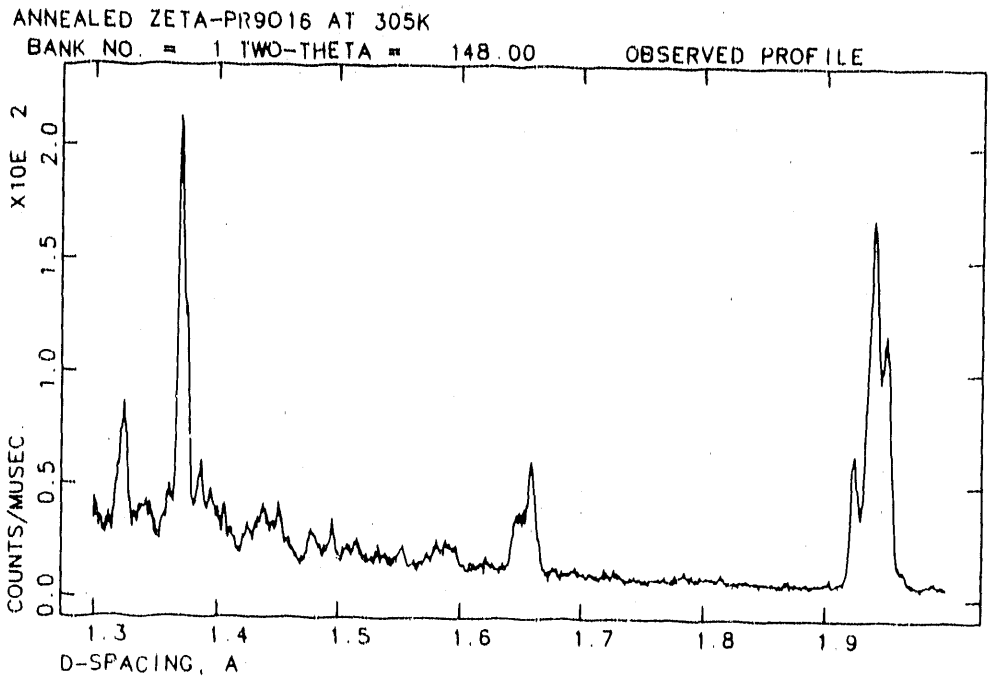

References:

Instrument used: *(please type)*	Local contact:	Proposal number: *(for LANSCE use only)*
NPD		236.2

Title:

Structure Refinement of the Complex Rare Earth Oxides - $Tb_{11}O_{20}$

Report received: *(for LANSCE use only)* 1/31/90

Authors and affiliations:

Robert B. Von Dreele — LANSCE, MS H805, Los Alamos National Laboratory, Los Alamos, NM 87545

Leroy Eyring — Department of Chemistry, Arizona State University, Tempe, AZ 85287

Experiment report:

The oxygen deficient rare earth oxide $Tb_{11}O_{20}$ ("delta" phase) was examined at room temperature on NPD. The diffraction pattern was first indexed as a pseudo-cubic cell for the sublattice reflections in the space group $F\bar{1}$ and a Rietveld refinement performed to give the lattice parameters: a=5.2874(2), b=5.2818(4), c=5.2856(3)Å, α=90.038(3), β=90.651(4), γ=89.473(5)°
The residuals for this fit were 11.6% for two histograms (+148° and +90° banks) and the agreement (Figure) was quite good over the sublattice reflections as anticipated. Transformation of this lattice to the true triclinic cell containing $Tb_{11}O_{20}$ was effected by the transformation:

$$\begin{bmatrix} 1 & -1/2 & 1/2 \\ 1/2 & 3/2 & -1/2 \\ -1/2 & 1 & 1 \end{bmatrix}$$

to give the lattice parameters:
a=6.5192, b=9.8779, c=6.4400Å, α=89.762, β=99.987, γ=96.326, V=405.89Å^3
in good agreement with earlier electron microscopic results. Analysis of the possible locations of the two oxygen vacancies within this unit cell with space group P1 shows that there is four possible models.
One of these has a 6-coordinated Tb atom and the others have only 7-coordinated Tb atoms. Work is continuing on this analysis.

Experiment report *(continued)*:

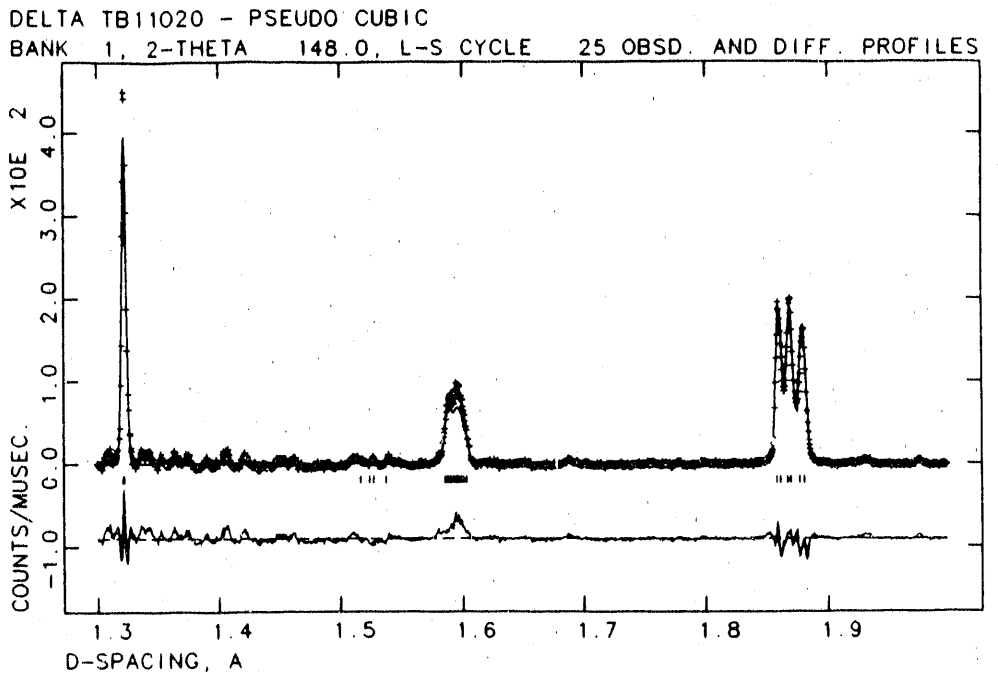

References:

Instrument used:	Local Contact:	Proposal number *(for LANSCE use only)*
NPD	Joyce A. Goldstone	252.0

Title:	Report received: *(for LANSCE use only)*
Evaluation of Strained Specimens by Neutron Diffraction	

Authors and affiliations:

Y. D. Harker, Mail Stop 7112, EG&G Idaho, Inc.,P.O. Box 1625, Idaho Falls, ID 83415
W. G. Reuter, Mail Stop 2210, EG&G Idaho, Inc., P.O. Box 1625,Idaho Falls, ID 83415
R. E. Schmunk, Mail Stop 7112, EG&G Idaho, Inc.,P.O. Box 1625, Idaho Falls, ID 83415
A. C. Lawson, MST-5, MS H805, Los Alamos National Laboratory, Los Alamos, NM 87545
Joyce A. Goldstone, LANSCE, MS H805, Los Alamos National Laboratory, Los Alamos, NM 87545

Experiment report

We conducted experiments on two samples: (a) a stainless steel rectangular bar with a notch machined to produce a stress field at the base of the notch and (b) a copper bar pulled in planar tension. Experiments with the stainless bar prove infeasible owing to the path length in in the stainless steel part.

We obtained data on the rectangular copper bar in an unstressed and stressed condition using the Neutron Powder Diffractometer (NPD) at LANSCE. The probed region (0.3 cm x 0.3 cm x 5 cm high) of the bar was defined by collimators in the incident and scattered beams. The volume excluded the surface to avoid non-uniformity of the strains near the surface region. The bar was stressed to 1% and 2% macroscopic strain in the direction perpendicular to the 5 cm height and in the plane of the bar. The bar was aligned at 45 degrees to the incident neutron beam and data were collected in only the ± 90° detector banks (see figures 1 and 2).

The geometrical arrangement of the sample and collimators permitted the measurement of the anisotropic response of the copper bar. Only the crystal planes whose normals bisect the incident and scattered beam directions will contribute to the measured diffraction pattern. This implies that given set of {hkl} planes, one detector bank (in the figure the -90°) will only see diffracting planes which are perpendicular to the applied stress. The other detector bank will see only difracting planes parallel to the applied stress. Copper is known to have a have anisotropy in its response to applied stress. So a large difference in the two detector banks is expected in the shift of diffraction peaks from the unstressed to stressed states.

This anisotropy in the response of copper was clearly seen in the collected data. Preliminary analysis of thirteen diffraction peaks plainly show this effect. The shift of all the diffraction peaks in the -90° detector bank showed compression of the lattice spacings of the planes perpendicular to the applied stress while the +90° data confirmed the expected increase in lattice spacings of the planes parallel to the applied stress. The ratio of the strain in the perpendicular to parallel direction allow calculation of the effective Poisson's ratio for each {hkl}. This measurement also yields the value of the macroscopic Young's modulus. In addition, the precision of the method is confirmed by the agreement of strain calculated from a family of planes (eg., 111, 222, etc.) and the variation of the strain for different families of planes (eg. comparison of 111 to 100) was precisely measured (see table).

This experiment is a prototype and validation measurement for future work on residual stress determinations on many materials. The cleverness of the arrangement of the sample at 45° to the incident beam and the availability of the ±90° detector banks permits detailed information not only about the strain state of the material but also its anisotropic response. The analysis of these data are yet incomplete and comparison to model calculations is planned. However, a few conclusions can be drawn from the current progress on the analysis. High resolution neutron powder diffraction is an excellent non-destructive technique for the measurement of internal residual strain, hence stress. The

Experiment report: (continued)
nature of three-dimensional stress fields may be investigated since this technique samples grains with a specifically chosen crystallographic axis. This has been illustrated by the (hkl) dependence of the measured strain. the precise determination of the strain as a function of (hkl) will allow comparison with calculational models.

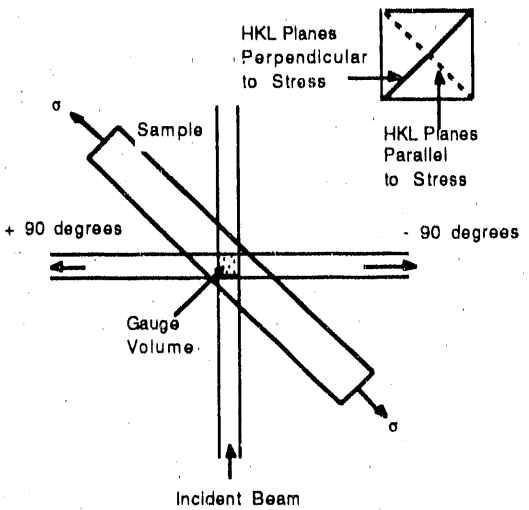

Figure1: Diffraction arrangements for strain measurements. The inset illustrates the diffraction planes giving rise to the +90° (⊥ planes) and -90° (|| planes)

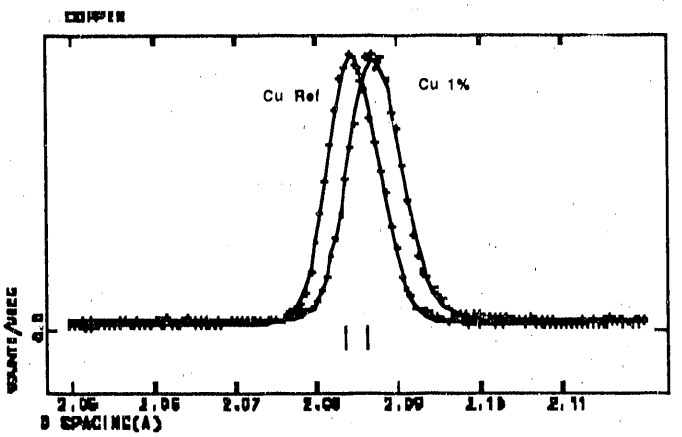

Figure 2: (111) diffraction peak of the reference and 1% strained copper bar. The ticks marks indicate the peak position.

Representative Shifts in Cu Diffraction Peaks

h k l	$[d - d_{(ref)}] / d_{(ref)}$ +90°	$[d - d_{(ref)}] / d_{(ref)}$ -90°
1 1 1	0.119(3)%	-0.097(7)%
2 0 0	0.209(3)%	-0.150(5)%
2 2 0	0.130(4)%	-0.117(3)%
2 2 2	0.113(5)%	-0.112(13)%

References:

Instrument used: *(please type)*	Local contact:	Proposal number: *(for LANSCE use only)*
NPD	R. B. Von Dreele	257.0

Title:	Report received: *(for LANSCE use only)*
Neutron Powder Diffraction Study of BeThN2	

Authors and affiliations:

Nathaniel E. Brese and Michael O'Keeffe
Department of Chemistry
Arizona State University
Tempe, AZ 85287 USA

Experiment report:

Juza and his co-workers synthesized BeThN2 by reacting Be_3N_2 and Th_3N_4 at 1500C and determined its hexagonal unit cell parameters to be a = 10.501 and c = 3.955 with Z = 8 (density 9.07) (1). They were unable to determine the structure (or even the spacegroup) of this material.

In order to maximize the Th-Th distances along the unique direction, we chose the acentric spacegroup P3m1. Thorium atoms positions were determined by guessing and minimizing the differences between the calculated and observed X-ray diffraction intensities using a simplex scheme (R =0.3). We are attempting a combined refinement of X-ray and time-of-flight neutron data. Currently, all but one of the N positions and the Be positions have been determined from difference Fourier maps. The Th atoms center fairly-regular capped trigonal prisms of N atoms. We are looking for tetrahedral sites for the Be atoms, since all known beryllium nitrides contain four-coordinate Be atoms.

Experiment report *(continued)*:

References:

1. A. -P. Palisaar and R. Juza, Z. Anorg. Allg. Chem. 384, 11 (1971).

Instrument used: *(please type)*	Local contact:	Proposal number: *(for LANSCE use only)*
NPD	R. B. Von Dreele	258.0

Title:

Neutron Powder Diffraction Study of Sr_2N

Report received: *(for LANSCE use only)*

Authors and affiliations:

Nathaniel E. Brese and Michael O'Keeffe
Department of Chemitry
Arizona State University
Tempe, AZ 85287 USA

Experiment report:

Sr_2N has been synthesized from the elements and its structure determined by time-of-flight neutron diffraction. Crystal data: $R\bar{3}m$, a = 3.8566(1), c = 20.6958(4) Å, V = 266.58(1) A^3, Z = 3, D_x = 2.13, T = 300 K, R_{wp} = 0.077, R_p = 0.056, reduced Chi-squared = 2.06 for 25368 profile points and 53 variables. Sr_2N crystallizes with the layered $CdCl_2$ structure as formerly proposed (1) (see Fig. 1). N atoms center flattened octahedra with six equal N-Sr distances of 2.6118(3) Å. The Sr-Sr distances in the octahedral layer are 3.8566(1) (6x) and 3.523(1) (3x). The Sr-Sr distances between layers are 4.726(1). It has been argued that Sr2N is actually $Sr_2N_xH_y$ (2,3), but the neutron data show the absence of any hydrogen contamination. Sr_2N is ametallic conductor with a weak temperature-independent paramagnetism.

Submitted to the Journal of Solid-State Chemistry.

Experiment report *(continued)*:

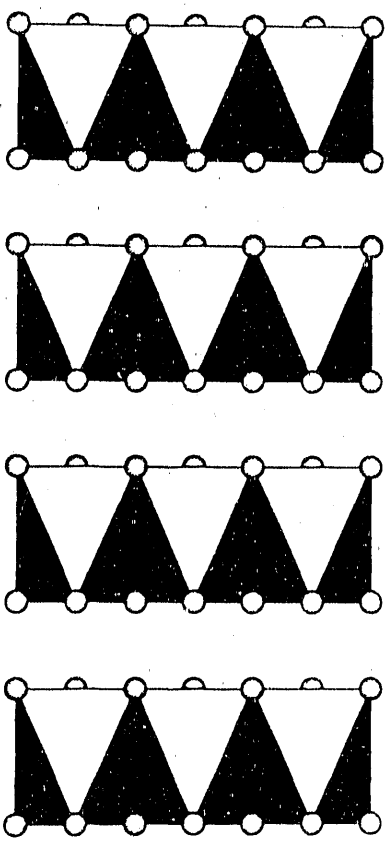

References:

1. J. Gaudé, P. L'Haridon, Y. Laurent and J. Lang, Bull. Soc. Fr. Mineral. Cristallogr. 95, 56 (1972).
2. J. -F. Brice, J. -P. Motte and J. Aubry, Rev. Chim. Miner. 12, 105 (1975).
3. F. Hulliger and F. Lévy (Eds.), Structural Chemistry of Layer-type Phases, D. Reidel, Dordrecht, Holland (1976)

Instrument used: *(please type)*	Local contact:	Proposal number: *(for LANSCE use only)*
NPD	R. B. VonDreele	260.0

Title:	Report received: *(for LANSCE use only)*
Structure of $BaCuO_2$	1/31/90

Authors and affiliations:

Daniel Partin and Michael O'Keeffe
Arizona State University

Experiment report:

According to the statistics of the GSAS package this refinement is complete, but when the potentials of the atoms are calculated it is obvious that somethis is amiss.

It was determined that the barium previously reported at 0,0,0 was not actually there, leaving a hole of greater than 7 A in diameter. This hole could possibly be occupied by CO_2 , as found in some of the 123 superconductors.

This necessitates that more work must be done to determine the composition.

Experiment report: *(continued)*

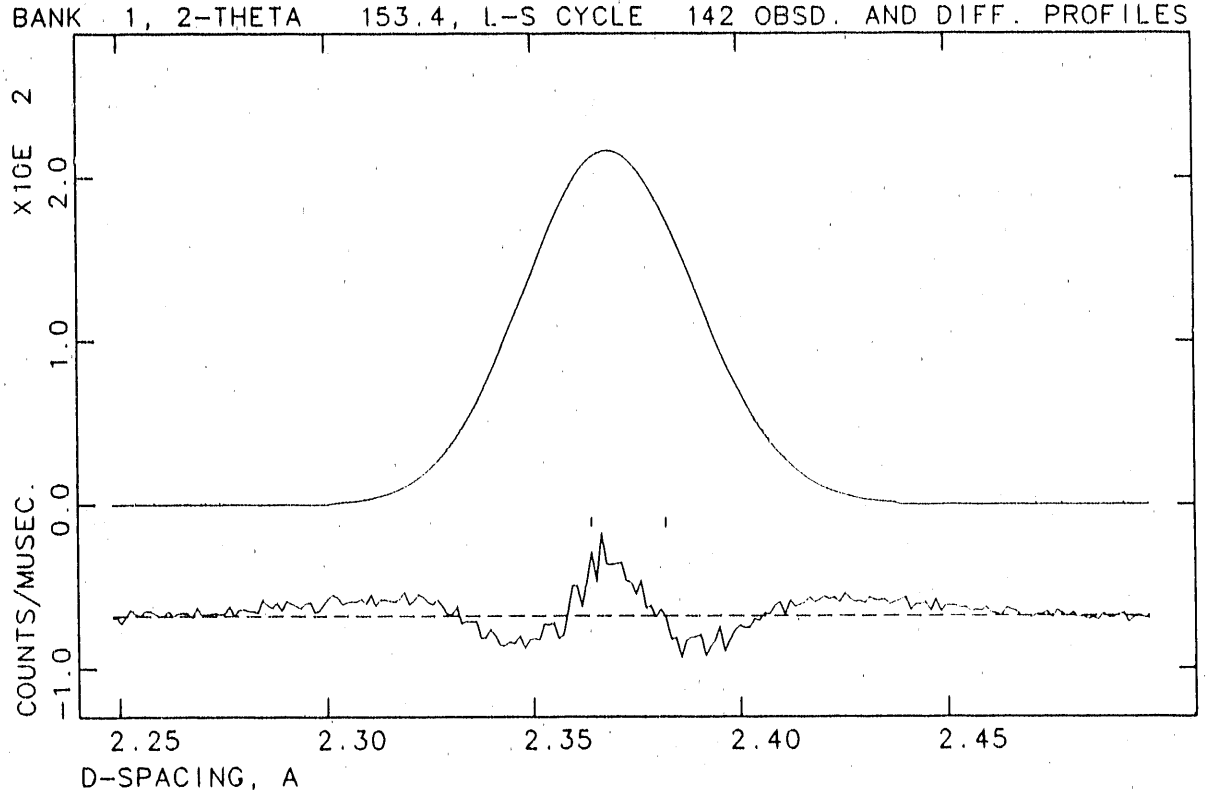

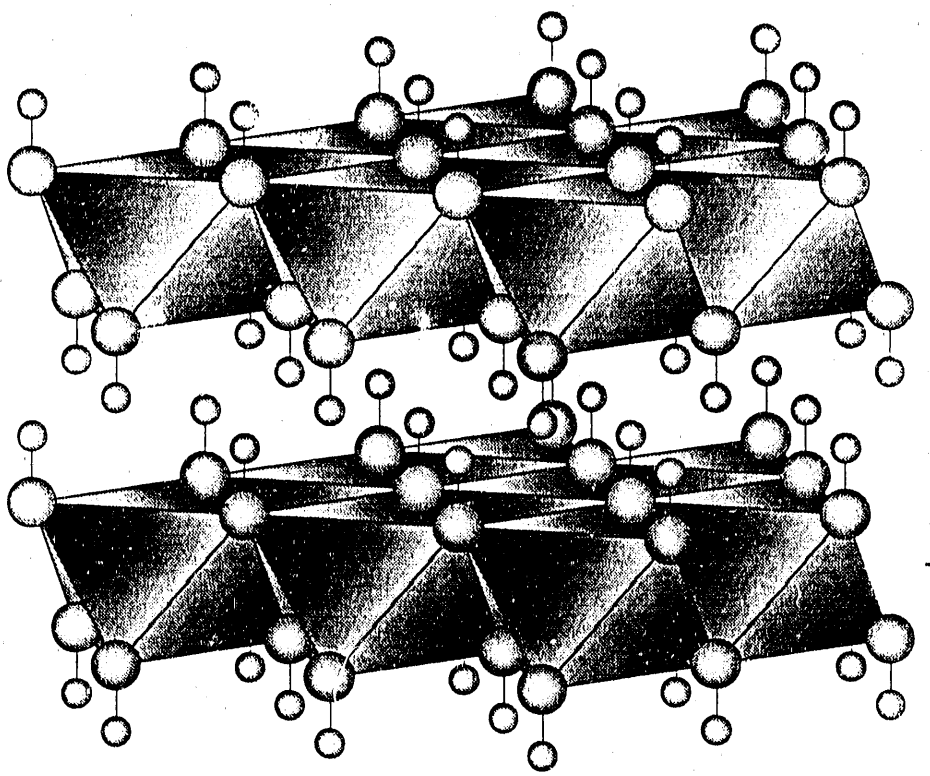

References:

Instrument used: *(please type)*	**Local contact:**	**Proposal number:** *(for LANSCE use only)*
NPD	R. B. Von Dreele	263.0
Title: Neutron Powder Diffraction Study of CuO		**Report received:** *(for LANSCE use only)*

Authors and affiliations:

Nathaniel E. Brese and Michael O'Keeffe
Department of Chemistry
Arizona State University
Tempe, AZ 85287 USA

R. B. Von Dreele
Manuel Lujan Neutron Scattering Center
Los Alamos, NM 87545 USA

Experiment report:

Time-of-flight neutron diffraction data were collected at 11K from a sample of CuO in a vanadium can. There is no evidence for magnetic ordering, although magnetic susceptiblity data show unusual behavior as CuO is cooled below room temperature. The final profile fit is shown in Fig. 1. Crystal data: $C2/c$, a = 4.6828(1) Å, b = 3.42052(7) Å, c = 5.1290(1) Å, β = 99.564(1)°, V = 81.013(4) Å^3, Z = 4, D_x = 6.52 , R_{wp} = 0.100, R_p = 0.073, reduced χ^2 = 2.319 for 11882 profile points from two detector banks (θ = 153, 90) using 43 variables. Cu atoms center rectangular planes of O atoms and form edge-sharing strings (distorted PdO structure). The Cu-O distances are 1.950(1) and 1.961(1) Å (each 2x) with corresponding O-Cu-O angles of 84.304(7)° and 95.696(7)°.

Experiment report: *(continued)*

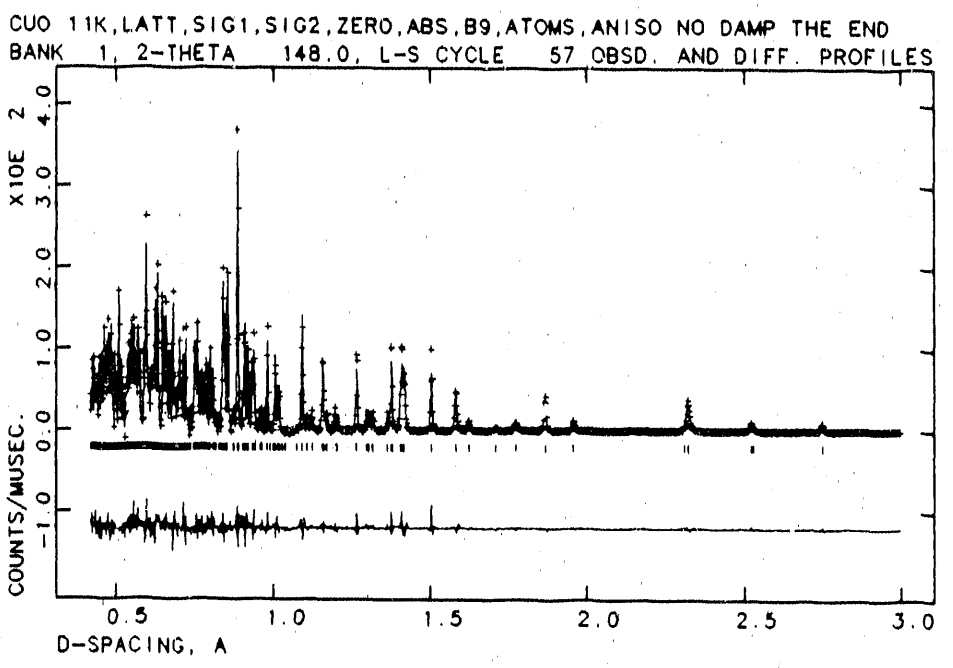

References:

Instrument used: *(please type)*	Local contact:	Proposal number: *(for LANSCE use only)*
NPD	Dr. Allen Larson	271.0

Title:

Electron density studies of Azidothymidine and related compounds.

Report received: *(for LANSCE use only)*

Authors and affiliations:

B. E. Robertson, Y. Y. Wei, R. J. Barton, University of Regina; A.C. Larson, LANSCE; L. Delbaere, S. Gupta, W. Quail, University of Saskatchewan.

Experiment report:

This experiment was of a preliminary nature, intending to explore the use of NPD for the collection of high quality neutron diffraction data for use in (X-N) deformation electron-density studies of organic compounds with biological activity, and which contain many hydrogen atoms.

A complete set of data was successfully obtained from the nucleoside analog, 5-methoxymethyl-2′-deoxyuridine. The compound is being developed for chemotherapeutic applications against the herpes viruses. It is very similar to azidothymidine (AZT), used against the human immunodeficiency virus, but is better suited for use in a first experiment because it contains only one molecule in the asymmetric unit of the structure, whereas AZT contains two molecules in the asymmetric unit.

The structure was partially refined while at LANSCE, using the crystallographic software currently under development at LANSCE; i.e., GSAS. It is intended that GSAS be installed on a VAX 8600 computer and that the refinement be completed in Regina as soon as time permits. However, the preliminary results of the refinement have provided much useful information.

The data was adequate for a conventional structural refinement of relatively low accuracy. We have attempted to use the hydrogen temperature factors in a parallel refinement using high-quality x-ray diffraction data, and have concluded that the neutron parameters are not superior to those obtained from the x-ray data. It is clear that it will be necessary to deuterate all or most of the hydrogen positions in the molecule in order to obtain data of sufficient quality for the (X-N) deformation-

Experiment report: *(continued)*

density refinement and further, that data from deuterated samples can be expected to be of adequate quality for the proposed calculations.

We have discussed the preparation of deuterated nucleoside analog compounds with Dr. Cliff Unkefer at LANL and we intend to apply for instrument time for the collection of data on deuterated samples in 1990.

The poor quality of the data is a consequence of the large amplitude of incoherent scattering by ^{1}H, creating an intense background beneath the coherently scattered diffraction amplitudes. The background curve obtained in the experiment provided an accurate experimental observation of the incident neutron beam wavelength distribution and revealed that it contained distinct edges. These edges are caused by the Bragg limit for diffraction by the neutrons in the aluminium windows through which they exit from the spallation source.

These results have been used to improve the parameters used to normalize time-of-flight data obtained on NPD to account for the variation in the incident beam wavelength distrubition.

References:

Single Crystal Diffractometer (SCD)

Single Crystal Diffractometer (SCD)

The Single Crystal Diffractometer (SCD) can be used to determine the crystal structures of a wide variety of materials. Neutrons are scattered from the crystalline sample onto an area detector (25 x 25 cm^2; position-sensitive; ^3He gas-filled counter), and the wavelength of the neutrons is determined by their time of flight from the source to the detector. To collect all the required data for a particular crystal, the orientation of the sample can be changed by rotations of the goniometer about φ and ω. The SCD has been used to study the structure of organometallic molecules that show a unique binding of H_2; crystal-structure changes at solid-solid phase transitions; twinned or multiple crystals; the texture analysis of polycrystalline materials that have been subjected to extreme geological environments; and crystal structures of materials under pressures of 10 to 20 thousand atmospheres. The instrument measures a large volume of reciprocal space at one time and therefore, can be used for studies of unknown incommensurate structures, diffuse scattering, etc. Nonambient sample environments can also be accommodated.

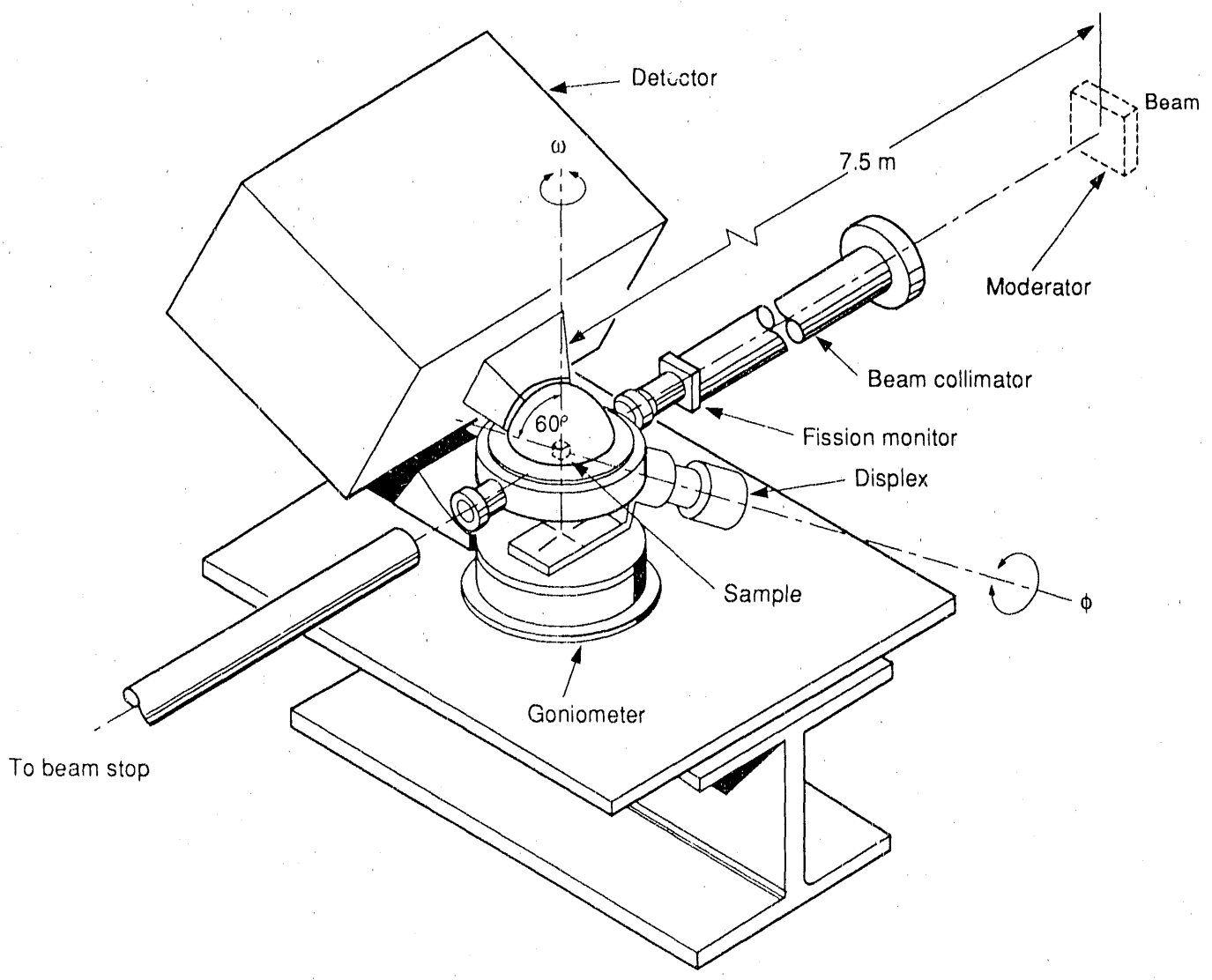

Instrument Details

Wavelength range, λ	0.5 - 5 Å
Beam diameter at sample	5.5 mm
Time resolution	~1%
Maximum lattice constant	~20 Å
Detector	1 multiwire (25 cm x 25 cm) at 90°
Detector resolution	2.5 mm
Moderator	Chilled water at 10° C
Sample environment	10 K to ambient
Sample size	0.25 - 25 mm^3
Experiment duration	1/2 day - 3 days per octant

Allen C. Larson, instrument scientist
Dennis Martinez, instrument technician

Instrument used: *(please type)*	Local contact:	Proposal number: *(for LANSCE use only)*
Single crystal neutron diffractometer	P. J. Vergamini A. C. Larson	239.0

Title: Neutron Structure of $Mo(CO)[(C_6D_5)_2PC_2H_4P(C_6D_5)_2]_2(H_2)\cdot xC_6D_6$ (benzene-d_6 solvate)

Report received: *(for LANSCE use only)* 4-15-90

Authors and affiliations:

Gregory J. Kubas, INC-4, Los Alamos, and local contact persons

Experiment report:

The title complex is of great interest because of its molecular hydrogen (H_2) ligand, which in this complex may possess an activated H-H bond with an H-H distance greater than the 0.80-0.82 Angstrom distances that have been found for three other dihydrogen complexes. Thus it is necessary to obtain neutron data to locate the hydrogen positions. Two x-ray structures had been done on two different solvated complexes: $Mo(CO)(dppe)_2(H_2)\cdot 3$benzene and $Mo(CO)(dppe)_2(H_2)\cdot 2$toluene (dppe= $(C_6H_5)_2PC_2H_4P(C_6H_5)_2$, i. e. the nondeuterated form of the ligand in the title complex). However, because of disorder between the H_2 and the trans-CO ligands, the H_2 could not be located (JACS, 1986, 108, 1339).[1] In order to aid the neutron experiment, the deuterated (partially, phenyl group positions) form of the phosphine ligand, dppe, was synthesized and used to prepare the title complex. Large single crystals were grown from benzene-d_6 solution by reacting $Mo(CO)(dppe\text{-}d_{20})_2$ (the unsaturated precursor) with H_2 in this solvent and allowing the resulting supersaturated solution to stand at ambient temperature. Well-formed crystals were deposited and a crystal of prismatic shape (about 1x1x1.5 mm in size) was mounted and used for the neutron experiment. Originally the intention was to use a D_2 complex to aid in location of the potentially disordered H_2 (or D_2) ligand. However, the H_2 species was inadvertantly prepared and used in the experiment. Fortunately the space group determined for the neutron sample was different from that

Experiment report *(continued)*:

of the samples used in the x-ray studies, making it likely that the neutron structure will not have a disorder problem. However, this meant that the neutron data set could not be readily solved based on known x-ray data. Thus there has been a delay in analyzing the data while ascertaining the best procedure to follow. It has been decided that the easiest route would be to obtain x-ray data on the crystals used for the neutron work to (a) determine whether a phase change occurred on cooling the sample to liquid helium temperature (the x-ray structure of the benzene solvate was done at ambient temperature---space group $P22_12_1$) or whether the composition of the neutron sample was different (e. g. the number of lattice solvent molecules might not have been three as for the x-ray sample) (b) to provide heavy atom positions to aid in solving the neutron data. The x-ray structure will be done at ambient temperature initially and at low temperature if necessary, as soon as the instrument is available in INC-4.

The unit cell determined from the SCD experiment is a = 12.98, b = 14.04, c = 19.85 Å and α = 90.55, β = 94.42 and γ = 114.06°. Triclinic, space group P1 or $P\bar{1}$.

Subsequent to collecting the neutron data, x-ray measurements have been carried out on other crystals from this same batch. The neutron unit cell was confirmed and a determination of the locations of the heavy atoms using x-ray data is in progress.

References:

1. Kubas, G. J.; Ryan, R. R.; Wrobleski, D. A. J. Am Chem. Soc. 1986, 108, 1339.

Instrument used: (please type)	Local contact:	Experiment no:
Single Crystal Diffractometer	Larson/Vergamini	240.0

Title:

Structure Refinement of Epidote ($Ca_2(Al,Fe)_3Si_3O_{12}(OH)$)

Authors and affiliations:

Joseph R. Smyth, R. Jeffrey Swope
Department of Geological Sciences
University of Colorado
Boulder, CO 80309–0250

Report received:
(to be filled in by LANSCE)
4-9-90

tes of experiment:

eptember 7–11, 1989

- ❑ Approved by external program committee
- ❑ Approved by internal program committee
- ❑ Part of LANSCE discretionary time

Experiment report:

The object of this experiment is to refine the crystal structure of a natural epidote in order precisely locate the hydrogen position(s). A single crystal of epidote of approximate composition, $Ca_2Al_{2.1}Fe_{0.9})Si_3O_{12}(OH)$, from Tyrol, Austria measuring 1.4 x 2.2 x 3.0 mm was mounted on the SCD instrument, and 20 histograms of data covering two octants of reciprocal space were collected over a period of 5 days (September, 7–11, 1989). A total of 1856 Bragg reflections were indexed, and the unit cell parameters ; a = 8.902(3) A, b = 5.628(2) A, c = 10.190(3), β = 115.28(2) determined by least squares refinement. The space group is $P2_1/m$.

The asymmetric unit contains 19 atoms of which 2 are on inversions, 14 lie on the mirrors, and 3 are in the general position. Positional and anisotropic thermal parameters for these atoms were refined from the Bragg intensity data to an $R_{wt}(F)$ of 0.076 for all reflections. Of two oxygens not bonded to Si in the structure, O(4) and O(10), it appears that all of the hydrogen is on O(10) and the position of this hydrogen has been refined to much greater precision than has been previously available.

Experiment report (continued):

This is study is not yet complete. An X–ray data set has been collected on the same material and is currently being used for a structure refinement. When this is complete, the positional and thermal parameters will be refined using the combined X–ray and neutron data sets. This should permit precise computation of electrostatic site potentials from which the distribution of oxygen isotopes between epidote and other phases as a function of temperature may be predicted. This should allow measured distributions of oxygen isotopes between epidote and other phases to be used to estimate equilibration temperatures of epidote–bearing metamorphic rocks.

Table 1. Preliminary Atom Positional Data for Epidote

Atom	X	Y	Z
Ca(1)	0.7570(5)	0.75	0.1517(4)
Ca(2)	0.6051(5)	0.75	0.4235(4)
Si(1)	0.3399(5)	0.75	0.0475(4)
Si(2)	0.6850(5)	0.25	0.2753(4)
Si(3)	0.1843(5)	0.75	0.3187(4)
M(1)Al	0.0	0.0	0.0
M(2)Al	0.0	0.0	0.5
M(3)Fe	0.2941(2)	0.25	0.2241(2)
O(1)	0.2340(2)	0.9935(4)	0.0408(2)
O(2)	0.3040(2)	0.9815(4)	0.3551(2)
O(3)	0.7954(2)	0.0141(4)	0.3394(2)
O(4)	0.0529(3)	0.25	0.1296(3)
O(5)	0.0422(3)	0.75	0.1461(3)
O(6)	0.0672(3)	0.75	0.4070(3)
O(7)	0.5145(3)	0.75	0.1805(3)
O(8)	0.5262	0.25	0.3094(3)
O(9)	0.6271(3)	0.25	0.0989(3)
O(10)	0.0832(3)	0.25	0.4297(3)
H	0.0557(7)	0.25	0.3260(6)

Los Alamos
Los Alamos National Laboratory
Los Alamos New Mexico 87545

Form number 1195 (12/87)

Instrument used:	Local contact:	Proposal number: (for LANSCE use only)
SCD	P.J. Vergamini	241 . 0

Title:	Report received: (for LANSCE use only)
Preferred Orientation in Experimentally Deformed Quartzite	

Authors and affiliations:

Hans-Rudolf Wenk	Dept. of Geology and Geophysics, Univ. Calif., Berkeley, CA 94720
Phillip Vergamini	LANSCE, LANL, Los Alamos, NM 87545
Allen C. Larson	LANSCE, LANL, Los Alamos, NM 87545

Experiment report:

Four samples of experimentally deformed quartzite were prepared and examined. These samples consisted of two pure quartzite samples and two samples which were 75% quartzite and 25% mica(muscovite). One sample of each pair was deformed 40% and the other was deformed 60%. A limited number of histograms were collected from each sample, only enough data to cover a band from the pole(the axial stress direction) to 90° from the pole were collected. This was expected to produce all of the information needed to define the pole figure of these samples.

The pole figure from the 60% deformed mixture sample is shown below as Figure 1 and pole density profiles obtained from this pole figure are shown in Figure 2, with the inverse pole figure for the quartz in this sample shown below in Figure 3.

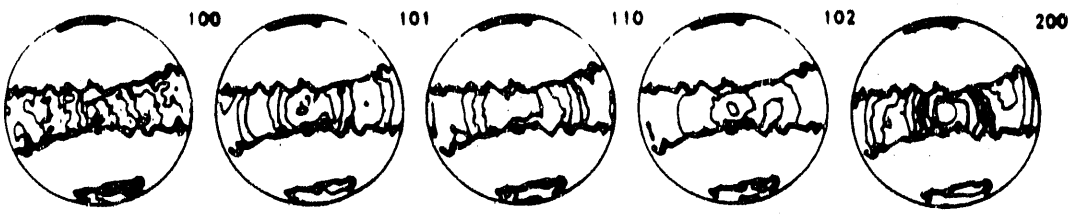

Figure 1. Partial pole figure coverage documenting approximate axial symmetry, equal area pro jection.

Experiment report *(continued)*

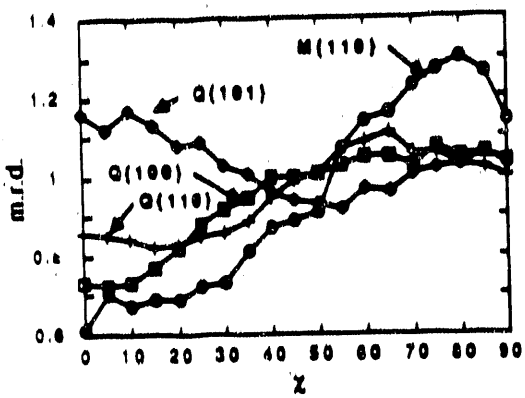

Figure 2. Pole density profiles for quartz from paral lel to perpendicular to the com pression axes for selected diffraction peaks in m.r.d. The profiles were averaged from pole fig ures in Fig. 7.

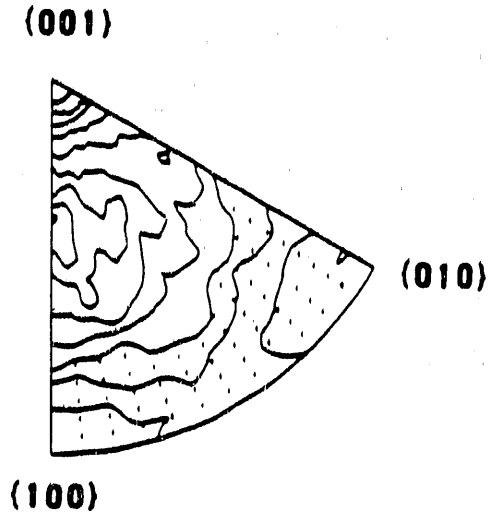

Figure 3. Inverse pole figure for quartz in experimentally deformed quartz-muscovite aggregate. Contours are in multi ples of a uniform distribution.

References:

Larson, A.C., P.J. Vergamini and H.R. Wenk (1989) "TOF measurements of pulsed neutrons for texture analysis of geological materials. Proc. M.R.S. (in press)

TOF MEASUREMENTS OF PULSED NEUTRONS FOR TEXTURE ANALYSIS OF LOW SYMMETRY MATERIALS

Allen C. Larson*, Phillip J. Vergamini* and Hans-Rudolf Wenk**
*Manual Lujan, Jr. Neutron Scattering Center, LANSCE, Los Alamos National Laboratory, Los Alamos, NM
**Department of Geology and Geophysics, University of California, Berkeley, CA

ABSTRACT

The single crystal diffractometer at LANSCE, SCD, provides an ideal capability for the study of preferred orientation in geological samples by time-of flight(TOF) measurement of pulsed neutrons. The 2-d position sensitive neutron detector with the large wave length range allows one to measure the complete distribution of intensities for several poles very quickly. Each histogram covers about $\pi^2/16$ radians of reciprocal space and contains information from all possible poles visible with the wave length range used, usually about 0.5 to 5.0Å. With this method complete pole figures of many lattice planes can be constructed from only 12 to 20 sample orientations as compared to over 1000 sample settings per lattice plane using conventional diffractometers.

Pole figures from measurements of experimentally deformed standard samples of calcite and quartzite with a known history of deformation provide information about deformation mechanisms and their temperature/strain history. This information can be applied to interpret preferred orientation of naturally deformed rocks.

INTRODUCTION

In many of the rocks composing the Earth's crust, mantle and core, mineral crystals display a preferred orientation distribution or texture. Among various origins of texture such as growth, flow of rigid particles in a rigid medium, recrystallization and dislocation glide, the latter is by far the most important mechanism. Rotations of crystals due to slip produce strong preferred orientation during tectonic deformation of the crust or during convection in the mantle. An understanding of texture development by plastic deformation helps us to understand dynamic processes within the earth. Also texture development produces anisotropy, eg. of seismic wave propagation, which needs to be taken into account for a quantitative interpretation of the earth's structure. One prerequisite in using textures for indicators of the geological history and structure is a need for quantitative texture measurements.

Traditionally X-ray diffraction has been used and this is sufficient for many applications. However neutron diffraction has some unique advantages for quantitative texture determinations. Weak absorption allows integration over sample volumes rather than surfaces. Also complete pole figures can be measured without

intensity corrections. With position sensitive detectors large ranges of the 2θ spectrum can be scanned at once and many poles recorded simultaneously. The time-of-flight measurements of pulsed neutrons combined with a 2D position sensitive detector offer the additional advantage of being able to scan large pole figure sectors of many pole figure simultaneously. We illustrate applications of this technique with experimentally produced quartz and calcite textures and the texture of a fluorapatite sample from a dinosaur bone.

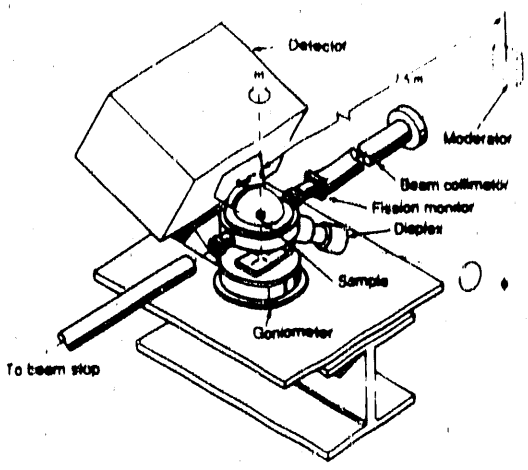

Figure 1. Schematic diagram illustrating the experimental setup of the SCD instrument at LANSCE. The sample is mounted on a two circle goniometer with a fixed χ-angle and the detector centered at 2θ=90° with the θ-axis tilted 45° from the ω-axis. Sample to the 25x25cm detector distance is 25cm.

EXPERIMENTAL PROCEDURE

The single crystal instrument at LANSCE is shown in Figure 1 [1]. This unique instrument uses a 2D position sensitive area counter positioned such that the θ axis makes an angle of 45° with the ω axis and the χ axis permanently set at 60°. Use of this instrument for pole figure measurement is described by Wenk, et al.[2].

This instrument can be used to examine about 80% of a sphere of reciprocal space. Only a small region on the bottom of the sphere is occluded. The reciprocal space coverage in the radial direction is illustrated in Figure 2 and Figure 3 shows the coverage of reciprocal space normally used for complete pole figures. Each histogram covers an area about 25° parallel to θ and about 50° perpendicular to θ.

The best way to handle the variation in detector efficiency, the geometric correction over the face of the detector and the variation in intensity due to the thermal neutron spectrum is to measure an isotropic sample and use its intensity data to calibrate or normalize the data. This can be approximated by summing the pole figure data from all histograms to obtain a self calibration. The only requirement in this is that the features in the pole figure be broad enough to provide a reasonable average value for all points on the detector.

Since the samples being examined on SCD are about 10 mm^3 in volume and the entire sample is placed in the incident beam, no corrections are needed for changes in the sample volume due to the angle of the incident and diffracted beams with respect to the sample surface. In addition no unusual background should arise and for samples lacking a strong incoherent scatterer the background is negligible,

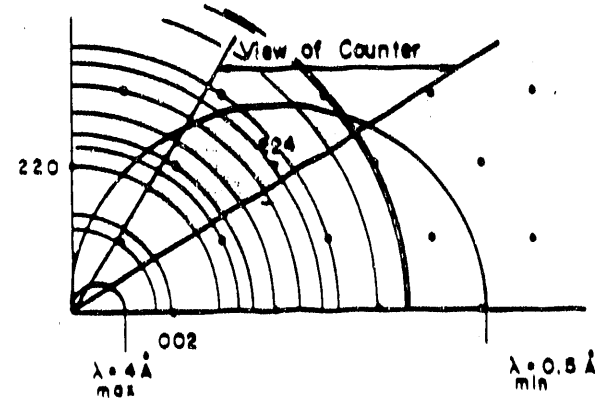

Figure 2. Diagram of a FCC reciprocal lattice showing traces of powder lines from lattice points and coverage of a histogram with the SCD detector.

as is the absorption for most geological materials.

The d-resolution obtainable on the LANSCE SCD instrument is dependent on the detector to sample distance, and in the setup usually used is $\Delta d/d$ = ca. 0.01.The major contribution to $\Delta d/d$ is the detector resolution and the effect of this can be easily improved by moving the detector from 25cm to 50cm. This however causes a decrease in pole figure coverage by a factor of about four. At 50cm the detector contribution to $\Delta d/d$ is ca. 0.005. With this resolution and a good peak to background ratio, measurements of pole figures for low symmetry geological materials having many closely spaced and weak diffraction peaks should be feasible.

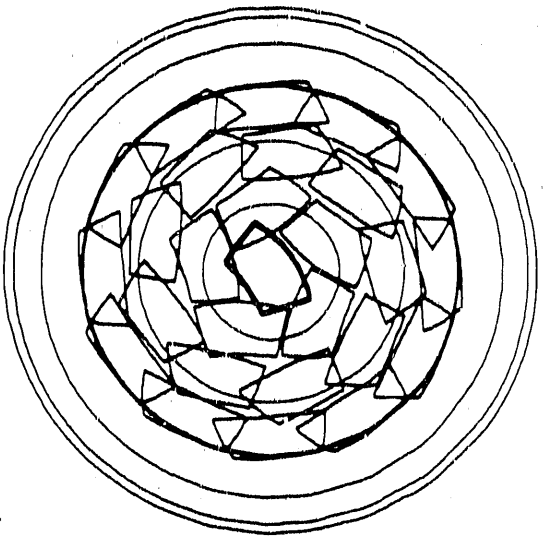

Figure 3. SCD detector coverage used to collect complete pole figures. An equal area plot.

RESULTS

The first example is an experimentally deformed limestone, $CaCO_3$. Deformation of 35% was in pure shear, at 400°C. The sample used in the texture analysis was a cube 0.8 cm on the side. The diffraction pattern of this trigonal mineral is considerably complex with five diffraction peaks in the range of interest between d=1.75 and 4.5Å (Figure 4). This sample is currently used as a "round robin" to determine the reliability of neutron diffraction pole figure determinations [3]. In Figure 5 LANSCE pole figure results are compared with measurements at ILL Grenoble with monochromatic neutrons and a 1-d position sensitive detector. Apart from a rotation difference which is due to a different sample orientation, pole figures are virtually identical, even for the very weak pole figure 110 for which counting statistics are poor.

The second sample is a mixture of 75% quartz and 25% muscovite, experimentally compressed by 60%. The quartz diffraction pattern is similar in complexity to calcite (Figure 6). Notice the weak diffraction peaks for muscovite which are barely above the background. Due to the axial symmetry of the deformation experiment and correspondingly of the pole figures, intensity profiles from parallel to perpendicular to the common axis are all that is necessary to describe the preferred orientation. With the detector window of 25° by 50° and ten sample settings we covered a large range (Figure 7). This was

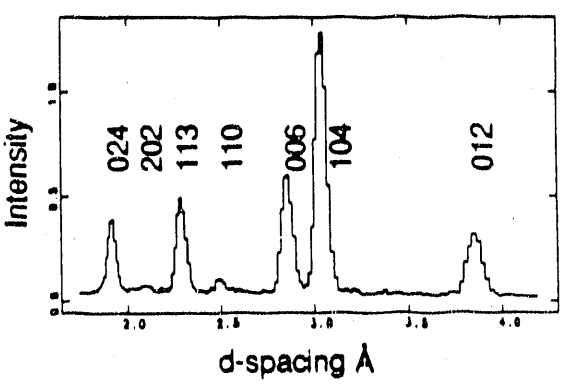

Figure 4. d-spectrum for limestone standard sample, K433, experimentally deformed by H. Kern, Kiel.

useful to establish an overall axial symmetry, also to note local deviations over which we were able to average. Texture profiles for quartz and muscovite are shown in Figure 8. From six partial pole figures we then calculated an inverse pole figure of the compression direction with the WIMV algorithm [4] which we present in Figure 9. The pole figure inversion shows good resolution with error values of less than 0.5% and is consistent with earlier observations [5]. With texture determinations on 4 samples of different composition and different degrees of deformation we could document that preferred orientation of quartz increases moderately in strength with increasing strain and is attenuated by interspersing muscovite in the sample.

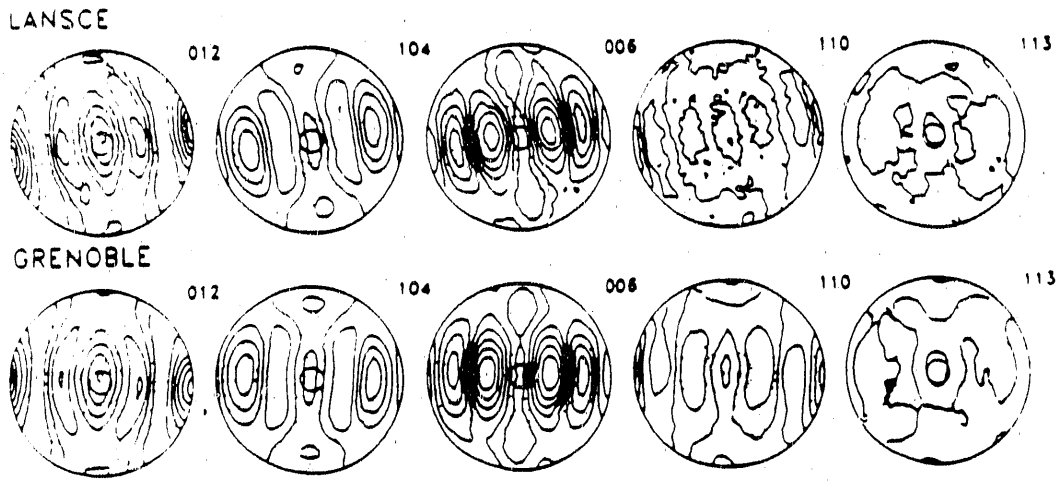

Figure 5. Comparison of five pole figures for experimentally deformed limestone,K433. Top was measured by TOF at LANSCE, bottom by monochromatic neutrons at ILL, Grenoble. Contours are in multiples of a random distribution, contours interval is 0.2, dotted regions are below 1 m.r.d., equal area projection.

A third geological sample is of biological origin. A fossil bone from a dinosaur found in the Seismosaurus locality in the southeastern San Juan Basin, Sandoval County, New Mexico shows a strong fabric of fluorapatite, $Ca_5F(PO_4)_3$ with *c* axes aligned in a single maximum, Figure 10, (002), and *a* and *b* axes distributed uniformly in a girdle perpendicular to the *c* axis maximum, Figure 10, (310). The example demonstrates that the original bone structure and the alignment of crystallites is still preserved after 140 million years.

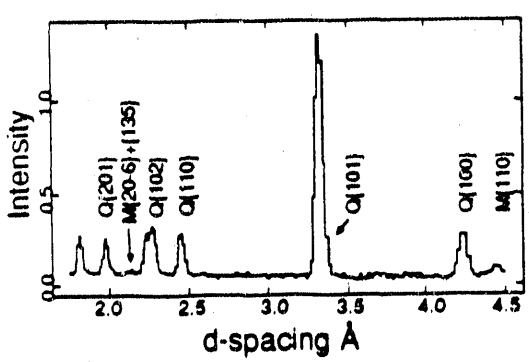

Figure 6. d-spectrum of a 75% quartzite, 25% muscovite mixture, Q505, deformed experimentally by J. Tullis, Brown. Notice weak peaks for muscovite.

CONCLUSIONS

The SCD and TOF neutron measurements at LANSCE were used to measure preferred orientation of geological materials with complex diffraction patterns. The method is efficient (about one hour per histogram), particularly for low symmetry compounds where the whole of reciprocal space is covered and should therefore also be attractive for ceramics such as high temperature superconductors [6]. At this point the experimental method could still be improved by allowing for larger samples and detectors with a wider coverage, e.g. of cylindrical shape. The data analysis should be extended to enable integration and deconvolution of overlapping peaks. Also measuring time could be reduced by sparser coverage of the pole figures which will require modifications of the algorithms to calculate the orientation distributions.

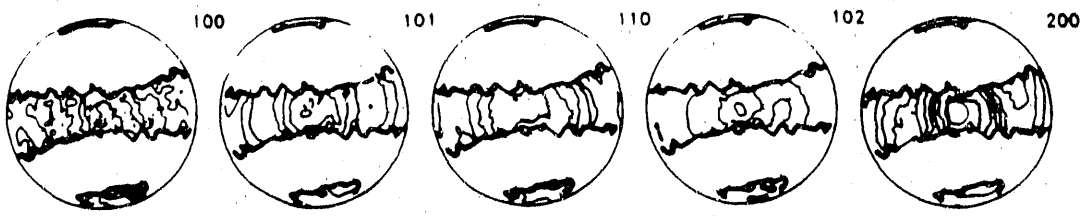

Figure 7. Partial pole figure coverage documenting approximate axial symmetry, equal area projection.

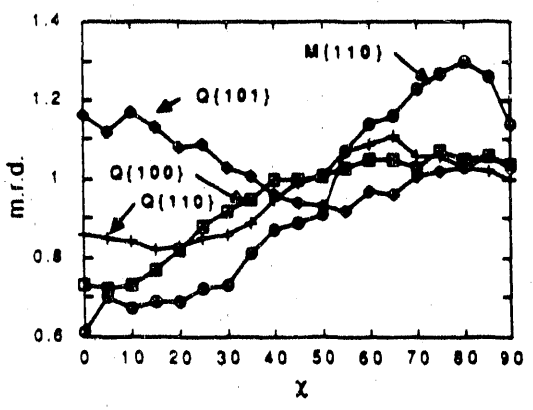

Figure 8. Pole density profiles for quartz from parallel to perpendicular to the compression axes for selected diffraction peaks in m.r.d. The profiles were averaged from pole figures in Fig. 7.

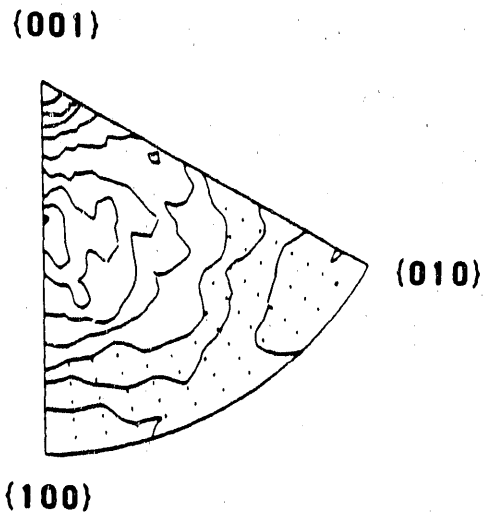

Figure 9. Inverse pole figure for quartz in experimentally deformed quartz-muscovite aggregate. Contours are in multiples of a uniform distribution.

Acknowledgements

We are appreciative for access to the LANSCE and support through IGPP Los Alamos and NSF EAR 870 9378. Hartmut Kern, Kiel and Jan Tullis, Brown University kindly provided the samples which were in this study.

This work was performed under the auspices of the US Department of Energy, Office of Basic Energy Sciences.

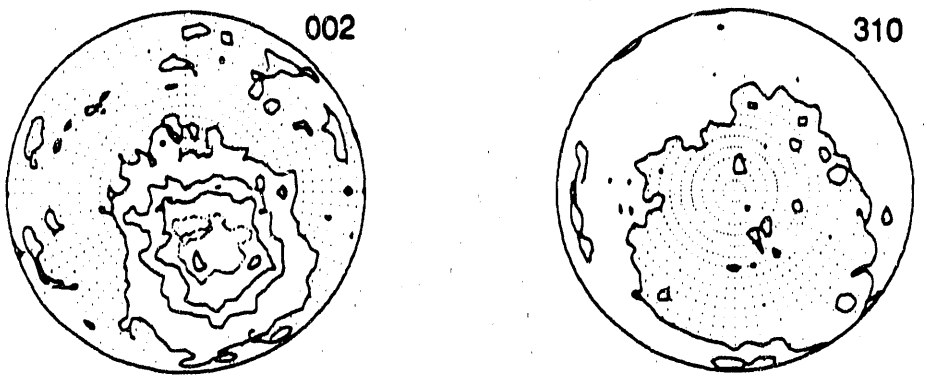

Figure 10. Pole figures of fluorapatite composing fossil bone of Seismosaurus. Contours at 0.2 m.r.d with regions below 1.0 dotted. Equal area projection.

REFERENCES

1. P.J. Vergamini, G.G. Christoph, R.W. Alkire and A.C. Larson, (Unpublished) (1987).

2. H.R. Wenk, P.J. Vergamini and A.C.Larson, Textures and Microstructures 8&9, 443-456 (1988)

3. H.R. Wenk, H. Kern, J. Pannetier, S. Höfer, W. Schäfer, G. Will and H.G. Brokmeier, Proceed. Int. Conf. Textures of materials, 8, 229-234. TMS, Warrendale.(1987)

4. J. S. Kallend and H.R. Wenk,Am. Soc. Metals, Annual Meeting (abstr.) (1989).

5. J. Tullis, J.M. Christie and D.T. Griggs , Geol. Soc. Am. Bull. 84,294-314(1973)

6. H.R. Wenk, J. Pannetier, G. Bussod and A. Pechenick, J. Appl. Phys. 65, 4070-4072 (1989).

Instrument used: *(please type)*	Local contact:	Proposal number: *(for LANSCE use only)*
SCD	P.J. Vergamini	242.D

Title:

Preferred Orientation of Apatite in Seismosaurus Bone

Report received: *(for LANSCE use only)*

Authors and affiliations:

Dr. David Gillette, State of Utah, Division of State History - Antiquities, Salt Lake City, UT 84101-1182

Dr. Phillip J. Vergamini, LANSCE, Los Alamos National Laboratory, Los Alamos, NM 87545.

Experiment report:

One of the largest dinosaurs discovered to date is a one hundred and forty-five million year old sauropod from the Morrison Formation (Upper Jurassic, 145 mya) of central New Mexico. The specimen is a partially articulated skeleton of a new dinosaur informally named "Seismosaurus", in allusion to its size; in life this individual was more than 110 feet long, the longest dinosaur known, and one of the largest. Excavation commenced in 1985, and will continue through at least the field season of 1990. This recent find in New Mexico has become the focus of a multi-disciplinary research effort based at the Los Alamos National Laboratory. As part of this effort, we at the Los Alamos Neutron Scattering Center (LANSCE) have been studying bone samples from the specimen by applying neutron scattering techniques at the LANSCE pulsed source. The Single Crystal Diffractometer (SCD) at LANSCE provides an ideal capability for the study of preferred orientation in the apatite mineral portion of the bone. We report here the first application of neutron texture studies to paleontology and our observation of preferred orientation in dinosaur bones.

Conventional wisdom regarding the preservation of fossil bone generally holds that "fossilization" is accomplished through "molecule-by-molecule" replacement. The intuitive notion that fossil bone is instead partially or wholly original, rather than "replaced," arises from the superb preservation of fine histologic detail in many specimens: "replacement" would destroy microscopic detail owing to stoichiometric incongruity. The few attempts to characterize the chemical composition of fossil bone have been mainly from Quaternary and Tertiary age localities, analyzed for purposes of extraction of organic molecules. This preliminary report describes this first analysis of the chemistry of dinosaur bone.

As part of a growing program at LANSCE, we have been developing techniques for utilizing the unique capabilities of both the pulsed neutron source and the geometry of the Single Crystal Diffractometer (SCD) to study preferred orientation in materials [1]. We are presently capable of routine texture studies of simple metallurgical to complex geological materials . Texture studies have been utilized in determining the history of materials in metallurgy and geology. More recently, the technique has been applied to the mineral portion of bone material[2]. Apatite ($Ca_5(PO_4)_3OH$) as grown in bone alongside collagen has a preference of the c-axis along the long, or load bearing, direction in bone, for structural purposes. An advantage of utilizing neutron diffraction for studying materials is the capability of sampling large volumes of material provided by the penetrating power of neutrons. In the particular application to bone material, a second advantage of neutrons over x-rays arises. The intensity of Bragg peaks corresponding to directions which are of most interest due to their alignment with certain other features in the bone is higher[3].

Our bone samples were selected from dense cortical bone in the ischium of Seismosaurus. The sample from the shaft of the ischium was taken by a hollow coring apparatus attached to a modified drill press. Two separate 3mm cubic samples of dense bone were cut from cores taken from the ischium of a Seismosaurus. The skeleton is preserved in the middle of a buff fluvial sandstone approximately 10 meters thick. Because sandstone is non-compressible, the bones are uncrushed and undistorted. They are preserved in fine detail, and contain little mineralization in pore spaces. The sandstone is presently porous, and presumably has been porous since its deposition, permitting frequent exchange of ground water and percolation of rainfall. Thus, the bones have not been geochemically isolated by unusual conditions of deposition or preservation, but instead are typical of dinosaur excavations.

Apatite is a major constituent (~70%) in bone. Chemical analysis of core samples of the Seismosaurus bone unearthed thus far indicate ~65% apatite. Detection of apatite, the crystalline portion of bone, is evidence of preservation of original material in dinosaur bone. However, the evidence is inconclusive unless post mortem deposition of apatite through geochemical processes and alteration of original material by pressure-temperature reactions can be ruled out. A hemisphere of reciprocal space was sampled utilizing the SCD at LANSCE which has the capability of collecting volumes of reciprocal space and therefore information about spatial distribution of intensity from several Bragg peaks at one time. Variations in the intensity of a particular Bragg peak allows us to extract information about preferred orientation of the microcrystalline structure.

Experiment report *(continued)*:

We looked for the preferred orientation of the crystalline apatite in a sample of the excavated bone material from a Seismosaurus ischium on the SCD using texture analysis techniques. Figures 1 and 2 show the extracted pole figures for the 002 (a) and 310 (b) reflections for samples 1 and 2 respectively. The center of the pole figure represents approximately the load bearing direction in sample 1 and we expect the c axis to be parallel to this mode. The pole figure for the 002 reflection shows a maximum in a very localized direction corresponding to this load bearing direction. The pole figure for the 310 reflection (sample 1) shows a maximum in a plane 90 degrees from the 002 maximum. The second sample was mounted such that the c-axis was perpendicular to the center of the pole figure. In figure 2a, maxima at 90 degrees to the center of the pole figure correspond to the c-axis or 002 reflection. Figure 2b (310), displays a planar band, again perpendicular to the c-axis (or load bearing) direction. This verification of crystallographic orientation of apatite crystals parallel to haversian systems in dinosaur bone eliminate post mortem changes from further consideration and support the notion of preservation of original material.

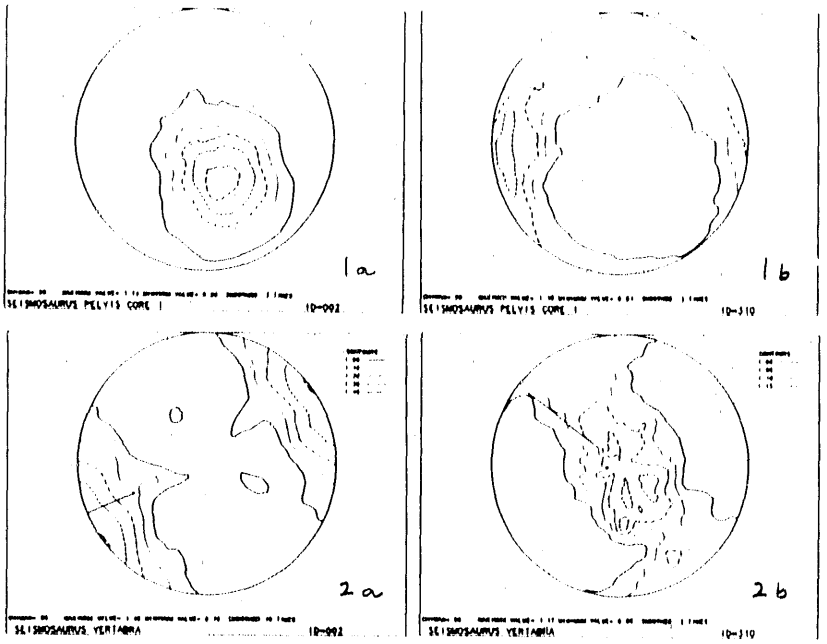

References:

[1] H.-R. Wenk, P.J. Vergamini, and A.C. Larson, Texture Analysis by Time-of-Flight Measurements of Spallation Neutrons With a 2 Dimensional Position Sensitive Detector, Texture and Microstructures, 819, 443-456 (1988).
[2] Allen C. Larson, Phillip J. Vergamini, and Hans-Rudolf Wenk, Proceedings of the Materials Research Society, Nov.27-Dec.1, 1989, Boston, Mass., in press, copy attached.
[3] G. E. Bacon, P. J. Bacon, and R. K. Griffiths, The Orientation of Apatite Crystals in Bone, J. Appl. Cryst. 12, 99-103(1979).

Instrument used: *(please type)*	**Local contact:**	**Proposal number:** *(for LANSCE use only)*
SCD	Angus Lawson	207.0

Title:

Elastic Neutron Scattering in Single Crystal V_7O_{13}

Report received: *(for LANSCE use only)*

5-5-90

Authors and affiliations:

Paul C. Canfield, Angus Lawson, Joe Thompson and Phil Vergamini,
Los Alamos National Laboratory, Los Alamos, New Mexico

Experiment report:

Data was collected on V_7O_{13} at T = 300 K and T = 20 K. Due to complexity of analysis and temperature instabilities during low temperature data collection, conclusive identification of a spin wave ground state at low temperature is, as of yet, not complete.

Instrument used: *(please type)*	Local contact:	Proposal number: *(for LANSCE use only)*
Single Crystal Diffractometer.	Dr. A. C. Larson Dr. Phil J. Vergamini	265.0

Title:

NEUTRON DIFFRACTION IN INCOMMENSURATE $Ba_2NaNb_5O_{15}$ AT LOW TEMPERATURE

Report received: *(for LANSCE use only)* 6-4-90

Authors and affiliations:

W. F. Oliver
Department of Physics
Arizona State University
Tempe, AZ 85287

J. F. Scott
Condensed Matter Laboratory
Department of Physics
University of Colorado
Boulder, CO 80309-0390

Experiment report:

Neutron diffraction experiments have been performed between 10 K and 250 K on single crystals of barium sodium niobate (BSN) using the single crystal diffractometer at LANSCE. The purpose of these experiments was to determine 1) the structure of the room temperature quasi-commensurate (QC) phase; 2) the structure and incommensurate (IC) nature of the doubly modulated structure below ~105 K; and 3) the nature of the locked phase below 30 K. Only BSN samples of pure stoichiometry exhibit the phase transitions below room temperature.

Three samples from different sources were studied during July and September of 1988 and September of 1989. Nineteen histograms were recorded in sample 1 at temperatures of 10, 21, and 90 K. Similar histograms were recorded in sample 2 at 10 K. In the third sample only three histograms were recorded, but at a range of temperatures between 80 K and 250 K. Our results will be summarized in the following paragraphs.

The data taken at 10 K and 21 K (samples 1 and 2) show a "locked-in" tetragonal structure with P4nc space-group symmetry and a unit cell of dimensions $a = 35.21 \pm 0.02$ Å and $c = 7.99 \pm 0.02$ Å. Residual discommensurations observed earlier by several groups[1,2] give rise to diffuse scattering along both [100] and [010] (see fig. 1b). At 90 K a 2q IC phase was observed consisting of an underlying lattice of point symmetry 4mm (cell dimensions of $a = 35.14 \pm 0.02$ Å and $c = 7.97 \pm 0.01$ Å) and a superlattice rotated by 90° in the ab plane (see figs. 1a and b). Superlattice reflections could not be indexed at 90 K as at lower temperatures.

Sample 3, unfortunately, did not have the correct stoichiometry to exhibit the low temperature phase transitions. We were however, able to determine that the structure of the quasi-commensurate phase (that below 546 K) belongs to the orthorhombic space group Bbm2 with lattice constants of $a = 35.09 \pm 0.15$ Å, $b = 17.62 \pm 0.06$ Å, and $c = 7.97 \pm 0.03$ Å. Residual discommensurations were also observed, but only along the [100] direction (again consistent with earlier observations), as unindexable reflections in the odd (00l)

Experiment report *(continued)*:

planes. From the Δh and Δk values of these reflections the parameter δ which characterizes the IC nature of the QC phase was determined to be $\delta = 0.012$. This parameter δ is related to the incommensurate wavevector $\underset{\sim}{k}_I$ in the following way:

$$\underset{\sim}{k}_I = (1+\delta)\left(\frac{\underset{\sim}{a}_t^* \pm \underset{\sim}{b}_t^*}{4}\right) + \frac{\underset{\sim}{c}_t^*}{2},$$

where a_t^*, b_t^*, and c_t^* refer to the tetragonal reciprocal-space lattice vectors of the high temperature normal phase (that above 582 K) from which the IC phases are formed upon lowering the temperature. Its value was not found to change for sample three over the temperature range studied. Our results are consistent with a recent electron microscopy study.[3]

Currently, I am waiting for data tapes of the earliest data runs to be sent here to ASU so that I may reanalyze those results in order to better characterize the 2q IC phase below 100 K. I will then write up a thorough report of our experiment and results for publication in Phys. Rev. B. Various aspects of this experiment have already been presented.[4]

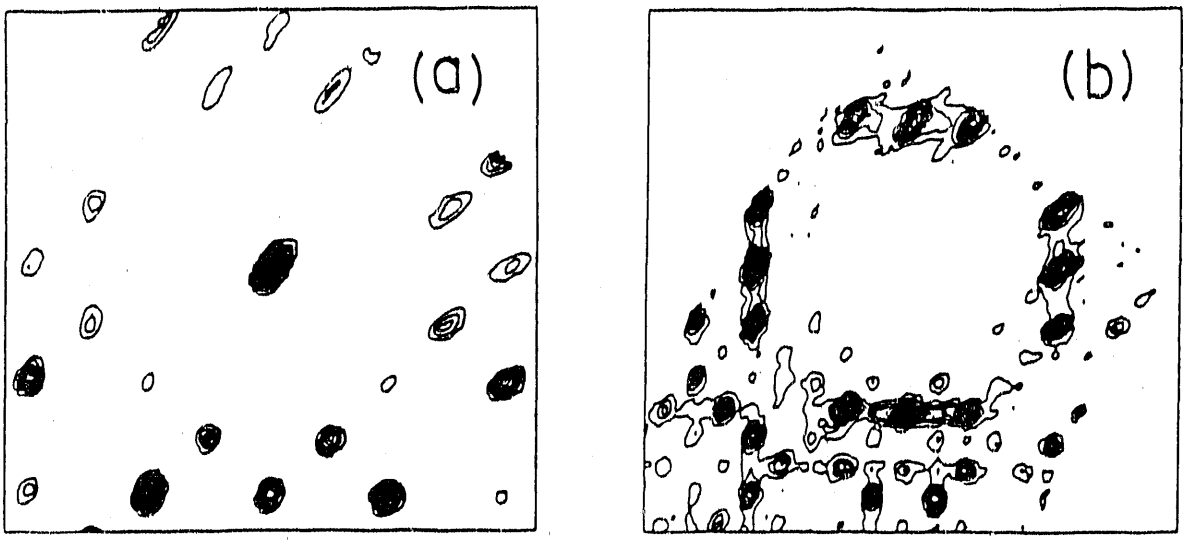

Figure 1. Neutron diffraction pattern for $Ba_2NaNb_5O_{15}$ at 10 K showing a slice through the h-k plane. (a) is centered at (0,0,10) and shows the underlying tetragonal structure of the commensurate phase, whereas (b) is centered at (0,0,7) and shows superlattice reflections of the "locked-in" IC modulation. Residual discommensurations give rise to diffuse scattering in the shape of rods in (b).

References:

1. Pan Xiao-qing, Hu Mei-shen, Yao Ming-hui and Feng Duan, Phys. Stat. Sol. (a) **91**, 57 (1985).
2. C. Manolikas, J. Schneck, J. C. Tolédano, J. M. Kiat and G. Calvarin, Phys. Rev. B **35**, 8884 (1987).
3. M. Verwerft, G. Van Tendeloo, J. Van Landuyt, and S. Amelinckx, Ferroelectrics **88**, 27 (1988).
4. W. F. Oliver, J. F. Scott, A. Shawabkeh, A. C. Larson, and P. J. Vergamini, Bull. Am. Phys. Soc. **35**, 795 (1990).

Instrument used:	Local contact:	Proposal number: (for LANSCE use only)
SCD	Phillip Vergamini	266 • 0

Title:	Report received: (for LANSCE use only)
Single Crystal Neutron Structure of 3-Trichloromethyl[2]Staffane	20 March 1990

Authors and affiliations:

Josef Michl — Department of Chemistry, The University of Texas, Austin, Texas 78712-1167

Gudipati S. Murthy — Ditto

Experiment report:

We are interested in the bicyclo[1.1.1]pentane structure for two reasons:

1. We are engaged in an attempt to develop a molecular-size "Tinkertoy" construction set for the assembly of artificial solids with pre-designed properties. The straight rods in this molecular civil engineering system are oligomers containing several bicyclo[1.1.1]pentane cages. They will be attached to connectors through functional groups located at both ends of the rods.

A detailed structural and spectroscopic characterization of these basic elements of the proposed construction set is needed. While we have been able to obtain reliable data on the location of the heavy atoms in about ten of these staffs by x-ray diffraction, none provided information on the location of the hydrogens. As mentioned below, the hydrogen positions are not obvious and we now wish to identify them by single-crystal neutron diffraction.

2. The problem of the exact location of the hydrogen atoms in the CH_2 groups of the bicyclo[1.1.1]pentane attracted attention soon after this hydrocarbon was first made. The hydrocarbon is unusual because of the very short non-bonded C-C distance(1.845Å), high degree of cyclobutane ring puckering(120°), small C-CH_2-C angle(73.3°), and a high strain energy(68 kcal/mol). The position of the hydrogen atoms is controversial[1,2].

Experiment report *(continued)*

If the CH_2 hydrogens make an HCH angle of 111°, only slightly smaller than expected from NMR coupling constants(114°), their non-bonded H...H distance is a mere 2.32Å and it has been proposed[1] that this is avoided by twisting the CH_2 groups, lowering the symmetry to D_3. Alternatively[2], the HCH angle could be unusually small(104°), accommodating the non_bonded H...H interaction in a reasonable fashion(2.45Å) and keeping the symmetry high, D_{3h}. Each of these two electron diffraction studies[1,2] arrived at a different conclusion. Our *ab initio* calculations favor the latter. We believe that the neutron diffraction study will resolve this long-standing question.

Unfortunately, the crystals of 3-Trichloromethyl[2]Staffane which were used for the data collection were somewhat small. This combined with the high hydrogen content of the compound, limited our ability to collect adequate data for the location of the hydrogen atoms on the bicyclo[1.1.1]pentane group. We are planning to pursue this problem by examining another material, one which has less hydrogen in the end groups.

References:

1. F. Chiang, S.H. Bauer, *J. Am. Chem. Soc.* **92**, 1614(1970)
2. A. Almenningen, B. Andersen and B.A. Nyhus, *Acta Chem. Scand.* **25**, 1217(1971).

Low-Q Diffractometer (LQD)

Low-Q Diffractometer (LQD)

The Low-Q Diffractometer (LQD) is designed for studying structures with dimensions in the range 10 to 1000 Å. Examples of problems that may be addressed include the following: structures of biological membranes; DNA/protein assemblies; large virus particles; nucleation and growth of voids in radiation-damaged bulk samples; phase separation in alloys; and intermolecular correlations in colloids and polymers. A significant feature of the LQD is that a broad range of Q (0.003-0.5 $Å^{-1}$) is measured in a single experiment without any changes to the physical configuration of the instrument.

The LQD requires an intense source of long-wavelength ("cold") neutrons. Therefore, a liquid-hydrogen moderator is used, which produces a neutron spectrum that peaks at about 2.4 Å and has usable flux from 0.3 to 20 Å. A pair of single-aperture collimator plates yields an angular resolution of 0.09° and a penumbra diameter of 10 mm at the sample. An optional five-hole-aperture converging collimator allows a four times increase in intensity without affecting the resolution.

At 20 Hz, the slowest neutrons used on the LQD fall 12 mm under the influence of gravity. Rather than increasing the size of the beam stop, neutrons whose parabolic trajectories strike the detector at its center are selected. The gravity-focusing device accomplishes this task by pushing the collimator exit plate upward at constant acceleration during each beam pulse.

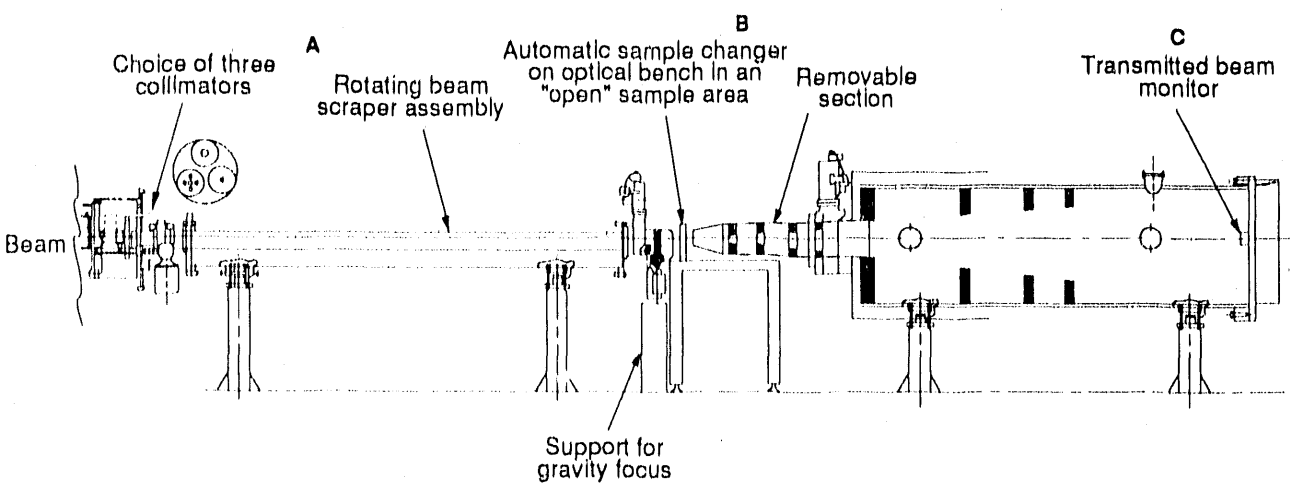

Instrument Details

Wavelength range, λ	0.2 - 15 Å at 20 Hz	
Scattering angle	6 - 60 mrad	
Q range	0.003 - 0.5 $Å^{-1}$	
Sample size:		
Single-aperture collimator	10 mm x 13 mm	
Multiple-aperture collimator	24 mm x 27 mm	
Detected intensity		
(single aperture, 30 μA):	$0.2 < \lambda < 1.6$ Å:	0.2×10^4 n/s
	$1.6 < \lambda < 5.0$ Å:	8.0×10^4 n/s
	$5.0 < \lambda < 15$ Å:	2.0×10^4 n/s
Detector	1 multiwire, 59 cm in diameter	
Moderator	Liquid hydrogen at 20 K	
Sample environment	Air, vacuum, closed-cycle refrigerator, or user supplied	
Experiment duration	10 minutes to 12 hours	

Philip A. Seeger, Instrument scientist
Rex P. Hjelm, Jr., Instrument scientist
Dennis Martinez, Instrument technician

Instrument used: *(please type)*	Local contact:	Proposal number: *(for LANSCE use only)*
LQD	Rex Hjelm	204.0

Title:
Spatial correlations and fractal geometry of gelling systems and Excluded phase structure in micellar and microemulsion systems

Report received: *(for LANSCE use only)*

Authors and affiliations:

Jess P. Wilcoxon, Organization 1153, Sandia National Laboratories, Albuquerque,NM U.S., (505) 846-3705
James E. Martin, Organization 1153, Sandia National Laboratories, Albuquerque, NM U.S., (505) 846-3705
E. W. Kaler, Department of Chemical Engineering, University of Delaware, Newark, Delaware, 19716, U.S., (302) 292-3553

Experiment report:

We focused our work on the microstructure of two types of complex fluid systems, gels and inverse micelles. The silica gel systems we studied were limited by the weak scattering from the samples but we did reach some interesting conclusions based upon our limited SANS data. We formed TMOS gels under two distinctly different regimes of growth. In the first case high base concentrations were used together with low salt concentrations. This would be expected to lead to high monomer surface charge and very little screening of the repulsive interactions between colloids. Thus, the early stages of growth would be slow (low sticking probability) and produce compact colloidal particles with sharp interfaces. This expectation was confirmed in our SANS data which showed $I \sim Q^{-4}$(Porod's law) at large Q. These ideas were also supported by our observations of the light scattering intensity vs growth time for this system. We found that the intensity per unit concentration vs growth time scaled with the cube of the particle radius, (measured independently by dynamic light scattering), as expected for compact colloidal particles. In the second kinetic regime we formed a TMOS gel with high salt and relatively low surface charge (low base) and found both rapid growth kinetics by light scattering measurements while SANS data gave $I \sim Q^{-2}$ characteristic of more ramified objects usually associated with diffusion limited growth. Thus, we established that the early stages of growth in gelling systems can have a major influence on the microstructure and can be controlled by simple surface charge screening. These observations are important since these short length scale correlations are apparently responsible for the very different viscoelastic properties of the final gels.

We were able to study many more of the inverse micelle and microemulsion systems of interest since scattering cross sections were larger for these systems than for the silica gels. We were interested in understanding how differences in microstructure and interactions in inverse micelles affect chemical reactions which take place in these systems. In particular we attempted to better understand the formation of colloidal metals or metalloids in these systems. In these reactions an otherwise insoluable metal salt (e.g. $NaAuCl_4$) is dissolved in a hydrocarbon solvent (e.g. octane) by use of a surfactant. We used nonionic surfactants in the family C_iE_j, where the value of i represents the number of carbons in the hydrocarbon portion of the amphiphile and j represents number of $O\text{-}C_2H_5$ groups in the hydrophilic portion of the molecule.

As is well known, surfactants often spontaneously self-associate to form aggregates called micelles when placed in water. When such groups are placed in a hydrocarbon solvent the amount of self-association is determined by the "chemical dipole" determined by the ratio of i:j. Systems in which the hydrophobic tails form an interface with the continuous oil phase are referred to as inverse micelles. Generally in water, the shape of the micelle (e.g. rod-like, spherical, or disc-like) is determined by packing considerations (e.g. the ratio of head group area to amphiphile molecular volume).

Experiment report: *(continued)*

In our first set of experiments we wanted see how changing the i/j ratio affected the microstructure for a fixed solvent, octane. We found that as we increased this ratio (making the surfactant less compatible with the hydrocarbon), the scattering intensity, I(Q=0), increased two orders of magnitude when changing from $C_{12}E_3$ to $C_{10}E_8$. Meanwhile Guinier analysis of the same data showed the radius of gyration to be <10 Å, 23 Å, and 40 Å for $C_{12}E_3$, C_6E_5, and $C_{10}E_8$ respectively. This implies either a corresponding increase in aggregation number (number of surfactants molecules/micelle) or the presence of nearby phase boundaries which would give rise to a significant increase in the osmotic compressibility.

It is interesting to note that all three of the above systems are single phase at all temperatures in the absence of metal salt. However, both C_6E_5 and $C_{10}E_8$ phase separate into two phases when sufficient quantities of $NaAuCl_4$ (0.03 M) is added. When only enough salt is added (.003 M) to ensure a single phase at room temperature, then both $C_{12}E_3$ and $C_{10}E_8$ are capable of forming highly monodisperse Au metalloids which are stable. However, C_6E_5 forms metal aggregates which rapidly sediment out of solution under the same reaction conditions. Since $C_{10}E_8$ and C_6E_5 have nearly identical chemical dipoles, the difference must be due to microstructure (e.g. a larger aggregation number in the former) which we see reflected in the SANS, not solely intermicelle interactions. However, this is not the entire story because the metalloid reaction kinetics is completely different in $C_{10}E_8$ compared to $C_{12}E_3$. Initially, we find large (~150 nm) purple metalloids are formed in the former system which evolve slowly (~24 hrs) to the small (~20-30 nm) red colloids which are rapidly formed (less than 60 seconds) in the latter system. Thus, it appears that increased attractive interactions in $C_{10}E_8$ compared to $C_{12}E_3$ are also important in the metalloid formation process and probably account for some of the differences in I(Q=0) values found in the SANS measurements on these systems.

We next compared the metalloid formation process for two very different surfactant/solvent systems, using identical surfactant concentrations, metal salt concentrations, and reaction conditions. Using SANS, we studied the bare micelle system, the system loaded with metal salt, and the final metalloid solution after reduction using N_2H_4. The first system, $C_{12}E_8$ in Octane, was a classical one (i.e. one forming droplet-like inverse micelles and capable of solubilizing significant amounts of water in the droplet interior). The second system was AOT in toluene. The latter cannot solubilize water at any appreciable level and thus is "non-classical." Both systems were capable of dissolving large amounts of metal salt and forming very monodisperse, small (~20 nm) spherical Au metalloids. No changes in SANS data were found between the bare and salt filled systems for AOT/toluene, while $C_{12}E_8$/octane data showed increases in I(0) and radius which could be associated with either increasing intermicelle interactions or an increase in droplet size due to swelling. Reduction to metalloids in both systems resulted in only small increases in I(0) for the AOT/toluene system, compared to an order of magnitude increase for the $C_{12}E_8$/octane system. Since the final metalloids were indistinguishable by TEM measurements, our preliminary conclusion is that intermicelle interactions were increased significantly in the $C_{12}E_8$/octane system during the metalloid formation process but not in the AOT/toluene system. The increase in intermicellar interactions is reflected in the I(0) increase observed upon salt addition in the former system. Although the mean metalloid size was nearly the same in both systems, the AOT/toluene system produced the most monodisperse metalloids obtained by *any* known method. We concluded that reducing attractive interactions (staying far away from phase boundaries) is an important aspect of metalloid formation and that interactions in oil continuous systems are much more important in the interpretation of SANS data than has been previously assumed.

References:

Instrument used: *(please type)*	Local contact:	Proposal number: *(for LANSCE use only)*
LQD	Rex Hjelm, Phil Seeger	208.0

Title:	Report received: *(for LANSCE use only)*
Small Angle Neutron Scattering Studies on PS/PMMA Diblock Copolymers	2/20/90

Authors and affiliations:

T. P. Russell
IBM Almaden Research Center
650 Harry Road
San Jose, CA 95120

Experiment report:

Small angle neutron scattering studies were performed on two different block copolymers of poly(styrene), PS, and poly(methyl methacrylate), PMMA, denoted P(S-b-MMA), as a.function of temperature. The molecular weights of the copolymers were ≃15,000 and in one case the PMMA block was perdeuterated,P(S-b-d-MMA), whereas in the other the full copolymer was perdeuterated, P(d-S-b-d-MMA). These studies paralleled the previous studies performed on P(d-S-b-MMA) as a function of temperature. The experiments were performed to determine the Flory-Huggins interaction parameter, χ, and its temperature dependence.

Experiments were performed at temperature over a temperature range from 100°C to 195°C in approximate 15°C increments. The data were corrected for parasitic scattering, electronic noise and detector homogeneity in the standard fashion and placed on an absolute level. In all cases, a single reflection was observed with no indication of a second order reflection characteristic of the lamellar morphology of a microphase separated, symmetric diblock copolymer. Consequently, assuming that the copolymers were phased mixed, the data were analyzed using the standard correlation hole scattering approach developed by Leibler[1] where the statistical segment length, b, and χ were adjusted to yield the best fit to the data.

For the P(S-b-d-MMA) copolymer, using b=8.5Å, the interaction parameter was found to be given by $\chi=(0.0292\pm0.002)+(3.188\pm0.4)/T$ where T is the absolute temperature. For the P(d-S-b-d-MMA) copolymer, on the other hand, using b=7.25Å, the interaction parameter was found to be given by $\chi=(0.0251\pm0.002)+(3.2\pm0.4)/T$. Previous experiments on P(d-S-b-MMA) yielded an interaction parameter given by $\chi=(0.0284\pm0.002)+(3.0\pm0.6)/T$. Thus, to within the experimental accuracy, the temperature dependent component of χ, appears to vary in each case. It is evident that the statistical segment lengths in the three cases are different. While these are all within the

Experiment report *(continued)*:

limits of the values found in the literature, the differences are quite real. Without this variation, reasonable fits to the scattering profiles could not be obtained using known values of the molecular weights. These results indicate that either there is an isotope effect due to the different labelling of the blocks or there are differences in the constitutions of the copolymers. This, for example, could arise from different tacticities of the PMMA portions of the copolymer. This latter possibility is being investigated by nuclear magnetic resonance.

References:

1. L. Leibler, Macromolecules, 15, 1283, (1982).

Instrument used: *(please type)*	Local contact:	Proposal number: *(for LANSCE use only)*
LQD	R. P. Hjelm, Jr.	221.0

Title:	Report received: *(for LANSCE use only)*
SANS Study of Ternary Microemulsion Gels	

Authors and affiliations:

Dr. C. Toprakcioglu, Cavendish Laboratory, University of Cambridge, UK

S. Radiman, Cavendish Laboratory, University of Cambridge, UK

L. E. Fountain, Cavendish Laboratory, University of Cambridge, UK

Experiment report:

We have studied the isotropic cubic liquid crystralline phases formed by the surfactant didodecyl dimethyl ammonium bromide (DDAB) when mixed with water and octane, using the techniques of small-angle neutron scattering (SANS), freeze-fracture electron microscopy, and rheology. Such liquid crystals are formed by the ordered arrangement of the aqueous and paraffinic microphases which are separated by a surfactant monolayer (or bilayer). The cubic phases can be visualised as "macrocrystals" with lattice constants of the order 100 Å instead of the usual few Å of typical crystalline solids. Thus, they give rise to Bragg scattering in the small-angle regime with thermal neutrons or X-rays. In particular, the LQD provides a sufficiently wide Q range to allow both principal and higher-order reflections to be observed in a single measurement for a wide range of lattice constants.

The water/DDAB/octane system has an extensive cubic domain, as shown in the phase diagram in Fig. 1. Samples are prepared by mixing the three components at ca.90–100°C and allowing the mixture to cool to room temperature. If the cooling rate is slow the system forms fairly large macrocrystals, some of which will have the right orientation to produce Bragg reflections on the detector. Successive cycles of melting and cooling reduce the size of the crystals, leading to what is essentially a powder diffraction pattern, as shown (radially averaged) in Fig. 2. The peaks can be indexed to a simple cubic or *bcc* structure (1:√2:√3), consistent with a constant-mean-curvature topology for these systems, which has the property of minimising the oil/water interfacial area for a given volume fraction. Conclusive indexing requires a detailed contrast-variation experiment.

These cubic phases may be technologically important, for instance, in producing novel porous materials with very small and virtually monodisperse pore size. A promising application is controlled drug delivery.

These results have been described in the LANSCE newsletter[1], and have been submitted for publication[2]. Further analysis is in progress.

Experiment report *(continued)*:

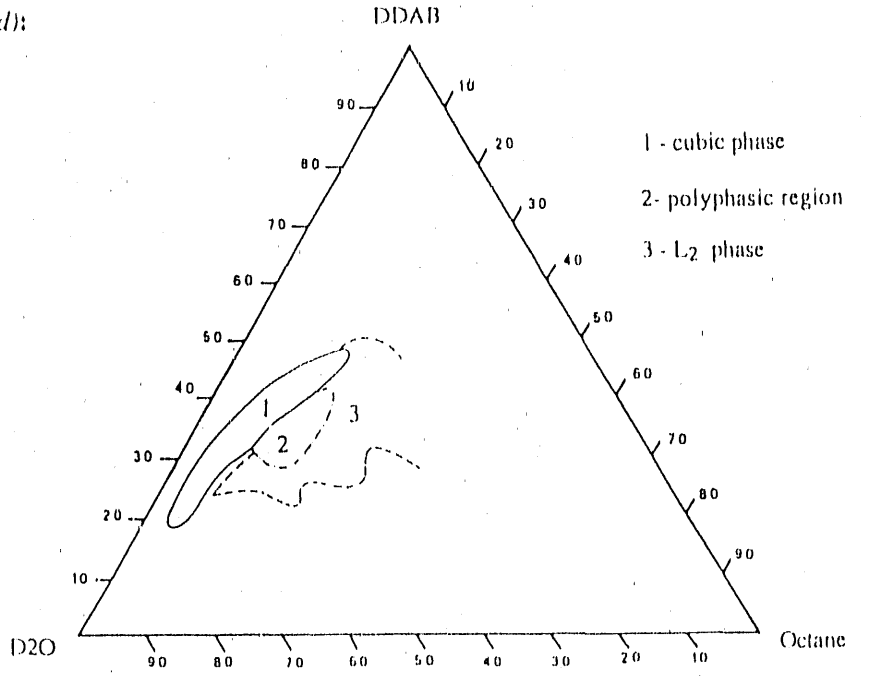

Fig.1 Phase diagram of DDAB/D2O/Octane.A thin region of colour birefringence occurs at the border between region 1 and 2.Region 2 has not yet been fully characterised.

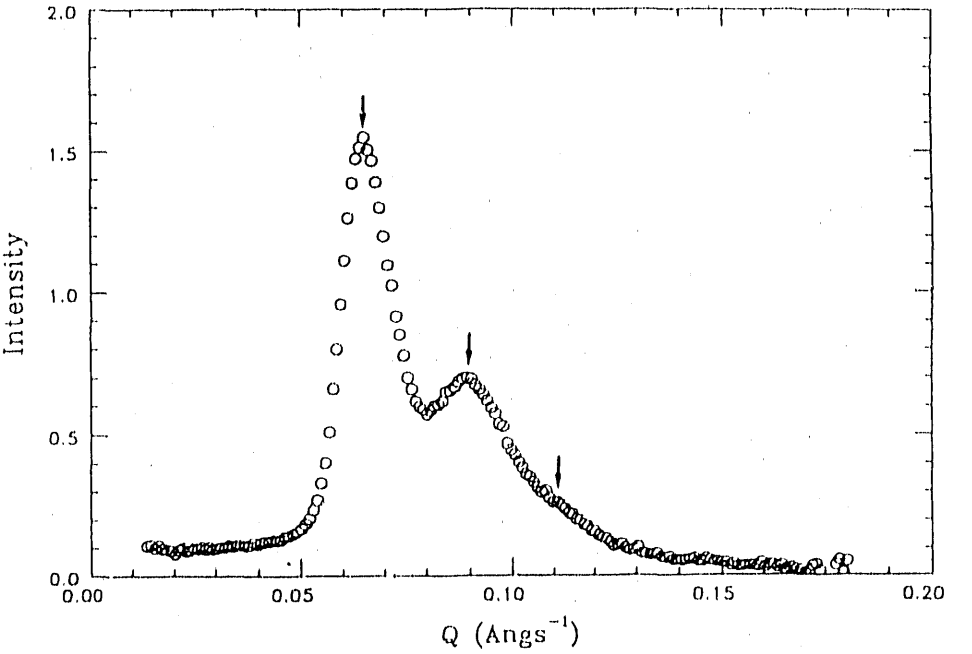

Fig.2 Sample of DDAB/D2O/Octane = 35.23/54.84/9.83 wt. % with water 50 % deuterated and oil fully hydrogenated.The peaks correspond to a spacing of $1:\sqrt{2}:\sqrt{3}$ with $2\pi/Q_{max}$=96.7 Å , for the principal peak.

References:

1. C. Toprakcioglu, "Small-Angle Scattering Studies of Cubic Ternary Systems," *from the tip of the LANSCE*, number 11, fall 1989

2. S. Radiman, C. Toprakcioglu, J.O. Raedler, A. de Vallera, and R.P. Hjelm, Jr., "Structural Investigation of Liquid Crystalline Phases of Ternary Surfactant Systems," Colloid and Interface Science (1990)

Instrument used: *(please type)*	Local contact:	Proposal number: *(for LANSCE use only)*
LOD	P. A. Seeger	2221.0

Title:	Report received: *(for LANSCE use only)*
NEUTRON SCATTERING STUDIES OF PHOSPHORYLASE KINASE STRUCTURE	

Authors and affiliations:

Trewhella, J., Rokop, S. E. Life Sciences Division, Los Alamos National Laboratory.

Blumenthal, D. K., Univeristy of Texas Health Center at Tyler, TX

Seeger, P. A., P-LANSCE, Los Alamos National Laboratory.

Experiment report:

BACKGROUND: Phosphorylase kinase (PK) is a large protein complex (approx. 1.3 million Daltons) present in high concentrations in skeletal muscle. Binding of hormone at the membrane surface of a muscle cell results in the formation of cAMP and activation of PK via cAMP-dependent protein kinase, leading to the eventual conversion of glycogen to energy for use by the cell. The activation of PK can also be brought about by calcium (for review see 1). PK consists of 16 subunits, made up of 4 identical copies of 4 different polypeptide chains denoted α,ß,γ,δ. Very little is known about the structure of the holoenzyme, or about the interactions of its subunits. The α-, ß- and δ-subunits of PK play regulatory roles, while the γ-subunit is responsible for catalytic activity. The δ-subunit of PK is responsible for the calcium dependent regulation of PK activity, and is identical to the multifunctional calcium-binding protein calmodulin. In most of the known calmodulin-target enzyme interactions calmodulin is only associated with the target enzyme when it binds calcium. In the case of PK, however, calmodulin remains an integral part of the multimeric protein assembly even in the absence of calcium.

We have studied calmodulin structure in solution extensively using small-angle X-ray and neutron scattering. Small-angle scattering particularly sensitive to changes in the relationship between the two globular domains of calmodulin that X-ray crystallographic studies indicate are connected by a solvent exposed α-helix (2). In our first X-ray scattering studies of calmodulin (3), we proposed that the interconnecting helix region of calmodulin was flexible in solution, and that on average the two globular lobes were closer together than observed in the crystal form. More recently, we have focused on X-ray and neutron scattering studies of the structures of calmodulin-peptide complexes as model systems for calmodulin-target enzyme interactions. The peptides used in these studies have been based on calmodulin-binding domains from target enzymes. In particular, we previously investigated the structure of calmodulin complexed with the 27-residue synthetic peptide, termed MLCK-I, using X-ray and neutron scattering (4). The MLCK-I peptide is based on the calmodulin-binding domain of myosin light chain kinase (MLCK). Upon binding to calmodulin, MLCK-I causes a dramatic contraction of the structure that brings the two globular lobes of calmodulin into close contact with each other (see figure below). Recently, two non-contiguous 25 residue peptide sequences have been identified in the γ-subunit of PK which bind to calmodulin synergistically and with nanomolar affinity (5). These two peptide sequences, designated PhK5 and PhK13, are thought to represent two distinct calmodulin binding domains that act in concert to bind calmodulin. The identification of <u>two</u> binding domains in the γ-subunit suggests a fundamentally different type of calmodulin-target enzyme association compared with MLCK and other target enzymes in which the calmodulin-binding domain appears to be contained in a relatively restricted region of the molecule.

Experiment report *(continued)*:

RESULTS: A contrast variation study of calmodulin complexed with PhK5 and PhK13 was completed by measuring neutron scattering data for 75% deuterated calmodulin complexed with non-deuterated PhK5 and PhK13 in solutions with different D_2O:H_2O ratios. In addition, X-ray scattering data were measured for calmodulin complexed with the PhK5 and PhK13 peptides individually as well as with the two peptides together. The structural parameters for the calmodulin + PhK5 complex are remarkably similar to those obtained previously for calmodulin + MLCK-I, indicating that there is a general contraction of the calmodulin on forming a complex with each of these peptides. The peptides PhK5 and MLCK-I have sequences that are predicted to have a high propensity for forming an amphipathic helix in solution, a characteristic believed to be a general property of many calmodulin binding domains in target enzymes. It is perhaps not surprising, therefore, that the nature of the interactions of calmodulin with MLCK-I and with PhK5 are similar. The data suggest that the MLCK-I and PhK5 peptides both bind in a central location with respect to the calmodulin. The structural parameters for the calmodulin + PhK13 complex are strikingly different from those for the calmodulin + PhK5 complex. The data indicate the PhK13 peptide binds in such a way that calmodulin is extended. The sequence of the PhK13 peptide is unlike the PhK5 peptide in that it has little amphipathic helix-forming propensity, but is more likely to form ß-structures according to Chou-Fasman analysis. When calmodulin binds simultaneously to PhK5 and PhK13, the complex appears to be very similar to the calmodulin + PhK13 complex. The results of the neutron scattering contrast series indicate that calmodulin itself is extended in the presence of the two peptides, quite unlike the case for either calmodulin + MLCK-I or calmodulin + PhK5. The fact that calmodulin contracts on binding PhK5 alone, but appears to respond differently when both PhK5 and PhK13 are present has significant implications for the interpretation of calmodulin-peptide interactions in terms of target enzyme binding mechanisms. The combined results of these neutron and X-ray scattering experiments have provided valuable new structural information concerning the interactions of calmodulin with the PK calmodulin-binding domain, and a manuscript on these results has been submitted to *Biochemistry* (6).

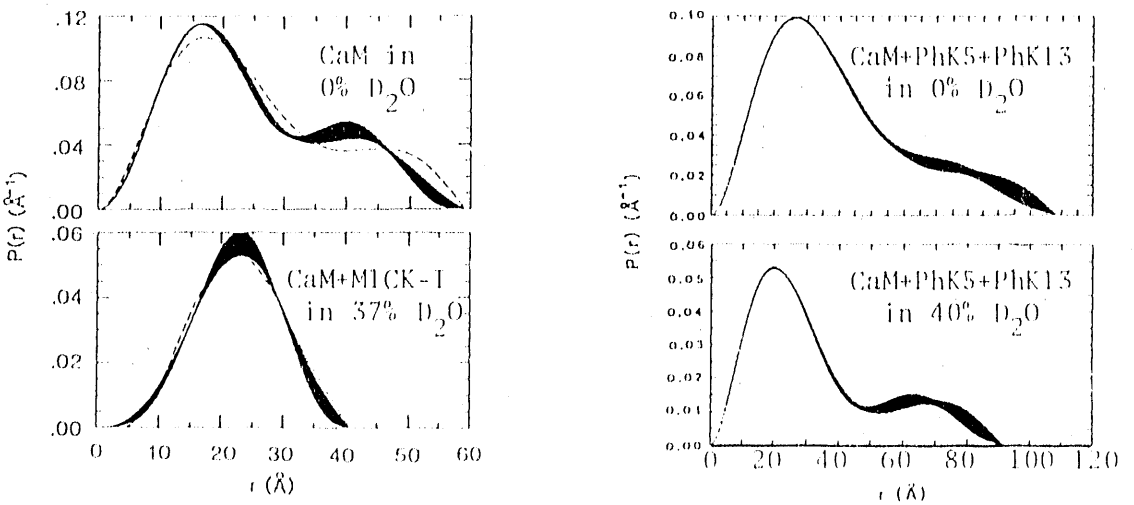

Figure: Vector distribution functions, P(r), calculated from neutron scattering data for the complexes indicated. The peptides are approximately solvent matched in 37-40% D_2O. The plots to the right are from the current experiments, those to the left are from the previous work and are given for comparison.

References:

(1) Picket-Gies, C.A., and Walsh, D.A., The Enzymes, 17:395, 1986 (2) Babu, Y. S., Sack, J. S., Greenhough, T. J., Bugg, C. E., Means, A. K., & Cook, W. J., (1985) *Nature (London) 315*, 37.

(3) Heidorn, D.B., & Trewhella, J. *Biochemistry 27*:909 (1988).

(4) Heidorn, D.B., Seeger, P.A., Rokop, S.E., Means, A.R., Crespi, H., & Trewhella, J. *Biochemistry 28*:6757 (1989).

(5) Dasgupta, M., Honeycutt, T., & Blumenthal, D.K., *J. Biol. Chem. 264*:8054 (1989).

(6) Trewhella, J., Blumenthal, D.K., Rokop, S.E., & Seeger, P.A. (1990) submitted to *Biochemistry*.

Instrument used: *(please type)*	Local contact:	Proposal number: *(for LANSCE use only)*
LQD	P. A. Seeger	223.0

Title:	Report received: *(for LANSCE use only)*
CALMODULIN STRUCTURE	

Authors and affiliations:

Trewhella, J., Rokop, S. E., Henderson, S., Life Sciences Division, Los Alamos National Laboratory.

Hobart, D., Palmer, P., Isotope and Nuclear Chemistry Division, Los Alamos National Laboratory.

Seeger, P. A., P-LANSCE, Los Alamos National Laboratory.

Experiment report:

BACKGROUND: The calcium ion is the major regulator of intra-cellular processes that occur on millisecond time scales. Regulation is generally achieved by Ca^{2+} binding to a protein and inducing a conformational change which allows the protein to activate a target enzyme. Calmodulin (CaM) is a ubiquitous Ca^{2+} binding protein known to regulate a wide variety of processes from neurotransmitter release to muscle contraction. We have been studying the solution structure of CaM as a free monomer in solution, and when it is interacting with target enzymes. Small-angle X-ray scattering data from CaM as a free monomer in solution do not agree well with its crystal structure. The crystal structure of CaM is unusual in that it shows two compact globular domains connected by an extended α-helix of about 9 turns, that is mostly exposed to solvent (Babu et al., 1985). There are two Ca^{2+}-binding sites in each globular domain. We have proposed an alternative model based on the solution scattering data (Heidorn and Trewhella, 1988). Our model preserves the structures of the two globular domains seen in the crystal form, but places them closer together, on average, by about 10 Å. This rearrangement requires flexibility in the interconnecting helix region. Small-angle neutron scattering data from CaM complexed with its binding domain from one of its target enzymes, myosin light chain kinase, support the idea that the interconnecting helix is flexible (Heidorn et al., 1989). These studies show that CaM adopts a much more compact structure when it binds the target enzyme domain. While there is a considerable body of indirect evidence to support the conclusions drawn from the small-angle scattering studies, the precise nature of the solution structure of CaM remains controversial. There are a large number of conflicting spectroscopic studies aimed at measuring the distance between the 4 Ca^{2+}-binding sites of CaM. If these distances were known, it would place important constraints on models for the structure in solution.

RESULTS: We have used neutron resonance scattering to measure the distances between Ca^{2+}-binding sites in CaM. ^{240}Pu has a strong nuclear resonance at 0.278 Å. At this wavelength the coherent scattering from ^{240}Pu is 1000 times that of any other nucleus present in a protein solution. Pu^{3+} has the same ionic radius as Ca^{2+}, and we were successful in stabilizing Pu^{3+} in a Tris buffer at pH 6 for several hours. We also established, using visible spectroscopy, that Pu^{3+} binds to CaM at 4 specific sites. Finally, we have shown that $4Pu^{3+}$•CaM activates one of its target enzymes (myosin light chain kinase) at least as efficiently as does $4Ca^{2+}$•CaM, indicating that structural data derived from $4Pu^{3+}$•CaM is relevant to the biologically active form of CaM.

Experiment report *(continued)*:

Neutron data were collected from D_2O solutions of $4^{240}Pu^{3+}$•CaM, $4Ca^{2+}$•CaM, $4^{149}Sm^{2+}$•CaM, as well as a D_2O buffer. Each of the CaM containing samples was approx. 50 mg/ml protein and the solution conditions were those for which CaM is known to be a soluble monomer. The $4^{149}Sm^{2+}$•CaM was measured because ^{149}Sm has a neutron scattering resonance near 1 Å, though it is broader than the ^{240}Pu resonance and not as strong. If the resonance scattering was measureable, however, future studies with ^{149}Sm would be a lot easier, in terms of safety issues and chemsitry, compared with Pu. To date, however, we have observed no resonance scattering in the $4^{149}Sm$•CaM data. On the other hand, Figure A shows very clearly the resonance scattering in the ($4^{240}Pu$•CaM - buffer) data. The peak in the scattering as a function of neutron time of flight occurs at approx. 870 μs, and within the experimental uncertainties this time of flight corresponds to a neutron wavelength of 0.278 Å. The width of the peak agrees well with the known width of the ^{240}Pu resonance. Figure B shows this resonance scattering data as a function of the scattering vector Q. Using a two point scattering model and searching for a minimum in χ^2 for the observed and caclulated scattering intensities, a separation distance of approx. 13 Å was determined for the scattering centers. This distance agrees well with the distance between the ion-binding sites within a single globular domain of CaM determined from the crystal data. This agreement is expected, though the distance has not been directly measured before for CaM in solution. The longer distance between ion binding sites in different domains (approx. 45 Å), would give rise to a higher frequency modulation of the two point scattering profile (Trewhella et al., 1990). Unfortunately, due to problems with the alignment of the collimation system on LQD (which could not be improved at the time of the experiment) the background levels were exceptionally high for these measurements, and hence the signal to noise ratio in the data is very high. As a result, the statistical errors prohibit analyzing for any such modulations, and the longer distance cannot be determined from the current data. Once the background problems are solved on LQD, however, it is anticipated that this experiment can be repeated and be an unqualified success. This technique provides a novel approach to structure determination in biological systems that has many other potential applications, including further experiments on CaM•target enzyme interactions.

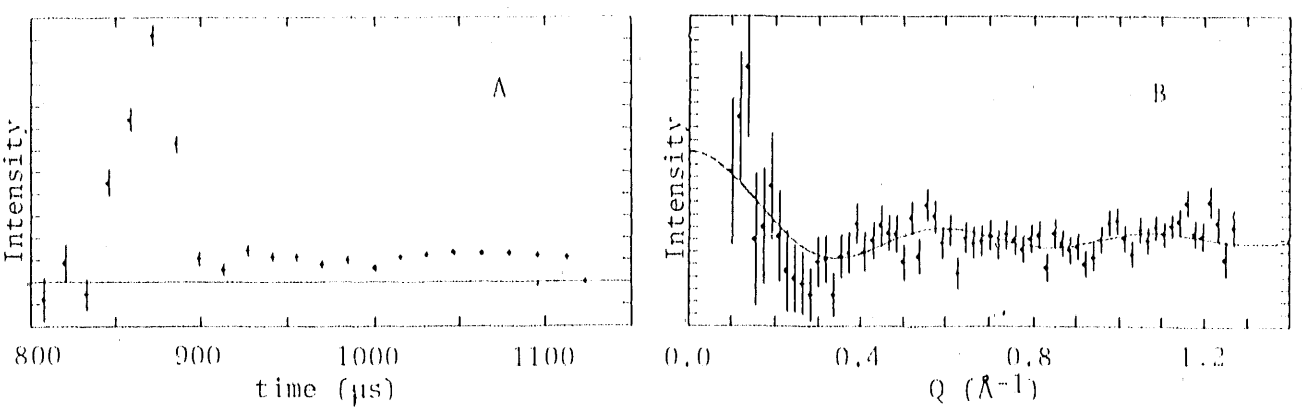

References:

Babu, Y. S., Sack, J. S., Greenhough, T. J., Bugg, C. E., Means, A. K., & Cook, W. J., (1985) *Nature (London) 315*, 37.

Heidorn D. B., & Trewhella, J., (1988) *Biochemistry 27*, 909.

Heidorn, D. B., Seeger, P. A. Rokop, S. E., Blumenthal, D. K., Means, A. R., Crespi, H., & Trewhella, J., (1989) *Biochemistry 28*, 6757.

Trewhella, J. Heidorn D. B., & Seeger, (1990) *J. Mol. Cryst. and Liq. Cryst.*, in press

Instrument used: *(please type)*	Local contact:	Proposal number: *(for LANSCE use only)*
LQD	Philip A. Seeger	225.0

Title: Dislocation-Hydrogen Correlation in Palladium

Report received: *(for LANSCE use only)*

Authors and affiliations:

John S. King University of Michigan

Brent J. Heuser University of Michigan

Experiment report:

This experiment was planned to search for the net dislocation scattering between deformed and undeformed single crystals of Pd and Cu. It is part of a study of net scattering from hydrogen (deuterium) clustering at or near dislocations in metals. The latter has been observed by us in polycrystal Pd, apparently with very good results.(1) However, dislocations alone have not been seen by us in Pd, whereas we, and others, have clearly seen this event in both single crystal and polycrystal Cu.(2)

Pairs of Cu and Pd samples were examined. One of each pair was deformed by rolling to a CW ≈70%. The normal for all wafer samples was close to [220]. The Cu samples were the same pair examined at ANL in 1987. Data were taken for all time slices but because of strong multiple Bragg forward scattering, only data above the Bragg cutoff (above time slice 65) could be used to search for dislocation scattering. Of special interest was (a)the increase in intensity for CW samples over the undeformed control samples (a net effect often ignored in earlier dislocation studies), and (b)the slope of intensity vs Q for the net in the Q range below ~ 0.025Å^{-1}. In this region a Q^{-3} behavior is expected from theory.(3)

Results were discouraging: (a)the net Pd scattering was negative. Over the range Q=0.009Å^{-1} to 0.025Å^{-1} the average ratio of intensity for deformed to reference Pd was 0.64; (b)the same comparison for Cu was positive but with a ratio of only 1.15. The Cu ratio is to be compared, for the same samples, to the 1987 ANL average value of 3.5 to 4.5. This gross discrepancy can only be attributed to the unlikely (to us) defect migration occuring over a two year shelf-life at room temperature. Otherwise there is a gross difference (also unlikely to us) between the reduction of these weak net signals between SAD and LQD. The purpose of the Cu data was just to make this comparison.

The negative Pd effect confirms a similar result we observe for polycrystal comparison. Although as yet we have no quantitative explanation, we think it may be due to extinction in coherent forward scattering. This is suggested by a distinctly different multiple Bragg behavior between Cu and Pd, which LQD allowed us to examine in very good detail.

Experiment report *(continued)*:

The leading multiple Bragg events are due to (111) planes at longer λ and then to the (200) planes. The scattering spatial profiles are complicated if the crystal orientation (220) is not closely collinear with the beam axis. This produces a double time slice peak. For reference Cu this was very large, the tilt indicated being of about 8° (later closely confirmed by wide angle measurements at U.M.). CW broadens and coalesces these double peaks. For reference Pd this was not so evident (although Pd samples measured on LQD in 1988 were double peaked). For reference Cu and Pd, a striking right cross was observed. The width of the arms of the cross are determined by the projected beams width, but the direction and length of the arms are due to rotation of the second scattering planes about the final k vector from the first event.[4] This produces, even for small mosaic spread, a line that sweeps across the detector face. The line directions of (111) and (200) are exactly 90° apart.

Table I shows the differences in peak counts and peak total areas for (111) in Cu and Pd. Table II shows the slopes observed for individual samples, and that for the Cu difference. The slopes on a Guinier plot are very nearly constant (within our large error limits) over the range in Q used, .009-.025Å^{-1}. Time slice data from 65 to 147 were used for the data of Table II.

TABLE I

Sample and Run No.	Peak ct. rate	FWHM	Peak Areas
Cu (reference), (1059)	390,000	0.0044 rads*	1,716
Cu (deformed), (1062)	720,000	0.093 rads	66,960
Pd (reference), (1065,1068)	70,000	0.027 rads*	1,860
Pd (deformed), 1063	29,000	0.112 rads	3,248

*Measured by 2-crystal scattering at U.M. Both ≃1.0 LQD time slice.

TABLE II

Sample and Run No.	n in Q^n
Cu (reference), (1059)	-2.83 ± 0.2
Cu (deformed), (1062)	-2.88 ± 0.2
Pd (reference), (1065,1068)	-3.30 ± 0.2
Pd (deformed), (1063)	-2.92 ± 0.2
Cu difference, (1062-1059)	-3.23 ± 0.5

10 transmissions and 6 sample runs in 22½ hours with beam up.

References:

1.) "SANS Measurement of Deuterium-Dislocation Correlation in Palladium", B. J. Heuser, G. C. Summerfield, J. S. King, and J. E. Epperson, MRS Symposium J.: Neutron Scattering for Materials Science, Boston, MA November 27 - December 2, 1989 (in publication).

2.) J. E. Epperson, G. Kostorz, C. Ortiz, P. Furnrohr, and K. W. Gerstenberg, Acta Metall. 27, 1363 (1979).

3.) H. H. Atkinson and P. O. Hirsch, Phil. Mag. 3, 213 (1958).

4.) A. Guinier and E. Guyon, J. Appl. Phys. 30, No. 5, 622 (1959).

Instrument used: *(please type)*	Local contact:	Proposal number: *(for LANSCE use only)*
LQD	P. A. Seeger	227.0

Title:	Report received: *(for LANSCE use only)*
ORDERING OF BIOLOGICAL ASSEMBLIES USING MAGNETIZED FERROFLUIDS	

Authors and affiliations:

T. Sosnick and J. Trewhella, Life Sciences Division, Los Alamos National Laboratory.

S. Charles, Physics Dept., University College of N. Wales, Bangor LL572UW U. K.

P. Yau and E.M. Bradbury, University of California at Davis and LANL

P. A. Seeger, P-LANSCE

Experiment report:

BACKGROUND: Small-angle scattering is widely used to study biological structures, but it suffers from the inability to determine a unique structure from the scattering because of the random orientation of the scattering particles. If one degree of freedom is removed by aligning the particles in one dimension, more detailed information about the structure can be determined. For example, diffraction peaks can be uniquely assigned to dimensions in the directions parallel or perpendicular to the applied field. Shearing forces and magnetic fields have been used with notable success to align a number of biological assemblies for structural studies. However, these techniques depend on specific physical properties of the a sembly and are not generally applicable to all problems of interest.

We have developed a new alignment technique that takes advantage of the properties of magnetized ferrofluids (1). Using modest magnetic fields, we have successfully aligned virus particles, with axial ratios of about 10:1, independent of their intrinsic magnetic properties. The viruses used in this development work (tobacco mosaic virus (TMV) and tobacco rattle virus (TRV)) were chosen because of their elongated shape and inherent structural stability. The alignment technique depends principally on the asymmetric geometry of the particle of interest and thus complements the existing techniques for magnetic alignment that depend on intrinsic diamagnetic anisotropy.

We are now interested in applying the ferrofluid system for alignment to chromatin structural studies. How a 2m length of DNA is packed into a 10μ nucleus in a replicable form is a fundamentally important question in biology. The packaging appears to be highly structured and the structure must be modulated during cell cycle to allow the genes to become more or less accessible to cellular control as needed. Chromatin consists of proteins associated with very long strands of linear DNA. When inactive chromatin is isolated from cell nuclei it comes in the form of chromatin fibers which can form order structures. Under certain ionic conditions (e.g. >40mM NaCl) the chromatin fiber is believed (2) to form a superhelix which has a nominal diameter of 300Å (3). This supercoil is believed to "tighten", increasing its mass per unit length, with increasing ionic strength. Numerous small-angle neutron and X-ray scattering experiments have been done on this structure, and diffraction peaks have been observed including one corresponding to a repeat distance of 11 nm. This peak could be due to either the helical

Experiment report *(continued)*:
repeat of the proposed supercoil, or to its diameter. Extensive model calculations have been performed (3) which associate the peak with the supercoil pitch but this assignment is not proven. If the chromatin fibers could be aligned using ferrofluids, the diffraction peaks could be uniquely assigned to particular structures. Importantly, the structural parameters determined would be for chromatin fibers in solution.

RESULTS: Neutron scattering data were measured for chromatin in deuterated ferrofluid using using the LQD in a previous experiment (Exp. 138), but the concentration of the chromatin was too low to derive any new structural information. The ferrofluid consisted of a magnetite core with deuterated detergent surfactants, and the carrier fluid was D_2O. The magnetic particles were approximately solvent matched to the D_2O in this preparation and thus did not contribute significantly to the scattering. If a non-ionic detergent surfactant is used for the ferrofluid preparation we have found that the biological structures we have studied retain their native structures in the ferrofluid.

The experiment was repeated this time at a much higher concentration, 10 mg/ml, and with longer fibers. Based on our previous work with TMV in ferrofluid we believed that these factors might help to increase the degree of ordering. In addition the increased chromatin concentration would improve the signal to noise ratio for the measurements. Neutron scattering data were measured for chromatin in deuterated ferrofluid for two different salt concentrations, 70 and 160 mM NaCl. The chromatin was diluted 1:1 with deuterated ferrofluid and measured in 4mm path length cuvettes with an applied magnetic field perpendicular to the neutron beam of about 5000 gauss. The neutron scattering data show evidence for alignment of the chromatin in both samples. In addition, the small-angle scattering from chromatin in ferrofluid and from chromatin in D_2O both with 70mM NaCl, indicates the structure of the chromatin is not perturbed by the ferrofluid. A^2 diffraction peak at $Q=0.02Å^{-1}$ in the direction perpendicular to the magnetic field was observed in the 160mM NaCl sample. This peak has been seen by others and is due to a 300Å distance in the direction perpendicular to the fiber axis. The peak has been attributed to a regular side-by-side packing distance of the fibers.

The degree of alignment found in these experiments is still significantly less than that observed previously for TMV in ferrofluid. Also, the scattering from the ferrofluid blank (which is subtracted to eliminate its contribution to the total scattering) was substantially greater than that observed with the previous ferrofluid preparations. This greatly reduced the signal-to-noise of the measurement and resulted in poor counting statistics. Because of these poor statistics coupled and the limited alignment, we were unable to assign directions to the diffraction peaks for $Q \geq 0.06Å^{-1}$. We have since improved the ferrofluid preparation and believe that we can produce a ferrofluid with about twice the magnetization and with magnetic particles that are better matched to the neutron scattering density of D_2O. With this improved ferrofluid we hope to repeat the chromatin experiments at a future date.

References:

(1) Hayter, J.B., Pynn, R., Charles, S., Skjeltorp, A., Trewhella, J.,Stubbs, G., & Timmins, P., Phys. Rev. Lett. **62**, 13, 1667 (1989).

(2) Bradbury, E.M., & Baldwin, J.P., in Supramolecular Structure & Function, Ed. Greta & Pifaf-Mrzlijak, Springer Verlag Berlin, p63-92, (1986)

(3) Bordas, J., Perez-Grau, L., Koch, M.H.J., Vega, M.C., and Nave, C., Eur. Biophys. J. **13**, 157 (1986); Bordas et al., ibid., 175

Instrument used: *(please type)*	Local contact:	Proposal number: *(for LANSCE use only)*
LQD	P. Seeger R. Hjelm	232.0
Title: Critical Phenomena in Binary Liquid Mixtures in Porous Glasses		**Report received:** *(for LANSCE use only)* 1-10-90

Authors and affiliations:

P. Wiltzius
S. B. Dierker

AT&T Bell Laboratories
Rm 1C-352,
600 Mountain Ave.
Murray Hill, NJ 07974

Experiment report:

During experiment # 232 we measured the structure factor $S(q)$ for the critical binary fluid mixture water-lutidine imbibed into various porous materials. The most extensively used material was porous *VYCOR* glass. We were able to measure mixtures with 15 different compositions at temperatures between 10 ℃ and 80 ℃. In addition we carried out exploratory experiments with different porous glasses (so-called *Controlled Pore Glasses)* and porous materials with radically different morphologies (*Anotec* membranes with channels arranged in a honey-comb structure).

An important aspect of experiments on fluids in Vycor is the ability to use contrast-variation techniques. Even though we knew the scattering density of Vycor to be $\rho_{Vycor}=3.6\times10^{10} cm^2$ and had appropriately prepared the fluid samples using mixtures of regular and heavy water, the first few measurements did not yield the expected $S(q)$ without a peak due to the porous glass. It turned out that our new anodized aluminum cell, which we had designed to ensure optimal temperature stability and uniformity, had a small angle scattering pattern with a peak at nearly the same q as Vycor. After the anodized layer had been milled off that problem was gone.

In the figure below, $S(q)$ is depicted as a function of temperature between 10 ℃ and 80 ℃. With current data analysis we get useful data for $0.008 \lesssim q \lesssim 0.2 \text{Å}^{-1}$. At low temperatures $S(q)$ is very small compared to dry *VYCOR* (maximum intensity around 50) as expected for an index matched sample. However, it is larger than $S(q)$ measured for Vycor filled with a mixture of 40 % H_2O and 60 % D_2O (intensity $\lesssim$0.1 mostly due to incoherent background). An important feature of the data is the change of the line shape of $S(q)$ from a single Lorentzian (limiting slope of -2 as $q \rightarrow \infty$), which is omnipresent in equilibrium phases, to a Lorentzian squared at high temperatures (limiting slope of -4 as $q \rightarrow \infty$). This is theoretically predicted to happen at a random field transition. We used a sum of a Lorentzian and a Lorentzian squared with the same correlation length ξ as a fit function for the data over the temperature range covered. Within the statistical uncertainty the fit could not be improved by allowing two different correlation lengths for the two different terms. This is in agreement with recent simulations of the random field transition. ξ increases only modestly from 20 Å at 10 ℃ in the one phase region to 60 Å at 80 ℃ at the random field transition. The knowledge of ξ establishes an important link between

Experiment report: *(continued)*

dynamics [1] and statics [2-4] of random field systems. With it we can analyze the relationship between the static correlation length ξ and the dynamic relaxation rate Γ and learn about hydrodynamics in confined and random media.

We want to point out that the statistical quality of the data obtained at *LANSCE* is very high, as might be judged by the error bars which in most cases are smaller than the symbols of the data points. For instance, we believe that the feature in the data around $q \approx 0.04$ Å^{-1} is real. The small bump is moving to lower q with rising temperature. This is more obvious in runs on other samples with different composition. Understanding features in $S(q)$ such as these is part of the overall difficult scattering problem, which currently deserves all our effort.

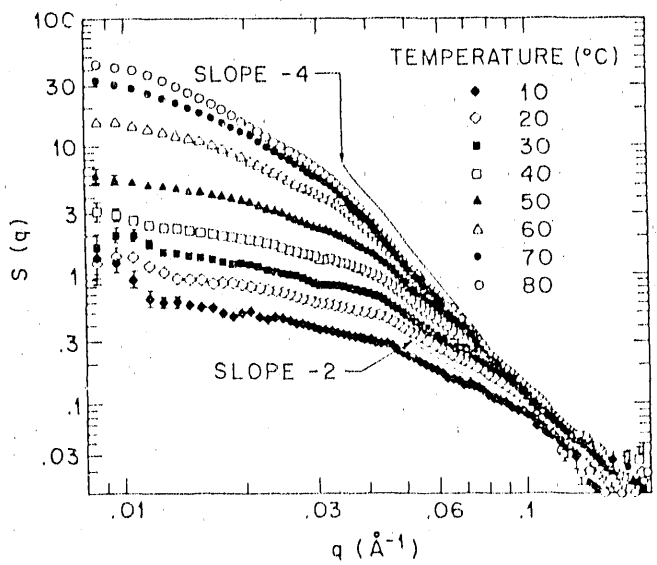

In order to study the influence of the ratio of pore size to pore volume on the random field and finite size effects we performed measurements on mixtures imbibed into *Controlled Pore Glasses* with pore sizes ranging between 170 Å and 3000 Å. The characterization of the dry glasses was succesfull. The data obtained from the glass samples filled with fluid mixture have a large component which is due to the fluid surrounding the glass grains (typical size 100 to 1000 micron). It appears that we have to reduce the amount of fluid that is not inside the porous glass in order to proceed with these experiments.

The third type of porous material used were *Anotec* filter membranes. Unfortunately these experiments did not work out the way we expected. Since the pore channels of the membrane were oriented in a direction parallel to the incident neutron beam most of the detected neutrons were reflected by the channel walls and not scattered.

Because most of our experiments were performed with contrast matched samples we had to deal with weak scatterers. The installation of the new five hole collimator was thus very timely and allowed a good turnover rate. Direct comparison of data taken on dry Vycor at the small angle facility in Oak Ridge with data taken at *LANSCE* indicates, however, that the q-resolution is better at Oak Ridge. This is probably due to methods employed in the preliminary data reduction, which is currently being fine tuned in collaboration with the resident instrument scientists.

References:

1. S. B. Dierker and P. Wiltzius, Phys. Rev. Lett. *58*, 1865 (1987).
2. P. Wiltzius, S. B. Dierker, and B, S, Dennis, Phys. Rev. Lett. *68*, 804 (1989).
3. P. Wiltzius, S. B. Dierker, Lansce Newsletter, *11*, 4 (1989).
4. S. B. Dierker and P. Wiltzius, Proceedings of the Materials Research Society, Fall Meeting 1989.

Instrument used: *(please type)* LQD	Local contact: P. A. Seeger	Proposal number: *(for LANSCE use only)* 245.0
Title: **Effects of H5 upon the Structure of the 195bp Nucleosome Particle**		Report received: *(for LANSCE use only)* 2/1/90

Authors and affiliations:

P. Yau [*], B. Imai [+], E.M. Bradbury [+], T. Sosnick [+], R. Hjelm^, and J. Trewhella [+].

[*] Biological Chemistry, School of Medicine, University of California, Davis, CA 95616
[+] Life Sciences Division, Los Alamos National Laboratory, Los Alamos, NM 87545
^LANSCE, Los Alamos National Laboratory, Los Alamos, NM 87545

Experiment report:

BACKGROUND: The basic structural subunit of chromatin is the nucleosome. It contains an octamer of histone proteins and a one molecule of lysine rich H1 or H5 along with about 200 base pairs (bp) of DNA which is wrapped twice around the octamer. This DNA is part of a continous piece that connects each of the octamers into a single chain. The primary function of the nucleosomes is to package the meter of DNA found in a eukaryotic nucleus into a compact yet accessible form. Accessibility of the DNA to the machinary of replication and transcription must be modulated at least in part by changes in chromatin structure. The purpose of the current experiment was to examine the changes in structural parameters of the nucleosome when H5 is removed. H5 is believed to bind external to the DNA and "seal off" the two turns of 167bp DNA as they exit. Potentially, H5 could alter the exit angle of the DNA from the histone core which would affect its accessibility and the relative orientation of the nucleosomes to each other. Importantly, the nucleosomes were reconstituted with a defined 195bp sequence of ribosomal DNA having a single positioning sequence. The use of the specific DNA removes the heterogeneity in DNA lengths and compositions present in previous experiments.

RESULTS: All samples showed signs of aggregation limiting analysis to data above $Q_{min}=0.02\text{Å}^{-1}$, or for data where $Q \bullet R_g > 0.9$. The values cited in the table are for a Guinier analysis out to $R_g \bullet Q = 1.3$. The P(r) analysis was similarly hindered by aggregation but did produce values for R_g which were in good agreement with the Guinier analysis. Generally, the derived values for R_g were slightly higher than found in previous work. The match point for the nucleosome with H5 was close to earlier values as was the value for the particle volume, V_c, derived from the slope of $\sqrt{I(0)}$ versus contrast. However, without H5, both the match point and V_c were higher than expected. This is probably the result a larger degree of aggregation in the H_2O sample without H5 giving rise to an anomalously high I(0) value.

The slope, α, of linear fit in the Stuhrmann plot is a reflection of non-uniform distribution of scattering intensity within the structure. A positive slope indicates that the larger scattering length component (i.e. the DNA) is generally on the outside of the protein. Though the statistics were poor, we did observe a factor of 2 decrease in α for the addition of H5. This is consistent with H5 binding on the exterior of the DNA.

Experiment report *(continued)*:
Structural Parameters Derived from X-ray and Neutron Scattering Data

Without H5:

$\%D_2O$	Guinier R_g	P(r) R_g	D_{max}	I(0)	√I(0)(cm)
100	38.5 ± 0.7Å	40.3 ± 0.7Å	140Å	0.0948	6.10 ± 0.04E-9
63	very small signal, no analysis possible				
40	no signal				
0	46.3 ± 4.0Å	45.6 ± 1.5Å	140Å	0.0576	7.17 ± 0.12E-9
X-rays	46.8 ± 1.9Å	46.7 ± 1.0Å	145Å	---	----

√I(0) vs contrast (using only the 0 and 100% data) gives $V_c = 191\ nm^3$ and a match point of 54% D_2O. From Stuhrmann plot R_c is approximately 43 Å.

With H5:

$\%D_2O$	Guinier R_g	P(r) R_g	D_{max}	I(0)	√I(0)(cm)
100	41.3 ± 1.0Å	41.7 ± 0.7Å	140Å	0.1966	6.38 ± 0.04E-9
75	very small signal and poor buffer statistics, no analysis possible				
25	very small signal and poor buffer statistics, no analysis possible				
0	44.7 ± 4.3Å	44.1 ± 1.5Å	130Å	0.0607	6.06 ± 0.11E-9
X-rays	46.7 ± 1.4Å	45.0 ± 0.4Å	130Å	---	----

√I(0) vs contrast gives $V_c = 179\ nm^3$ and a match point of 49% D_2O. From Stuhrmann plot, $R_c = 42.9$ Å.

CONCLUSIONS: In the H_2O measurements, for which the DNA contribution to the scattering dominates, we do observe a slight decrease in R_g and a 15 Å decrease in the maximum linear dimension, D_{max}, for the particle upon the addition of H5. A marginal increase in R_g was observed in the 100% D_2O measurements in which the scattering from the protein dominates. These data are consistent with the DNA folding back around the histone core upon the binding of H5.

These result provide some indication of the possible structural changes of the nucleosome induced by H5-binding. However, to quantitate these changes, it is essential to repeat the measurements. We believe that we can prepare samples which are not agreggated by working at lower concentrations. Lower sample concentrations will require longer neutron scattering data acquisition times, but should lead to the critical information required to understand the modulation of chromatin structure induced by H5-binding.

References:

Instrument used: *(please type)*	Local contact:	Proposal number: *(for LANSCE use only)*
LQD	Dr. Rex P. Hjelm Jr.	246.0

Title:

Neutron Scatter Studies of the Structures of Transcription Factor TFIIIA Complexes with i) the 5S Gene DNA; ii) 5S Gene mRNA and iii) the Nucleosome Containing the 5S Gene

Report received: *(for LANSCE use only)*

Authors and affiliations:

Bradbury, E. M.	University of California, Davis and LANL
Schroth, G. P.	University of California, Davis
Cook, G.	University of California, Davis
Gottesfeld, J. J.	Scripps Institute
Hjelm, R. P. Jr.	LANSCE

Experiment report:

BACKGROUND

Transcription Factor IIIA (TFIIIA) is a 40,000 molecular weight protein which binds to DNA sequences in the 5S ribosomal gene and is required for transcription of the gene by RNA polymerase III. It makes contact with its 50 base-pair binding site through nine zinc-finger DNA binding motifs. The entire 5S gene is 120 b.p. in length and TFIIIA binds at positions +45 to +95 relative to the transcription start site. This internal promoter is called the internal control region (ICR). Using a circular permutation assay, we have previously shown that binding of TFIIIA to the ICR induces a bend in the DNA (Schroth et al.). A contrast variation neutron scattering study of the TFIIIA-DNA complex was initiated in order to determine more precise structural information about the complex.

RESULTS

Technical difficulties prevented successful completion of the experiments. The initial plan was to run four contrast match points of 0, 35, 65 and 100% D_2O. This would have allowed the determination of the radius of gyration (R_G) and a P(R) analysis of the DNA and protein components of the complex. During the course of the experiments at LANSCE, there were problems in maintaining an adequate beam current. Most of the data that was collected was very difficult to interpret due to the presence of a large contaminant in the samples that was scattering more strongly than the complex itself. One of the initial runs in 100% D_2O, did give an encouraging R_G of approximately 40 Å. This represents a considerable compaction of the 54 b.p. DNA which has a calculated R_G of approximately 53 Å. This result is consistent with the model of the DNA being tightly bent about the protein core. The subsequent runs were run after a delay and all showed evidence of the large, strongly scattering contaminant. The time dependence of the appearance of the contaminant suggests that it may be due to aggregation of the complex with time.

Experiment report *(continued)*:

CONCLUSIONS

The limited amount of useful data which was collected gives indications that support the biochemical evidence that the DNA is bent in the TFIIIA-DNA complex. Unfortunately, lower D_2O scattering data, which would have indicated the conformation of the protein component was unusable. In the future, the complexes will be reconstituted immediately preceding the actual scattering experiment and kept under stringent non-oxidizing conditions which should help minimize the aggregation potential of the complexes.

References:

Schroth, G. P., Cook, G. R., Bradbury, E. M. and Gottesfeld, J. J. (1989) *Nature 340*, 487-488.

Instrument used: *(please type)*	Local contact:	Proposal number: *(for LANSCE use only)*
LQD	Rex Hjelm	248.0

Title:	Report received: *(for LANSCE use only)*
Excluded Phase Structure in Micellar and Microemulsion Systems	1/19/90

Authors and affiliations:

Eric W. Kaler
Department of Chemical Engineering
University of Delaware
Newark, DE 19716

Jess P. Wilcoxon
Division 1152
Sandia National Laboratory
Albuquerque, NM 87105

Experiment report:

During this experimental session, we made measurements on three different micellar and microemulsion systems, including one in which spontaneous vesicles form.

Our initial plan was to examine the scattering from nonionic surfactant mixtures at temperatures above their lower consulate temperature. In this case, the solutions contain two phases, one rich in surfactant and the other quite lean. We have indications from light scattering experiments that there may be anomalously large structures—of 1000 Å scale—in the dilute phases. Thus our first experiment was to examine the surfactant lean phase of $C_{12}E_5$ in D_2O, and $C_{12}E_6$ with added NaCl in D_2O at 25° C. [Here the notation C_iE_j indicated an ethoxylated alcohol with alkane tail lengths of carbon number i and hydrophilic head groups containing j ethylene oxide unites.] In the SANS q-regime, we had hoped to see q^{-4} Porod scattering, but the scattered intensity was too low over the obtainable q-range (greater than 0.015 $Å^{-1}$) for this weak scatterer for a significant signal to be recorded.

We then tried some experiments that worked; namely a series of measurements on inverted or water-in-oil microemulsions made with nonionic surfactants. In this case, water is contained in small pools (droplets) stabilized by a surfactant film. These systems display the usual upper critical temperature behavior and so can be made one phase near room temperature. These microemulsions can solubilize substantial amounts of material (salts) into their water cores, but the nature of the droplets depends sensitively on the details of the mixture. We measured $C_{12}E_3$, C_6E_5, and $C_{10}E_8$ surfactants in deuterated octane and toluene with and without added water. We also examined inverted microemulsions made with the ionic surfactant AOT as a function of the water/surfactant ratio w_o, but at high w_o the spectra are significantly effected by interdroplet interactions. We are presently interpreting this scattering in terms of the usual models of colloidal scattering (1), but there are surprises. In particular, the scattering of microemulsions formed with d-toluene is qualitatively different from that in octane. More details of these experiments are given in the report of Wilcoxon and Martin.

Experiment report *(continued)*:

Finally, we used a portion of this beam time to characterize a new surfactant structure we have just discovered (2), namely the spontaneous vesicles formed in mixtures of cationic and anionic surfactants. We have reported a general method of preparing spontaneous, equilibrium vesicles of controlled size, surface charge, or permeability from commercially available surfactants. Vesicles formed immediately upon combining aqueous mixtures of two commercially available, single-tailed surfactants with oppositely charged head groups. The curvature of the mixed surfactant bilayers (which controls size and shape), the vesicle wall thickness (which controls permeability), and the sign and magnitude of the surface charge (which controls vesicle interactions and stability against aggregation) can be determined by the relative amounts and the chain length of the individual commercially available surfactants used. We have characterized these vesicles using a variety of methods, and we carried out preliminary SANS characterization of the vesicles formed in aqueous mixtures of cetyl trimethylammonium tosylate (CTAT) and sodium dodecylbenzene sulfonate (SDBS).

A typical scattering curve is shown in Figure 1 for SDBS/CTAT vesicles at a weight ratio of 3/7 and a total surfactant concentration of 2%. The measured data span the expected range from Guinier scattering at low q to Porod scattering a high q. A detailed model of the micell-vesicle transitions in this mixture is being constructed and will allow a quantitative fit of the measured scattering. We have verified that the measured R_g of 180 Å is consistent with the size measured by light scattering.

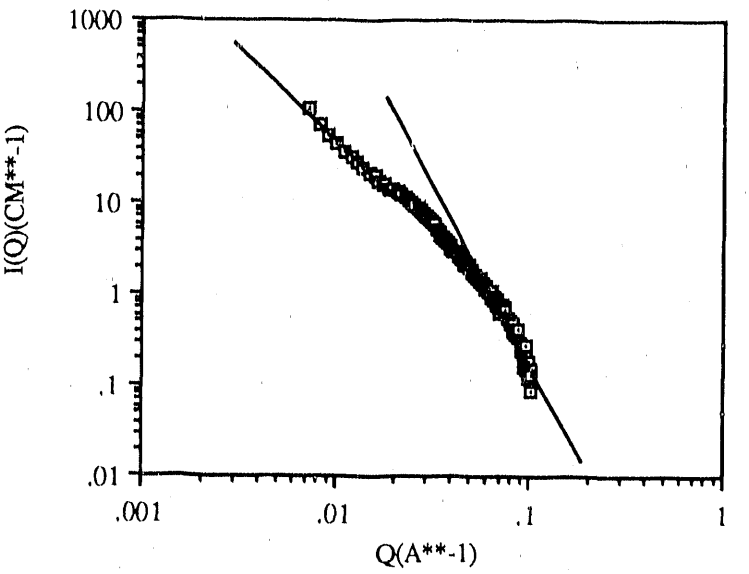

Figure 1. Log-log plot of the scattering from SDBS/CTAT vesicles at a weight ratio of 3/7 and a total surfactant concentration of 2%. The lines indicated q^{-2} and q^{-4} scattering at low and high q respectively; the average radius of gyration is 180 Å.

References:

1. "Modelling Small Angle Scattering from Colloidal Suspensions," E. W. Kaler, J. Appl. Crys. 21, 729 (1988).
2. "Spontaneous Vesicle Formation in Aqueous Mixtures of Single-Tailed Surfactants," E. W. Kaler, A. K. Murthy, B. E. Rodriguez, and J. Zasadzinski, Science 245, 1371 (1989).

Instrument used: *(please type)*	Local contact:	Proposal number: *(for LANSCE use only)*
LQD	R.P. Hjelm	250.0

Title: Summary of the Analysis of SANS Studies of DPPC/DiC7PC Solution

Report received: *(for LANSCE use only)*

Authors and affiliations:

Tsang-Lang Lin, Nat. Tsing-Hua Univ., Hsin-Chu, Taiwan 30043
S.-H. Chen, MIT, MA 02139
M. F. Roberts, Boston College, MA 02167

Experiment report:

See attached report.

Experiment report *(continued)*:

References:

T. L. Lin, S. H. Chen and M. F. Roberts,
"Temperature Dependence of the Growth of diC7PC Micelles Studied by Small-Angle Neutron Scattering"
Submitted to J. Phys. Chem. (Dec. 1989).

Summary of the Analysis of SANS Studies of DPPC/DiC_7PC Solution

Tsang-Lang Lin*, S.-H. Chen**, M. F. Roberts†

*Dept. Nuclear Eng., Nat. Tsing-Hua Univ., Hsin-Chu, Taiwan 30043.

**Dept. Nuclear Eng., MIT, Cambridge MA02139.

†Dept. Chemistry, Boston College, Chesnut Hill, MA02167.

Feb. 5, 1990

Methods of Analysis :

1. The Guinier Plots

By plotting $\ln(I(Q))$ versus Q^2 as shown in Fig. 1, one obtains the scattering amplitude I_0 and the radius of gyration as listed in Table I and Table II. It is obvious that this system is very polydisperse or contains rods or disks, or polydisperse small unilamelar vesicles. The scattering intensities distribution deviates far from the straight line of the Guinier plot. There is a indication of the existence of large globular particles as can be seen from the fast increase in the neutron scattering intensity at Q near zero.

2. The Kratky-Porod Plots

By plotting the $\ln(I \cdot Q^2)$ versus Q^2, one could obtain the thickness of the particles if the scattering intensity data fall on a straight line in the middle-Q region. Figure 2 shows such plots for DPPC/DiC_7PC

in 100% D_2O and in 80% D_2O. The obtained thickness is listed in Table III. This method is not applicable for some cases.

3. The Plot of Contrast Variation

Figure 3 shows the plot of the square root of I_0 versus $\%H_2O$ in the solution. The slopes are proportional to the square root of concentration and the square root of mean aggregation number. These four series of external contrast variation measurements should have the same slopes if their concentration are the same and the I_0 has been accurately obtained. The straight lines are drawn to pass the predicted contrast match points.

3. Model Fitting : Polydisperse Unilamellar Vesicles

The best fit is shown in Figure 4 and the enlarged Figure 5 for the DPPC/DIC_7PC in 100% D_2O. This model does not fit the measured spectrum very well. The scattering in the Q-range from above 0.01 $Å^{-1}$ is due to 14.6% of the added materials. The other 85.4% materials must form large globular particles and they contribute to the large scattering intensities in the very small Q-region. The size distribution of the vesicles needed to fit the data are shown in Fig.6. Their bilayer thickness is kept at 46 Å during the fitting.

4. Model Fitting : Bilayer Disks

The results of Kratky-Porod plots indicate the small particles are most likely disks of radius R and thickness L. The result of fitting is

shown in Fig.7. The goodness of fitting is better than that of polydisperse vesicles. The radius of the disk is found to be 94.5 Å and L=44 Å. The scattering in the Q-range above 0.01 $Å^{-1}$ is due to 18% of the added material. The rest of the material again forms large globular particles, could be large multi-lamellar vesicles, but not large unilamellar vesicles. They could also be large aggregates (clusters) of disks, vesicles, or micelles.

Table I The scattering amplitudes obtained by Guinier plots.

$\%D_2O$	P/P	D/P	P/D	D/D
1.0	15.07±0.05	0.521±0.006	16.97±0.06	0.3174±0.005
0.8	9.05±0.03	N/A	10.74±0.04	0.1604±0.003
0.6	2.348±0.014	0.582±0.005	2.76±0.02	1.300±0.008
0.4	0.8225±0.008	2.021±0.015	0.890±0.009	2.667±0.013
0.2	0.0352±0.003	4.963±0.04	0.0044±0.0001	5.707±0.03

Table II The radius of gyration obtained by Guinier plots.

$\%D_2O$	P/P	D/P	P/D	D/D
1.0	70.9	79.7	76.3	84.5
0.8	73.9	N/A	76.3	46.2
0.6	71.2	63.9	77.9	72.1
0.4	70.5	74.5	80.4	70.9
0.2	56.5±4.3	84.2	56.9	75.1

P: Protonated D: Deuterated

DPPC/DiC_7PC = 20mM/5mM

Table III The thickness L obtained by Kratky-Porod plots.

$\%D_2O$	P/P	D/P	P/D	D/D
1.0	42.6±6	N/A	47.6±0.9	N/A
0.8	44.2±7	N/A	45.9±0.9	N/A
0.6	42.6±7	N/A	44.5±2	[illegible]0
0.4	41.6±3	N/A	43.9±4	30.3±1.9
0.2	N/A	N/A	N/A	37.3

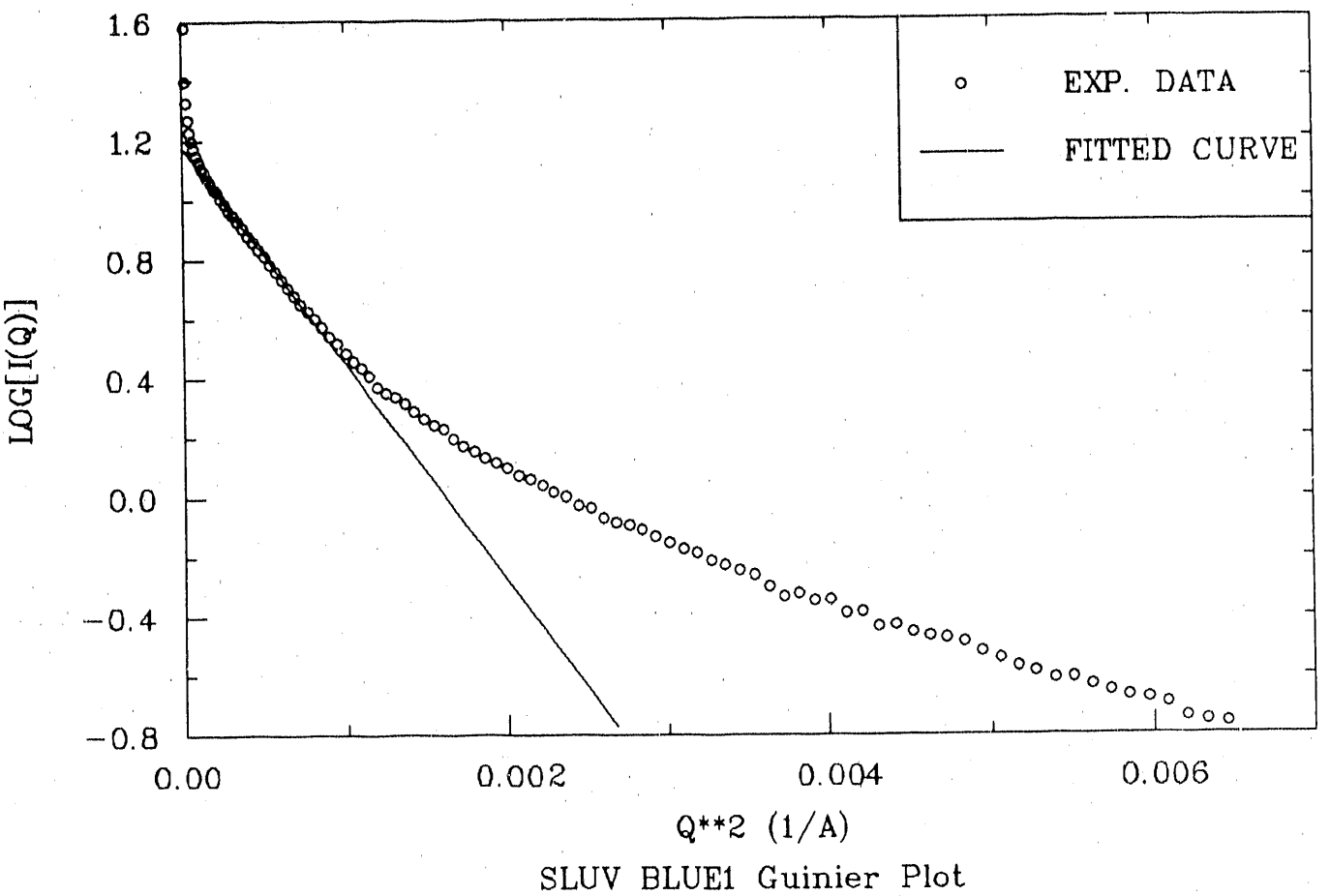

SLUV BLUE1 Guinier Plot

BLUE1

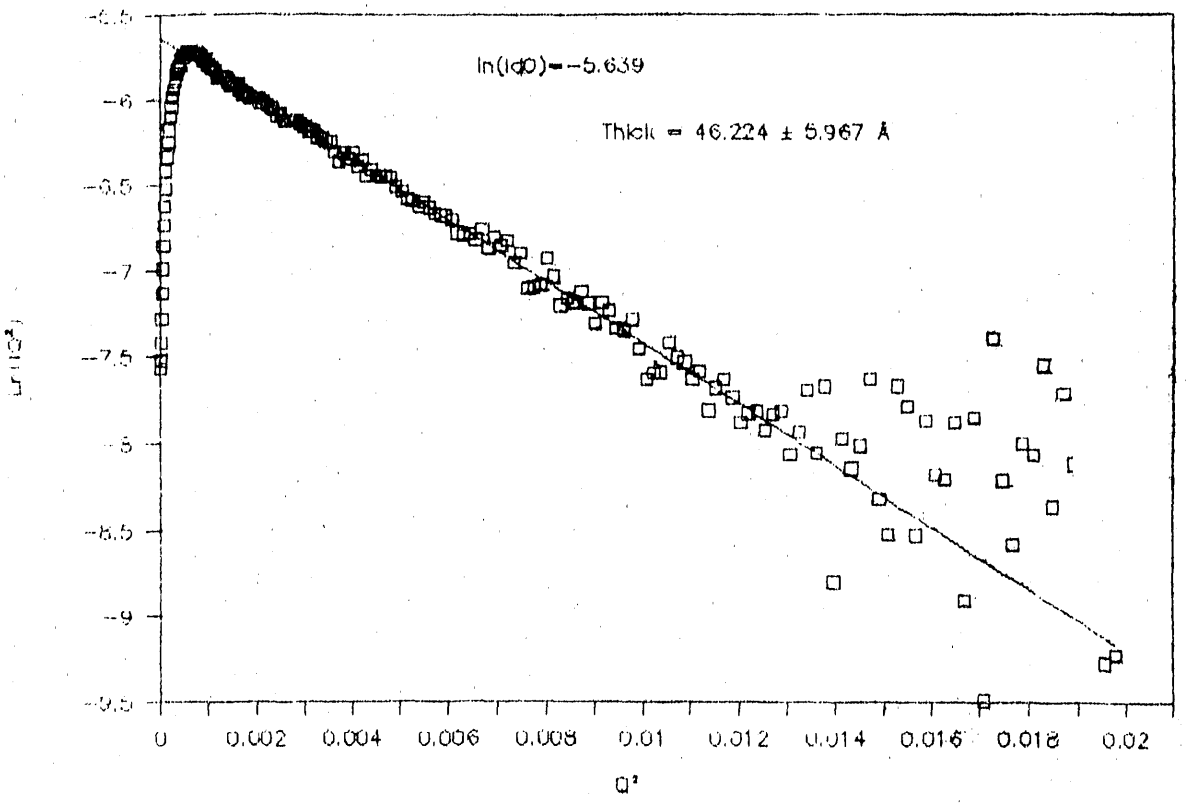
ln(Id0)=-5.639
Thick = 46.224 ± 5.967 Å
-6
-6.5
-7
-7.5
-8
-8.5
-9
-9.5
0
0.002
0.004
0.006
0.008
0.01
0.012
0.014
0.016
0.018
0.02
Q²

BLUE2

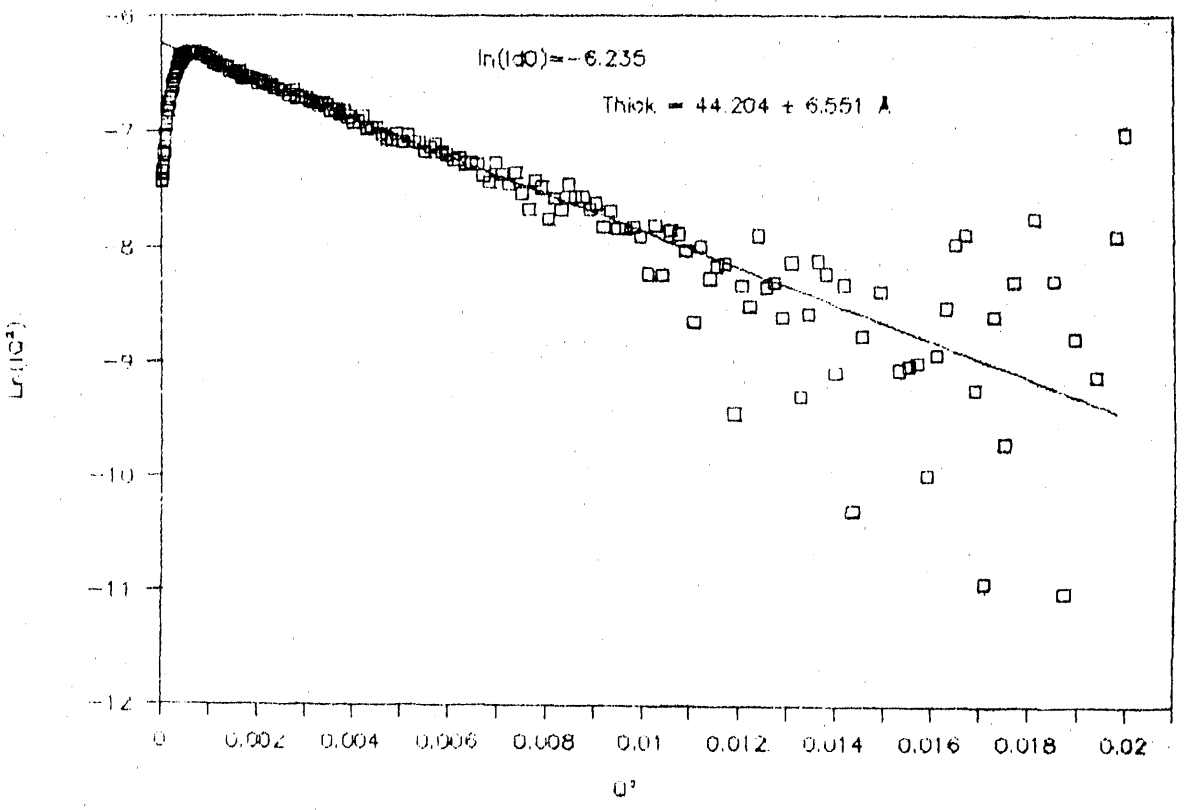
ln(Id0)=-6.235
Thick = 44.204 ± 6.551 Å
-7
-8
-9
-10
-11
-12
0
0.002
0.004
0.006
0.008
0.01
0.012
0.014
0.016
0.018
0.02
Q²

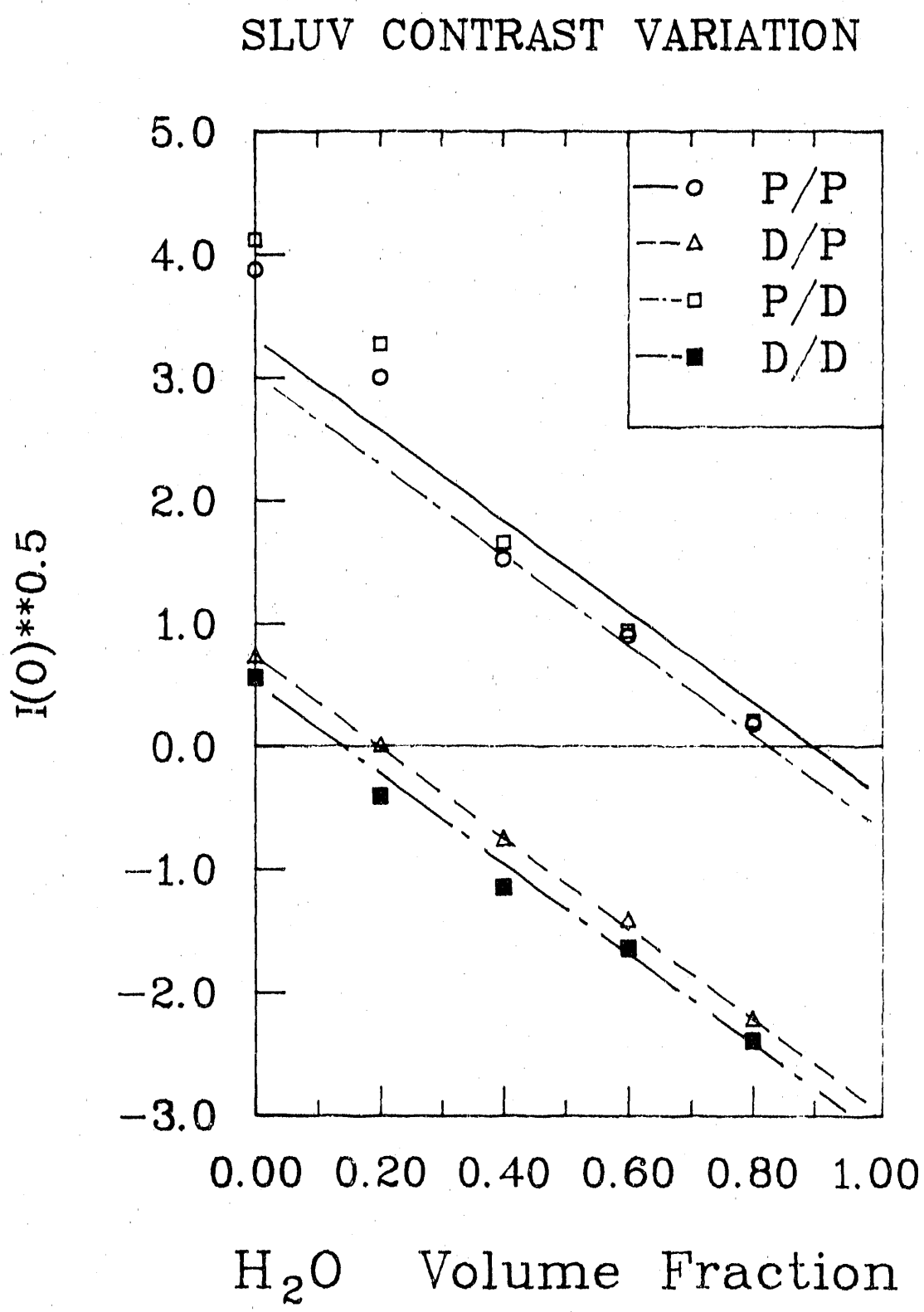
SLUV CONTRAST VARIATION
5.0
4.0
3.0
2.0
1.0
0.0
−1.0
−2.0
−3.0
I(0)**0.5
P/P
D/P
P/D
D/D
0.00
0.20
0.40
0.60
0.80
1.00
H2O Volume Fraction

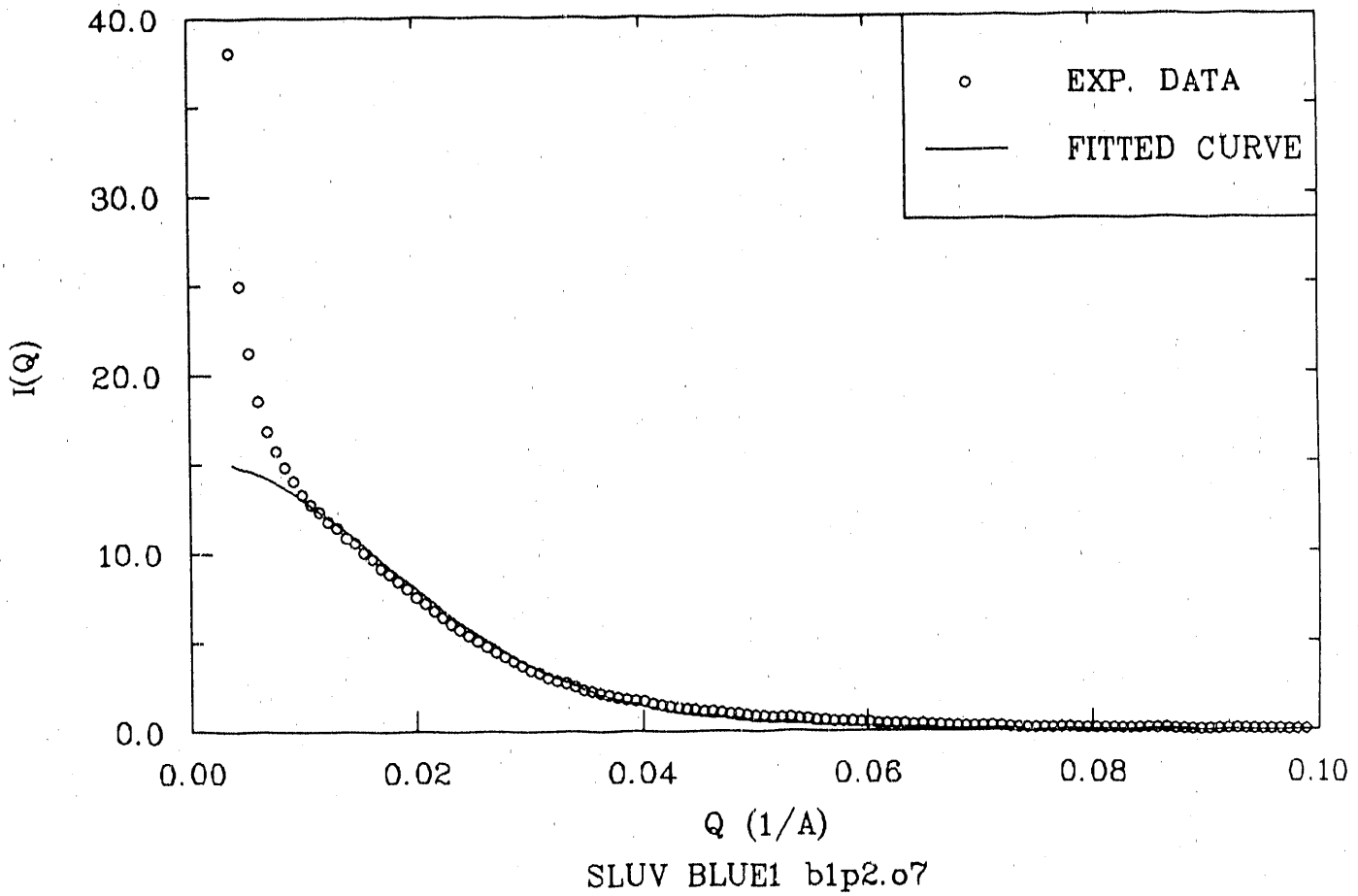
40.0
30.0
20.0
10.0
0.0
I(Q)
0.00
0.02
0.04
0.06
0.08
0.10
Q (1/A)
EXP. DATA
FITTED CURVE
SLUV BLUE1 b1p2.o7

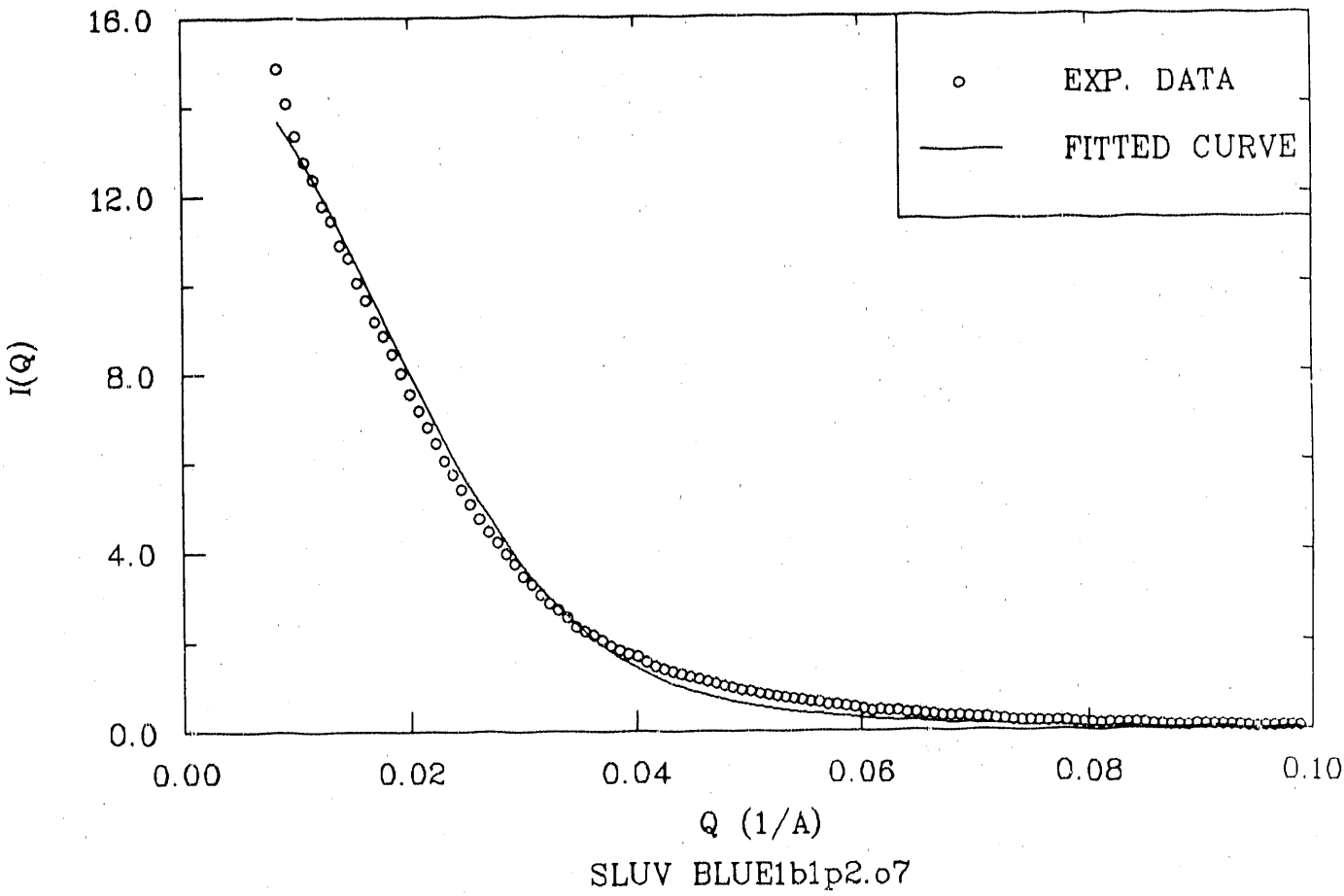
16.0
12.0
8.0
4.0
0.0
I(Q)
0.00
0.02
0.04
0.06
0.08
0.10
Q (1/A)
EXP. DATA
FITTED CURVE
SLUV BLUE1b1p2.o7

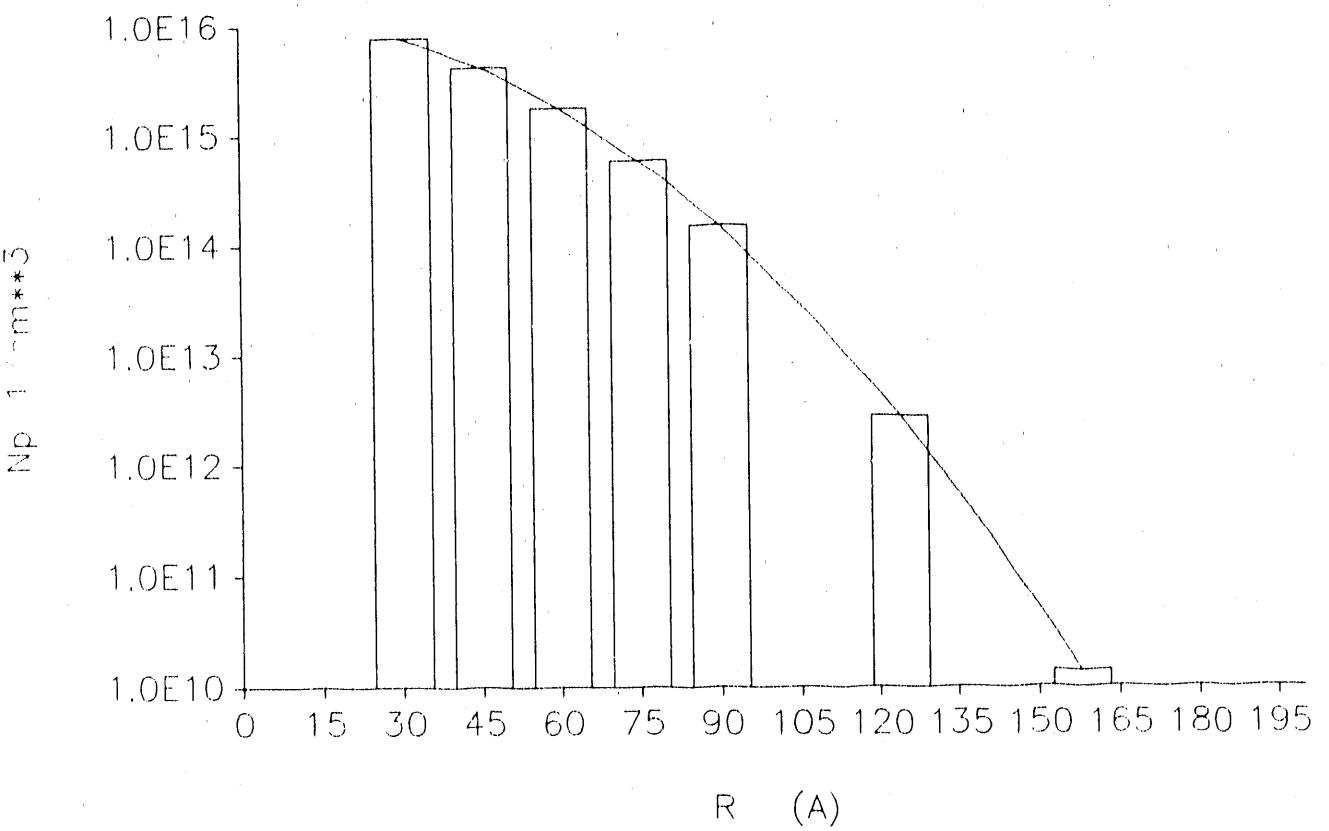
1.0E16
1.0E15
1.0E14
1.0E13
1.0E12
1.0E11
1.0E10
0 15 30 45 60 75 90 105 120 135 150 165 180 195
R (A)

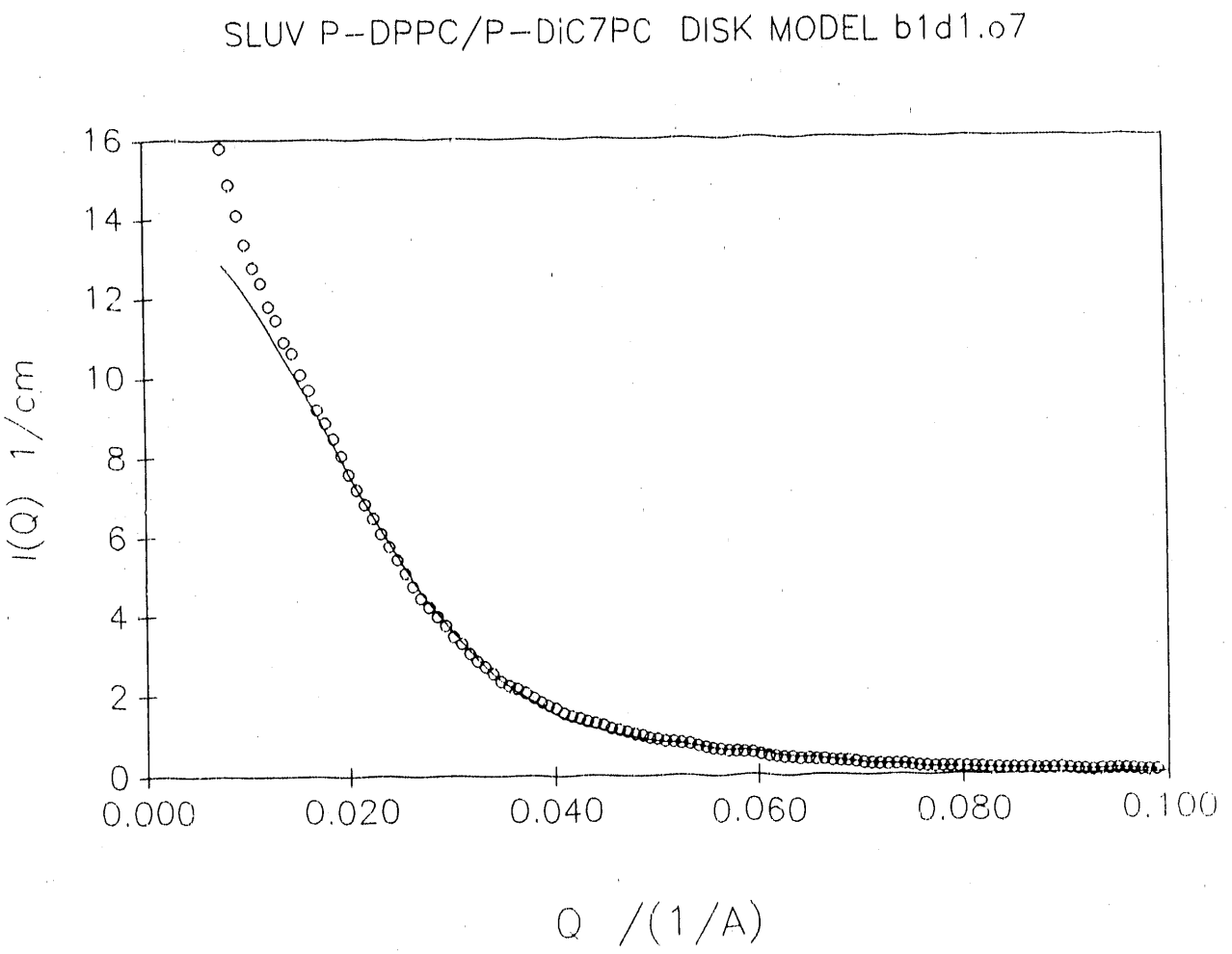
SLUV P-DPPC/P-DiC7PC DISK MODEL b1d1.o7
I(Q) 1/cm
16
14
12
10
8
6
4
2
0
0.000
0.020
0.040
0.060
0.080
0.100
Q /(1/A)

Instrument used: *(please type)*	Local contact:	Proposal number: *(for LANSCE use only)*
LQD	Phil Seeger	254.0

Title:	Report received: *(for LANSCE use only)*
Structure of Molecular Composites	1/31/90

Authors and affiliations:

D. W. Schaefer, J. E. Mark, and L. R. Gilliom
Department 1810
Sandia National Laboratories
P. O. Box 5800
Albuquerque, NM 87185

Experiment report:

Molecular composites (MC) are multicomponent systems that are homogeneous on scales larger than 1μm. These materials offer new strategies for the enhancement of material properties beyond that possible for single phase materials.

We studied two classes of reinforced elastomers. In both cases, the reinforcing glassy phase was precipitated in situ, by chemical means. The base elastomers were polydimethylsiloxane and polybutadiene.

For PDMS, a variety of fillers were studied including polystyrene, silica, titania and zirconia. Our goal was to develop synthetic strategies whereby the degree of filler ramification could by controlled by chemical parameters. Our results show that most systems yield particulate fillers with smooth surfaces. In some cases, however, bicontinuous fillers as well as polymeric mass-fractal fillers were produced.

We also studied the kinetics of the development of particulate fillers for the silica/siloxane system. Fig. 1, for example, shows the development of the scattering profile as a function of reaction time. The initial unreacted sample shows large scale phase separation which is complemented by precipitation of 100Å particulates which have fractally rough surfaces during growth. Upon drying, smooth surfaces result as indicated by the D-11 data shown in Fig. 1 for the dry sample.

We also studied catalytically deuterated 1-2 and 1-4 polybutadiene. In this case, we hoped the homogeneously dispersed catalyst would give glassy polystyrene domains whose morphology could be controlled by catalytic conditions. Figs. 2 and 3 compare the 1-2 and 1-4 systems. For 1-4 some increase in scattering is observed in the .05 A^{-1} region with no evidence of distinct domains. For 1-2 on the other hand, a distinct peak appears indicating either enhanced crystallinity or highly correlated domains. The former is inconsistent with measured differential thermal analysis data and the latter is inconsistent with monotonic increase in the peak height from 0-100%. Therefore, the origin of the peak remains a mystery.

Experiment report: *(continued)*

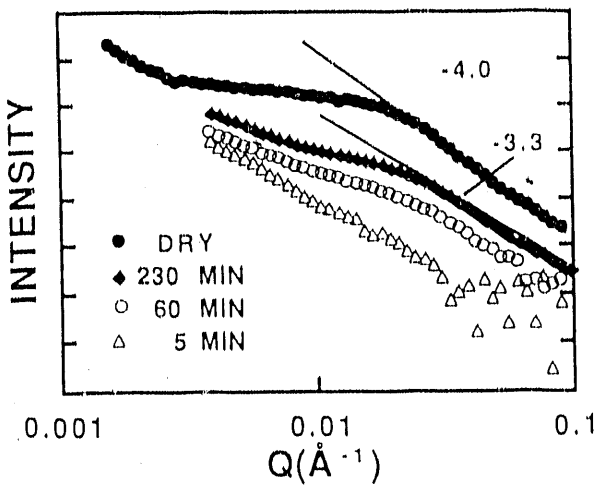

FIGURE 1. PDMS KINETICS RUN PICT

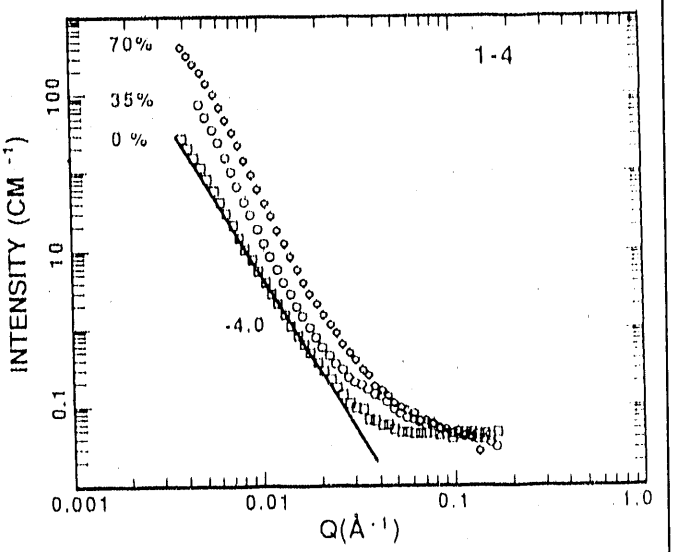

FIGURE 2. RAW14.PLT

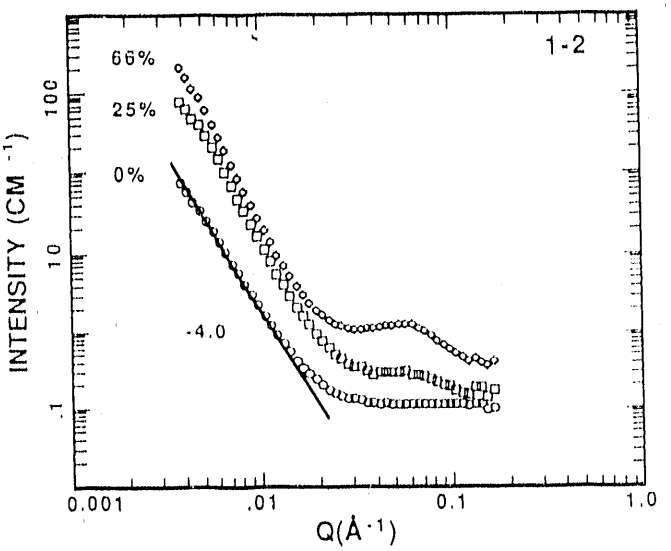

FIGURE 3. RAW12.PLT

References:

D. W. Schaefer, J. E. Mark, D. McCarthy, Li Jian, and Phil Seeger, in Polymer Based Molecular Composites, Ed by D. W. Schaefer and J. E. Mark (Pittsburgh, Materials Research Society, 1990) P. xxx.

L. R. Gilliom, D. W. Schaefer, and J. E. Mark in Polymer Based Molecular Composites, Ed by D. W. Schaefer and J. E. Mark (Pittsburgh, Materials Research Society, 1990) P. xxx.

D. W. Schaefer, C. J. Brinker, D. Richter, B. Farago, and B. Frick, Phys. Rev. Lett. submitted.

Instrument used: *(please type)*	Local contact:	Proposal number: *(for LANSCE use only)*
LQD	R.P. Hjelm	268.0

Title:

SMALL-ANGLE NEUTRON SCATTERING FROM MIXED BILE SALT-LECITHIN COLLOIDS

Report received: *(for LANSCE use only)*

Authors and affiliations:

R. P. Hjelm — LANSCE
P. Thiyagarajan — IPNS, Argonne National Laboratory
H. Alkan — Department of Pharmaceutics, University of Illinois, Chicago

Experiment report:

INTRODUCTION: We have been investigating the morphology of particles formed in mixed colloids of bile salt and lecithin in aqueous solution. These are of interest as models of the structure and action of bile, which is important in the transport of lipid waste products from the liver, such as cholesterol, and in the solubilization of lipids in the digestive tract. These systems are of general interest in understanding the physical chemistry of mixed colloid systems, and may find uses in industrial processes. In our previous work we showed that in certain parts of the bile salt-lecithin phase map long rods are present [1-3]. Maximum entropy analysis of the data [3] indicates that the rods are formed by association of globular micelles. These discoveries are not in accord with the currently held model [4,5] of mixed micelle formation in this system. In other parts of the isotropic phase there is a transition from rod-like forms to vesicles. We have shown that this transition is thermally induced and is reversible. The vesicles consist of single lecithin bilayers, and we find that the radius is temperature-dependent---they become substantially smaller with higher temperature. We were interested in determining if the aggregation of micelles into rods is affected by temperature. We therefore made observations on the temperature-dependence of scattering in preparations known to contain only globular micelles. We also wanted to obtain more information on the structure of the globular micelles. We therefore ran a contrast variation study on these samples.

Experiment report *(continued)*:

RESULTS: Further structural characterization of the phase map confirmed that initial globular particle elongate on dilution. However, for samples having a lecithin to glycocholate molar ratio of 0.5 at a total lipid concentration of 15mg/ml there was no observable temperature-dependence over a range from 15° to 45 ° C. This implies that, unlike the rod-vesicle transition and the processes of bile salt leaching from the vesicle, $\Delta H \approx 0$ for micelle aggregation. Contrast variation studies on the globular particles show in D_2O a radius of gyration of approximately 24 A. This is consistent with our earlier determinations [2,3]. Stuhrmann analysis of the contrast-dependence of Rg suggest that a higher scattering length density component of the system is toward the outer portions of the micelle. This would be the bile salt and the phosphatidylcholine molety of the lecithin.

References:

References:

1. Hjelm, R.P., Thiyagarajan, P., and Alkan, H. (1988), *J. Appl. Cryst.*, **21**, 858-863.
2. Hjelm, R.P., Thiyagarajan, P., and Alkan, H. (1990), *Mol. Cryst. Liq. Cryst.*, (in press).
3. Hjelm, R.P., Thiyagarajan, P., Lindner, P., Alkan, A., and Schwahn, D. (1990), *Prog. colloid polymer Sci.*, **82** (in press).
4. Schurtenberger, Mazer and Kanzig (1985), *J. Phys. Chem.*, **89**, 10492-1049
5. Startk, R.E. et al., (1985) *Biochemistry*, **24**, 5599-5605

Instrument used: *(please type)*	Local contact:	Proposal number: *(for LANSCE use only)*
LQD	Phil Seeger / Rex Hjelm	273.0

Title:

Inelastic Scattering Effects in TOF SANS

Report received: *(for LANSCE use only)*

21990

Authors and affiliations:

Rex P. Hjelm, Jr. LANSCE

Phil Seeger LANSCE

P. Thiyagarajan IPNS Division, Argonne National Laboratory

Experiment report:

The measurements described here partially covered one aspect of the proposal to evaluate inelastic effects in TOF-SANS measurements, namely to evaluate the importance of such effects in samples of known size and structure in different mixtures of H_2O and D_2O. There was insufficient discretionary time to carry out the remainder of the program.

EXPERIMENTAL: Colloidal silica gels stated by the manufacturers to be spherical particles and to be of well characterized sizes where used in these measurements. The first, LS-30, tradename LUDOX, manufactured by Dupont, is a 30% silica gel of average particle diameter 120 Å. The second 1115, tradename NALCOAG, and manufactured by Nalco, has particle diameter of 40 Å and is a 15% silica gel. The third, 1130 (also from the NALCOAG product line) has an average diameter of 80 Å. The silica gel content is 30%. In each, samples were prepared by diluting stock solutions to 2% W/V. Care was taken with pH and NaCl concentration to stabilize the solutions. Samples were made in 100%, 60% 40%, 20% and 0% D_2O, the exception being 1115 for which the highest D_2O content was 86%. Not all solutions could be measured, measured, due to lack of time. It was planned to do each measurement with the MgO filter in and out, but again time considerations limited the procedure to only 1115 in 86% and 0% D_2O.

Analysis of the curves at small Q is done using the Guinier analysis. A radius of gyration was extracted from this analysis if a sufficiently good Guinier region was obtained.

RESULTS: Scattering curves where measured for each sample between $Q \approx 0.008$ and 0.08 Å^{-1}. The range was limited due to high background near the beam stop from collimator internal scattering. LS30 in 100% D_2O gave an $Rg = 72$ Å. This corresponds to a spherical particle diameter of 186Å, significantly larger than the size quoted by the manufacturer. 1115 gave $Rg = 55$ Å, corresponding to a diameter of 140 Å. This again is considerably larger than stated by the manufacturer. No value of Rg could be extracted from scattering of 1130, as the Guinier analysis gave a continuously upward curving line. This suggests aggregation in 1130. Radii of gyration comparable with those in D_2O were obtained for LS30 and 1115 in other percentages of D_2O, with the obvious exception of 60% D_2O--the contrast match point of silica gel. No significant differences were observed in the Guinier analysis between 1115 sample with the MgO filter in or out.

Experiment report *(continued)*:

At larger Q values it was noted that the background scattering always exceeded the foreground when the D_2O content was lass than 80%. This is a potentially serious problem which has been observed in other contrast variation experiments, as well. The most important observations in this regard were at the contrast match point (60% D_2O) for these systems, where, apart from a small internal correlation hump at low Q, the scattering is expected to be featureless. This is indeed observed, but the ratio of foreground to background is not 1.0, but rather some smaller number between 0.7 and 0.8 and is constant with Q. We do not yet know the reason for this, but possibilities include unaccounted differences in incoherent scattering and or insufficient measurement of the transmitted beam.

CONCLUSIONS: *1)* We cannot verify with these measurements the correctness of Rg measured on a TOF-SANS instrument, due to the large discrepancy with the manufacturer's measurements of the particle diameter. Consultation with the manufacturers revealed that the samples may have aggregated. This is a common occurrence in silica colloids which are more than a few months old, as these were. Further, we have measured Rg values for other materials such as polystyrene beads and ribosomes which match expectations, so it seems unlikely that the problem is with the instrument or data reduction procedures.

2) There are no obvious effects from down scattering of epithermal neutrons at least down to Q ≈ 0.008 $Å^{-1}$., as evidenced by the lack of significant differences in the scattering with the instrument in the filter in and filter out configuration. We do not yet know how this matches expectations for LQD in this Q range.

3) There are, as yet, unexplained effects at high-Q which cause the background signal to be higher than the foreground. The fact that the ratio of the two tends to be independent of Q in regions where the scattering is expected to be featureless, suggests incoherence or problems with normalization.

References:

Instrument used: *(please type)*	Local contact:	Proposal number: *(for LANSCE use only)*
LQD	Rex Hjelm	275.0
Title: Studies of High T_c Superconductors using Small-angle Neutron Scattering Techniques.		**Report received:** *(for LANSCE use only)* 2/1/90

Authors and affiliations:

M. Yethiraj, T. O. Brun	P-LANSCE
R. N. Silver	T-11
J. O. Willis	P-10

Experiment report:

We have carried out a search for a flux lattice in $La_2CuO_{4+\delta}$ single crystals at 10K in a magnetic field of 1.25kOe applied parallel to the c-axis. We found no signal due to flux lines in the sample. However, we observed a very strong signal (Bragg peak) corresponding to a periodicity of approximately 600 Å. This scattering appears below 200K and has no field dependence. This peak, we believe, is due to the phase separation (ref. 1) and not due to twinning, since it can be shown that scattering from phase separated domains will be much stronger than scattering from the twin boundaries. If this interpretation is correct, the phase separated domains form a layered structure with the layers stacked in a direction perpendicular to the c-axis, which is an entirely unexpected result.

Further work is needed to pinpoint the source of the scattering that has been observed (ref. 2). Since it is believed that one of the phases in the two-phase system is normal (i.e. non-superconducting), the structure of flux line lattice with the field parallel to the crystalline c-axis is unpredictable. Experiments are also needed to measure scattering from flux lines in materials that do not show any phase separation (ref.3).

Experiment report *(continued)*:

REFERENCES

[1] J. Goldstone, J. Schirber and J. Thompson, personal communication

[2] M. Yethiraj, T. O. Brun, R. N. Silver and J. Schirber, proposal submitted to EPAC

[3] M. Yethiraj, T. O. Brun and R. N. Silver , proposal submitted to EPAC

Instrument used: *(please type)*	Local contact:	Proposal number: *(for LANSCE use only)*
Low-Q Diffractometer	Dr. Phil Seeger Dr. Rex Hjelm	286.0

Title:	Report received: *(for LANSCE use only)*
Characterization of Film Formation From Polystyrene Latex Particles via SANS	

Authors and affiliations:

L. H. Sperling
Whitaker #5, MRC
Lehigh University
Bethlehem, PA 18015

Andrew Klein
Building A, Chem. Eng.
Lehigh University
Bethlehem, PA 18015

J. N. Yoo
Whitaker #5, MRC
Lehigh University
Bethlehem, PA 18015

Experiment report:

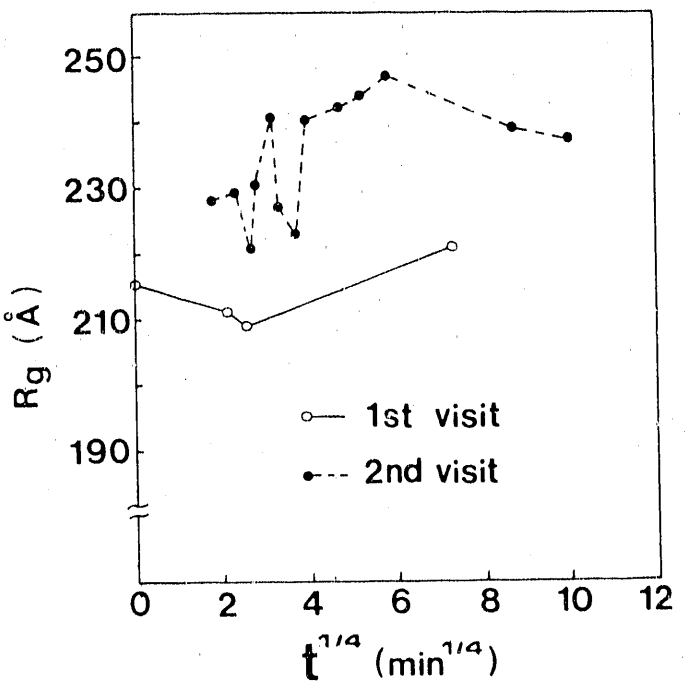

Figure 1. Deuterated latex particle radii of gyration as a function of annealing time, showing the discrepancy between the two sets of SANS data.

Experiment report: *(continued)*

SANS studies on the interdiffusion proesses in film formation from high molecular weight (Mw = 2,000,000 g/mol) polystyrene were investigated. The latexes, 270 A in radius, were mildly molded to full density (minimum interdiffusion), then annealed at 152 C for times ranging from five minutes to seven days. For SANS purposes, samples were prepared containing 6% of deuterated latexes. Thus, the deuterated material was substantially surrounded with protonated material. The object was to investigate the relationship between the diffusional penetration depth of the polymer chains and the tensile strength of the films. Experimentally, we watched the apparent expansion of the polystyrene latex spheres with annealing time.

After an apparent induction period, the films gained tensile strength with time to the one-fourth power. Ultimate tensile strength of 30,000,000 N/sq.m was developed at a penetration depth of 40 to 50 A. The latter is comparable to the radius of gyration of the critical entanglement molecular weight. This result confirms and extends the results on a previous set of samples annealed at 144 C.

The Lehigh University team visited LANSCE twice during the 1989 season. Due to the fact that the beam time was shortened during the first visit, a continuation was arranged for 85 days later. During this time, the samples were at room temperature conditions. Discrepancies between the data obtained before and after the intermission suggested a possible 15 A diffusion during this period, see Figure 1. Other possible sources of the difference were instrumental calibration, film thicknesses, etc. While these are considered unlikely, the data at this time are inconclusive on this point.

In a separate set of measurements, the radius of gyration of several polystyrene latexes (still in dispersion) used in previous experiments (at NIST), as well as for the present set of experiments, were determined. These experiments were entirely successful, adding an improved starting point in the interdiffusion experiment. The results of this experiment were incorporated in two papers, one already submitted to Macromolecules, and the other about to be submitted. Pending resolution of the above mentioned discrepancy, this third set of data will also be submitted to Macromolecules.

References:

1. J. N. Yoo, L. H. Sperling, C. J. Glinka, and A. Klein, submitted to Macromolecules, "Characterization of Film Formation from Polystyrene Latex Particles via SANS:. 1. Moderate Molecular Weight.

2. J. N. Yoo, L. H. Sperling, C. J. Glinka, and A. Klein, "Characterization of Film Formation from Polystyrene Latex Particles Via SANS: II. High Molecular Weight," to be submitted to Macromolecules.

Instrument used: *(please type)*	Local contact:	Proposal number: *(for LANSCE use only)*
LQD	Phil Seeger	289.0

Title:	Report received: *(for LANSCE use only)*
Radius of Gyration of Ribosomal RNA Protein in situ	5-5-90

Authors and affiliations:

Peter Moore, David Harrison; Yale University, Dept. of Chemistry, New Haven Connecticut

Experiment report:

A Pavlov and Serdyuk[1] style experiment was begun using isotopically labeled 30S particles. The basis of the method relies on subtracting two different scattering curves of the same multicomponent particle that have been identically prepared except that one of the common components has different extent of deuteration. Upon analysis of the preliminary scattering curves from these samples, it was determined that the samples differentially aggregated during the course of transport from New Haven to Los Alamos. On the basis of this fact, it was decided that there was no useful information to be learned from continuing the experiment.

To exploit the remaining beam time, it was decided that calibrating LANSCE with a biological sample that was well characterized would be valuable to the neutron scattering community. 50S ribosomal subunits were used as a sample in a contrast variation experiment. These particles were considered not abnormally large and they have been well characterized.[2] Both Guinier and **P**(r) analysis were carried out at Los Alamos for scattering curves measured at 20%, 40%, 80%, and 100% D_2O by Jill Trewhella. These two types of analyses showed good agreement with each other. Using this data, Stuhrmann[3] plots ($\sqrt{I}$ vs. $\%D_2O$, and R_g^2 vs. $\sqrt{I}$) were carried out to calculate the match point of the 50S particle as well as the radius of gyration of the subunit and its protein and RNA components.

Experiment report *(continued)*:

	This Data[4]	Previous Results[2]
R_c	76 Å	70±1 Å
R_P	101 Å	100±4 Å
R_R	60 Å	50±4 Å

Analysis of these data indicate that the samples may have been slightly aggregated. However, they seem to be in fairly good agreement with the previous characterization from monochromatic neutrons.

[1]Pavlov, M. Yu. and Serdyuk, I. N., J. Appl. Cryst.(1987), **20**, 105

[2]Crichton, R.R., Engleman, D.M., Haas, J., Koch, M.H.J , Moore, P.B., Parfait, R., and Stuhrmann, H.B. (1977)*Proc. Natl. Acad. Sci. USA* **74**, 5547

[3] Stuhrmann, H.B. and Kirste, R. G. (1967) *Z. Phys. Chem.* **56**, 334

[4]This Data was the result of interpretation of P(*r*) analysis using a data range of 0.015Å^{-1} ≤ Q ≤ 0.09Å^{-1}

P(*r*) Analysis

%D_2O	R_g	I_o	d_{max}	χ^2(d.f.)
20	68.3±.3	1.076±.008	190	87.7(45)
40	64.4±.5	0.310±.004	195	106(45)
80	88.8±1.5	0.674±.019	270	47.6(43)
100	79.5±.26	2.255±.017	205	53.4(44)

Instrument used: *(please type)*	**Local contact:**	**Proposal number:** *(for LANSCE use only)*
LQD		290.0
Title: Compressibility of Powders		**Report received:** *(for LANSCE use only)*

Authors and affiliations:

see attached

Experiment report:

see attached

[Abstract submitted to COPS II, Alicante, Spain, May 6-9, 1990]

SMALL-ANGLE NEUTRON SCATTERING STUDY OF FUMED SILICA POWDER COMPACTION.

Alan J. Hurd[1,2], Gregory P. Johnston[2], and Douglas M. Smith[2].

[1]Sandia National Laboratories, Albuquerque, New Mexico 87185-5800 USA,

[2]Center for MicroEngineered Ceramics, University of New Mexico, Albuquerque, New Mexico 87131 USA

ABSTRACT

In a previous study of fumed silica by mercury porosimetry (1), we established an inverse dependence of the powder compressibility κ on applied pressure p, heralded by power-law differential volume vs pressure curves. Independent small-angle neutron scattering (SANS) measurements, undertaken to establish microstructure, indicated a decreasing zero-angle intensity, $S(q\to 0)$, with increasing sample compression.

Preliminary analysis indicated that, like the compressibility κ, $S(q\to 0)$ is inversely proportional to pressure. It is well known from studies of systems in thermodynamic equilibrium that $S(q\to 0)$ is proportional to κ; our results suggested an analogous relation for systems in mechanical equilibrium (but not thermodynamic equilibrium).

In this paper, we have tested this relationship, in the low pressure regime, by correlating the scattered neutron intensity from samples in various degrees of compression. We find that, while the intensity does decrease with increasing compression (after removing the effects due merely to greater sample density) as expected according to the compressibility analogy, the dependence is not the same as that found by mercury porosimetry.

Compressed fumed silica has been studied as a percolating system by several groups (2-4); we have not yet attempted such an analysis.

This work was supported by Sandia National Laboratories under Department of Energy Contract DE-AC04-76-DP00789, Los Alamos National Laboratory under DOE Contract W-7405-ENG-36, and the UNM Center for MicroEngineered Ceramics.

REFERENCES

1.- D. M. Smith, G. P. Johnston, and A. J. Hurd, J. Colloid Interface Sci., in press.

2.- F. Ehrburger and J. Lahaye, J. Phys. France 50, 1349 (1989).

3.- J. Forsman, J. P. Harrison, and A. Rutenberg, Can. J. Phys. 65, 767 (1987).

4.- J. M. Heintz, F. Weill, and J. C. Bernier, Mater. Sci. and Engin. A109, 271 (1989).

Instrument used: *(please type)*	**Local contact:**	**Proposal number:** *(for LANSCE use only)*
LQD	Rex Hjelm	291.0

Title:	**Report received:** *(for LANSCE use only)*
Static Ising-Mean Field Crossover in Binary Polymer Mixtures	3/26/90

Authors and affiliations:

F. S. Bates, J. H. Rosedale, P. Stepanek, T. P. Lodge; University of Minnesota
R. P. Hjelm; Los Alamos National Laboratory
G. H. Frederickson, P. Wiltzius; AT&T Bell Laboratories

Experiment report:

SEE ABSTRACT, NEXT PAGE

Experiment report *(continued)*:

Abstract Submitted
for the March 1990 Meeting of the
American Physical Society

November 14, 1989

Date

Static Ising-Mean Field Crossover in Binary Polymer Mixtures. F.S. BATES, J. H. ROSEDALE, P. STEPANEK, T. P. LODGE, University of Minnesota; R. [redacted], Los Alamos National Laboratory; G. H. FREDERICKSON, P. WILTZIUS, AT & T Bell Laboratories--A low molecular weight binary mixture of cis-1,4,polyisoprene and partially deuterium labelled poly(ethylene-propylene) exhibiting a critical temperature and composition of T_c = 38°C and ϕ_c = 0.60 was studied between 40 and 100°C by small angle neutron scattering. A crossover from Ising-like (i.e., universal) critical behavior to mean-field behavior occurs for this system at T_x = 73°C. An analysis based on the Ginzburg criterion demonstrates that this result is consistent with a prior study [1] involving a high molecular weight polymer mixture where $T_c - T_x \cong 2$°C.

1. D. Schwahn, K. Mortensen, and H. Yee-Madeira, *Physical Review Letters* 58, 1544 (1987).

Timothy P. Lodge
Signature of APS Member

Timothy P. Lodge
Department of Chemistry
University of Minnesota
207 Pleasant St. S.E.
Minneapolis, MN 55455

References:

Instrument used: *(please type)*	Local contact:	Proposal number: *(for LANSCE use only)*
LQD	P. A. Seeger	293.0

Title:

FRACTAL DIMENSIONS OF CARBON BLACKS

Report received: *(for LANSCE use only)*

Authors and affiliations:

Michel Gerspacher, Sid Richardson Carbon Company, Fort Worth, TX

P. A. Seeger, P-LANSCE, Los Alamos National Laboratory.

Experiment report:

Discretionary time was used to demonstrate the feasibility of using the LQD for determination of the fractal dimension of the surfaces of various commercial carbon blacks which are used to enhance properties of rubber compounds. This is a preparatory measurement in a program to study the nature of the interaction of elastomer molecules with the carbon black surface; this is an unsolved question of extreme importance in the rubber industry[1]. Product improvements by even 1% could result in huge savings in the automobile industry, for instance through extended tire life and/or improved fuel economy.

Three samples were run: N234, which is a strongly reinforcing filler; N330, which has intermediate properties; and N762, which does not strengthen rubber significantly when used as a filler. All carbon blacks are very strong scatterers, and the major problem was that with samples approximately ¼-mm thick the count rates were too high for the detector, leading to some miscoding of positions. Average data collection time was 5 minutes. An additional run was made on N234 with a sample made by sprinkling powder on Scotch tape. Data collection in this case was for 30 minutes. Power-law fits have been made to each data set in the range $0.04 < Q < 0.09$ Å^{-1}, as shown in the accompanying figure. The implied fractal dimension for all three samples is 2.40 ± 0.05.

These results were presented[2] at a meeting of the Rubber Division of the American Chemical Society. Additional discussion of the significance and experimental approach, and references, are included in a 1990 LANSCE proposal entitled "Surface Interaction Between Active Carbon Black Surfaces and Elastomeric Chains."

Experiment report *(continued)*:

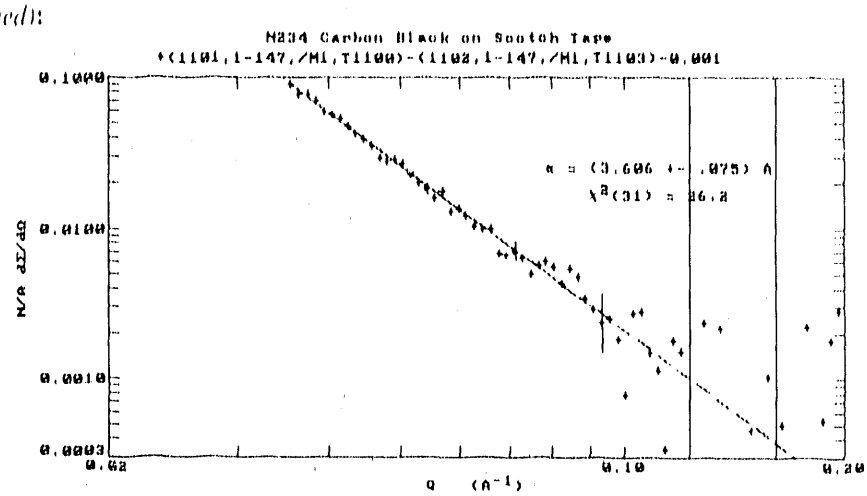

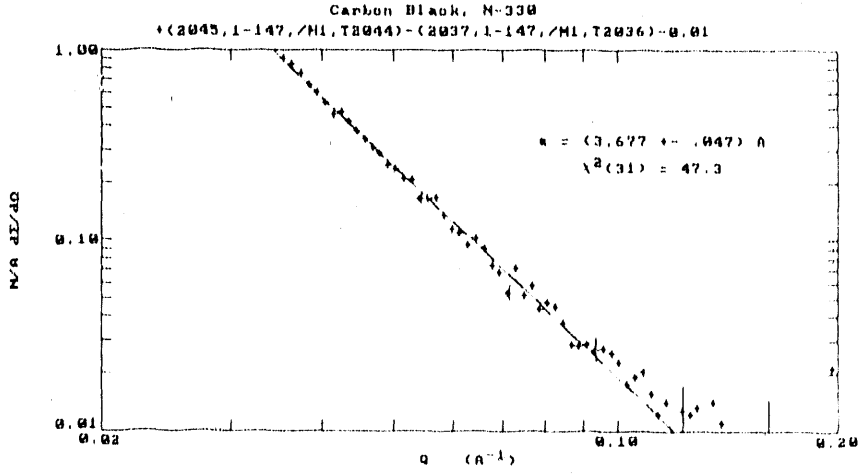

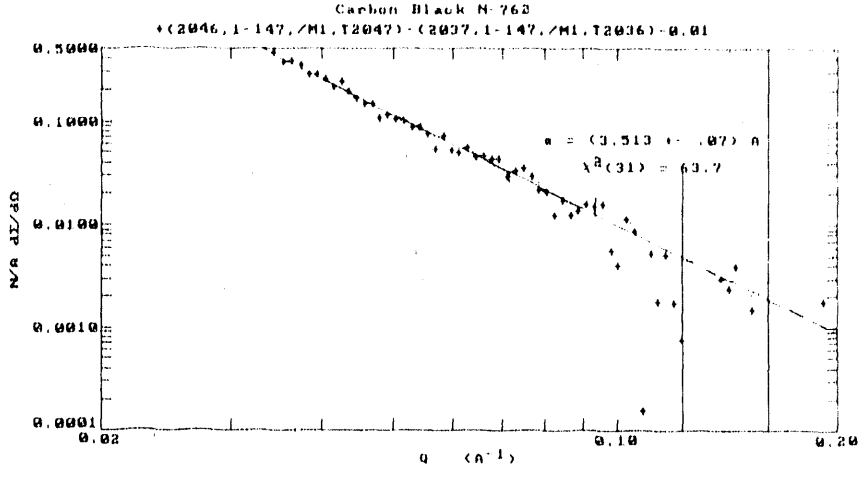

References:

1. Donnet, J.B. and Voet, A., "Carbon Black, Physics, Chemistry, and Elastomer Reinforcement" (Marel Dekker, New York, 1976).

2. Seeger, P.A., "Determination of Fractal Dimensions by Small-Angle Neutron Scattering: Equipment and Techniques," Rubber Division, ACS, Detroit, MI, Oct. 17-20, 1989, Paper No. 3.

Instrument used: *(please type)*	Local contact:	Proposal number: *(for LANSCE use only)*
LQD	Rex P. Hjelm, Jr.	269.0

Title: Disposition of ^{149}Sm Ions in ^{149}Sm-CMPO Aggregates in C_6D_6 Using Resonante Small Angle Neutron Scattering	Report received: *(for LANSCE use only)* 219190

Authors and affiliations:

P. Thiyagarajan, IPNS, Argonne National Laboratory
H. Diamond, CHM, Argonne National Laboratory
Rex P. Hjelm, Jr., LANSCE, LANL, Los Alamos
P. Seeger, LANSCE, LANL, Los Alamos
J. E. Epperson, MSD, Argonne National Laboratory

Experiment report:

INTRODUCTION:

The availability of intense pulsed spallation neutron sources, such as IPNS, LANSCE, ISIS etc, producing intense neutron beams with wavelengths in the region of 1 to 15 A offers new and unique possibilities for the use of small angle neutron scattering (SANS) in structural studies of proteins and other biological systems containing metals, organometallics, polymers containing metals and metallic alloys. Conventional SANS techniques are useful to study parameters such as the size, shape, molecular weight, polydispersity etc of the systems. However, if the SANS measurements are made using neutrons with wavelengths in the region of the resonance of an element (label) distributed in a system, significant changes in the signal can be seen which has the information on the distribution of the resonance species. This technique is called resonance small angle neutron scattering (RSANS). Since the pulsed neutron sources operate using the time-of-flight techniques using a beam of wide wavelength region, typically 1 to 15 A, macromolecules containing labels with resonance in this wavelength region, both SANS and RSANS from the system can be measured in a single experiment. The signal in the resonance region of a label in a macromolecule will yield information on the label distribution, while the signal from off-resonance region will provide all the information one can obtain from the conventional SANS. It is important to cite that there are analogous techniques using x-rays exist which are small angle x-ray scattering (SAXS) and anomalous small angle x-ray scattering (ASAXS). The ASAXS technique, being a very weak effect, became possible only with the advent of powerful synchrotron x-ray facilities with tunable wavelengths and has been applied to the determination of intermetallic distances in proteins and partial structure functions of phase separating metallic alloys.

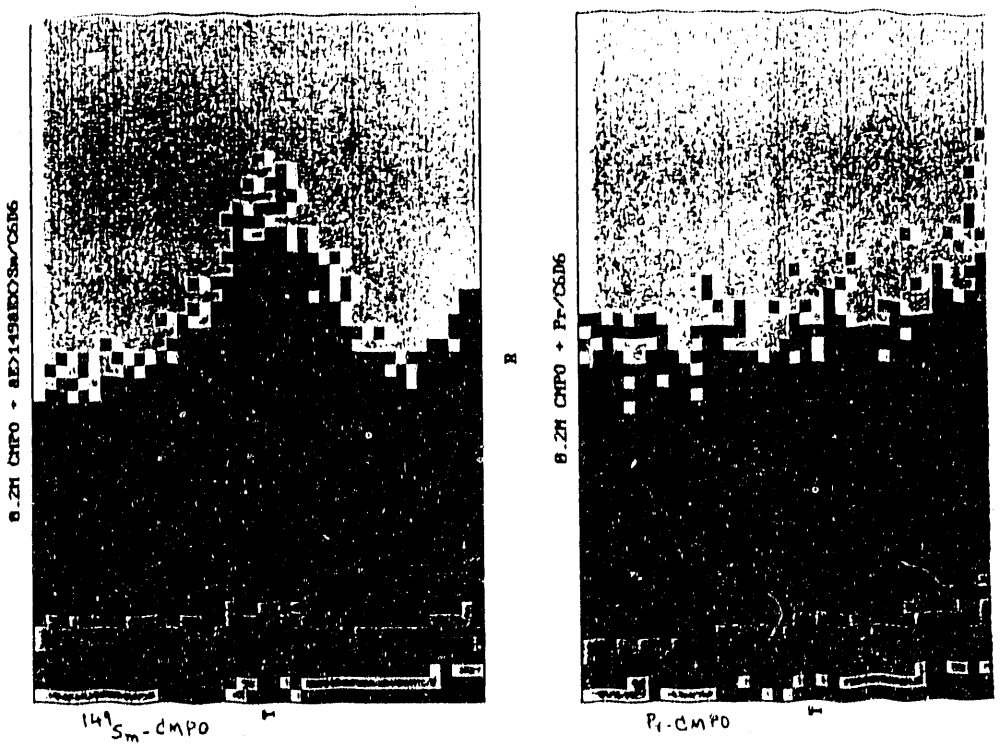
0.2M CMPO + 8D149BDSm/C6D6
149Sm-CMPO
0.2M CMPO + Pr/C6D6
Pr-CMPO

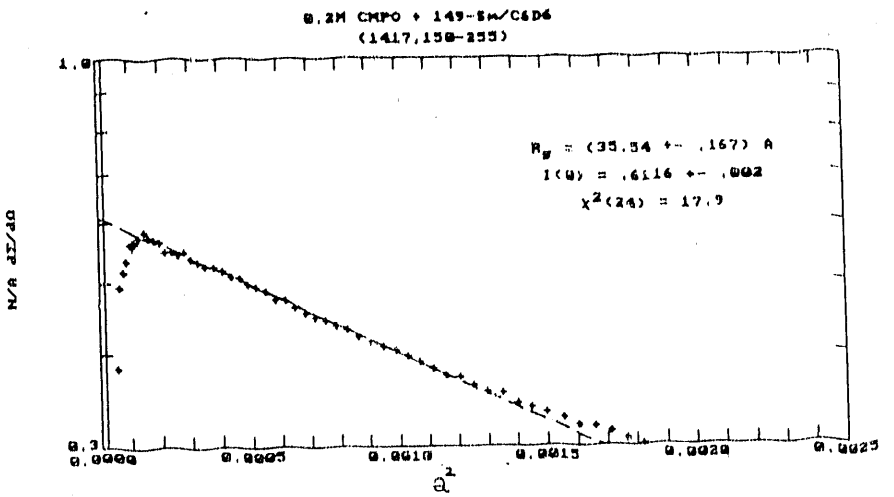
0.2M CMPO + 149-Sm/C6D6
(1417,150-255)
R_g = (35.54 +- .167) A
I(0) = .6116 +- .002
χ^2(24) = 17.9
N/A dΣ/dΩ
q^2

Fig. 1

Experiment report *(continued)*:

Recently we have studied the structure of the aggregates formed by the Praseodymium-CMPO [octyl(phenyl)-N,N-diisobutylcarbamoylmethyl phosphine oxide] complexes in organic solvents (Thiyagarajan et al., 1988). These studies showed that Pr-CMPO complexes in C6D6 form aggregates with a rod shape with a radius and length around 10 and 300 A respectively. We believe that the particle formed is a polymer wherein the metal ions are interspaced by the extractant CMPO. It is however cannot easily be confirmed by techniques such as EXAFS or NMR. It would be interesting to find out whether the particle is formed due to polymerization of metal-CMPO complex serving as a monomer or due to some form of aggeregation of extractant and metal ions. The RSANS can provide this information as we can measure the correlations related to the resonace labels from this technique.

on LQD

We carried out SANS measurements on the 0.2M CMPO-149Sm and 0.2M CMPO-Pr complexes in C6D6 by removing the MgO filter in the beam in order not to attenuate the neutrons in the region of 0.9 A. The usual configuration for the LQD instrument is running the experiments with the cold MgO crystal filter in the beam thus attenuating the neutrons with wavelengths below 2 A. Our experiment was the first one requiring the MgO filter to be out of the beam and this caused some problems setting up the experiment. The difficulties that we had to face were the dead time effects in the upstream monitor and the area detector as well as problems with the data acquisition software to collect data. This resulted in loss of about 1 day's beamtime and we could not get good enough statistics to analyse the data in the resonance region. However the data shown in Fig.1 clearly demonstates that these experiments are feasible. Two important results emerged from this study. First the OFF RESONANCE region shows that the 149Sm-CMPO system in C6D6 forms particle with size similar to that of pr-CMPO. There is an excess of coherent scattering in the resonance region for the 149Sm-CMPO when compared to that for pr-CMPO. This is quite encouraging and we believe that this technique will provide direct information on the disposition of the 149Sm ions in the aggregate. Data of higher statistical precision is needed to achieve that.

References:

Thiyagarajan, P., Diamond, H. and Horwitz, E. P. (1988) J. App. Cryst 21,848-852.

Experiment report *(continued)*:

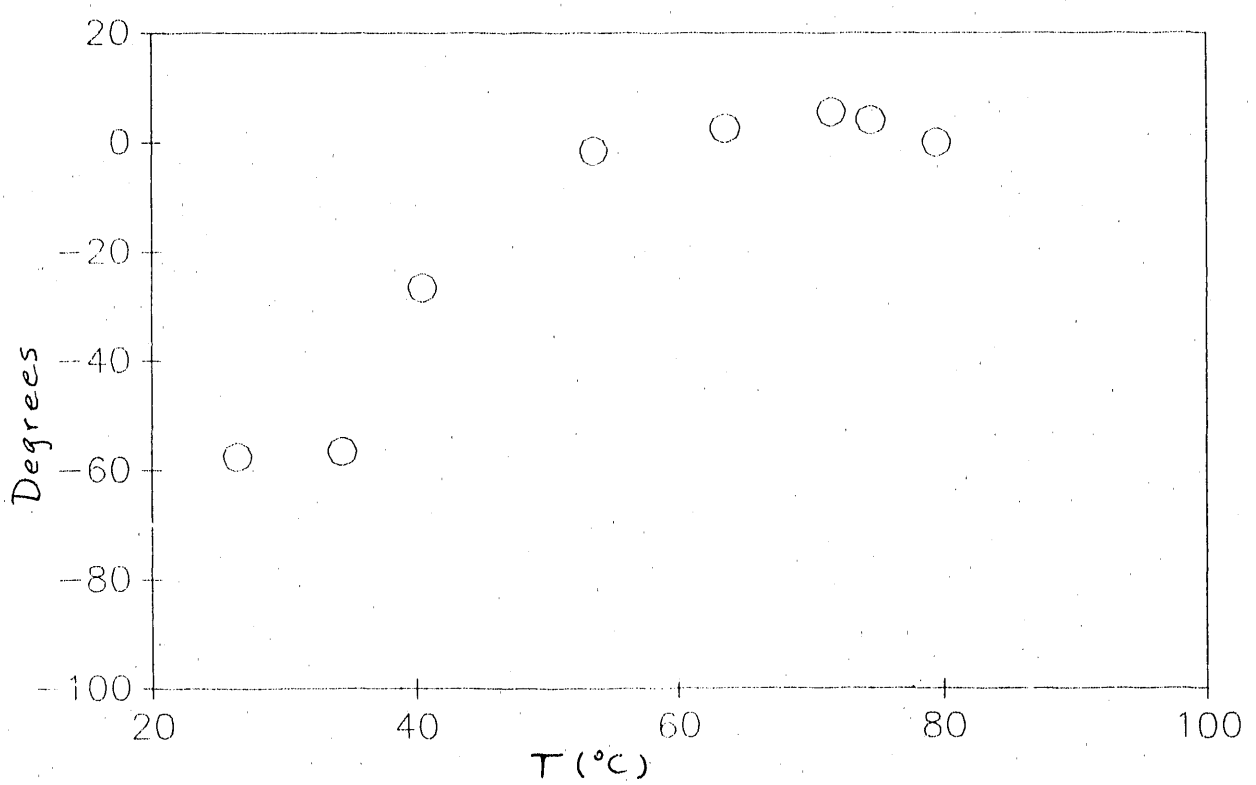

Figure 2: Smectic layer rotation as a function of temperature.

References:

Instrument used: *(please type)*	Local contact:	Proposal number: *(for LANSCE use only)*
LQD	Dr. Rex Hjelm	288.0

Title:

Neutron Scattering Investigation of a Sheared Binary Colloidal Suspension

Report received: *(for LANSCE use only)*

2/9/90

Authors and affiliations:

G.C. Straty, H.J.M. Hanley and J. Pieper
Thermophysics Division
National Institute of Standards and Technology
Boulder, Colorado 80303

Experiment report:

Experiments were carried out from 5-7 Sept., 1989 to investigate the structure of a mixture of colloidal particles, specifically a mixture of polystyrene latex and silica (ludox) spheres in water. Results are reported for the mixture at rest and under shear. The shearing apparatus was that constructed for the NIST facility with minor adaptations for the LQD spectrometer. A feature of the work was that the mixture was contrast matched by appropriate mixing of D_2O and H_2O in the aqueous medium. It is proposed to present the work in two publications; a letter and a Faraday Discussion paper if accepted.

The results are summarized in the abstract of a submitted letter publication, as follows:

ABSTRACT

The intensity of neutrons scattered from a well characterized binary colloidal suspension are reported. Results are given for the system at rest and under shear. Partial intensities were obtained by selective contrast matching. The experiments were carried out at the LQD pulse-source facility at the Los Alamos national laboratory. The shearing cell was a modification of the apparatus constructed for experiments at the reactor facility of the National Institute of Standards and Technology.

The mixture consisted of 92 nm polystyrene latex and 54 nm silica particles in water at a mixture volume fraction of 0.15, with a nominal polystyrene/silica number ratio of 1.7 to 1. The polystyrene and the silica were contrast matched by appropriate mixing of D_2O and H_2O in the aqueous medium. All solutions investigated were stabilized at a pH of 7 and contained an NaOH ion concentration of about 40 μM/1.

Experiment report *(continued)*:

Estimates of partial structure factors are given. The shear influenced behavior of the mixture is compared and contrasted with that from pure polystyrene under equivalent conditions. Indications are that the tendency of the polystyrene to order at rest, and under shear, is suppressed by the addition of the smaller silica particles. We demonstrate that the well known fluid mixture approximation that the structure factor, or the radial distribution function, of the components should scale with the particle radii is not valid for this mixture in which one species is substantially bigger than the other.

References:

Supplement to Report on Experiment 288, Sept 1989

Our previous experiments should be considered successful, however they should also be considered preliminary since the data analysis was somewhat clouded by apparatus and sample problems and our unfamiliarity with the LQD. Specifically:

Shearing experiments involve the examination of asymmetry in the vector Q maps caused by shear. Extensive analysis of the 2-D data have revealed, previously unrecognized, areas where LQD instrument improvements/adjustments are necessary.

We were unable to use the gravity focuser during the shearing experiments because its operation caused substantial mechanical vibration. This vibration prevented us from doing the precise alignment of the shearing apparatus' rotating elements which is absolutely necessary. Analysis of the 2-D Q maps obtained from the experiments, without the gravity focuser, revealed, as expected, a considerable loss in resolution in the Y direction. However, analysis of zero shear data, obtained with the gravity focuser operating, revealed similar, although somewhat smaller, loss of resolution in the Y direction, leading to the conclusion that the gravity focuser was perhaps detuned for these runs. Circular averaging of the data distorted the intensity peek shapes which are important to us in this work.

The vibration problem has since been corrected by decoupling the gravity focuser from the sample mounting area. A periodic check of the gravity focuser tuning will be made during subsequent experiments.

For the colloid work it is necessary to push the LQD to its lowest Q limits. Our unfamiliarity with LQD and the relation between (a) the TOF slices used in the analysis, (b) the resolution of the instrument and (c) the minimum Q resulted in our inability to recognize problems with a few samples which only became obvious after the fact. Reanalysis of the data using only a few of the higher time channels revealed evidence of previously unrecognized problems, either multiple scattering or interference effects, which should be eliminated or reduce to more tolerable level in future experiments.

The shearing cell is a Couette-type concentric cylinder apparatus where samples are located in the annular gap between a stationary inner cylinder and rotating outer cylinder. Some modifications to the shearing apparatus are planned for the next series of experiments. New sample cells are being constructed which will allow better temperature control and the ability to look off-axis in order to sample a component of the shear perpendicular to the incident beam direction. Cells will also have a smaller annular gap to reduce multiple scattering and allow higher shear rates.

We believe that we can do much better work now that we are aware of the pitfalls and are more familiar with LQD. LQD staff have worked closely with us on resolving these problems and we feel future work will be of mutual benefit.

Surface Profile Analysis Reflectometer (SPEAR)

Surface Profile Analysis Reflectometer (SPEAR)

The Surface Profile Analysis Reflectometer (SPEAR) views a liquid-hydrogen moderator maintained at 20 K. The moderated neutrons are collimated into two beams within the LANSCE target's bulk biological shielding. The beams are inclined downwards at angles of 1.5° and 1.0° to the horizontal and converge at a common sample position 8.73 m from the moderator. A specially designed mercury shutter allows the beams to be operated either independently or simultaneously. As defined by the in-shield collimation, the vertical resolution of each beam ($D\Theta/\Theta$) is ±5% for horizontal surfaces, and the horizontal resolution ($D\Theta$) is ±0.25°.

A "T_o chopper" is located 5 m from the moderator in a heavily shielded cave just outside the bulk shield. This chopper rotates a 300-mm-long nickel slug into the beam during the initial flash of high-energy neutrons and gamma rays and significantly reduces the background that limits reflectivity measurements. At the midpoint of the beam line (6.19 m) is the frame-overlap chopper, which consists of a thin neutron-absorbing disc with two opposing 90° segments removed. Rotating at one half of the PSR repetition rate, this chopper defines the wavelength band (1-16 Å or 16-32 Å) to be used and suppresses frame-overlap background pr[illegible] between these frames.

A 2-m length of the beam path is accessible between the frame-overlap chopper and the sample position. This section allows for further tailoring of the incident beam. Possible modifications include slits for fine horizontal collimation of the beam for in-plane or diffuse scattering studies and polarizers for magnetic depth profile measurements.

A goniometer at the sample position allows solid samples to be tilted to change the angle of incidence of the beam relative to the reflecting surface. For the study of liquid surfaces, sample containers (e.g., Langmuir troughs) must be isolated from external sources of vibration. SPEAR uses an EVIS vibration isolation system (Newport Corporation), which supports the sample and actively dampens vibrations transmitted through the floor or air.

Three detector systems are available for use on SPEAR: a single ^3He detector for use in low reflectivity studies; a single linear position-sensitive detector with 1-mm resolution when high angular resolution is required; and a bank of twenty 12.5-mm-diameter x 300-mm-long linear position-sensitive detectors (3-mm resolution) stacked side by side, forming a two-dimensional detector for studies of off-specular scattering.

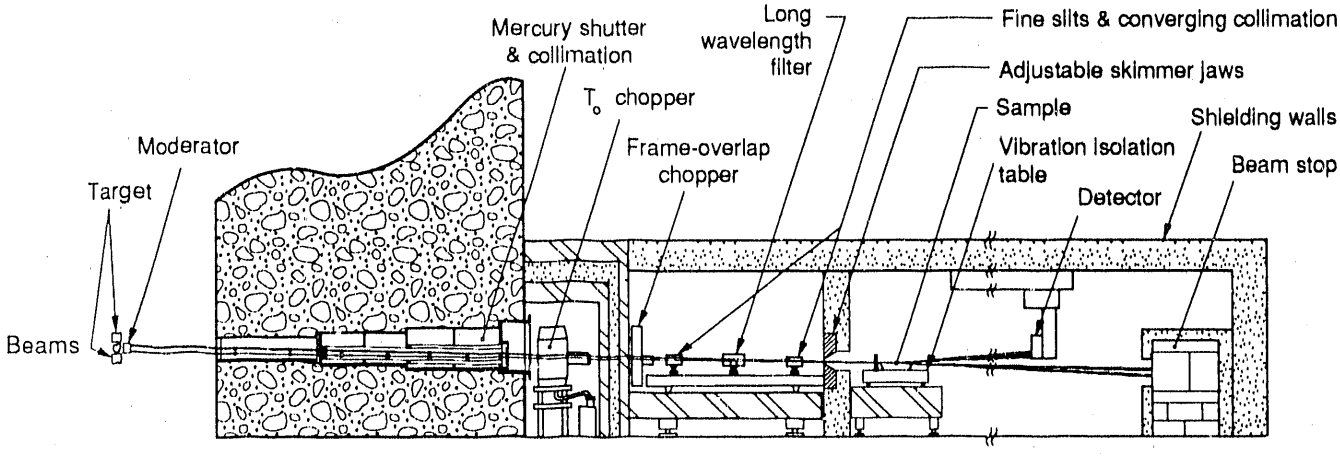

Instrument Details

Moderator-to-detector distance	12.38 m
Wavelength frames at 20 Hz	$1 < \lambda < 16$ Å
	$16 < \lambda < 32$ Å
Q range (horizontal sample)	$0.007 < Q < 0.3$ Å^{-1}
Beam cross-section at sample position (maximum sample acceptance)	5-mm high x 50-mm wide (1° beam)
	7.5-mm high x 50-mm wide (1.5° beam)
Moderator	Liquid H_2 at 20 K

Neutron flux at sample position for 1.5° beam at 60 μA:

$1 < \lambda < 6$ Å	3.4×10^5 n/cm^2/s
$6 < \lambda < 16$ Å	3.3×10^4 n/cm^2/s
$16 < \lambda < 32$ Å	2×10^2 n/cm^2/s

Detectors	Single ^{3}He tube
	1-mm resolution linear ^{3}He position-sensitive detector
	3-mm x 12.5-mm resolution ^{3}He position-sensitive-detector array (250 mm x 300 mm area)
Minimum reflectivity	10^{-6}
Typical run duration	30 min to 6 hr

Greg Smith, instrument scientist
Bill Hamilton, instrument scientist
Ross Sanchez, instrument technician

Instrument used: *(please type)* SPEAR	Local contact: Bill Hamilton/Greg Smith	Proposal number: *(for LANSCE use only)* D-0
Title: Neutron Reflectivity Investigation of the Surface-Induced Ordering Process for Symmetric, Diblock Copolymers		Report received: *(for LANSCE use only)*

Authors and affiliations:

T.P. Russell
IBM Research Division, Almaden Research Center

W.A. Hamilton and G.S. Smith
Manuel Lujan, Jr Neutron Scattering Center
Los Alamos National Laboratory

Experiment report:

Diblock copolymers are polymers constructed from two different homopolymers (polymers made up of n times a single monomer constituent). In the microphase separated state, diblock copolymers can exhibit spherical, cylindrical, or layered morphologies. The behavior of copolymers in the bulk has been studied by many different laboratories and has provided important insights into the interactions occurring between the two different block constituents. The characteristics of diblock copolymers at surfaces and interfaces in the solid state has, on the other hand, received considerably less attention. However, the use of block copolymers as agents for compatibilizing two immiscible homopolymers (i.e. in recycling of mixtures of different plastics) and as surface active components in a multicomponent system has focused attention to the interfacial and surface activity of block copolymers.

We used neutron reflectivity measurements taken on SPEAR (the Surface ProfilE Analysis Reflectometer) at LANSCE to make preliminary investigations of the block morphology within films of symmetric diblock copolymers of polystyrene (PS) and polymethylmethacrylate (PMMA). These films were prepared in a phase mixed state by spinning solutions of these copolymers in toluene onto a flat silicon substrate. Annealing of these films at 170 °C for 24 h has been shown to produce dramatic orientation of PS and PMMA rich microdomain layers parallel to the surfaces of the films[1]. This alignment results in a periodic arrangement of the block phases that persists evenly throughout the entire thickness of the film. Further, it has been shown that during the annealing process this multilayer order is established from the film interfaces and proceeds inward (PS exhibits an affinity for the free surface and PMMA is preferentially located at the film/substrate boundary). The final ordering of the film is dictated by several factors which will compete as it is established. The final bilayered structure is quantized to a half integral fraction of the final layer thickness, however initially the phase separated layers established at the film interfaces are not necessarily so restricted. Furthermore, the mixed phase state density of the film will be different to the separated phase (PS and PMMA) densities so the overall thickness of the film will change during the ordering process.

Our experiment was designed to investigate the formation of the microphase domain structure during the annealing process. Specifically, at what stage and in what manner the necessary spatial phase relationships between layer structures beginning at the film's free surface and substrate boundary are established. Selective deuteration of the homopolymers was used to enhance neutron optical contrast between PS and PMMA rich regions. (Our copolymer is PSH-

Experiment report *(continued)*:

PMMAD, with each homopolymer having a molecular weight of 50,000.) The reflection coefficient for neutrons is very nearly proportional to the modulus-squared of the Fourier transform of the neutron contrast profile of the surface, which is manifested as an interference pattern modulation of the reflected signal. This makes the technique exquisitely sensitive to variations of the microphase domain thicknesses and spatial phase between these structures as the multilayer structure is established[2].

The figure shows reflectivity as a function of the reflected neutron scattering vector for three stages in the annealing procedure (the profiles have been have been separated over the log scale): Unannealed - the reflection profile shows the even interference fringe pattern of due to homogeneous mixed phase film 2030 Å thick; Annealled for 24 h at 170 °C - the bilayer microphase order is fully established within a film of total thickness 1700 Å; and an intermediate stage in the annealing/ordering process (3 h at 170 °C) showing the interference pattern of a morphology sharing aspects of both structures. This data is currently being analyzed using both conventional (model fitting) and maximum entropy techniques.

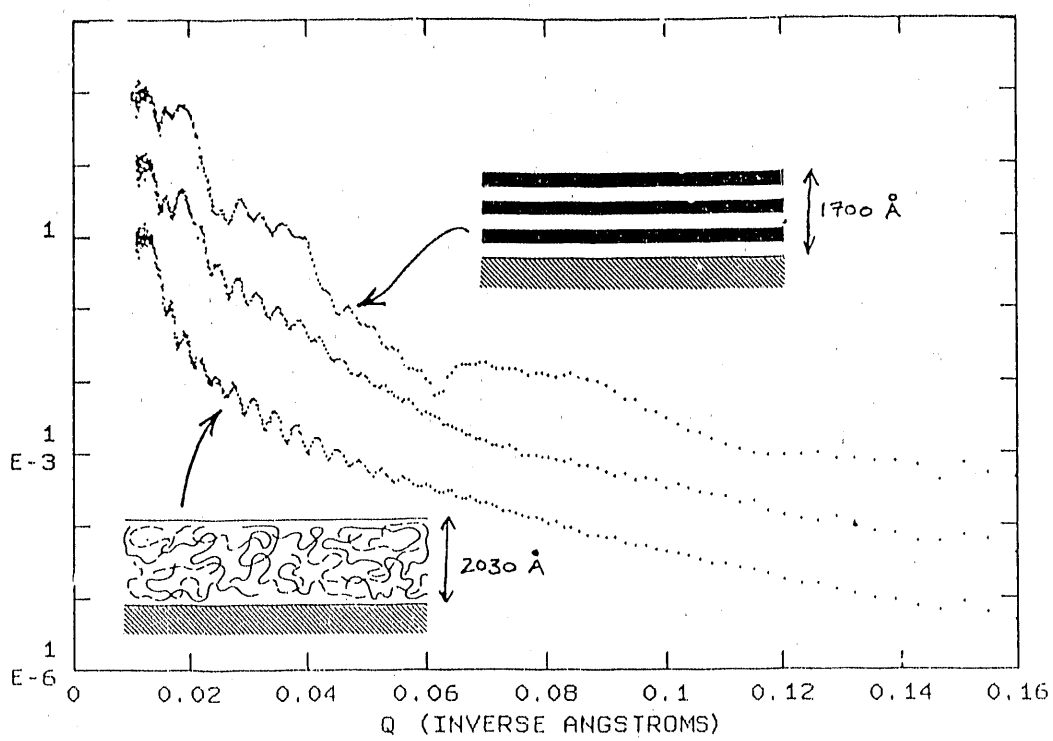

References:

1. G. Coulson, T.P. Russell, V.R. Deline and P.F. Green, *Macromolecules* **22**, 2581 (1989).

2. S.H. Anastasiadis, T.P. Russell, S.K. Satija and C.F. Majkrzak, *Physical Review Letters* **62**, 1852 (1989).

Instrument used: *(please type)*	Local contact:	Proposal number: *(for LANSCE use only)*
SPEAR	Bill Hamilton	D-29.0

Title:
Reflectivity Studies of Ni/Ti Neutron Mirrors

Report received: *(for LANSCE use only)* 4-5-90

Authors and affiliations:

E.M. Larson and A.F. Jankowski
Lawrence Livermore National Laboratory
Chemistry and Materials Science Department
Livermore, CA 94550

W.A. Hamilton and G.S. Smith
Los Alamos National Laboratory
P-LANSCE
MS H 805
Los Alamos, NM 87545

Experiment report:

Multilayers, as Mn/Ge [1] and Fe/Ge[2], used for grazing incidence polarization of neutrons provide an improvement in reflected intensity over conventional Ni mirrors. The multilayer is a replacement for a ferromagnetic crystal which selectively Bragg reflects neutrons of one spin state as a consequence of interference between the nuclear and magnetic contributions. The multilayer 'supermirror' provides the possibility of even higher reflectivities (>95%) to grazing angles beyond twice the critical angle of a Ni mirror [3,4] for all wavelengths, thus serving as a wide band-pass monochromator. Examples include 15-20 layer pair structures of Fe/Ag or Ni/Ti with d-spacing of 260-290 Å, nominally, for neutron wavelengths of 1-4 Å.

The samples were prepared and characterized at LLNL and the results of analyses described elsewhere [5]. An initial characterization of the multilayer crystallinity was undertaken using conventional θ-2θ Bragg x-ray diffraction. Grazing angle scans clearly show Bragg peaks due the layer pair spacing of the Ni/Ti structure. A full scan (2θ = 15°-100°) indicated the amorphous or microcrystalline nature of the Ti components, due to the lack of any well defined (hkl) reflections, and the (111) texturing of the Ni layers.

Neutron reflection measurements were taken for the multilayer 3-88-0908B over the Q range 0.01-0.2 $Å^{-1}$. As expected, we observe unit reflectivity due to Bragg scattering from the multilayer at Q values well beyond the critical edge for Ni, figure A (the dashed line is the calculated reflectivity for a simple Ni surface and the nominal structure appears as an inset). Neutron analysis of the structure has proceeded to the point that features in the measured and calculated reflectivity profiles can be matched in Q, but are not yet fitted. We have also not included a realistic interfacial roughness variation throughout the multilayer. Roughness has been included in the simplest possible way: a "generic" 11 Å roughness over all surfaces, obviously a very crude estimation. With these limitations admitted, we have been unable to confirm the 260 Å bilayer repeat distance claimed in reference 5. Q values of the gross features of our reflectivity profile indicate a repeat distance of 240±5 Å. This is consistent with the small angle x-ray data presented as figure 1 (a) in that paper, which would seem to indicate a bilayer repeat spacing of 245±7 Å. Our data would further seem to indicate that most of the difference can be explained by a lessened Titanium thickness; probably closer to 85 Å than 110 Å. A significantly different value for the 150 Å Ni thickness has been ruled out, since even slight

Experiment report *(continued)*:

adjustment (~5 Å) of this layer has a very noticeable effect on the calculated critical reflectivity edge position at low Q, while it appears relatively insensitive to the Ti thickness, owing to the much lower scattering length density in these layers. Our best effort to this moment appear in figure B, with the calculated reflectivity with allowance for instrument resolution for a 240 Å bilayer: Ni(155 Å)/Ti(85 Å).

While these measurements are in some disagreement with the larger value from electron microscopy data their preliminary nature is obvious from the discrepancies between the calculated and measured reflectivities. It is also important to note that, while the electron microscopy numbers are derived from the well defined layers near the base of the multilayer, both the small angle x-ray and neutron reflectivities depend on correlations over its entire thickness. The progression of the interfacial roughness through the multilayer would have significant effects on the reflectivity. To a first approximation, roughness appears as a "smoothing" of the depth averaged scattering length density profile, which would tend to depress high Q features in the reflectivity profile. There is some evidence for this in figure B. Further, the severity of the distortion in the upper layers ("The Ti layer traverses a path approximately twice its constituent width in the direction of composition modulation" [5]) results in a scattering problem that is beyond the scope of a simple reflectivity calculation.

These problems could be avoided in future in a series of samples; beginning with a single bilayer and working up to true multilayers. Characterization of the type reported in reference 5 could then be used to obtain quantitative estimates of the effect of the progressive coarsening observed in the layer structure on its neutron optical characteristics; information that will be of value in future attempts to create true broadband supermirror multilayers.

Figure A

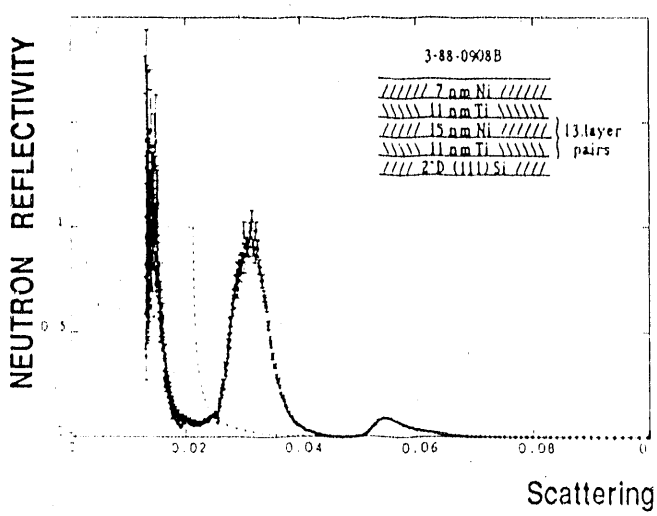

Figure B

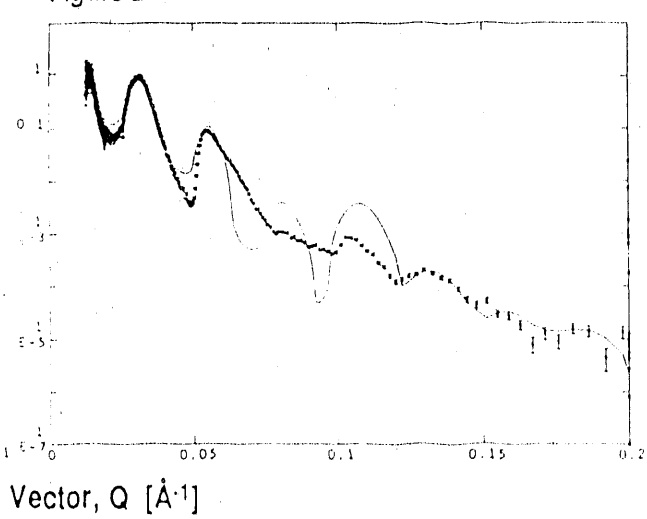

Scattering Vector, Q [Å^{-1}]

References:

1. B.P. Schoenborn, D. Caspar & O. Kammerer, *J. Appl. Cryst.* **7**, 508 (1974).
2. J.W. Lynn, J.K. Kjems, L. Passell, A.M. Saxena & B.P. Schoenborn, *J. Appl. Cryst.* **9**, 454 (1976).
3. F. Mezei, *Commun. Phys.* **1**, 81 (1976).
4. F. Mezei, SPIE Vol. **983** *Thin Film Neutron Optical Devices* (1988), in press.
5. A.F. Jankowski & M.A. Wall, *Thin Solid Films* **181**, 305-312 (1989).

Instrument used: *(please type)*	Local contact:	Proposal number: *(for LANSCE use only)*
Spear	Greg Smith	220.0

Title:

Segment density of an end adsorbed block copolymer in a homopolymer melt

Report received: *(for LANSCE use only)*

Authors and affiliations:

E J Kramer - Materials Science and Engineering
Cornell University

L Norton - Materials Science and Engineering
Cornell University

R A L Jones Materials Science and Engineering
Cornell University
(Present address: Cavendish Laboratory
Cambridge University, UK).

Experiment report:

We have made neutron reflectivity measurements of layers of deuterated polystyrene grafted to a silicon interface by short adsorbing blocks of poly (vinyl pyridine), in a matrix of normal polystyrene of various molecular weights. The samples were prepared by spin casting thin films (thicknesses in the range ~ 50 Å -350 Å) onto silicon wafers. Thicker films of normal polystyrene (thicknesses of order 1 μm) were then floated onto water and picked up on the wafers. Figure 1 shows the reflectivity of such as sample as made, plotted as the product Rk^4 against k, where k is the perpendicular component of neutron wave-vector, and R is the reflectivity. In order to have an accurate and absolute measure of the angle of reflection an 2-d position sensitive detector was used; unfortunately however the rather high background of the detector used meant that reflectivities could be measured only down to about 10^{-4}. The prominent fringing is due to interference between reflection from the front and back of the block copolymer layer, and allows us to ascribe a thickness of 350 Å to the block copolymer film as cast. The reflectivity of a similar sample after annealing is shown in figure 2. The fringing has disappeared, indicating that the interface beteen the deuterated PS-PVP layer and the normal polystyrene layer has become diffuse. The solid line indicates the best fit to a parabolic type profile - this shape might be expected by analogy to solution experiments [1].

Experiment report *(continued)*:

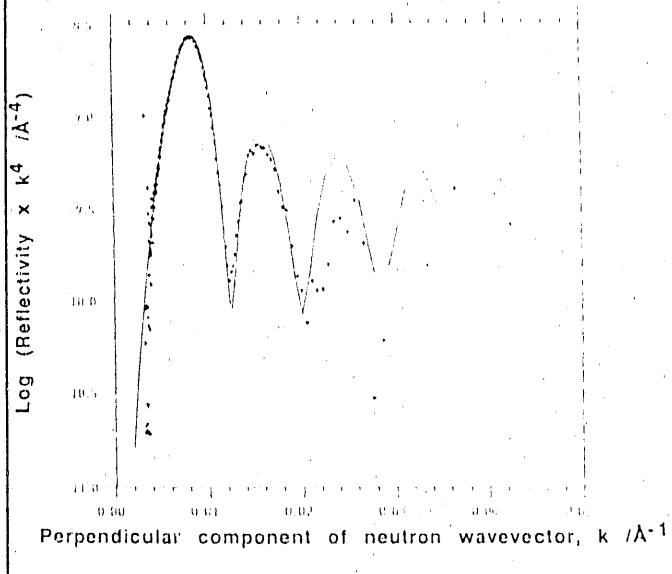

Figure 1.

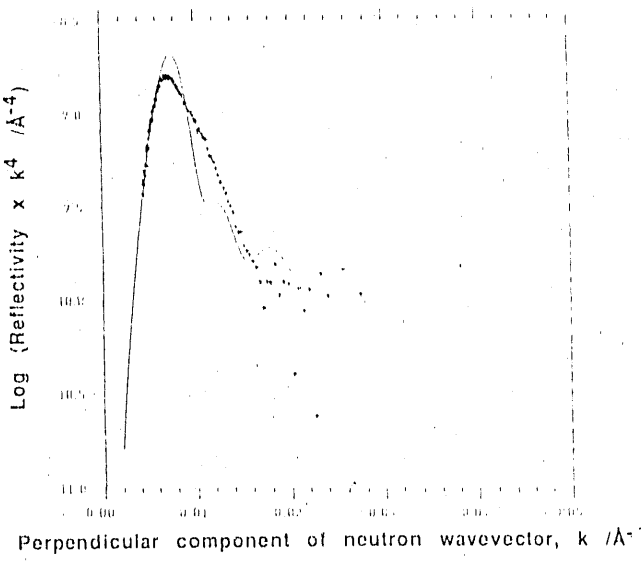

Figure 2.

This type of profile leads to less dramatic fringing arising from the discontinuous first derivative in the theoretical profile; however the data shows no fringing at all. This is not a surprise as the theoretical arguments leading to this prediction assume the idealisation of infinite molecular weight. Systematic deviations from the theoretical fit remain, however, indicating qualitatively that the actual profile is flatter than a parabolic profile. Again, this is predicted qualitatively by recent theory for rather high surface coverages [2], although the possibility of non-equilibrium effects cannot be ruled out. Efforts are continuing to find a functional form which better represents the data.

References:

1. H.Toprakcioglu, J.Field, H.Stanley, R.C.Ball, J.Penfold, to be published

2. M.E.Cates, D.Shim, J.Phys (Paris) **50** 3535 (1989)

Filter Difference Spectrometer (FDS)

Filter Difference Spectrometer (FDS)

The Filter Difference Spectrometer (FDS) measures changes in the energies of neutrons scattered by a sample in the beam. Scattered neutrons reach the detectors via polycrystalline Be or BeO filters, which will only pass neutrons that fall within the energy bandwidth of the filters. This determines the final energy of the scattered neutrons. Energy transfers can then be calculated from the time of flight of the neutron from the source to the detector. The use of both Be and BeO filters allows different spectra to be taken, which results in much improved resolution. Data can also be corrected using a model filter-response function using either a numerical filter-difference-method or maximum-entropy-method deconvolution. Energy resolution can thereby be improved to 1.5 - 2% of the energy transfer over most of the range of the spectrometer. Because it detects neutrons over a very large solid angle, the FDS is most useful for measurements requiring high sensitivity, such as the vibrations of molecules adsorbed on surfaces.

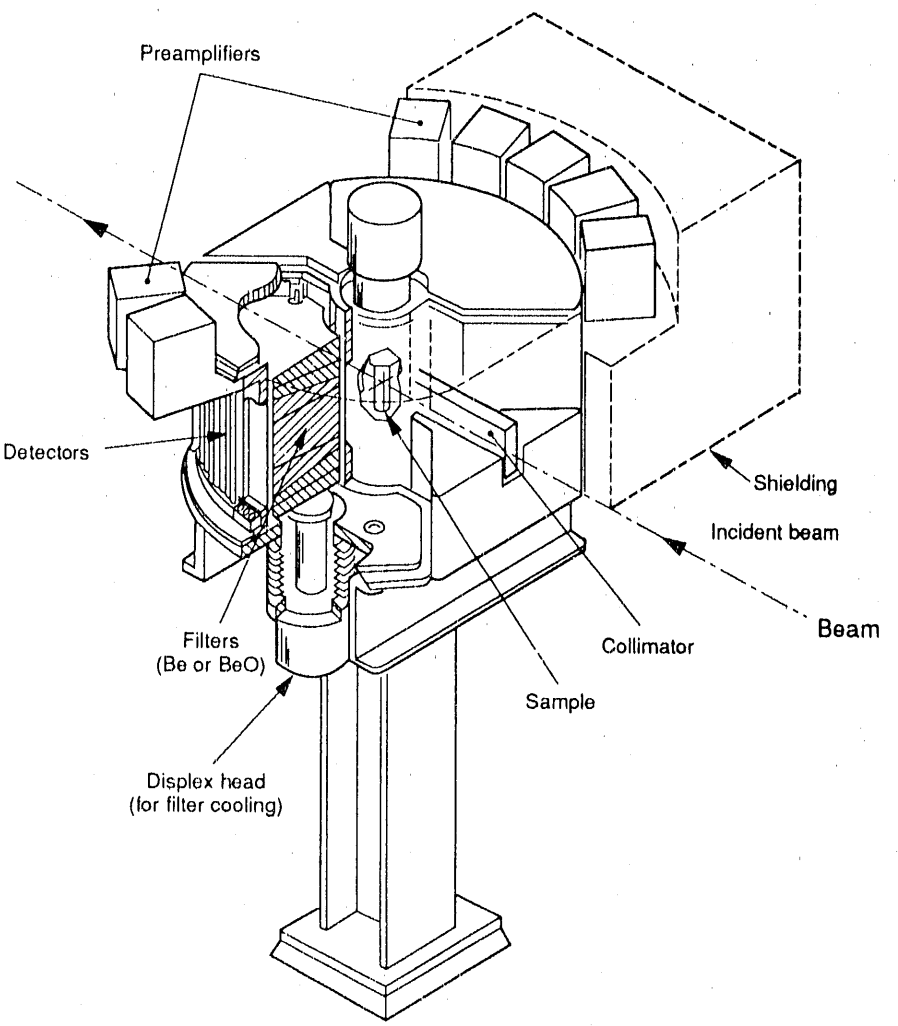

Instrument Details

Energy-transfer range	37 - 620 meV (300 - 5,000 cm^{-1})*
Q range	1.5 - 17 $Å^{-1}$
Energy-transfer resolution	1.5% - 6.5% , depending on data treatment
Beam size at sample	2.5 cm wide x 10 cm high
Detectors	60 ^3He (1.3 cm diameter)
Filter analyzers	5 Be, 5 BeO, each subtending a scattering angle of 18°; refrigerated
Moderator	Chilled water at 10° C
Sample environment	10 - 300 K, closed cycle refrigerator; furnace temperature limit 400° C
Sample size	0.5 - 100 grams
Experiment duration	2 hours - 2 days

**In certain cases the range can be extended to elastic scattering.*

Juergen Eckert, instrument scientist
Ross Sanchez, instrument technician

Instrument used: *(please type)*	Local contact:	Proposal number: *(for LANSCE use only)*
FDS	Juergen Eckert	D 34.0
Title: Inelastic and quasielastic neutron scattering studies of TMMB		**Report received:** *(for LANSCE use only)*

Authors and affiliations:

Gordon J. Kearley — Institut Laue Langevin

Juergen Eckert — LANSCE

Experiment report:

$(CH_3)_4NMnBr_3$ (TMMB) is a quasi one dimensional linear chain compound and at room temperature is isostructural with the much studied model compound $(CH_3)_4NMnCl_3$ (TMMC). However, these compounds undergo phase transitions at 144 and 126K, respectively, this transition being first order for the bromide but nearly second order for the chloride. There are no structural data for the low-temperature phase of TMMB but the transition is thought to be brought about by the ordering of the $(CH_3)_4N^+$ ions. Motions of the cations or their components can be investigated directly via inelastic and quasielastic neutron scattering. The low energy INS spectra of TMMB at low temperatures (~10K) are dominated by an peaks in energy gain and loss of around 36 cm^{-1}. These peaks are almost certainly due to librational motions of the cation as a whole and reflect a rather low hindrance potential. As the temperature is increased, these motions become increasingly damped and the inelastic peaks broaden, move to lower energy, and a central a quasi-elastic component develops. However, the intensity of the quasielastic component is greater than that expected simply from the damped harmonic oscillator and further its profile strongly suggests the presence of two components of different widths. Within the limits of the data the spectra can be quantitatively reproduced using either a model in which there are two types of cation with different rotational barriers or a model in which the cation is appreciably distorted from cubic symmetry. At temperatures above that of the phase transition (at around 150K) the spectrum become somewhat intractable in that the inelastic peaks remain, but are weak and poorly resolved, and a third very broad quasielastic contribution appears. Quantitative analysis of these spectra has proved exceptionally difficult but it is clear that there is a dramatic change of some element of the cation dynamics at this phase transition.

FDS RESULTS

In order to obtain more information about the effective symmetry of the cation and the possibility of multiple site occupancy we have obtained the high resolution high-energy INS spectrum. In fact the diagnostic region lies between 200 and 600 cm^{-1} in which we would expect to see four characteristic bands: symmetric and antisymmetric methyl torsions and similarly symmetric and antisymmetric C-N-C deformations. Basically if there are two crystallographically distinct cations in the structure we would expect to see a simple doubling of the bands whilst if there is a reduction of symmetry some degeneracies will be lifted.

In the raw data from FDS four intense bands are indeed seen at 216, 304, 368 and 465 cm^{-1} which are readily assigned as above, respectively, but there is little sign of either band doubling or splitting. In the "Mezei"-treated data however, a low-frequency shoulder is just resolved on antisymmetric methyl torsion peak, this being a molecular T-mode. The maximum entropy reconstruction spectrum is even more

Experiment report: *(continued)*

encouraging in that it shows a clearly resolved doublet at 280 and 297 cm^{-1} with the intensities being in the approximate ratio of 1:2. Assuming that there are no other unresolved splittings we can conclude that T-modes are split into A+E whilst E-modes (symmetric C-N-C deformation) are left degenrate. By elementary group theory this leads to the following possible effective symmetries of the $(CH_3)4N$ ion: D_{2d}, C_{3v}, S_4 or C_3.

This information should enable the quasielastic neutron scattering data to be analysed unambiguously which is obviously a vital starting point for understanding the phase transitions in these materials.

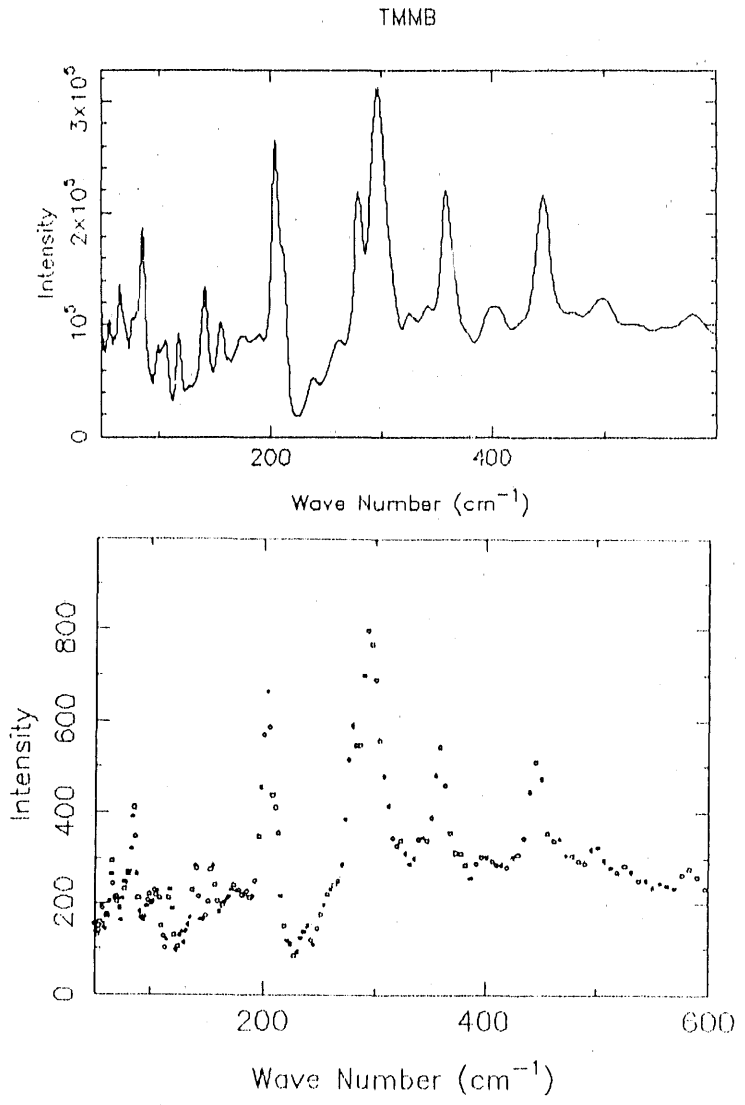

Fig. 1. FDS data on TMMB, T=12K. MaxEnt reconstruction (top) and "Mezei" - treatment (bottom)

References:

Instrument used: *(please type)*	**Local contact:**	**Proposal number:** *(for LANSCE use only)*
FDS	Juergen Eckert	D-35.0
Title: Molecular Hydrogen Complexes of Cobalt		**Report received:** *(for LANSCE use only)*

Authors and affiliations:

Juergen Eckert	LANSCE
Claudio Bianchini	Studio della Stereochimica ed Energetica dei Composti di Coordinazione, C.N.R., Firenze, Italy
Alberto Albinati	Istituto di Chimica Farmaceutica, Universitá di Milano, Italy

Experiment report:

We have investigated the first molecular hydrogen complexes of cobalt, $[(PP_3)Co(H_2)]^+$, where PP_3 (= $P(CH_2CH_2PPh_2)_3$) is a tripodal phosphine ligand (scheme I) in which all four phosphine donors are tied together [1]. This is in contrast to the related complexes such as $[FeH(H_2)(Ph_2PCH_2CH_2PPh_2)]^+$ with diphos ligands, where relatively easy exchange between hydride and dihydrogen ligands is observed [2] in solution. In the Co compound of the present study strong metal-dihydrogen binding is in fact observed with the attendant high degree of H-H bond activation. This is indicated, for example, by the large value of J(H,D) (=27.8 Hz) in $[(PP_3)Co(HD)]^+$.

While the Ir analog of our compound forms an octahedral cis-dihydride under all conditions, the Rh analog shows stable dihydrogen binding in solution above 173K [3]. The Co complex, on the other hand, appears to retain its trigonal-bipyramidal (TBP) shape even in the solid state as indicated by an X-ray diffraction study [1]. This strongly suggest dihydrogen coordination, as the classical cis-dihydride would require an octahedral geometry about the Co.

We have therefore examined two samples of $[(PP_3)Co(H_2)]^+$ on the high resolution time-of-flight spectrometer IN5 at the Institut Laue-Langevin and on the FDS at LANSCE. One of these samples was crystallized with $(PF_6)^-$, the other with $(BPh_4)^-$. Differential spectra for the FDS require the use of two

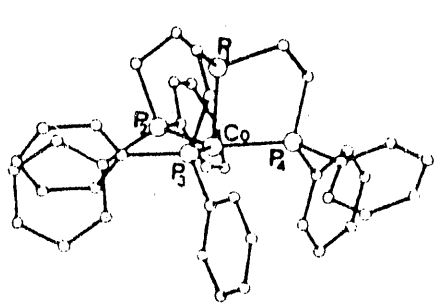

I

X-ray structure of $[(PP_3)Co(H_2)]^+$. The dihydrogen ligand could not be located, but is expected opposite P_1.

Experiment report: *(continued)*

"blank" samples, which were, respectively, the (D_2) and (N_2) analogs.

In the IN5 experiments we were unsuccessful in observing the rotational tunneling spectra of the H_2 ligands. The reason for this may well be that the barrier to rotation in these cases is too high, so that the tunnel splitting is too small to be observable. Since there is an approximately exponential dependence of tunnel splitting on the barrier height small changes in metal-H_2 binding can easily make the latter unobservable. It is, of course, also possible that there is no, or only a small amount of H_2-ligand in these complexes.

High frequency vibrational data on the FDS for the two compounds are shown in Fig. 2. The spectrum for the $(PF_6)^-$ compound is rather similar to others [4] obtained by this technique, except that it is shifted to higher energy. In fact, if we were to assign the peak at 400 cm^{-1} to the Co-(H_2) torsion, the corresponding rotational tunnel splitting of about 0.04 meV would have been difficult to observe with the conditions used in the IN5 experiment.

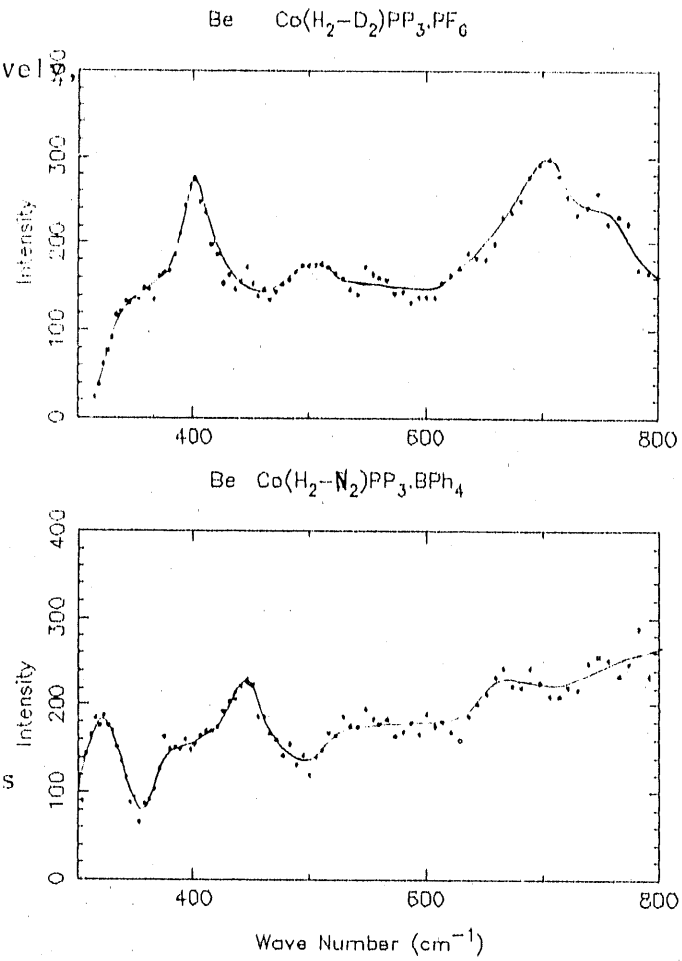

Fig. 2 Differential spectra (Be only) of the two forms of $[(PP_3)Co(H_2)]^+$.

Peaks at 500, 700 and 750 cm^{-1} in the top figure could then be assigned to $Co(H_2)$ deformation modes and some possible Co-hydride bending modes, whereby the presence of a mixture of classical and non-classical binding would be indicated. The data on the $(BPh_4)^-$ analog is less conclusive at this time. Further analysis of these data, as well as that of related complexes is in progress, as well as independent attempts (single-crystal diffraction, solid state NMR) to ascertain the presence of the dihydrogen ligand in the solid state.

References:

1. C. Bianchini, C. Mealli, A. Meli, M. Peruzzini and F. Zanobini, J. Am. Chem. Soc. 110, 8725 (1988).
2. M. T. Bautista, K. A. Earl, R. H. Morris and A. Sella, J. Am. Chem. Soc. 109, 3780 (1987).
3. C. Bianchini, C. Mealli, A. Meli, M. Peruzzini and F. Zanobini, J. Am. Chem. Soc. 109, 5548 (1987).
4. J. Eckert, G. J. Kubas, J. H. Hall, P. J.Hay, and C. M. Boyle, J. Am. Chem. Soc., in press (1990).

Instrument used: *(please type)*	Local contact:	Proposal number: *(for LANSCE use only)*
FDS	Juergen Eckert	11-D-36
Title: Vibrational spectroscopy of Acetanilide Isotopomers		**Report received:** *(for LANSCE use only)*

Authors and affiliations:

B. I. Swanson — INC-4, LANL
J. Eckert — LANSCE, LANL
P. Vorderwisch — HMI, Berlin, FRG

Experiment report:

We have obtained low temperature vibrational spectra of the acetanilide isotopomers $C_6H_5NHCOCH_3$, $C_6D_5NDCOCH_3$, $C_6H_5NHCOCD_3$ and $C_6H_5NDCD_3$ as part of our program to study intermolecular vibrational coupling in biological building block molecules, such as glycine [1] and DL-Alanine [2]. This work is aimed at obtaining information on energy transfer mechanisms. In the case of ACN there has been considerable interest in its vibrational spectra because of anomalies in the IR and Raman spectra. A variety of explanations have been given for these anomalies [3] including the formation of solitons or alternatively, the presence of a Fermi resonance.

Because of the large intensity changes that are associated with replacement of H atoms by deuterium, INS can be extremely useful in pinpointing intermolecular vibrational coupling which may play a role in energy transfer phenomena. If, for

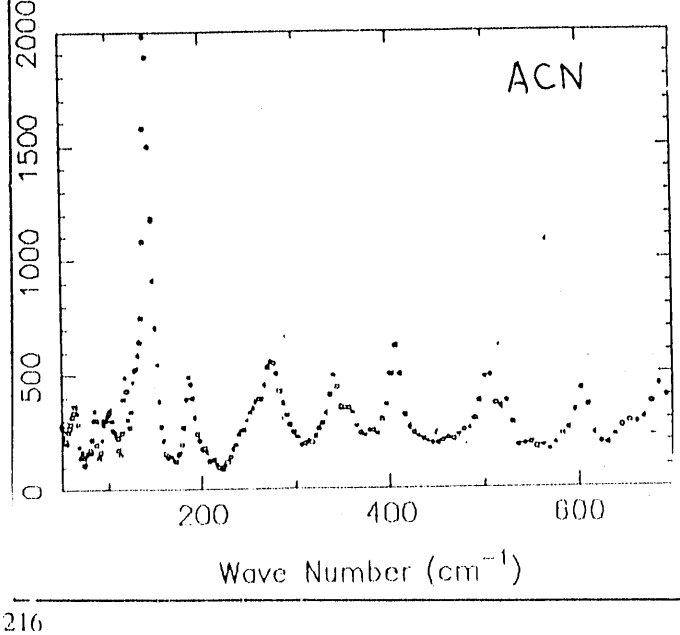

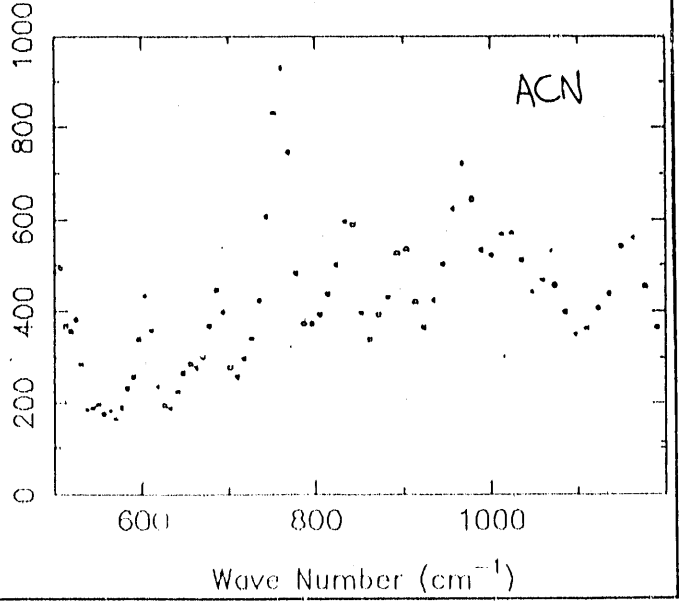

Experiment report: *(continued)*

example, deuteration on one molecular group causes intensity changes in vibrational modes of another, such coupling may be indicated.

Spectra obtained on the FDS at 12K are shown in the figures of ACN (left), ACN with the phenyl ring deuterated and the hydrogen bond as well (right, top) and ACN with the methyl group deuterated (right, bottom). The last sample did not receive sufficient beam time, as the source was shut down for the end of the cycle. All spectra shown were treated with the "mezei method".

We are now in the process of analyzing these data in conjunction with the large amount of optical data we have taken. In addition, we are carrying out a refinement of the force constant model with an NCA on neutron intensities and optical frequency data by means of the program CLIMAX [4], which had to be altered to handle a system of this size.

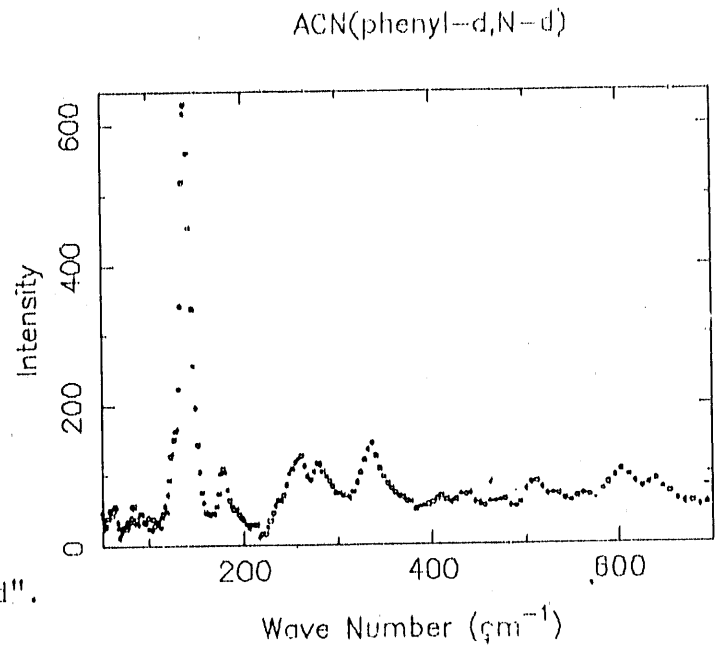

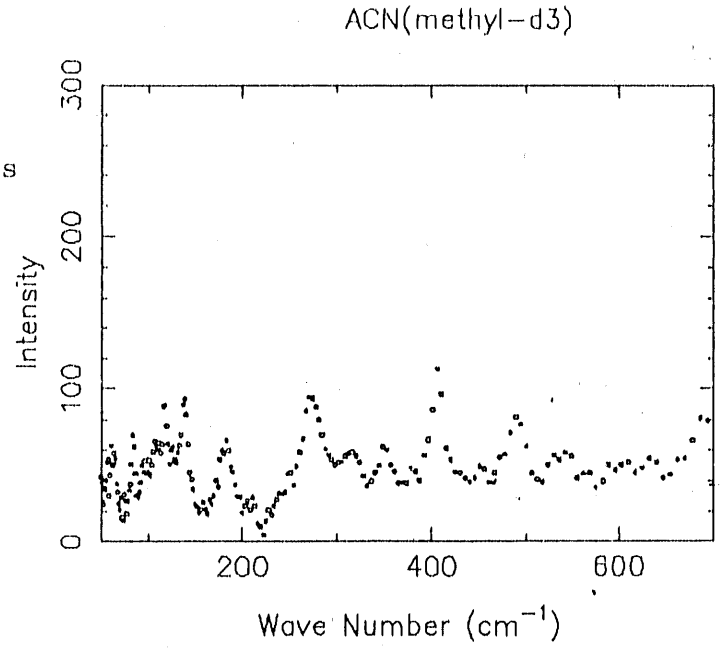

References: 1. S.F.A.Kettle, E. Lugwisha, J. Eckert and N. K. McGuire, Spectrochim. Act. 45A, 533 (1)989).
2. S.F.A. Kettle, E. Lugwisha, P. Vorderwisch and J. Eckert, Spectrochim. Act. (in press, 1990)
3. B. Swanson, and C. Johnston, Chem. Phys. Lett.114, 547 (1985); and references therein.
4. G. J. Kearley [personal communication]

Instrument used: (please type)	Local contact:	Experiment no:
FDS	J. Eckert R.B. Von Dreele	D-37

Title:

IINS Study of Metal-Ammonia Solutions Trapped in TiS_2

Authors and affiliations:

E.W. Ong and W.S. Glaunsinger, Dept. of Chemistry, ASU;

J. Eckert, LANSCE, Los Alamos National Laboratory

Report received:
(to be filled in by LANSCE)

Dates of experiment:

- ☐ Approved by external program committee
- ☐ Approved by internal program committee
- ☒ Part of LANSCE discretionary time

Experiment report:

Definitive evidence was recently found showing that metal-ammonia solutions of lithium and alkaline earths, held in the van der Waals gaps of titanium disulfide formed solvation complexes. This study was initiated to explore the molecular energetics within these intercalates. A series of three samples with varying calcium contents (x = 0.032, 0.065, 0.099) was studied on the FDS. These compounds follows the generic formula:

$$(NH_3)_u[Ca^{2+}_x(NH_3)_B](NH_4^+)_yTiS_2 \qquad 0.00 \le x \le 0.12 \ .$$

Their stoichiometry varies approximately as: B 3x, y 0.22-2x, and u varying about u = 0.6-B-y for low x ; u = 0.4-B-y for high x. This set of variations was designed to find the energies and motional modes of the solvation complexes. The figures below shows: 1) IINS spectra for the x = 0.099 sample and 2) IINS spectra for x = 0.032 sample. The peak near 480 cm^{-1} can be associated with the complex, those near 300-350 cm^{-1} can be associated with the loose ammonia $(NH_3)_u$.

More work is needed to further understand these systems. Time is being requested for the 1990 run cycle.

Experiment report (continued):

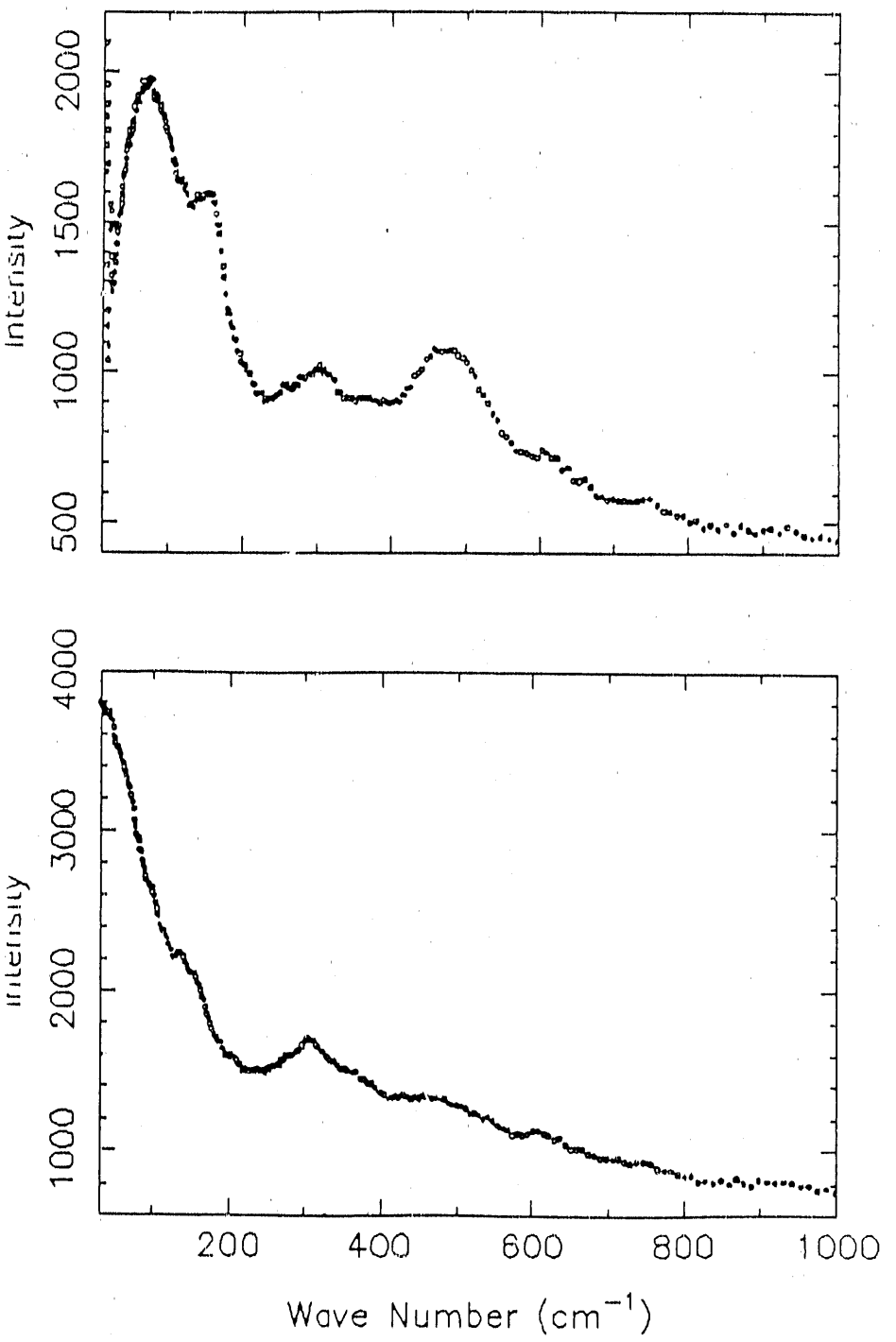

Los Alamos
Los Alamos National Laboratory
Los Alamos, New Mexico 87545

Form number 1195 (12/87)

Instrument used: *(please type)*	Local contact:	Proposal number: *(for LANSCE use only)*
FDS	Juergen Eckert	210
Title: Dynamics of very short hydrogen bonds		**Report received:** *(for LANSCE use only)* 2/1/90

Authors and affiliations:

Prof. Horst Küppers, Mineralogisches Institut der Universität Kiel, Olsenhausenstr. 40, D-2300 Kiel, FRG

Juergen Eckert LANSCE

Experiment report:

We are carrying out a program designed to fully chracterize the dynamics of H in extremely short (R(OO)≲ 2.45 Å) hydrogen bonds. For such systems the antisymmetric stretch ν(OHO) occurs at very low frequency in a spectral region where it is often difficult to assign from optical data. Moreover, it is frequently mixed with other modes and therefore rather broad.In INS on the other hand, entirely different factors govern the intensities of the modes, and in addition, we can utilize the ability to orient the Q-vector either parallel or perpendicular to the displacement vector of the mode under investigation. It is, of course, necessary that the crystal structure is such that all H-bonds point in the same direction.

The principal compound under study has been Li-H-Phthalate-Dihydrate, which has one of the shortest hydrogen bonds known with R(OO) = 2.39 Å. The bond direction is parallel to the crystallographic a-axis of its orthorhombi structure. During our most recent allocation of beam time we performed single crystal studies of the H- and D (on the H-bond and the hydration water) isotopomers in a (110) orientation parallel and perpendicular to the H-bond as well as single crystals of ring-deuterated material in a (101) orientation.

Some of the new single crystal data is shown in Fig.'s 1 and 2, and a comparison of the powder spectra of all three isotopomers is shown in Fig. 3. These additional data have reduced the uncertainties in our assignments of the H-bond vibrations, but have also revealed an unexpected complication that arises from the crystal water molecules. These are

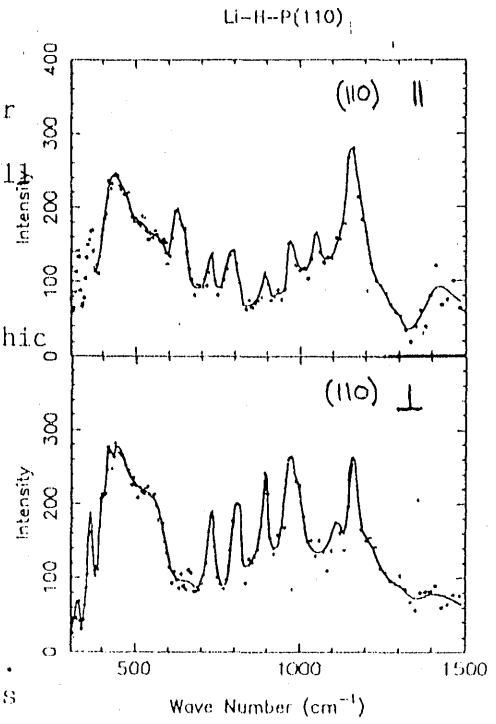

Fig. 1. Li-H-Phthalate INS spectra; (110) orientation. Data are "Mezei"-treated.

Experiment report: *(continued)*

also oriented in a way such that a vector from one H to the other (on a given water molecule) is parallel to the H-bond of the Phthalate ion. Some of the vibrational modes of the water molecules therefore have intensities with similar directional dependencies as the H-bond. Fig. 1, for example shows a very pronounced peak at about 630 cm^{-1} in the parallel configuration. So does, in fact, Fig. 2, which has an additional mode at about 730 cm^{-1} with roughly the same dependence. One of these would be assigned to ν(OHO), whereas the other is ν_R (H_2O), one of the hindered librations of the water molecules. It will require intensity calculations to help sort this problem out. These have been initiated using the profile fitting routine CLIMAX (G.J. Kearley) with NCA.

In another case we have the overlap of the ν_2(H_2O) mode with the in-plnae bend (OHO) in the region between 1600 and 1700 cm^{-1}. Here the data in Fig. 2 allow the identification that the latter is on on the higher side of the broad peak around 1700 cm^{-1}, while δ(OHO) is to be assigned as the peak in the top of the figure, i.e. at 1630 cm^{-1}. The out-of-plane bend, γ(OHO), is quite clearly discernible at about 1180 cm^{-1} in the powder data of the ring-deuterated compound (fig.3).

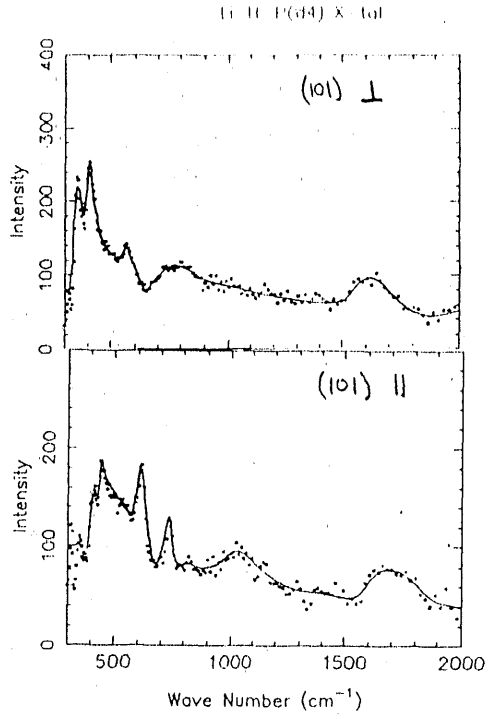

Fig.2. Ring-deuterated Li-H-Phth.

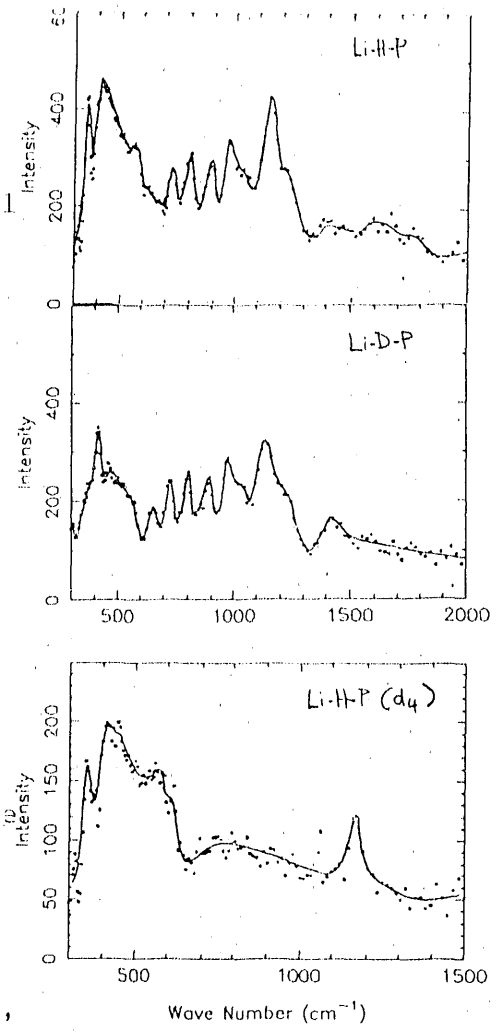

Fig. 3. Powder data of the three isotopomers of Li-H-Phthalate

This is the most detailed set of INS data on any short hydrogen bonded system to date. We are therefore in the process of using intensity calculations to complete the assignments and to obtain a more detailed picture of the dynamics of this very short hydrogen bond.

References:

Instrument used: *(please type)*	Local contact:	Proposal number: *(for LANSCE use only)*
FDS	J. Eckert	216.0

Title:	Report received: *(for LANSCE use only)*
Inelastic Neutron Scattering in NH_4F-I and NH_4F-II	

Authors and affiliations:

M. C. Aronson P-10 LANL

J. Eckert LANSCE

J. D. Thompson P-10 LANL

A. C. Lawson MST-5 LANL

Experiment report:

We have proposed an inelastic neutron scattering study of the structural phase transition observed in NH_4F at room temperature with the application of approximately 4 kbar pressure. The structure of the low pressure phase, NH_4F-I, can be described[1] as hexagonally close packed layers of fluorine atoms with the NH_4^+ ions sitting on alternate tetrahedral sites with three-fold rotational symmetry. Recent neutron powder diffaction measurements[2] revealed that the high pressure phase, NH_4F-II, differed by the presence of layers containing two inequivalent tetrahedra, in which the NH_4^+ ions sit either on a threefold axis, as in NH_4F-I, or in a non-symmetric position. Consequently, it was expected that the degeneracy of the NH_4^+ torsional mode, observed at 555 cm^{-1} in NH_4F-I at 1 bar,[3] should be lifted in NH_4F-II.

Inelastic neutron scattering measurements were performed on NH_4F in a beryllium-copper pressure clamp using the Filter Difference Spectrometer(FDS). The sample spectra at 1 bar and 6 kbar are reproduced in Figure 1. After subtracting the pressure cell background, the NH_4^+ torsional mode at 1 bar is easily resolved at 560 cm^{-1}. In addition there is a water libration mode at 640 cm^{-1}, a phonon density of states feature at 280 cm^{-1}, and an unidentified peak at 400 cm^{-1} which we tentatively ascribe to Fluorinert, the pressure transmitting medium. The primary effect of 6 kbar pressure on this spectrum is to substantially broaden the NH_4^+ torsional mode.

Experiment report *(continued)*:

The broadening of the NH_4^+ torsional mode is qualitatively in agreement both with the introduction of low symmetry NH_4^+ sites under pressure and with the distortion of the NH_4^+ ions themselves, as detected in the neutron powder diffraction measurements. Namely, the degeneracy of rotational energy levels of NH_4^+ ions on the symmetric tetrahedra is lifted on the nonsymmetric tetrahedral sites. However, due to the low symmetry of both the NH_4^+ "rotor" and the potential in which it moves, little quantitative can be said without a more extensive study of the NH_4F-I,II energy level configuration.

In this experiment, we have shown that the rotational energy levels of NH_4F are sensitive to the structural differences between NH_4F-I and NH_4F-II. In addition, we have demonstrated that even with the stringent sample volume constraints imposed by beryllium copper pressure cells, inelastic neutron scattering experiments to pressures of 18 kbar are feasible on the FDS.

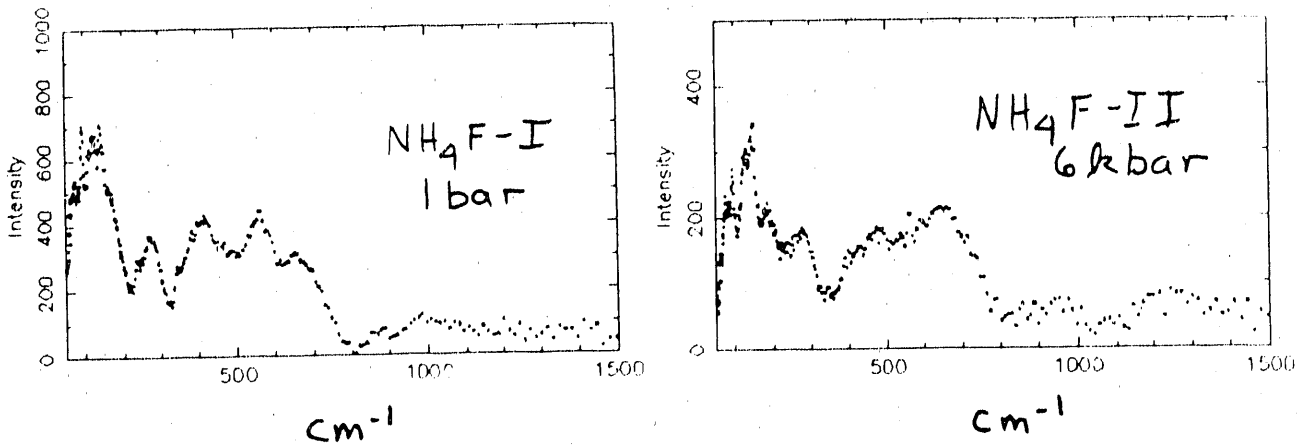

References:

1. H. W. W. Adrian and D. Feil Acta Cryst. A25 438-444 (1969)
2. A. C. Lawson, R. B. Roof, J. D. Jorgenson, B. Morosin, and J. E. Schirber (to be published, Acta Cryst. B)
3. J. Eckert and J. Goldstone (unpublished).

Instrument used: (please type)	Local contact:	Experiment no:
FDS	J. Eckert	247.0

Title:
Inelastic neutron scattering measurements on amino-guadinium salts

Authors and affiliations:

S.F.A. Kettle

School of Chemical Sciences

University of East Anglia

Norwich NR4 7TJ U.K.

Report received:
(to be filled in by LANSCE)

Dates of experiment:

- ❑ Approved by external program committee
- ❑ Approved by internal program committee
- ❑ Part of LANSCE discretionary time

Experiment report:

One aspect of the Raman phenomenon which has attracted attention in recent years is the so-called virtual state. It now seems clear that phenomena can occur during its lifetime although direct evidence of this is extremely limited. The work carried out at Los Alamos had as its aim the test of a hypothesis of the origin of the broad bands (half-width ca 2000 cm^{-1}) seen in the Raman spectra of some strongly hydrogen-bonded amide systems. It having been established by a variety of methods that the broad bands are not due to fluorescence (they are independent of the exciting wavelength, for example), the most likely explanation is that they indicate proton tunnelling in the virtual excited state. For this explanation to be credible, it has to be established that the vibrational ground state is normal (by comparison with species not showing the broad bands). Because of the infrared manifestations of hydrogen bonding (also broad bands, although narrower than their Raman counterparts), and consequent difference between 'broad band' and 'reference' species, infrared spectroscopic measurements are rather ambiguous. Inelastic neutron scattering measurements provide an ideal method of comparing 'broad band' and 'reference', the relatively low resolution of the method being unimportant.

With one exception, all of the 'broad band' species studied

Experiment report (continued):

in the present work were nitrates. The exception is guadinium fluoride, a species which also shows the broad Raman band phenomenon. Its INS spectrum is compared in Figure 1 with those of the nitrate (broad band) and chloride(reference), both recorded last year. Clearly, the vibrational ground states of all three are very similar. The fluoride spectrum is helpful in that it seems to indicate that weak features at ca 900 cm^{-1} and 650 cm^{-1} in the nitrate are not nitrate modes made visible by coupling with protonic vibrations. Further data refinement (vide infra) should estblish this point.

Clear similarities between the vibrational ground states of both aminoguadinium nitrate (broad band) and chloride (reference) were found, again implicating the virtual state in the broad-band Raman phenomena (Figure 2). The same can be said for triaminoguadinium nitrate (broad band) and chloride (reference) for the region above 500 cm^{-1} (Fig.3). Differences below this frequency almost cetainly result from the superposition of two peaks in the nitrate of what are separate features in the chloride. It is planned to establish this point by running an additional triaminoguadinium salt (probably the sulphate) at the earliest opportunity.

Finally, the present measurements offer the unusual possibility that, for a limited number of compounds, inelastic neutron scattering measurements offer a higher effective resolution than do either infrared or Raman. It is therefore of interest to deconvolute the data with, for instance, the instrument resolution function, and so enhance the resolution. Only limited work has so far been done on this but the results are encouraging. The bottom spectum in Fig.4 shows the Be filter data on aminoguadinium chloride, for which good infrared and Raman data are available for comparative purposes. The middle spectrum shows the improved resolution resulting from incoprorating BeO data in a filter difference spectrum. Finally, at the top is shown the filter difference data subject to a MEZEI analysis, a deconvolution program which at the present time seems to give more meaningful results than does maximum entropy.

Summary Inelastic Neutron Scattering Studies carried out at Los Alamos provide strong support for the existence of a novel Raman virtual-state phenomenon in strongly hydrogen bonded amino-guadinium nitrates. It may well be that with suitable data processing of the INS results, detailed vibrational data can be obtained for these species, data that would otherwise be unobtainable.

Figures are on a separate sheet

Los Alamos
Los Alamos National Laboratory
Los Alamos, New Mexico 87545

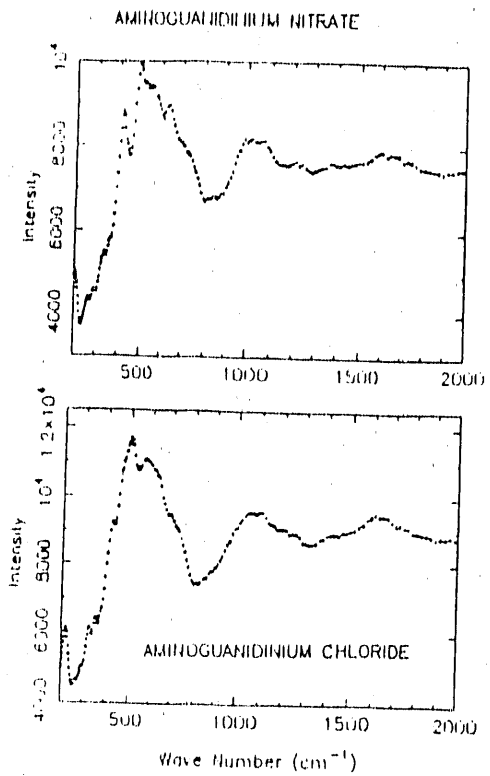

Figure 2

BESUM

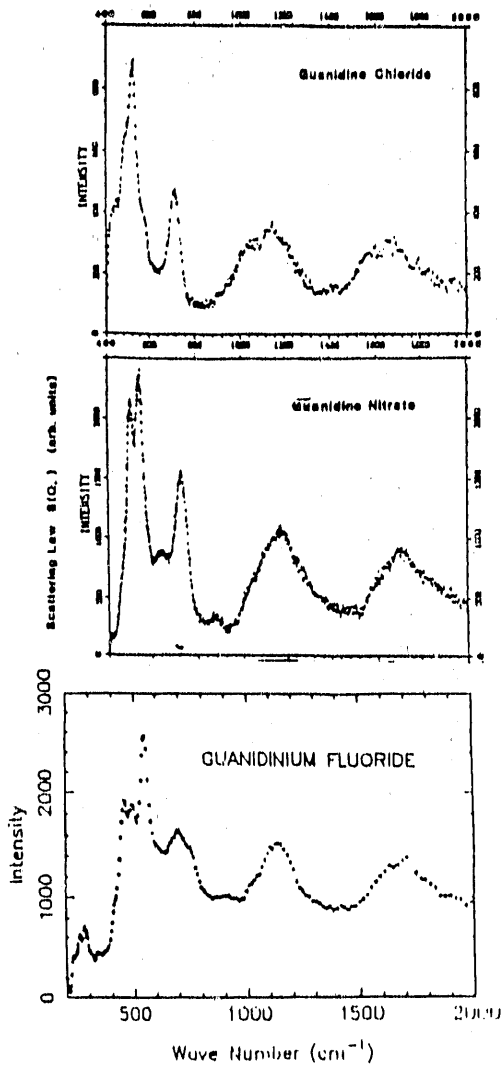

Figure 1

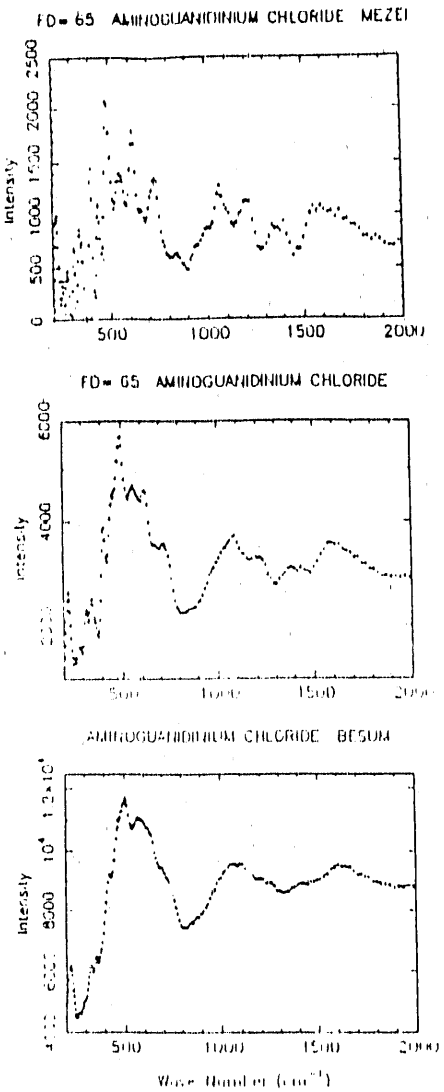

Figure 4

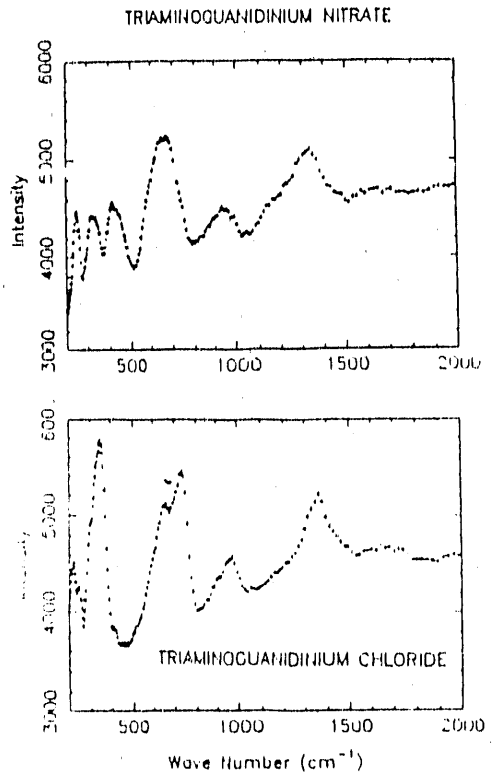

Figure 3

BESUM

Instrument used: *(please type)*	**Local contact:**	**Proposal number:** *(for LANSCE use only)*
FDS	Juergen Eckert	249.0

Title: Hydride dynamics in transition metal cluster compounds

Report received: *(for LANSCE use only)*

Authors and affiliations:

Alberto Albinati, Universitá di Milano, Italy
Juergen Eckert, LANSCE
Luigi M. Venanzi, ETH Zuerich, Switzerland

Experiment report:

As part of our vibrational and structural studies of model systems for heterogeneous catalysis and metal-hydride chemistry we are investigating the dynamics of the hydride ligands in transition metal complexes and cluster compounds. Neutron vibrational spectroscopy can be particularly useful in identifying the vibrational modes associated with the brdiging hydride ligands because of its sensitivty to hydrogen motions. If howeve:, al large number of other protons are in the molecule, a difference technique has to be utilized. In this method the hydride ligand in question is deuterated in a second sample, and the spectrum of the latter subtracted from the former. In this way the vibrational modes of the other ligands (e.g. phenyl rings) are subtracted out provided that coupling between these and the hydride is negligible. While assignment of the hydride vibrations is frequently possible with optical techniques (1), it is sometimes rather difficult because of severe line broadening or interference of other modes.

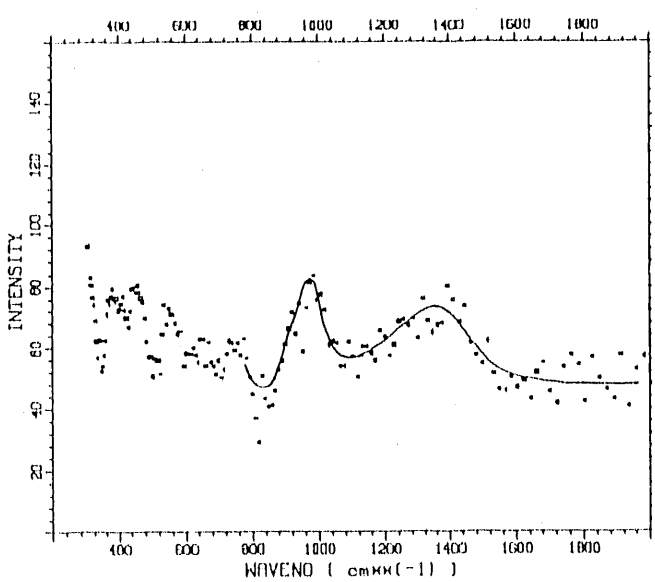

Fig. 1. Differential (Be) spectrum of Ph-$(PEt_3)_2$Pt-H-Pt$(PEt_3)_2$-Ph

We have now completed the study of three Pt-H-Pt complexes with Pt-Pt distances ranging from 3.01 Å to 3.24 Å. In none of these compounds has the hydride been located by the

Instrument used: *(please type)*	Local contact:	Proposal number: *(for LANSCE use only)*
LQD	Rex Hjelm	277.0

Title:

Small Angle Neutron Scattering from a Smectic Liquid Crystal

Report received: *(for LANSCE use only)* 2-9-90

Authors and affiliations:

Thomas P. Rieker and Rex P. Hjelm

Manuel J. Lujan Jr. Neutron Scattering Center (LANSCE)
Los Alamos National Lab.
Los Alamos, NM 87545

Experiment report:

INTRODUCTION: Thermotropic Liquid Crystals are organic molecules which self-organize into various ordered phases as the temperature is altered. Each of these phases is characterized by a distinct combination of partial orientational and translational order. Rod shaped thermotropic molecules are in general composed of a central rigid core with flexible aliphatic chains attached at each end. This class of molecule often exhibits smectic (layered) phases in which the molecules align end-to-end with a typical interlayer spacing of 30 Angstroms and an in-plane spacing of 5 Angstroms. Small angle neutron scattering (SANS) and powder diffraction experiments were undertaken to investigate the evolution of these parameters and to ultimately determine the molecular conformations and packing geometries present in the various phases.

EXPERIMENTAL RESULTS: Small angle neutron scattering on the Low Q Diffractometer (LQD) was performed on an unaligned 2 mm thick bulk sample of $D_{21}C_{10}O(C_6H_4)COO(C_6H_4)0C_6D_{13}$ in order to probe the interlayer spacing as spacing as a function of temperature and the relative tilt of the core and tail regions. Several very interesting results were obtained:

1) The neutron scattering pattern observed for the unlayered nematic phase was unexpectedly similar to those observerd for the smectic phases.

2) Second order scattering was observed for the smectic phases, see Fig. 1.

3) In the smectic phases a Debye-Scherrer ring was observed, corresponding to small angle scattering from a powder of smectic layers . However, the scattering was non-uniform around the ring, concentrating into two broad peaks (+/- q) about the transmitted neutron beam. These peaks rotate by approximately 60 degrees as the sample is cooled through the smectic phases to the crystalline phase. In the crystalline phase the rotation ceased. Figure 2 shows this rotation as a function of temperature.

Experiment report *(continued)*:

3) The interlayer spacing was observed to shrink and then expand in a manner that is atypical for the phase sequences of this sample.

A 100 micrometer thick aligned sample of the above material sandwiched between paralle quartz plates was also prepared. However, this sample appears to have been too thin since coherent scattering from this sample was not observed even after collecting data for a 24 hour period.

CONCLUSIONS: We have observed a novel reorientation of the smectic layering structure in a bulk liquid crystal sample and an atypical change in the interlayer spacing. These effects are due to packing and conformational changes of the liquid crystal molecules. We propose that the central rigid cores of the molecules are becoming more ordered and that they become staggered relative to one another as the temperature is reduced. Further study by small angle neutron and X-ray scattering techniques will be needed to confirm this model.

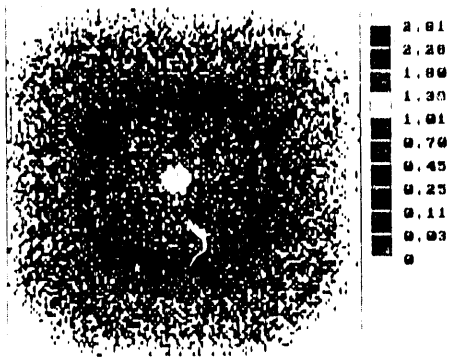

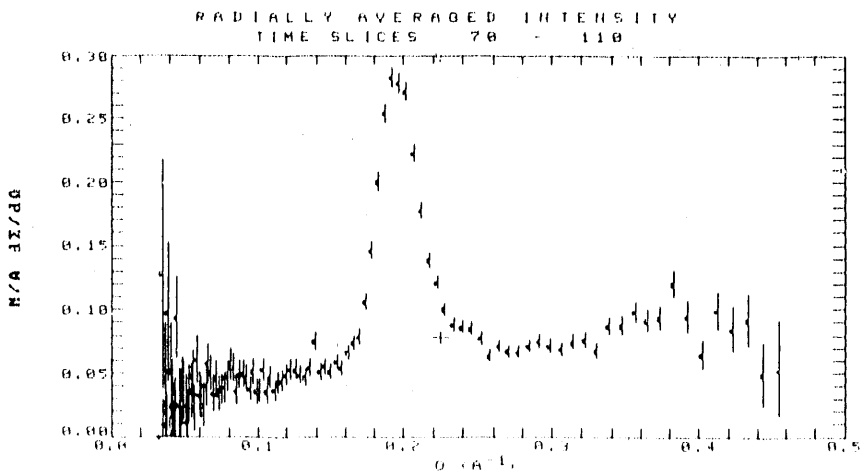

Figure 1: (a) Scattering pattern observed for the smectic A phase in the thermotropic liqiuid crystal; $D_{21}C_{10}O(C_6H_4)COO(C_6H_4)OC_6D_{13}$. (b) Radial distribution of the above scattering pattern. Note the second order peak.

Experiment report: *(continued)*

structural studies carried out to date (2). Approximate Pt-H-Pt bond angles can be derived by extending the C-Pt vectors (compound 1) on either side to the midpoint. This gives 145° for complex 1, for example.

Our data can be analyzed in a rather preliminary way and the(PtHPt) stretching modes assigned by using the simple model for bridging hydrides where there is just one stretching force constant, and use of made of the fact that H is much lighter than the Pt atom. In this case (1) the ratio ν_{as}/ν_{s} is related to tan(θ/2) where θ is the Pt-H-Pt bond angle. Since the Pt-Pt distances are known the Pt-H distance can be estimated. On this basis we can make the following assignments:

	Pt-Pt	ν_{as}	ν_{s}
1	3.24	1415	925
2	3.09	1280	990
3	3.01	1260	1020

where the frequencies are in units of cm^{-1} and the Pt-Pt distance in Å. This yields a Pt-H distance of about 1.9, and bond angles ranging from 114 to 103°. These are smaller than the "theoretical" value as is quite common in such systems.

Further vibrational analysis is in progress, in particular the assignment of the Pt-H-Pt deformation modes and a more detailed consideration of the chemical bonding on the Pt and the resulting geometry of the hydride bridge.

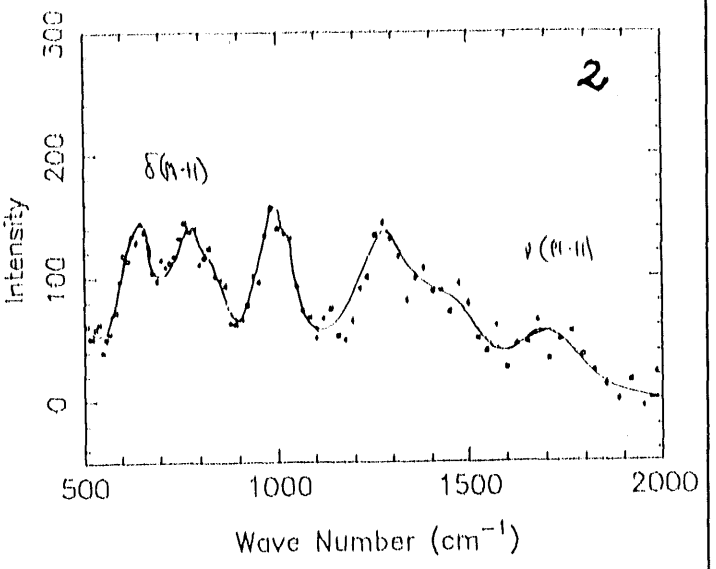

Fig. 2. Differential spectrum (be) of H-$(PEt_3)_2$Pt-H-Pt$(PEt_3)_2$-Ph(d_5)

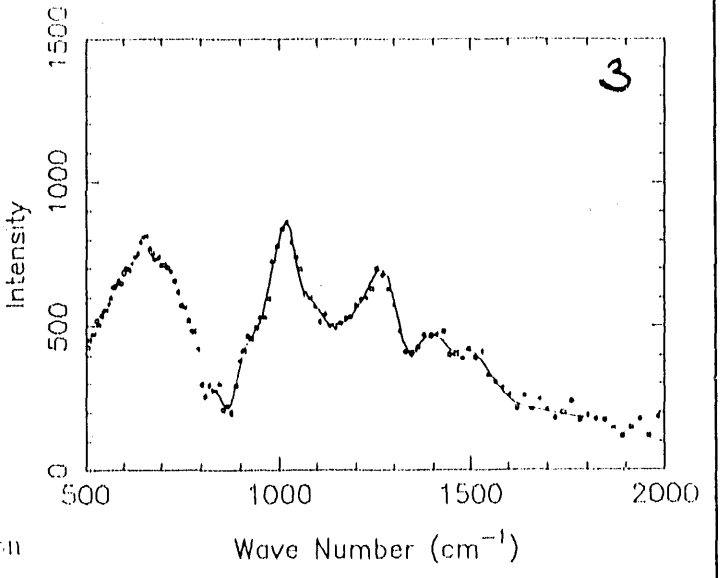

Fig. 3. Differential spectrum (Be) of (C_6F_5)-$(PMe_3)_2$Pt-H-Pt$(PMe_3)_2$-(C_6F_5)

References:

1. C. B. Cooper III, D. F. Shriver and S. Onaka, Adv. Chem. 167, 232 (1978).
2. D. Carmona, R. Thouvenot, L. M. Venanzi, F. Bachechi and L. Zambonelli, J. Organometallic Chem. 250, 589 (1983).

Instrument used: *(please type)*	Local contact:	Proposal number: *(for LANSCE use only)*
Filter Difference Spectrometer. (FDS)	J. ECKERT	284 + 285

Title:
(a) Interstitial Hydrides in Metal Clusters. (284)
(b) Vibrational Coupling in the Solid State. (285)

Report received: *(for LANSCE use only)*
5/1/90

Authors and affiliations:

R.P.White and G.J.Kearley - Institute Laue Langevin, France
U.A.Jayasooriya - University of East Anglia, U.K.
J.D.Corbett - Iowa State University of Science and Technology, U.S.A.
J.Eckert - Los Alamos Nat. Lab., U.S.A.

Experiment report:

(b) The second experiment was an attempt to investigate the probable presence of heterionic vibrational coupling between totally symmetric metal-ligand modes in the compound $[Cr(NH_3)_6]_2[MoS_4]_3$. No conclusive evidense for such an effect was found. This was mainly because of the unavailability of the ^{15}N substituted compound in time for the experiment, due to some unexpected difficulties encountered during the preparation. However, the measurements conducted on the torsional and librational modes of these ions have shown them to be in very shallow potential surfaces. This observation may be of significance in the context of some intriguing resonance Raman spectral results of these compounds which are presently under investigation.

Experiment report: *(continued)*

(a) The first experiment was the search for the optic modes of the interstitial hydrogen in the cluster compound $Li_6Zr_6Cl_{18}H$. Four energy transfers were observed (Figure) with those at 480 and 790 cm^{-1} assignable to the interstitial with the other two at 280 and 190 cm^{-1} assigned respectively to the terminal and bridging chlorine ligands. These observations may be rationalised in terms of a model where the hydrogen occupies a μ_3-bridging position within the octahedral interstitial site with a Zr-H distance of *ca.* 2.0 Å. These conclusions are in good agreement with an NMR study of this compound where the proton was described as 'rattling' within the Zr_6 cavity.[1] Therefore we assign a localised μ_3 geometry for the proton on a vibrational time-scale but showing fluxionality amongst the eight such possible sites on an NMR time-scale. This work is being prepared for publication.

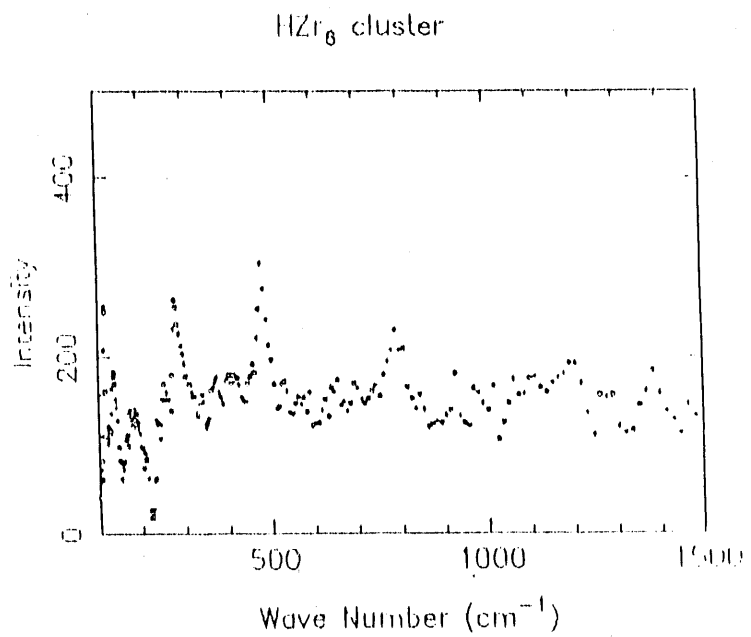

References:

1 P.J.Chu, R.P.Ziebarth, J.D.Corbett and B.C.Gerstein, J.Amer.Chem.Soc., **1988**, *110*, 5324.

Constant-Q Spectrometer (CQS)

Constant-Q Spectrometer (CQS)

The Constant-Q Spectrometer (CQS) is an inelastic scattering instrument designed for the study of collective atomic vibrations and analogous magnetic phenomena waves. A pulsed white beam of neutrons from the source illuminates a sample, which is normally a single crystal. After scattering at the sample, the neutrons are intercepted by a large germanium or copper analyzer that diffracts the neutrons into an array of 96 detectors. The essence of the method is to measure the change in neutron energy when scattering takes place. This is achieved by the analyzer in conjunction with the conventional time-of-flight technique.

The CQS has two principal features: first, the rich higher-energy spectrum at a pulsed source makes this machine suitable for the study of higher-energy collective excitations (50 meV and above), and second, the mapping capability of the instrument makes it suitable for survey work.

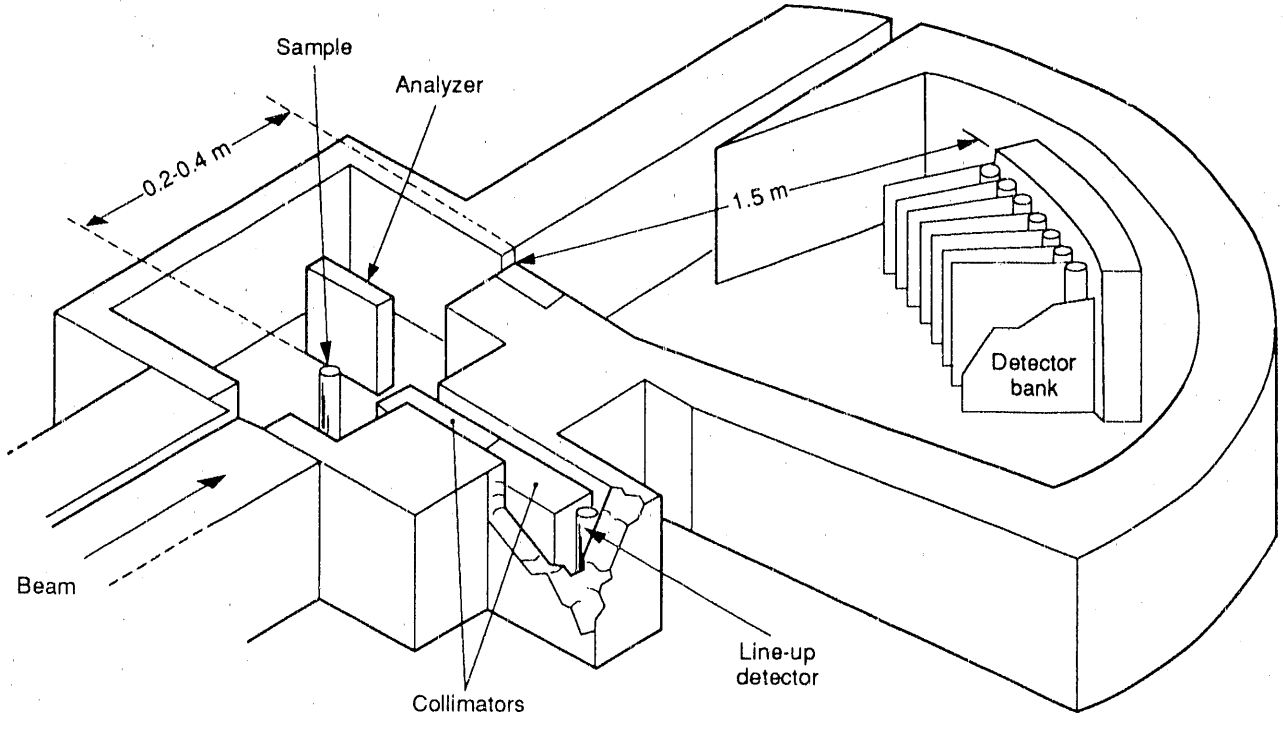

Instrument Details

Detectors	Movable bank of 96 ^{3}He (1.3 cm diameter), 0.57° apart
Detector range	10 - 70°
Energy-transfer resolution	4 - 10%
Analyzer planes	Ge (hh*l*), Cu (hh*l*)
Beam size at sample	2.5 cm wide x 5 cm high
Moderator	Chilled water at 10° C
Sample environment	Closed cycle refrigerator
Experiment duration	~1 week

Robert Robinson, instrument scientist
Eric Larson, instrument technician

New Instruments

PHAROS
μeV Spectrometer

Chopper Spectrometer (PHAROS)

The new chopper spectrometer, PHAROS, is intended to provide 0.5% incident energy resolution for incident energies between 50 meV and 2 eV. The spectrometer is located on flight path 16 with a sample position 20 m from the moderator, which is currently water at room temperature.

Phase I of the construction is ready (Fig. 1a) and consists of an evacuated, shielded flight path for low-angle scattering ($1^\circ < \varnothing < 10^\circ$). The spectrometer is suitable for low-angle studies such as neutron Brillouin scattering and magnetic excitations.

Phase II of the construction will be completed by April 1991 (Fig. 1b). The spectrometer will then be a high-resolution, general-purpose chopper spectrometer with 10 m^2 of detectors covering scattering angles between -10° and 140°. PHAROS will then be able to accommodate the full range of inelastic scattering experiments, including phonon density of state, magnetic excitations, momentum distributions, crystal-field levels, chemical spectroscopy, and measurements of $S(Q,\omega)$ in disordered systems. In addition, the low-angle detectors can be used at distances between 4 and 10 m, with scattering angles down to 1°, and will be suitable for high-resolution inelastic studies at low Q.

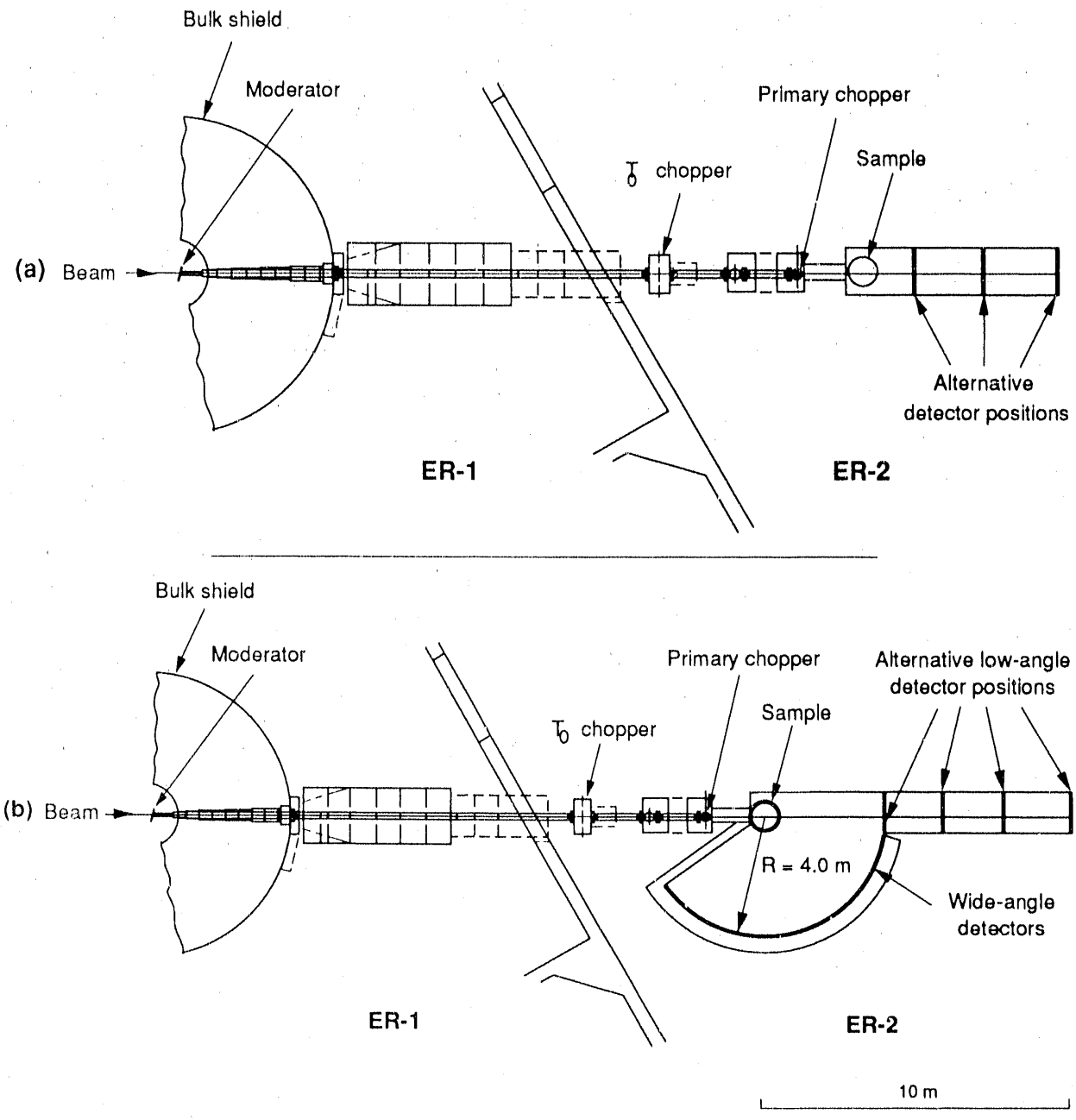

Instrument Details

Moderator-chopper distance	18 m
Chopper-sample distance	2 m
Moderator	12.5 x 12.5 cm^2 room temperaure H_2O
Chopper frequency	600 Hz
Chopper diameter	10 cm
Chopper slit spacing	1 mm or more
Sample size	up to 5 cm x 7.5 cm
Incident energy resolution	$\Delta E_f/E_i = 0.5\%$

Phase I (April 1990)

1 m^2 of detectors at 3.5 m from the sample; scattering angle between 1° and 12°.

Phase II (April 1991)

9 m^2 of detectors at 4 m from the sample; scattering angle between -10° and 140°;
1 m^2 of detectors in forward scattering position at 4 - 10 m from the sample

Robert Robinson, instrument scientist
Eric Larson, instrument technician

10 μeV Spectrometer

The 10 μeV spectrometer is a new time-of-flight backscattering instrument for quasielastic and high-resolution inelastic spectroscopy. This instrument will be installed in 1991. The incident neutron energy is measured by time of flight through a long incident flight path of 30 m. The energy of the scattered neutrons (about 2 meV) is determined from backscattering from single crystals of graphite or silicon. The instrument is to be installed on flight path 11, which is one of the three flight paths viewing the liquid-hydrogen moderator. The combination of this moderator and neutron beam guides between the moderator and the sample maximizes the neutron flux incident on the sample in the energy region between 1 meV and 4 meV.

The new spectrometer is designed for studies of diffusion and low-frequency dynamics. Examples of future experiments are reorientational and tunneling motions in molecular crystals, motion of molecules on surfaces, and dynamics of simple biological systems.

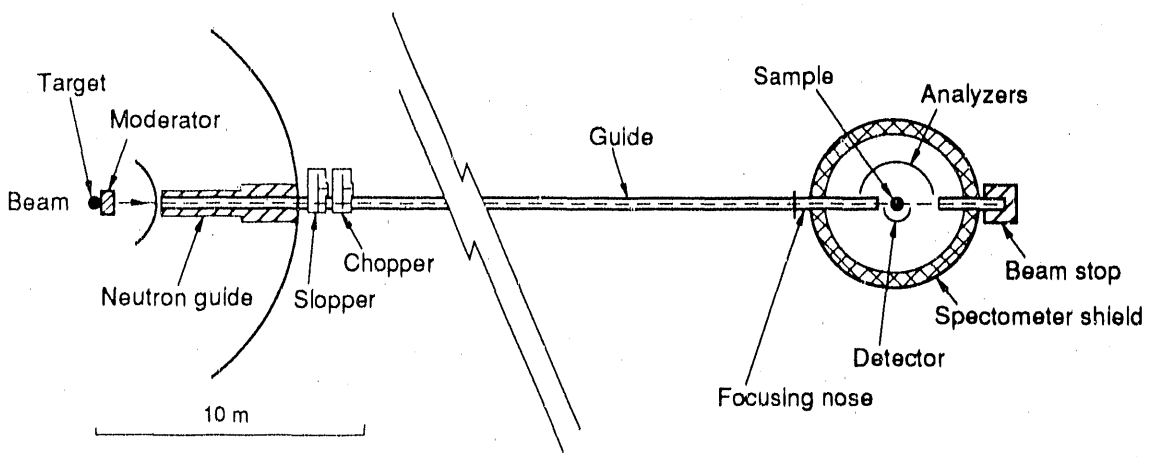

Instrument Details

Quasielastic scattering:	
Final energy	2 meV
Q range	0.035 $Å^{-1}$ - 2 $Å^{-1}$
Resolution	10 μeV
Inelastic scattering:	
Energy transfer range	0 - 50 meV
Q range	1 $Å^{-1}$ - 10 $Å^{-1}$
Resolution	1% of incident energy (FWHM)
Moderator	Liquid H_2 at 20 K
Sample size	3 cm x 3 cm

Torben Brun, instrument scientist
Ross Sanchez, instrument technician

LANSCE User Group
Science Seminar
Abstracts

November 1989

Finite Element Modeling and Neutron Diffraction Measurement of Residual Stress in Stainless Steel and Zircaloy-2

Elane C. Flower
Lawrence Livermore National Laboratory
Livermore, California
and
Stuart MacEwen
Chalk River Nuclear Laboratory
Chalk River, Ontario

The objective of these studies has been to compare calculations of deformation-induced residual stress in test-specimen measurements made by neutron diffraction. The fact that neutrons penetrate into the bulk of the material, allows one to experimentally measure strains that are similar to those calculated by the finite element method. The numerical analysis was performed at LLNL using the NIKE2D finite element program. Neutron diffraction experiments were carried out on the L3 triple-axis spectrometer at the NRU reactor, Chalk River, in the diffraction mode. In our stainless steel specimens, the strains measured at a location depended upon the choice of (hkl) since the stainless steel is elastically anisotropic. As expected, the calculated values of residual elastic strain were between the values measured on the (111) planes and the (002) planes. To determine values of residual stress from experimental data, we used the Reuss approximation (single-crystal constants and hkl strains) and an average approximation (using bulk constants, averaged strains (111) + (002) /2). The Reuss approximation did not yield a unique value of stress indicating a non-linear relationship between stress and strain. Reasonable agreement was found by average approximation. The Zircaloy-2 has an hcp crystal structure, is plastically anisotropic, and exhibits a strength differential (SD) between compression and tension. In our FE model we included the strength differential and used a Hill's anisotropic flow criteria. Agreement between calculated and experimental results depended not only on the choice of (hkl), but on the deformation mode, i.e., whether in tension or compression. The relationship between strain and stress cannot be adequately expressed with single- crystal constants and linear approximations. The work of MacEwen and Tome to analyze diffraction data in Zircaloy-2 will be discussed.

Texture Analysis by TOF of Pulsed Neutrons

H. R. Wenk and K. Bennett
University of California
Berkeley, California
and
A. Larson and P. Vergamini
Los Alamos National Laboratory
Los Alamos, New Mexico

Traditionally preferred orientation in deformed materials has been measured by x-ray diffraction. A detector is set at a given diffraction angle for a particular lattice plane (hkl) and intensities are recorded for different specimen orientations. This way a single incomplete pole figure can be constructed from a set of measurements. Neutron diffraction offers new possibilities.

- Due to minimal absorption, orientation distribution of bulk materials, rather then of thin surfaces can be determined.
- Since there is no defocusing effect, complete pole figures can be measured directly.
- With position-sensitive detection, we can measure a large 2d range, a large pole figure sector, or both at once.

Textures have been measured in conventional neutron sources (e.g., at MBS), with 20 one-dimensional position-sensitive detectors (e.g., at ILL and Risø) and with pulsed neutrons (e.g., at Dubna). The LANSCE facilities offer new possibilities by combining TOF measurements of pulsed neutrons and a 2d position-sensitive detector. This allows both simultaneous coverage of a wide d-spectrum (many peaks) and a large orientation region (pole figure segment). The method effectively permits measurement of the full orientation-distribution on line and is especially attractive for in situ observation of texture development during deformation, recrystallization, and transformations. Due to the simultaneous 2d coverage and the possibility of peak deconvolution, it is ideal for compounds with low crystal symmetry, such as geological materials and HTSC ceramics.

We will illustrate results by comparing LANSCE measurements of a standard sample of calcite with measurements at other facilities. We will also present data from geological, metallurgical, and biological materials and discuss applications of quantitative texture analysis. Finally, we will explore improvements of existing facilities to design instrumentation for state-of-the-art texture analysis.

Neutron Diffraction Measurements of Residual Stress in Engineering Components

T. M. Holden
Atomic Energy of Canada, Ltd.
Chalk River Nuclear Laboratories
Chalk River, Ontario

The key advantage of neutron diffraction is that measurements may be made of residual strain at depth in engineering components in a non-destructive fashion. The simple ideas for exploiting the penetration of the neutron in measuring the desired component of strain at any point in the sample will be explained. The method is applied to the problems of determining the strain field around a crack in welded line pipe and the strain field associated with a single pan weld in a stainless steel plate. The latter example naturally leads to a discussion of weld texture and its influence on elastic properties.

Grain interaction strains in anisotropic materials such as zircalloy, even though they do not constitute a macroscopic strain field, are technologically important. The approach taken to measuring and interpreting the residual strains in highly textured, rolled zircalloy plate will also be discussed.

Future directions for development of the method will be briefly discussed.

Dynamics of the Molecular Hydrogen Ligand in Metal Complexes

Juergen Eckert
Los Alamos National Laboratory
Los Alamos, New Mexico

The recently discovered metal complexes that bind hydrogen in molecular form are the first examples of ligand coordination solely via interaction of a metal center with an s-bonding electron pair. An experimental probe of the electronic details of dihydrogen coordination is, therefore, clearly desirable. We have used inelastic neutron scattering techniques to observe some of the high-frequency vibrations of the metal-dihydrogen fragment as well as the low-frequency tunnel splitting of the rotational ground state of the dihydrogen ligand on a series of such complexes where either the metal center or the large stabilizing ligands are changed. These studies clearly demonstrate the importance of the form of the direct metal-dihydrogen interaction in the origin of the rotational barrier that is determined from the neutron scattering experiments. Our most recent studies include several examples of complexes where questions of a possible equilibrium between polyhydride and dihydrogen ligand formation have arisen both in solution studies and in the solid state as well as those where the dihydrogen ligand is bound so strongly that the rotational tunneling becomes unobservable by neutron scattering.

Theoretical Studies of Transition Metal Complexes of Molecular Hydrogen

P. Jeffrey Hay, C. A. Boyle, and E. M. Kober
Los Alamos National Laboratory
Los Alamos, New Mexico

The structures, energies and reactions of transition metal complexes of molecular hydrogen have been investigated using ab initio electronic structure techniques. The rotational barriers for H_2 in $M(CO)_3(PR_3)_2(H_2)$ species have been calculated for M=Mo and W and for various phosphine alkyl groups (R). These barriers have been compared to the experimentally determined barriers by Eckert using inelastic neutron scattering. Another series of investigation explores mechanistic pathways that may explain the experimentally observed interconversion of H_2 and D_2 molecules to HD involving $Cr(CO)_4(H_2)(D_2)$ complexes.

Structure of Inverse Micelles and Microemulsions

Jess Wilcoxon,
Sandia National Labs
Albuquerque, New Mexico
and
Eric Kaler
University of Washington
Seattle, Washington

A combination of techniques has established that surfactants at low concentrations in aqueous solvents aggregate to form droplet-like structures that swell upon the addition of oil. Much less is known regarding the types of possible structure adopted by surfactants in non-aqueous solvents, such as cyclohexane or toluene. For example, in the well-studied ionic AOT (surfactant) linear-saturated-hydrocarbon system, SANS and light scattering have established that a droplet-like inverse system exists that swells upon the addition of water. This is demonstrated by an increase in both the mass (increase in scattering intensity) and size (decrease of the diffusion coefficient). However, when either AOT or a wide range of nonionic surfactants in the family C_iE_j are solubilized in cyclohexane or toluene, no increases in either quantity is found, even upon addition of large amounts of water (molar water: surfactant ratios of up to w_o~40). By using SANS, we show that the structural units in such solutions have characteristic sizes of <10 Å and cannot be considered true inverse micelle structures. By systematically adjusting the water-like nature (increasing j) in a series of surfactants (C_iE_j) for fixed solvents, we establish the evolution of these inverse systems from small surfactant clusters to classical droplet-like aggregates. Introduction of metal salts into the interior of these inverse systems followed by reduction to form surfactant-stabilized metal colloids allows us to study the structure of these systems by both SANS and electron microscopy. Not surprisingly, the non-droplet systems produce remarkable small metal colloids (diameters ~20 Å), while the droplet-like systems produce larger, and somewhat more polydisperse, colloids.

Structure of Multiphase Silicates

Dale W. Schaefer
Sandia National Laboratories
Albuquerque, New Mexico

Because of the rich chemistry of silica-containing materials, silicates are promising candidates for the development of new materials whose structure and properties can be controlled via precursor chemistry. We have used small-angle scattering along with powder diffraction to elucidate the structure of a variety of silicates from porous glasses to complex molecular composites. Structure is traced to polymer branching and polymerization-induced phase separation in precursor phases. For silica-toughened siloxane elastomers, the structure of the two-phase molecular composite has dramatic effects on the mechanical properties.

Work done in collaboration with J. E. Mark.

Neutron Studies on Copolymers

T. P. Russell
IBM Almaden Research Center
San Jose, California

Small-angle neutron scattering (SANS) and neutron reflectivity (NR) have been used to characterize the morphology of symmetric, diblock copolymers of polystyrene, PS, and polymethylmethacrylate, PMMA. Either block of the copolymer was perdeuterated to provide sufficient neutron contrast. SANS on the diblock copolymers has been used to evaluate the segmental interaction parameter, x, characterizing the interactions between the PS and PMMA segments. X was found to be linearly dependent upon the absolute temperature. However, the temperature coefficient was quite small indicating that x was dominated by entropic contributions. This result is most unusual for diblock copolymers. NR studies on thin films of these copolymers have revealed details on the morphology of copolymers that have been unattainable by other techniques. In particular, the interface between the PS and PMMA can be quantitatively described by a hyperbolic tangent function with an effective width of 50 Å. Calculated values of the interfacial width using x measured by SANS are ca. 30 Å, i.e., 40% lower than the observed value. This discrepancy points to shortcomings of current understandings of the interfacial behavior of polymers.

Small Angle Neutron Scattering Study of Critical Binary Fluids in Porous Glasses

P. Wiltzius and S. B. Dierker,
AT&T Bell Laboratories
Murray Hill, New Jersey

We have previously found that for binary liquid mixtures of 2.6 lutidine and water imbibed into porous VYCOR glass, the phase behavior—as well as the temperature dependence of composition fluctuations—exhibit a wealth of novel features.[1] These can be understood as resulting from a combination of finite-size and random-field effects. Elastic-light-scattering measurements have provided important evidence for a transition from complete to partial wetting behavior.[2] However, SANS is better matched to studying the short-length scale structure of the fluid mixture inside the porous medium.

We measured with SANS the static structure factor S(Q) as a function of temperature and composition. By choosing appropriate mixtures of regular and heavy water, we adjusted the scattering length densities of the liquid and the glass to be equal on average. The, thus determined, S(Q) of the liquid changes from a Lorentzian in the one-phase region to a Lorentzian squared at the random-field transition, in agreement with predictions of the Random Field Ising Model. Measurements of the evolution of S(Q) and of the correlation length with temperature will be presented and discussed.

1. S. B. Dierker and P. Wiltzius, Phys, Rev. Lett. 58, 1865 (1987).
2. P. Wiltzius, S. B. Dierker, and B. S. Dennis, Phys, Rev. Lett. 62, 804 (1989).

The Rod to Vesicle Transition in Bile Salt-Lecithin Mixed Aqueous Colloids

Rex P. Hjelm, Jr. and Devinderjit S. Sivia
Los Alamos National Laboratory
Los Alamos, New Mexico
P. Thiyagarajan
Argonne National Laboratory
Argonne, Illlinois
Hayat Alkan
University of Illinois
Chicago, Illinois
and
Dietmar Schwahn
Kerforshungsanlage Jülich
Jülich, West Germany

The concentration-induced and thermally-induced transitions from rod-like forms to vesicles in mixed aqueous colloids of the bile salt, glycocholate, and lecithin are studied using small-angle neutron scattering. The concentration-induced formation of rods occurs by aggregation of small, globular mixed micelles into large linear aggregates. Extended networks of rods are observed as a transitional form between rods and vesicles. Vesicles formed at the highest concentrations are quite large and decrease in size as the total lipid concentration is lowered. All vesicles appear to consist of single lipid bilayers. The temperature dependence of particle morphology is also considered. Of particular interest is the thermally-induced transition from rods to vesicles, which shows extended networks as intermediate forms. The transition is reversible.

Effect of Oxygen on Structure and Superconductivity in Lanthium Cuprates

J. E. Schirber, B. Morosin, E. L. Venturini, and D. S. Ginley
Sandia National Laboratories,
Albuquerque, New Mexico
and
G. Kwei, J. Goldstone, Z. Fisk, and S-W. Cheong
Los Alamos National Laboratory
Los Alamos, New Mexico

Oxygen introduced by high pressure-high temperature treatment produces bulk superconductivity near 40 K in both La_2CuO_4 and $La_{1.6}Sm_{0.2}Sr_{0.2}CuO_4$. The LaSmSrCuO material is in the T° phase, which is an unusual marriage of the 6-fold Cu-O coordination found in La_2CuO_4 and the four-fold Cu-O coordination found in Nd_2CuO_4 (the precursor for the recently discovered n-type superconductor.) The Cu-O coordination is five-fold in the T° structure. Controversy exists as to the nature and location of the excess oxygen driving the superconductivity in these systems. Because of the current unavailability of any spectroscopy capable of probing this excess oxygen directly, the best hope for clarification of this issue would appear to be careful neutron diffraction studies. Recent studies of La_2CuO_{4+d} and $(LaSmSr)_2CuO_4$ using the Neutron Powder Diffractometer at LANSCE will be described and compared with previous neutron diffraction results.

Particle Size Measurements of Palladium

J. W. Conant
Los Alamos National Laboratory
Los Alamos, New Mexico

Palladium hydride is one of the most exhaustively studied hydrides in science. It is said to have two phases, alpha with an H/Pd in the range of 0 to 0.07 (depending upon the isotropic strain existing in the crystal) and beta with an H/Pd = 0.65 at room temperature (although two other phases have been reported by Sermon, et. al.) We feel that the alpha phase may be a surface phenomenon, with the small quantities of hydrogen trapped in a subsurface layer, rather than a true hydride, in which the hydrogen is randomly dispersed in the octahedral sites of the palladium fcc lattice as reported by many others. The volume of the subsurface layer seems to account for all of the hydrogen present if all of its sites are filled with hydrogen without requiring any hydrogen to be resident in the bulk. Differential Scanning Calorimetry studies by Chou and Vannice seem to substantiate this contention. Our hypotheses are also supported by inelastic neutron scattering and thermal desorption measurements.

We have undertaken a comprehensive study of the particle sizes of a variety of palladium powders before hydriding in an effort to compute the amount of hydrogen that could be occluded based on the specific surface (a function of the volume of the subsurface) of the powders. Measurements were made at LANSCE (HIPD) and ARL (GPPD). Line-broadening estimations of particle size were made using the GSAS version of the Rietveld technique and the results were compared to x-ray data. Studies concerning the take up of hydrogen using Sievert's (gas titration) techniques are also being run on the same materials in an effort to correlate the hydrogen occlusion in the "alpha phase" with particle size. The progress of our investigations will be reported.

Neutron Scattering Studies of Chromosome Structural Elements

Morton Bradbury
Los Alamos National Laboratory
Los Alamos, New Mexico

Similar to all higher organisms, human-cell nuclei contain extraordinary amounts of DNA,—a total of 2.04 meters in length subdivided into 46 chromosomes and contained in a cell nucleus 5 to 10 x 10^{-6} m. Determination of the modes of packaging DNA into chromosomes is central to our understanding of chromosome functions. Digestion of chromosomes in cell nuclei by micrococcal nuclease, an enzyme that cuts the DNA double helix, shows that the DNA is packaged into a repeating subunit called the nucleosome, which contains about 200 base pairs (bp) of DNA, an octamer of histone proteins ($[H2A,H2B]_2[H3_2,H4_2]$) and a fifth histone H1. Further digestion with micrococcal nucleases reveals well-defined subnucleosomal particles; the chromatosome that contains 168 bp DNA; the histone octamer and one H1 and the nucleosome core particle that contains 146 bp DNA and the histone octamer. The structure of the core particle has been solved at low resolution by neutron scattering techniques and at higher resolution by x-ray and neutron diffraction.

Neutron scattering techniques have powerful applications to the structures of two component biological systems because of the different scattering lengths of the two isotopes of hydrogen: ^1H [b = -0.38.10^{-12} cm] and ^2H [b = +0.67.10^{-12} cm]. The other elements found in biological systems have b values in the rand of +0.51 to -0.94.10^{-12cm}. Therefore, to a first approximation, the scattering-length density (SLD) of a biological molecule will be determined by the proportion of 1H it contains. SLDs of protein and DNA are 0.20.$10^{11}cm^{-2}$ and 0.38.$10^{11}cm^{-2}$, respectively. These values are contained within the range of values that can be obtained with mixtures of ^1H_2O [SLD = -0.06.$10^{11}cm^{-2}$] and ^2H_2O [SLD = +0.63.$10^{11}cm^{-2}$]; the SLD of DNA is matched by a water mixture of 63% ^2H_2O:37% ^1H_2O and that of protein by 40% ^2H_2O:60% ^1H_2O. Neutron scattering studies of nucleosomes particles in different mixtures of ^1H_2O and ^2H_2O have given unique structural information on the spatial organization of the protein and DNA. Such a neutron-contrast-matching study gave the solution structure of the core particle, and this has been shown to be essentially correct by x-ray crystal-structure determinations. Our current research is to use neutron scattering to investigate the effects of chromatin variables associated with chromosome functions on the structure of the nucleosome and chromatin.

These studies were carried out in collaboration with Drs. Jill Trewhella and Rex Hjelm.

Structures in Ca^{2+}-Dependent Biochemical Regulation Studied by Neutron Scattering

Jill Trewhella
Los Alamos National Laboratory
Los Alamos, New Mexico

Biochemical regulation is a central problem in the study of life processes. For healthy biochemical function, a myriad of processes must be carried out in the appropriate order and at the appropriate rates. There are a number of messengers that play key roles in regulatory mechanisms both within and between cells to ensure proper function. The divalent calcium ion is the principal biochemical messenger that acts in the regulation of intra-cellular processes that occur on short time-scales. Examples of such processes include muscle contraction, neurotransmitter release, the generation of energy for cellular metabolism, etc. Calcium-dependent regulation is generally achieved when Ca^{2+} binds to a calcium-binding protein, which is then able to bind to a target enzyme and activate it. The calcium "modulator" protein calmodulin is the major intracellular receptor for calcium.

The solution structure of calmodulin and its interactions with two target enzymes have been studied using x-ray and neutron scattering. Neutron resonance scattering from calmodulin, in which the Ca^{2+} has been substituted with $^{240}Pu^{3+}$, has been measured in an attempt to determine the distances between the four ionbinding sites in the protein. Interestingly, the calmoduin.$4Pu^{3+}$ complex activates at least one target enzyme as efficiently as does calmodulin.$4Ca^{2+}$. Calmodulin—complexed with its binding-domain from myosin light-chain kinase, as well as with two-binding domains from the catalytic subunit of phosphorylase kinase,— has been studied using small-angle scattering and contrast variation. Information about the nature of the calmodulin target-enzyme interactions has been obtained and has contributed to our current understanding of the molecular basis for Ca^{2+}-dependent regulation.

Understanding Reflectivity

William Hamilton
Los Alamos National Laboratory
Los Alamos, New Mexico

In recent years, the reflection of neutrons from surfaces has emerged as a new technique for the investigation of interface and multilayer structures over the range from 10 to 10,000 Å. The method shares most of the unique advantages associated with conventional neutron scattering, including contrast control by isotopic substitution and sensitivity to magnetic structures. This talk will present an introduction to the surface profile information available from neutron-reflection measurements.

Redox and Solvation Phenomena in Transition Metal Disulfide Intercalates

M. J. McKelvy, V. G. Young Jr., E. W. Ong, G. L. Burr, and W. S. Glaunsinger
Arizona State University
Tempe, Arizona
and
R. B. Von Dreele
Los Alamos National Laboratory,
Los Alamos, New Mexico

Ammonia and metal-ammonia intercalates of the transition metal disulfides (TS_2) can be described as ammonia-solvated cation intercalates. Intercalation of ammonia into TS_2,T=Ti,Nb, and Ta hosts is not a simple molecular insertion reaction. Redox reactions resulting in the cointercalation of ammonium accompany ammonia intercalation. These intercalates possess a variety of structural phenomena, depending on the relative strength of their guest-guest and guest-host interactions. These phenomena include solvated cation complex formation, ammonia reorientation, and distorted ammonia geometries. The characterization of these, as well as other phenomena, the investigation of selected intercalates by the Rietveld refinement of NPD data, and future directions will be discussed.

Neutron Diffraction in Incommensurate Barium Sodium Niobate at Low Temperatures

W. F. Oliver
Arizona State University
Tempe, Arizona

Stoichiometric $Ba_2NaNb_5O_{15}$(BSN) undergoes a phase transition at 105 K upon cooling from a nearly commensurate orthorhombic phase ($Ccm2_1$) to a doubly modulated incommensurate (IC) structure of underlying tetragonal symmetry. Dielectric measurements reveal another possible phase transition at ~40 K. The 2Q IC structure between 40 K and 105 K also appears to exist between ~565 K and 582 K; and thus, the 105 K transition is thought to be a reentrant transition. We have performed neutron diffraction studies on two samples of BSN at 10 K, 21 K, and 90 K to elucidate its true structure in these low temperature phases. At the two lowest temperatures probed, the structure is found to be "locked-in" to a structure with P4nc symmetry. Between is indicated a phenomenon also observed in other structurally IC systems. The results of these experiments and possible extensions of this work will be discussed.

The Structure of High Temperature Superconductors: the 1989 Vintage

George H. Kwei
Los Alamos National Laboratory
Los Alamos, New Mexico

Structural work on high-transition-temperature superconductors and related compounds from the 1989 run cycles at the Manuel Lujan, Jr. Neutron Scattering Center will be presented. These range from temperature-dependent and dopant studies of $YBa_2Cu_3O_7$, to studies of oxygen stoichiometry in superoxygenated T and T* phase materials, and to some newly discovered superconducting materials. Recent structural work on the superconductor, $TlBa_{1.2}La_{0.8}CuO_5$, produced by reduction rather than oxidation of the CuO_2 planes will be highlighted.

Index

Author	Proposal No.	Page
Albinati, A.	249.0	228
	35.0	214
Alkan, H.	268.0	174
Aronson, M. C.	216.0	222
Barton, R.	271.0	106
Bates, F. S.	291.0	186
Bernhardt, J.	272.0	42
Bianchini, C.	35.0	214
Blumenthal, D.	222.0	142
Bradbury, E. M.	229.0	148
	245.0	152
	246.0	154
Brese, N.	14.1	14
	14.2	16
	257.0	98
	258.0	100
	263.0	104
Brun, T.	275.0	178
Burr, G. L.	31.0	6
	32.1	8
	32.2	10
	100008.0	56
	100009.0	58
	19.1	72
	19.2	74
	203.3	80
	203.4	82
Buschow, K. H. J.	10.0	4
	33.0	24
Canfield, P.	207.0	127
Charles, S.	229.0	148
Chen, H. S.	250.0	158
Cheong, S-W.	280.2	52
	281.2	69
Claytor, T.	21.0	22
Conant, J. W.	100008.0	56
	100009.0	58
Cook, G.	246.0	154
Corbett, J.	284.0	230
	285.0	230
Cort, B.	212.0	28
	218.0	84
	227.0	88
Delbaere, L.	271.0	106
Diamond, H.	269.0	190
Dierker, S. B.	232.0	150
Eckert, J.	34.0	212
	35.0	214
	36.0	216
	37.0	218
	210.0	220
	216.0	222
	249.0	228
	284.0	230
	285.0	230
Epperson, J. E.	269.0	190
Eyring, L.	236.1	92
	236.2	94
Farago, B.	253.0	38
Fisk, Z.	280.2	52
	281.2	69
Foltyn, E.	218.0	84
Fountain, L. E.	221.0	140
Frederickson, G. H.	291.0	186
Frick, B.	253.0	38
Garzon, F. H.	281.2	69
Gerspacher, M.	293.0	188
Gillette, D.	242.0	124
Gilliom, L.	254.0	172
Ginley, D. S.	31.0	6
	32.1	8
	32.2	10
	4.0	66
	203.1	76
Glaunsinger, W. S.	19.1	72
	19.2	74
	203.2	78
	203.3	80
	203.4	82
	37.0	218
Goldstone, J. A.	8.0	21
	278.0	60
	4.0	66
	281.2	69
	251.0	70
	19.1	72
	19.2	74
	218.0	84

Author	Proposal No.	Page
Goldstone, J. A.	226.0	86
	227.0	88
	235.0	90
	252.0	96
Gottesfeld, J. J.	246.0	154
Gray III, G. T.	243.0	34
Gupta, S.	271.0	106
Hamilton, W.	276.0	46
	0.0	202
	29.0	204
Hanley, H. J. M.	288.0	196
Harker, Y. D.	252.0	96
Harrison, D.	289.0	182
Henderson, S.	223.0	144
Heremans, C.	272.0	42
Heuser, B.	225.0	146
Hjelm, R. P.	245.0	152
	246.0	154
	268.0	174
	273.0	176
	291.0	186
	269.0	190
	277.0	193
Hobart, D.	223.0	144
Hults, W.	281.1	54
Hurd, A. J.	290.0	184
Imai, B.	245.0	152
Iqbal, Z.	279.0	48
Jankowski, A. F.	29.0	204
Jayasooriya, U. A.	284.0	230
	285.0	230
Johnston, G. P.	290.0	184
Jones, R. A. L	220.0	206
Kalceff, W.	237.0	30
	238.0	32
Kaler, E.	204.0	136
	248.0	156
Kearley, G. J.	34.0	212
	284.0	230
	285.0	230
Kettle, S. F. A.	247.0	224
King, J. S.	225.0	146
Kirk, D.	100008.0	56
Klein, A.	286.0	180
Kramer, E. J.	220.0	206
Kubas, G. J.	239.0	112
Küppers, H.	8.0	21
	33.0	24
	210.0	220
Kwei, G. H.	16.1	18
	16.2	20
	279.0	48
	280.1	50
	280.2	52
	281.1	54
	4.0	66
	281.2	69
Larson, A. C.	17.0	36
	267.0	40
	235.0	90
	271.0	106
	239.0	112
Larson, A. C.	241.0	116
Larson, E. M.	29.0	204
Lawson, A.	10.0	4
	21.0	22
	33.0	24
	212.0	28
	243.0	34
	280.1	50
	100008.0	56
	100009.0	58
	218.0	84
	226.0	86
	227.0	88
	252.0	96
	207.0	127
	216.0	222
Lin, T-L.	250.0	158
Lodge, T. P.	291.0	186
Mark, J. E.	254.0	172
Martin, J. E.	204.0	136
McCarron, E. M.	251.0	70
McKelvy, M.	32.1	8
	32.2	10
	203.1	76
	203.2	78
	203.3	80
	203.4	82
Michl, J.	266.0	130
Moore, P.	289.0	182
Morosin, B.	4.0	66
Mosley, W. C.	205.0	26
Murthy, G.	266.0	130
Norton, L.	220.0	206
O'Keeffe, M.	13.0	12
	14.1	14
	14.2	16
	257.0	98
	258.0	100
	260.0	102
	263.0	104
Oliver, W. L.	265.0	128
Olivier, B. J.	253.0	38
Ong, E. W.	16.1	18
	16.2	20
	279.0	48
	19.1	72
	19.2	74
	37.0	218
Palmer, P.	223.0	144
Parise, J. B.	8.0	21
	251.0	70
Partin, D.	13.0	12
	260.0	102
Pieper, J.	288.0	196
Quail, W.	271.0	106
Radiman, S.	221.0	140
Ramakrishna, B. L.	16.1	18
	16.2	20
	279.0	48
Reuter, W. G.	252.0	96
Richter, D.	253.0	38
Rieker, T. P.	278.0	60

Author	Proposal No.	Page
Rieker, T. P.	277.0	193
Roberts, M. F.	250.0	158
Robertson, B. E.	271.0	106
Robinson, R. A.	10.0	4
	16.1	18
	16.2	20
	33.0	24
Rokop, S. E.	222.0	142
	223.0	144
Rosedale, J. H.	291.0	196
Russell, T. P.	208.0	138
	208.0	138
	0.0	202
Sabine, T. M.	237.0	30
	238.0	32
Schaefer, D. W.	253.0	38
	254.0	172
Schirber, J. E.	280.2	52
	4.0	66
Schmunk, R. E.	252.0	96
Schroth, G. P.	246.0	154
Scott, J.	265.0	128
Seeger, P. A.	222.0	142
	223.0	144
	229.0	148
	273.0	176
	293.0	188
	269.0	190
Silver, R. N.	275.0	178
Sivia, D.	21.0	22
Smith, D. M.	290.0	184
Smith, G. S.	276.0	46
	0.0	202
	29.0	204
Smith, J. L.	281.1	54
Smyth, J.	240.0	114
Sosnick, T.	229.0	148
	245.0	152
Sperling, L. H.	286.0	180
Spirilet, J. C.	212.0	28
Stepanek, P.	291.0	186
Straty, G. C.	288	196
Subramanian, M. A.	8.0	21
Swanson, B. I.	36.0	216
Swope, R. J.	240.0	114
Tadloch, W.	100008.0	56
Thiyagarajan, P.	268.0	174
	273.0	176
	269.0	190
Thompson, J. D.	280.2	52
	281.2	69
	207.0	127
	216.0	222
Toprakcioglu, C.	221.0	140
Torrie, B.	17.0	36
	267.0	40
	235.0	90
Trewhella, J.	222.0	142
	223.0	144
	229.0	148
	245.0	152
Vance, L.	238.0	32
Vaninetti, J.	21.0	22
Venanzi, L. M.	249.0	228
Venturini, E. L.	4.0	66
Vergamini, P.	241.0	116
	242.0	124
	207.0	127
Viskoe, D.	21.0	22
Voderwisch, P.	36.0	216
Von Dreele, R. B.	10.0	4
	31.0	6
	32.1	8
	32.2	10
	14.2	16
	16.1	18
	16.2	20
	8.0	21
	33.0	24
	212.0	28
	237.0	30
	17.0	36
	267.0	40
	276.0	46
	280.2	52
	100009.0	58
	278.0	60
	251.0	70
	19.1	72
	19.2	74
	203.1	76
	203.2	78
	203.3	80
	203.4	82
	235.0	90
	236.1	92
	236.2	94
Walters, R. T.	205.0	26
Ward, J. W.	212.0	28
Wei, Y. Y.	271.0	106
Wenk, H. R.	241.0	116
White, R. P.	284.0	230
	285.0	230
Wilcoxon, J. P.	204.0	136
	248.0	156
Willis, J. O.	275.0	178
Wiltzius, P.	232.0	150
	291.0	186
Wuensch, B. J.	272.0	42
Yau, P.	229.0	148
	245.0	152
Yethiraj, M.	21.0	22
	275.0	178
Yoo, J. N.	286.0	180
Young, Jr., V. G.	31.0	6
	32.1	8
	32.2	10
	19.1	72
	19.2	74
	203.1	76
	203.2	78
	203.3	80
	203.4	82

•U.S. GOVERNMENT PRINTING OFFICE 1990-0-773-034/20101

END

DATE FILMED

11 / 08 / 90